ESSAYS IN EMPIRICAL ASSET PRICING

by

HAO CHANG

A Dissertation submitted to the

Graduate School - Newark

Rutgers, The State University of New Jersey

In partial fulfillment of the requirements

for the degree of

Doctor of Philosophy

Graduate Program in Management

Joint with Graduate Program in Statistics in the School of Graduate Studies

written under the direction of

Professor Yangru Wu and Professor Rong Chen

and approved by

_____

_____

_____

_____

Newark, New Jersey

May, 2020

Copyright page:

ABSTRACT OF THE DISSERTATION

ESSAYS IN EMPIRICAL ASSET PRICING

By Hao Chang

Dissertation Director:

Professor Yangru Wu and Professor Rong Chen

This dissertation includes four essays on empirical asset pricing as well as the application of state-space models in this area. The first essay seeks to reconcile the debate about the price effect of risk-neutral skewness (RNS) on stocks. We document positive predictability from short-term skewness, consistent with informed trading, and negative predictability from long-term skewness, consistent with skewness preference. A term spread on RNS captures different information from long- and short-term contracts, resulting in stronger predictability. The quintile portfolio with the lowest spread outperforms that with highest spread by 14.64% annually. The information difference between short- and long-term options explains the pricing difference of their RNS, providing a potential resolution to the debate.

The second essay uses a novel sequential Monte Carlo method, the mixture Kalman filter (MKF), to detect periodically collapsing rational bubbles in stock prices. The stock-dividend-bubble system is expressed in a state-space model with Markov regime switching. We apply the MKF to estimate the model for simulated and actual stock data. Our methodology captures the bubble dynamics more successfully than the model without regime-switching, and identifies major bubble collapsing episodes in our sample period.

The third essay explains why the correlation between oil price and 10-year TIPS break-even inflation increased dramatically after the financial crisis. We develop a shadow-rate no-arbitrage term structure model to fit nominal yields, TIPS yields and inflation forecasts, and estimate it using the Extended Kalman Filter. Based on the model estimation, we provide empirical evidences showing that the puzzle is because when interest rates bind at the zero lower bound, investors doubt the effectiveness of monetary policy to control deflation. We justify this mechanism theoretically under a general equilibrium framework.

The last essay develops an arbitrage-free Nelson-Siegel term structure model with economic factors, estimates the model using the Kalman Filter and reveals the information content of treasury term premium through model decomposition. We find foreign carry trades and cross-border investments have been the key drivers of negative treasury term premium in recent years due to monetary divergence. This poses challenges to conventional term structure models using US-exclusive macro variables to explain treasury dynamics.

Acknowledgements

It is my pleasure, to my best memory, to pay my special regards to all the people who advised, inspired, motivated, and supported me through my entire joint Ph.D. study in Finance and Statistics.

Firstly and most importantly, I would like to express my deepest gratitude to my co-advisors, Prof. Yangru Wu and Prof. Rong Chen. I would like to thank my Finance advisor, Prof. Yangru Wu, for his guidance on my research about empirical pricing of equities and other asset classes, for advising me how to think and write academically, and for his invaluable suggestions and encouragement on my career development. I will never forget many weekends I spent with him discussing about research ideas and writing papers together. I would like to thank my Statistics advisor, Prof. Rong Chen, for his guidance on my research about the application of non-linear state-space model in finance and for helping me expand my horizons in mainstream statistics research. I enjoyed all the time conducting interdisciplinary research under Prof. Wu and Prof. Chen's guidance. Without their enlightenments and support, the completion of this dissertation would be impossible.

Secondly, I wish to give many thanks to my outside committee member Prof. Yacine Ait-Sahalia from Princeton University, for providing me his insightful comments on my dissertation and systematically teaching me advanced technologies about interest rate term structure, continues-time asset pricing and financial econometrics. It was a great honor for me to have a chance to take his two graduate courses at Bendheim Center for Finance through Rutgers-Princeton Exchange Program. Without learning from him, I was not able to finish last two essays in my dissertation.

Additionally, I would also like to thank my other committee members, Prof. Zhaodong (Ken) Zhong, Prof. Daniela Osterrieder, Prof. Steffen Hitzemann and Prof. Han Xiao, for providing their intuitive enlightenments on my dissertation. I greatly benefited from discussions with Prof. Zhong about empirical literature in derivatives markets and many discussions with Prof. Hitzemann about how to develop dynamic stochastic general equilibrium models to justify empirical findings theoretically.

I would like to thank many other faculty members at RBS, including Prof. Ivan Brick, Prof. Cheng-Few Lee, Prof. Jin-Mo Kim, Prof. Tavy Ronen, Prof. Simi Kedia, Prof. Ben Sopranzetti, Prof. Zhengzi (Sophia) Li, Prof. Phil Davies, Prof. Yichuan Liu, Prof. Vikram Nanda, Prof. Andrzej Ruszczynski, Prof. Xiaodong Lin, etc., and many other facuty members at the Department of Statistics, including Prof. John Kolassa, Prof. William E. Strawderman, Prof. Cun-Hui Zhang, Prof. David E. Tyler, Prof. Javier Cabrera and Prof. Zhiqiang Tan, etc., for providing general guidance and/or teaching me during my Ph.D. study.

Furthermore, I wish to thank some scholars outside Rutgers University, such as Prof. Renraw Chen from Fordham University, Prof. Liuren Wu from Baruch College and Prof. Turan Bali from Georgetown University, for giving me deep insights on my research. Sincerely thanks to Dr. Min Wei from the Federal Reserve Board of Governors, who systematically taught me literature about fixed income pricing, Macro finance and monetary policies when I took her course at Princeton University. The last two essays of my dissertation were persistently inspired by her recent top publication about TIPS market. I also thank Prof. Paul Borochin from University of Miami for his helpful suggestions and contribution on our collaborated project about risk-neutral skewness.

This is also an opportunity to thank my colleagues at RBS, including Peixuan Yuan, Xinjie Wang, Weike Xu, Ge Wu, Bo Zhou, Yaqing Xiao, Xin Cheng, Cheng Gao, Yankuo Qiao, etc., and my colleagues at the department of statistics, including Liang Wang, Linglin

He, Yilei Zhan, Yi Chen, etc., for helpful discussions and general support. I am very grateful to Liang Wang for his important contribution to our collaborated work about the mixture Kalman fiter. I enjoyed a lot of discussions with him, which advanced and enhanced my knowledge on sequential Monte Carlo methods. In addition, I owe my thanks to Xiaoyang (Sean) Dong at Bendheim Center for Finance in Princeton University, who was my teaching assistant when I learned from Prof. Yacine Ait-Sahalia and Dr. Min Wei. I learned a great deal from him about hands-on experience for estimating continuous-time asset pricing models with a huge number of parameters as well as economic intuition for global macro strategy through our joint work on negative treasury term premium.

I am proud to be the first student in Rutgers history to purse the joint Ph.D. program in Management (Finance) and Statistics across Newark and New Brunswick campuses. I am indebted to all relevant administrators in the Office of the Senior Vice President for Academic Affairs of Rutgers Universitywide, the Office of the Dean at RBS, the Office of the Dean at the Graduate School - Newark, the Office of the Dean at the School of Graduate Studies, Ph.D. program in Management and Ph.D. program in Statistics, for the tremendous support. Thanks to Rutgers University for providing me such a fantastic opportunity to conduct high-quality interdisciplinary research across campuses.

Finally, I can't be more grateful to my family for their love, understanding and tireless support. Special thanks to my wife, Yan Xue, my parents and my parents-in-law. Without their support, I would not be able to complete this dissertation. I am also grateful to my sons Bowen and Evan, for bringing me eternal happiness, passion and motivation.

Dedication

To my parents Junjie and Huilan, my wife Yan and my sons Bowen and Evan

Table of Contents

List of Tables

List of Figures

Chapter 1

The Information Content of the Term Structure of Risk-Neutral Skewness

(Jointly with Paul Borochin and Yangru Wu)

1.1 Introduction

The behavioral and rational models of Brunnermeier et al. (2007), Mitton and Vorkink (2007), and Barberis and Huang (2008), in which investors exhibit a preference for securities with positive skewness, have motivated a large empirical literature on whether positively skewed securities are overpriced and earn negative average excess returns. As most historical estimates of skewness provide poor forecasts of future skewness (Boyer et al., 2010), empirical studies commonly use option data to estimate investor expectations of skewness.

To date, existing studies have produced mixed evidence for whether option-implied risk-neutral skewness carries a positive or negative premium in the cross-section of equity returns. Consistent with skewness preference theory, Conrad et al. (2013) find a negative relation between risk-neutral skewness (RNS) and future equity returns. This approach implicitly assumes that option and stock markets reflect the same information and that option-implied skewness proxies for expected underlying skewness. Thus, positive option-implied skewness combined with skewness preference among investors in the underlying asset leads to low expected returns.

This assumption is challenged by findings of information differences between the option and equity markets. Ait-Sahalia et al. (2001) demonstrate that the risk-neutral density

estimated from the S&P 500 options is different from a density inferred from historical index returns, suggesting that the option market includes a "peso problem" jump dynamic unobserved in the underlying asset. Consistent with an information difference between two markets, other studies contradict Conrad et al. (2013) by demonstrating that RNS can positively predict future stock returns (Xing et al., 2010; Bali and Murray, 2013; Stilger et al., 2017; Bali et al., 2019). While Bali and Murray (2013) focus on the returns of a hedged asset with skewness exposure, part of their analysis confirms a positive relationship between RNS and the underlying asset. Stilger et al. (2017) suggest that the difference between the Conrad et al. (2013) results and others are driven by the aggregation of RNS across time periods. In this study, we consider the role of the option maturity horizon in defining the relationship of RNS with the cross-section of underlying returns.

Xing et al. (2010) suggest that informed option traders purchase out-of-the-money (OTM) put options before downward jumps in the underlying stock, which drives up the volatility of OTM puts and consequently leads to a steeper slope of the implied volatility function translating to a more negative RNS per Bakshi et al. (2003). Furthermore, Stilger et al. (2017) find this trading activity mainly concentrates on stocks that are perceived as relatively overpriced by investors and costly to sell short. Therefore, hedging demand for underlying positions or speculation on pessimistic expectations causes informed investors to buy OTM puts or sell OTM calls, also pushing down RNS. As information is transmitted from the option market to the stock market, these relatively overpriced stocks with low RNS subsequently underperform, producing a positive relation between RNS and future realized equity returns. Bali et al. (2019) find that option-implied skewness is positively related to future expected returns from analyst forecasts and implied cost of capital calculations.

Our study contributes to this ongoing debate between two empirical views on RNS by considering its term structure: we find that short-term options have more informed traders consistent with the view that positive RNS predicts positive underlying returns because it reflects market beliefs. We also find that long-term options have more uninformed hedgers

consistent with the skewness preference view that positive RNS predicts negative underlying returns because it results in overbidding. We build the intuition for the potential to reconcile informed trading and skewness preference using a multi-period equilibrium model where investors have heterogeneous skewness preferences and information sets, detailed in Section 1.2.

Importantly, our theoretical results show that when there is a small proportion of informed investors, the risk premium for RNS is negative. In this case, RNS is predominantly determined by uninformed investors' expected skewness for assets. Uninformed investor preferences thus result in more demand and lower subsequent return for positively-skewed assets. Conversely, when the proportion of informed traders increases, the RNS risk premium turns positive. In this case, RNS reflects informed traders' superior information about the true skewness of assets. Thus for a stock with higher RNS, its true skewness should be higher than what uninformed investors expect. When the information becomes public afterwards, the demand for the stock increases, pushing up its price and generating a positive relation between RNS and subsequent return.

We empirically test whether the direction of RNS return predictability varies with the maturity of the options used to compute it. In other words, we test the predictability of the underlying returns across the term structure of RNS, as we hypothesize that the proportion of informed traders may vary across options with different maturities. If differently informed investor types have different maturity preferences and thereby produce market segmentation across option maturities, the resulting RNS estimated across different maturity horizons may contain distinct information sets. While we cannot directly map trades to investor types, we can conjecture that informed traders may prefer to use short-term options due to lower costs while hedgers may need longer-maturity contracts. Our findings confirm this conjecture.

We use the OptionMetrics Volatility Surface file from 1996 to 2015 to calculate monthly

RNS at the 1-, 3-, 6-, 9-, and 12- month maturities for a large sample of U.S. stocks. We estimate RNS for each security at each time horizon using the model-free method of Bakshi et al. (2003) and analyze the cross-sectional predictive relationship between the RNS at different maturities with subsequent monthly underlying returns. The results indicate that this relationship exhibits a monotonic pattern, which is significantly positive for the short-term (1 month), insignificant for the middle-term (6 months), and significantly negative for the long-term (12 months). In particular, a strategy that is long the equal-weighted quintile portfolio with the highest 1-month RNS and short the equal-weighted quintile portfolio with the lowest 1-month RNS yields a risk-adjusted[1] return (alpha) of 0.95% per month with a t-statistic of 5.78, while the same strategy based on 12-month RNS produces a corresponding alpha of -0.56% per month with a t-statistic of -2.52. The positive predictability of future equity returns from short-term RNS is consistent with informed trading (Xing et al., 2010) and hedging (Stilger et al., 2017) interpretations, while the negative predictability from the long-term RNS is consistent with skewness preference (Bali and Murray, 2013; Conrad et al., 2013).

Since the short-term RNS has positive predictive power for returns while long-term RNS has the opposite, we capture the different information sets on the two ends of the RNS term structure by constructing a term spread of RNS defined as 12-month RNS minus 1-month RNS. We demonstrate that this spread effectively combines the two information sources and yields even stronger negative return predictability for the underlying asset using a portfolio sorting approach. A trading strategy that is long the equal-weighted quintile portfolio with the highest term spread and short the equal-weighted quintile portfolio with the lowest term spread yields an alpha of -1.22% per month with a t-statistic of -6.61 after controlling for the Fama and French 3 factors, Carhart momentum factor, and Pastor and Stambaugh (2003) liquidity factor. We confirm these results with a Fama and MacBeth

[1]We use the FFCP5 benchmark model that combines the Fama and French (1993) beta, size, and book-to-market factors, the Carhart (1997) momentum factor, and the Pastor and Stambaugh (2003) liquidity factor. Alternative benchmarks produce similar results.

(1973) cross-sectional regression.

To further explore the extent of the information impounded in the term structure of RNS, we test whether short- and long-term RNS have differing predictive power for firms' standardized unexpected earnings (SUE) using a Fama and MacBeth (1973) regression. We find that the short-term RNS is a positive predictor of SUE, suggesting that it captures option traders' superior information about earnings. Simultaneously, we find that long-term RNS is a negative predictor of SUE, consistent with overvaluation due to skewness preference. As a robustness check for the information content of RNS across different maturities, we also test its ability to predict future stock price crashes. Consistent with the previous results, we find a significantly negative (positive) relationship between the short-term (long-term) RNS and future price crashes. Notably, the predictive power of short-term RNS persists for at least 6 months. Furthermore, consistent with Stilger et al. (2017), we demonstrate that the positive predictability of future equity returns from short-term RNS is strongest for overpriced and short-sale constrained underlying stocks, indicating that the short-term RNS reflects hedging demand. In addition, we provide some direct evidence showing that the long-term RNS reflects skewness preference. We compare long-term RNS with two recent well-known physical skewness measures exhibiting negative predictive power for equity returns consistent with the skewness preference literature, maximum daily return over the previous month (MAX) (Bali et al., 2011) and expected idiosyncratic skewness (EIS) (Boyer et al., 2010). We find that our long-term RNS measure not only has strong positive correlation with these physical skewness proxies, but also complements them in identifying low expected return stocks with lottery-like payoffs.

We find that the term structure of RNS is largely explained by two principal factors, a level and a slope, similar to findings for the yield term structure by Nelson and Siegel (1987), Litterman and Scheinkman (1991) and Christensen et al. (2011). The RNS term structure slope factor, which is most significantly related to both cross-sectional and time-series stock returns, is significantly related to the Welch and Goyal (2008) macroeconomic

state variables for the equity premium in vector autoregressive models.

We help to reconcile the ongoing debate about the direction of the skewness anomaly by demonstrating the existence of a term structure of RNS and its differential information content across option maturities. We find evidence consistent with informed trader preference for hedging underlying stock positions or speculating by trading short-term options. This interpretation is intuitive for several reasons. First, mispricing in the stock market can be corrected over a short time horizon (Bali et al., 2011). Second, short-term options are more sensitive to the variation of the underlying stock's price, thus providing more protection to hedgers or a more leveraged position to speculators. Third, the short-term option market is usually more liquid and thus imposes lower trading costs.

The RNS implied by short-term options deviates away from the expected skewness of the underlying stock due to informed trading. As the option term increases, informed traders have monotonically decreasing hedging/speculating demand for the corresponding option contracts due to increasingly unfavorable timing, exposure, and liquidity characteristics. Being increasingly less affected by informed trading, these longer-term options more closely mirror the distribution of the underlying stock. As a consequence, the skewness implied by the long-term options tends to reflect the equity market's expected skewness of the underlying stock and carries a negative risk premium. These patterns are consistent with Holowczak et al. (2006), who find that the informativeness of option prices increases when option trading activity generates net sell or buy pressure on the underlying stock and even more so when the pressure coincides with deviations between the stock and options prices. Thus, the price effect of RNS across its term structure is determined by a combination of informed option traders' hedging/speculative demand and the equity market's expectations about the skewness of the underlying stock.

The remainder of this paper is organized as follows. Section 1.2 provides the theoretical motivation for this research. Section 1.3 describes the data and variable construction.

Section 1.4 documents the differing explanatory power of the short- and long-term RNS on the cross-section of equity returns. Section 1.5 illustrates a novel anomaly, the term spread of RNS, that captures the difference in the information content of RNS at different maturities. Section 1.6 examines the information content in the term structure of RNS by relating it to earning surprises, price crashes, and investors' hedging demands. Section 1.7 identifies an RNS term structure similar to that of interest rates, and finds that the "slope" factor has a significant relation with macroeconomic variables related to expected equity returns. Section 1.8 concludes.

1.2 Theoretical Model

In this section we use an equilibrium model to show how informed trading and skewness preference can be reconciled with each other and can lead to different pricing effects on future stock returns. Our model builds on the equilibrium asset pricing model of Mitton and Vorkink (2007), who use a one-period economy with two type of investors with heterogeneous preference for skewness to generate the negative risk premium of skewness. The first type, which is referred as a "Traditional Investor", has a mean-variance utility function. The second type, the "Lotto Investor", has identical preferences to the traditional investor over mean and variance but also has preference for skewness. We extend Mitton and Vorkink (2007) by changing the one-period economy to a multi-period economy and dividing the lotto investor type into two subtypes, the "Informed Lotto Investor" and "Uninformed Lotto Investor". Informed lotto investors are able to estimate the skewness of risky securities more accurately than uninformed ones. By making these extensions, we bring the role of informed trading into the asset pricing framework and demonstrate its ability to generate a positive skewness risk premium.

Following Mitton and Vorkink (2007), we assume that the investable universe consists of three risky assets and a riskless bond that pays an interest rate r per period. $\mathbf{V}$ denotes the

covariance matrix of the three risky assets one period ahead. In addition, the distribution of asset returns are allowed to be skewed. In a departure from Mitton and Vorkink (2007), we assume that there are n periods in the economy and that all risky securities pay off at time n. The current time is time 0. In this example we set $n = 10$ without loss of generality.

The future wealth of each investor type is denoted as W and its mean, variance and skewenss are $E(W)$, $Var(W)$ and $Skew(W)$. We assume all types of investors know $\mathbf{V}$. At a certain time t, they believe the distribution of asset returns are i.i.d in each of the remaining periods from time t to time n.

The "Traditional investor" has a standard quadratic utility function over wealth

$$U(W) = E(W) - \frac{1}{2\tau} Var(W), \tag{1.1}$$

where W is the future wealth and τ ($\tau > 0$) is the coefficient of risk aversion. The "Informed Lotto investor" has a mean-variance-skewness utility function:

$$U(W) = E(W) - \frac{1}{2\tau} Var(W) + \frac{1}{3\phi} Skew(W). \tag{1.2}$$

Here ϕ ($\phi > 0$) is the coefficient controlling preference for skewness. A preference for positive skewness is indicated by positive values of ϕ. Here we assume the informed Lotto investors know the true value for the idiosyncratcic skewness and coskewness of all risky assets so they can estimate $Skew(W)$ precisely.

The third investor type, the "Uninformed Lotto investor", has the same utility function but his/her estimate for the idiosyncratic skewness of a stock may be biased. Therefore, this type's estimate for the third moment of the future wealth, $\widehat{Skew(W)}$, which measures the downside risk of his/her future wealth, may deviate from its true value $Skew(W)$. The

corresponding preference is given by

$$U(W) = E(W) - \frac{1}{2\tau}Var(W) + \frac{1}{3\phi}\widehat{Skew(W)}. \tag{1.3}$$

For simplicity, we assume every uninformed lotto investor believes his/her skewness estimate is correct and he/she doesn't know about the existence of informed lotto investors. We further assume that traditional investors don't care about the third moment of their wealth distribution when making investment decision. Thus, whether or not they are informed about the skewness of the joint distribution of risky assets has no effect on asset prices and asset holdings of this investor type in equilibrium.

Let $\mathbf{X}_j^{(t)} = \left[x_{j,1}^{(t)}, x_{j,2}^{(t)}, x_{j,3}^{(t)}\right]'$ be an 3×1 vector that denotes every j-th type investor's dollar amount in each of the three risky assets at time t. Let $\mathbf{R}^{(t,n)} = \left[R_1^{(t,n)}, R_2^{(t,n)}, R_3^{(t,n)}\right]'$ denote the average return of each period from time t to time n in equilibrium. The wealth these investments generate at time n is $W_j^{(n)} = W_j^{(t)}(1+(n-t)r)+\mathbf{X}_j^{(t)'}(n-t)(\mathbf{R}^{(t,n)}-r\mathbf{1})$. Here $W_j^{(t)}$ represents every j-th type investor's endowment at time t. For simplicity, we assume simple interest in this economy.

The objective of each investor type is to maximize his/her utility function, such as equation (1.1), (1.2) or (1.3), subject to their budget constraint. In the spirit of Mitton and Vorkink (2007), a traditional investor's demand function is given by,

$$\mathbf{X}_T^{(t)} = \tau\left((n-t)\mathbf{V}\right)^{-1}(n-t)(\mathbf{R}^{(t,n)} - r\mathbf{1}) = \tau\mathbf{V}^{-1}(\mathbf{R}^{(t,n)} - r\mathbf{1}). \tag{1.4}$$

Here subscript T signifies traditional investors. As the distribution of 3 risky assets are believed to be i.i.d, $(n-t)\mathbf{V}$ are believed to be the covariance matrix of 3 risky assets from time t to time n.

For an informed lotto investor, the solution is described by the following equation,

$$(n-t)(\mathbf{R}^{(t,n)} - r\mathbf{1}) - \frac{1}{\tau}(n-t)\mathbf{V}\mathbf{X}_{IL}^{(t)} + \frac{1}{\phi}\left[\left(x_{IL,1}^{(t)}(n-t)\mathbf{M}_1 + x_{IL,2}^{(t)}(n-t)\mathbf{M}_2 + x_{IL,3}^{(t)}(n-t)\mathbf{M}_3\right)\mathbf{X}_{IL}^{(t)}\right] = 0, \quad (1.5)$$

where subscript IL signifies informed lotto investors and $\mathbf{M}_1$, $\mathbf{M}_2$, and $\mathbf{M}_3$ are matrices defined as

$$\mathbf{M}_i = \begin{bmatrix} M_{i11} & M_{i12} & \cdots & M_{i1n} \\ M_{i21} & M_{i22} & \cdots & M_{i2n} \\ \vdots & \vdots & \ddots & \vdots \\ M_{in1} & M_{in2} & \cdots & M_{inn} \end{bmatrix} \quad (1.6)$$

with $i = 1, 2, ..., n$ and where arbitratry elements of $\mathbf{M}_i$, denoted as M_{ijk}, is denoted as $M_{ijk} = E\left[(R_i - \bar{R}_i)(R_j - \bar{R}_j)(R_k - \bar{R}_k)\right]$ and $\bar{R}_i = E\left[R_i\right]$. R_i is the return of Asset i in one period. Three general types of skewness elements exist in the 'M' skewness matrices: M_{iii}, which represents the idiosyncratic skewness of Asset 'i', M_{iik}, which represents the curvilinear interaction of Asset 'i' and 'j', and M_{ijk}, which represents the triplicate product moment of the Assets 'i', 'j' and 'k'. The above equation (1.5) can be simplified as,

$$(\mathbf{R}^{(t,n)} - r\mathbf{1}) - \frac{1}{\tau}\mathbf{V}\mathbf{X}_{IL}^{(t)} + \frac{1}{\phi}\left[\left(x_{IL,1}^{(t)}\mathbf{M}_1 + x_{IL,2}^{(t)}\mathbf{M}_2 + x_{IL,3}^{(t)}\mathbf{M}_3\right)\mathbf{X}_{IL}^{(t)}\right] = 0. \quad (1.7)$$

Here we assume informed lotto investors know $\mathbf{M}_1$, $\mathbf{M}_2$, and $\mathbf{M}_3$. While uninformed lotto investors may not have such information. Their estimation of $\mathbf{M}_1$, $\mathbf{M}_2$, and $\mathbf{M}_3$ at time t are denoted as $\hat{\mathbf{M}}_1^{(t)}$, $\hat{\mathbf{M}}_2^{(t)}$, and $\hat{\mathbf{M}}_3^{(t)}$. Therefore, for uninformed lotto investor, the solution is implied by the following equation,

$$(\mathbf{R}^{(t,n)} - r\mathbf{1}) - \frac{1}{\tau}\mathbf{V}\mathbf{X}_{UL}^{(t)} + \frac{1}{\phi}\left[\left(x_{UL,1}^{(t)}\hat{\mathbf{M}}_1^{(t)} + x_{UL,2}^{(t)}\hat{\mathbf{M}}_2^{(t)} + x_{UL,3}^{(t)}\hat{\mathbf{M}}_3^{(t)}\right)\mathbf{X}_{UL}^{(t)}\right] = 0. \quad (1.8)$$

We assume without loss of generality that the total investment in each risky asset at time

0 is $D = 100$, and that the total number of investors is $N = 300$. Among all investors, the proportion of traditional investors and informed lotto investors are P_T and P_{IL}, respectively. Therefore, the proportion of uninformed lotto investors is $P_{UL} = 1 - P_T - P_{IL}$. We fix the the proportion of traditional investors to be 1/2, i.e., $P_T = 1/2$. And by default we set the proportion of each type of lotto investors to be 1/4, i.e., $P_{IL} = P_{UL} = 1/4$. To clear the market, at time t, we have the following conditions:

$$\mathbf{X}_T^{(t)} N P_T + \mathbf{X}_{IL}^{(t)} N P_{IL} + \mathbf{X}_{UL}^{(t)} N (1 - P_T - P_{IL}) = D\mathbf{1}. \tag{1.9}$$

By solving equations (1.4), (1.7), (1.8), and (1.9), we can obtain the equilibrium return from time t to time n for 3 risky assets, $\mathbf{R}^{(t,n)}$, and the equilibrium holdings for risky assets of one investor of all types, $\mathbf{X}_T^{(t)}$, $\mathbf{X}_{UL}^{(t)}$ and $\mathbf{X}_{IL}^{(t)}$.

Table 1.1 presents the parameters we use to obtain the numerical solutions to our theoretical equilibrium model. Following Mitton and Vorkink (2007), we use the same parameters of the risk-aversion and skewness preference parameters (τ, ϕ) and the covariance matrix $(\mathbf{V})$ elements, and we assume that the return distributions of Assets 1 and 3 are completely characterized by the first two moments (i.e., no skewness). Asset 1 represents a large-cap stock with low variance and high average correlation to other stocks, and Asset 3 represents a small-cap stock with high variance and low average correlation to other stocks. However, the return distribution of Asset 2 is allowed to be skewed, and its skewness is allowed to be idiosyncratic, which is equivalent to setting $M_{ijk} = 0$ for all i, j, k except for the case $i = j = k = 2$.

We assume the information about M_{ijk} is known to all investors, with the exception that informed and uninformed lotto investors may have a different understanding of the value of M_{222}, i.e., these two types of investors may have different opinions about how skewed the return distribution of Asset 2 is. Given these specifications, equation (1.7) and (1.8) can

be simplified as,

$$(\mathbf{R}^{(t,n)} - r\mathbf{1}) - \frac{1}{\tau}\mathbf{V}\mathbf{X}_{IL}^{(t)} + \frac{1}{\phi}[0, M_{222}{x_{IL,2}^{(t)}}^2, 0]' = 0, \tag{1.10}$$

and

$$(\mathbf{R}^{(t,n)} - r\mathbf{1}) - \frac{1}{\tau}\mathbf{V}\mathbf{X}_{UL}^{(t)} + \frac{1}{\phi}[0, \hat{M}_{222}^{(t)}{x_{UL,2}^{(t)}}^2, 0]' = 0. \tag{1.11}$$

We assume that at time 0, informed lotto investors learnt the true value of M_{222}, while the uninformed lotto investors are not able to do this until time 1. The uninformed lotto investors' estimation for M_{222} at time 0 is denoted as $\hat{M}_{222}^{(0)}$. Under this framework, we can study the role of informed trading in determining the equilibrium return of assets from time 0 to time 1, $\mathbf{R}^{(0,1)}$, especially the equilibrium return of Asset 2, $R_2^{(0,1)}$.

We compute $\mathbf{R}^{(0,1)}$ in two steps. First, at time 0, we solve the equilibrium average one-period return of risky assets from time 0 to time n, $\mathbf{R}^{(0,n)}$. Second, at time 1, we solve the average one-period return from time 1 to time n, $\mathbf{R}^{(1,n)}$. Then $\mathbf{R}^{(0,1)}$ is computed as $\mathbf{R}^{(0,1)} = n\mathbf{R}^{(0,n)} - (n-1)\mathbf{R}^{(1,n)}$.

The RNS of Asset 2 at time 0 can be proxied by the idiosyncratic skewness of Asset 2 implied by the equilibrium asset prices, assuming all lotto investors, including both informed and uninformed, have the same information. We denote the RNS of Asset 2 by $\tilde{M}_{222}$. It satisfies the following equation,

$$(\mathbf{R}^{(t,n)} - r\mathbf{1}) - \frac{1}{\tau}\mathbf{V}\mathbf{X}_{L}^{(t)} + \frac{1}{\phi}[0, \tilde{M}_{222}^{(t)}{x_{L,2}^{(t)}}^2, 0]' = 0, \tag{1.12}$$

where $\mathbf{X}_L^{(t)}$ is the average holding of each lotto investor, which can be calculated as $\mathbf{X}_L^{(t)} = \left(\frac{P_{IL}}{P_{IL}+P_{UL}}\right)\mathbf{X}_{IL}^{(t)} + \left(\frac{P_{UL}}{P_{IL}+P_{UL}}\right)\mathbf{X}_{UL}^{(t)}$. Therefore, $\tilde{M}_{222}^{(t)}$ is given by

$$\tilde{M}_{222}^{(t)} = \phi\left[\frac{1}{\tau}\mathbf{V}\mathbf{X}_L^{(t)} - (\mathbf{R}^{(t,n)} - r\mathbf{1})\right]_2 / {x_{L,2}^{(t)}}^2. \tag{1.13}$$

Our main focus is to study relationship between the RNS of Asset 2 at time 0, $\tilde{M}_{222}^{(0)}$, and the subsequent return of Asset 2 from time 0 to time 1, $R_2^{(0,1)}$ under different scenarios. To begin with, we study the special scenario where $\hat{M}_{222}^{0} = M_{222}$, i.e., uninformed investors know the true value of the idiosyncratic skewness of Asset 2 at time 0. In this case, uninformed lotto investors and informed lotto investors have the same demand for each risky asset in equilibrium and can be classified as the same type of investors, which is the "Lotto Investor" in Mitton and Vorkink (2007). Thus we expect a negative correlation between $\tilde{M}_{222}^{(0)}$ and $R_2^{(0,1)}$, as suggested by Mitton and Vorkink (2007). The asset returns and asset holdings of one investor of each type given different RNS values are shown in the Figure 1.1. We can see that as the RNS of Asset 2 increases, lotto investors have more demand for holding Asset 2 and the return of Asset 2 decreases.

The above relation between RNS and subsequent return of Asset 2 also holds when the change of RNS is purely driven by the change of skenwess estimate of uninformed lotto investors, while the true value of skewness is fixed. For example, let us set the true value of Asset 2's skewness to be 0.1, i.e., $M_{222} = 0.1$, and let uninformed lotto investors' skewness estimate $\hat{M}_{222}^{(0)}$ vary from -0.3 to 0.3. Then the corresponding asset returns and asset holdings of one investor of each type given different RNS values are shown in Figure 1.2. In this case, when RNS increases, the skewness estimate of uninformed lotto investors increases, so the demand for holding Asset 2 from uninformed lotto investors increases and Asset 2 tends to be overpriced. Therefore, the return of Asset 2 goes down. At the same time, the demand for holding Asset 2 from informed lotto investors and traditional investors decreases.

When the change of RNS is purely driven by the change of true value of skewness and the skewness estimate of uninformed lotto investors is fixed, the informed trading may play a dominant role and result in a positive relationship between RNS and stock return. For example, let us set the skewness estimate of uninformed lotto investors to be 0.1, i.e., $\hat{M}_{222}^{(0)} = 0.1$, and set the true value of skewness M_{222} to vary from -0.3 to 0.3, then the

corresponding asset returns and asset holdings of one investor of each type given different RNS values are shown in the Figure 1.3. In this case, when RNS increases, the true value of skewness increases, so the demand for holding Asset 2 from informed lotto investors increases and that from uninformed lotto investors and traditional investors decreases. When the buying demand from informed lotto investors becomes large enough, the RNS reflects the predictive information for the true skewness. Higher RNS suggests that true skewness should be higher, so there should be more demand for Asset 2 after uninformed lotto investors realize the true skewness of Asset 2 at time 1. Correspondingly its price goes up at time 1. Because of their superior information, informed lotto investors buy Asset 2 from other investors in advance (at time 0) and make profits when its price increases at time 1.

In reality, the change of RNS can be driven by the changes of both true skewness and uninformed lotto investors' skewness estimate. So its relation with future stock return can be either positive or negative, depending on how much effects the inside information has on trading in equilibrium, e.g., how much the proportion of informed traders is. To study this question, we let the proportion of informed lotto investors change and check the correlation between RNS and future stock return. And we generate RNS series by changing both true skewness value and uninformed lotto investors' skewness estimate. In particular, we generate $\hat{M}_{222}^{(0)}$ by the uniform distribution between -0.15 to 0.15 and M_{222} by the uniform distribution between -0.3 to 0.3. We keep the proportion of lotto investors to be 50%, but let the proportion of informed lotto investors over all lotto investors change from 0 to 100%. Given specific values of $\hat{M}_{222}^{(0)}$, M_{222} and the proportion of informed lotto investors, we compute the RNS at time 0 and return from time 0 to time 1 for Asset 2. Therefore, given a certain proportion of lotto investors, we can compute the correlation between RNS and Asset 2's subsequent return. The correlation against the proportion of informed lotto investors over all lotto investors is shown in the Figure 1.4.

Based on Figure 1.4, when there is a small proportion of informed lotto investors, the relation between RNS and subsequent asset return is negative. This is because given a small

number of informed lotto investors, RNS is predominately driven by the skewness estimate of uninformed lotto investors. Thus it mainly reflects the skewness estimate of uninformed investors as well as the their demand for holding Asset 2. In this case, informed traders successfully hide their inside information in asset prices. When the proportion increases to some threshold (16%), the correlation becomes positive and continues to increase when the proprotion increases. This results from the fact that as the number of informed lotto investors increases, RNS starts to reflect the informed traders' predictive information about Asset 2's skewness. The correlation reaches the peak when the proportion of informed traders arrives at a certain point (67%). After that if the number of informed traders continue to increase, the correlation decreases. The correlation becomes negative after the proportion exceeds 88%, because as most of lotto investors are informed lotto investors, their belief about Asset 2's skewness tends to become "public information" rather than "inside information", and skewness preference starts to dominate the relation between RNS and stock return again. When the proportion reaches 100%, all lotto investors are "informed investors" and the true skewness of Asset 2 becomes completely public. Thus there is no ground for informed trading, and the correlation drops to a very negative value, which is close to -1 in this example.

For simplicity, we do not formally bring options into this equilibrium model. If we extend the model by formally adding options at different moneyness, we can expect to obtain similar findings as options provide more vehicles for hedging or speculation and help to back out the implied skewness of stocks. Our empirical findings in the remaining part of this essay about the negative risk premium of the long-term RNS are consistent with the negative relation between RNS and future stock return when the proportion of informed investors is small as shown in Figure 1.4. Furthermore, our findings about the positive risk premium of short-term RNS in the remaining part of this essay are consistent with the positive relation between RNS and future stock return when informed traders are more prevalent, as shown in Figure 1.4. These empirical results are consistent with the

theoretical equilibrium, as we will demonstrate that short-term RNS contains more accurate firm-specific information than long-term RNS does.

1.3 Data and Variable Construction

We first describe the data and the methods used to compute risk-neutral skewness across different maturities, as well as other firm characteristics for each individual stock. Our sample is from January 1996 to December 2015.

1.3.1 Risk-Neutral Skewness

On the last trading day of each month, firm i's option-implied skewness for a given maturity is calculated using the model-free methodology of Bakshi et al. (2003). To compute the RNS τ periods ahead, we need to use the authors' method to compute the τ-period value of payoffs to the second, third, and fourth power of the underlying stock's risk neutral log returns. To implement this approach in practice, OTM call and put options with continuous strikes expiring in τ periods would be required. However, traded options are available only at irregular strikes and maturities, and thus option-implied risk-neutral skewness measures at a constant maturity are unlikely to be observed since option maturities decay daily but contracts are issued at weekly frequency at most. To deal with this data issue, studies using risk-neutral moments (see, e.g., Bakshi et al., 2003, Conrad et al., 2013, and Stilger et al., 2017) aggregate daily options data that falls in a window of time to maturity τ, computing RNS for a horizon equal to the mean of maturities within the group. For example, Stilger et al. (2017) use daily prices for all OTM options with τ between 10 and 180 days to calculate option-implied skewness with an average maturity across different stocks of 86.56 trading days. If more than one contract with different τs are available for options with a specific strike price, the authors choose the option with the smallest τ. We denote this method as "maturity bin" method.

One drawback of the "maturity bin" method is that options with different moneyness have different maturities within each bin, which cause the implied risk-neutral density with an average τ to actually contain information for horizons different from τ. For instance, suppose that the spot price is \$100, and of contracts falling in the τ bin from 10 to 180 days, the shortest available maturity for an OTM put option with strike price \$80 is 30 days, while that for OTM call option with strike price \$120 is 150 days. By using the "maturity bin" method, information impounded in the one-month put and five-month call options would be reflected in the option-implied risk-neutral density with an average τ close to 3 months. Since the main purpose of this paper is to explicitly investigate information differences across the term structure of RNS, this method prevents a clean decomposition by maturity.

To mitigate this issue, we instead use standardized option implied volatilities in the Volatility Surface file from OptionMetrics. The file contains the interpolated volatility surface for each security on each day, obtained using a kernel smoothing algorithm. The Volatility Surface file encompasses information on standardized call and put options with maturity of 30, 60, 91, 122, 152, 182, 273, 365, 547, and 730 calendar days, at deltas of 0.20, 0.25, 0.30, 0.35, ..., 0.75, and 0.80 (with similar but negative deltas for puts). A standardized option is included only if enough traded option prices are available on that date to accurately interpolate the required values. The traded options data is first organized by maturity and moneyness and then interpolated by a kernel smoother to generate an implied volatility value at each of the specified interpolation grid points. In addition to option price information such as implied volatility, option premium, and strikes, a measure of the accuracy of the implied volatility calculation, denoted as dispersion, is also provided for each security/maturity/moneyness combination. A larger dispersion indicates a less accurate interpolation.

We use all standardized OTM options maturing in 30, 91, 152, 273, and 365 days to calculate RNS for 1, 3, 6, 9, and 12 months respectively, denoted as RNS1M, RNS3M, RNS6M, RNS9M and RNS12M. The OTM call (put) options are options with deltas of

0.45 (-0.45), 0.40 (-0.40), 0.35 (-0.35), 0.30 (-0.30), 0.25 (-0.25), and 0.20 (-0.20). To optimally execute the tradeoff between excluding less accurate data while keeping the sample as large as possible, we filter out stocks of which at least one implied volatility for a moneyness/maturity combination has a dispersion measure that is larger than 0.2[2]. In unreported robustness checks, we have examined filtering rules with different dispersion thresholds and found that both stricter and looser rules produce results similar to those reported in the subsequent analysis. In addition, we only keep securities that have traded options with non-missing trading volume and non-zero open interests from the OptionMetrics price data file. Finally, we use the trapezoidal rule to compute the integrals to evaluate the quadratic, cubic, and quartic contracts following Bakshi et al. (2003).

Of the five resulting maturities, we define the 1-month and 12-month to be the short-term and long-term RNS, respectively. To integrate the different information contained in these two variables we also define the term spread of RNS (RNSTS) as the difference between the long-term and short-term RNS.

1.3.2 Other Firm Characteristics

To compute portfolio returns and stocks' idiosyncratic volatilities, we collect daily and monthly stock returns, market values and trading volumes from the Center for Research in Security Prices (CRSP). We calculate market value (MV) as the the closing share price times the number of shares outstanding. We obtain the annual book value of the firm from COMPUSTAT and then compute the book-to-market ratio (BM) as the the ratio between book value and market value. We also compute a series of control variables such as stock illiquidity (ILLIQ) proxied by Amihud's (2002) price impact ratio, stock return momentum (MOM) and reversal (REV).

---

[2]The mean (95% quantile) for the dispersions of implied volatility for 1, 3, 6, 9, and 12 months are 0.0320 (0.1250), 0.0196 (0.0706), 0.0162 (0.0556), 0.0138 (0.0486) and 0.0132 (0.0463) respectively.

To test the firm-specific information impounded into the RNS at different maturities, we construct two variables representing significant firm-specific events. One is the standardized earnings surprise variable (SUE), which is defined as the actual earnings minus analysts' forecast scaled by end-of-quarter price following Livnat and Mendenhall (2006). The other is the monthly price crash indicator (CRASH), which equals one for a firm-year that experiences one or more crash days during the month, and zero otherwise. A crash is defined as a 3-σ negative daily return relative to daily historical volatility based on Hutton et al. (2009), Kim et al. (2011a) and Kim et al. (2011b) and detailed in Appendix 1.A.

To control for option liquidity and price pressure issues, we also collect data on option volume and open interests from the option price file in IvyDB's OptionMetrics. To proxy for the hedging demand of options we construct three measures: the put-to-all option volume ratio (PAOV), the aggregate open interest ratio (AOI), and the Zmijewski (1984) Z-score, following Stilger et al. (2017). In addition, we use the maximum daily return over the last month (MAX) and expected idiosyncratic skewness (EIS) as proxies for stock overvaluation and lottery-like payoffs, and idiosyncratic volatility (IVOL) relative to the Fama and French (1993) model as a proxy for short-sale constraint. The construction of firm characteristics and option measures is detailed in Appendix 1.A.

1.3.3 Summary Statistics

Table 1.2 presents summary statistics for the RNS of different maturities, the term spread of RNS, option volume and open interests, as well as all firm-specific characteristics. We report the number of firm/month observations, means, medians, standard deviations as well as 5th and 95th percentiles across stocks during the sample period.

Carr and Wu (2003) and Foresi and Wu (2005) observe that the risk-neutral distribution of index returns becomes more negatively skewed as option maturity increases. We find this pattern also exists for individual stocks. Table 1.2 shows that the mean and median

of RNS become more negative with maturity. To the extent that the RNS reflects investor beliefs, this is consistent with expectations of higher probability of disaster or crash events in individual equities. One possible reason is that as the time horizon increases, risk-averse investors require larger compensation for bearing crash risk. Since the risk-neutral density is the product of the risk premium and physical density adjusted by risk-free rate, the long term risk-neutral density becomes more negative than short term risk-neutral density does. An alternative explanation is that the short-term density contains different information than the long-term.

Table 1.3 shows the correlation among our main variables. The lower triangular of the correlation matrix presents Pearson correlations between each pair, while the upper triangular of the correlation matrix reports the non-parametric Spearman correlation matrix. As maturity increases, the corresponding RNS has less correlation with 1-month RNS. For example, as maturity increases from 3 months to 12 months, the Pearson (Spearman) correlation between the corresponding skewness and RNS1M decreases from 0.50 (0.54) to 0.25 (0.30). This is consistent with a divergence between the information contents in the short-term and long-term risk-neutral skewness.

1.4 RNS Term Structure and Return Predictability

We demonstrate that the RNS of different maturities has differential predictive power for future returns of the underlying asset. We then consider how this difference in predictability matches the contradictory results in the empirical literature, advancing a potential way to reconcile the negative predictability consistent with skewness preference (Conrad et al., 2013; Bali and Murray, 2013) with the positive predictability consistent with informed trading (Xing et al., 2010) and hedging demand (Stilger et al., 2017).

We document the differential predictive power of short- vs long-term RNS using a portfolio sorting approach. Each month, we rank all sample firms in ascending order according

to their RNS estimates on the last trading day and assign them to quintile portfolios. This sorting procedure results in 5 equal-weighted portfolios per RNS measure. Since we have five observations in the RNS term structure, we obtain a total of 25 portfolios, with returns sampled at monthly frequency over the period February 1996 through December 2015. We fit common benchmark models to the portfolios to test for abnormal performance indicative of predictive power across the RNS term structure. The t-values in the estimations are computed using Newey-West standard errors with five lags to account for possible autocorrelation and conditional heteroscedasticity.

In Table 1.4, we present the results of abnormal portfolio returns relative to our benchmarks for equal-weighted portfolios across the RNS term structure. Panels A, B, C, D, and E report abnormal returns over the subsequent month of the portfolios sorted by 1-, 3-, 6-, 9-, and 12-month RNS, respectively. We use five standard asset pricing models as benchmarks: the Capital Asset Pricing Model (CAPM), the Fama and French 3-factor model (FF3) (Fama and French, 1992; Fama and French, 1993), the Fama and French 5-factor (FF5) model (Fama and French, 2015), the Carhart 4-factor model (Carhart, 1997), and the Fama and French 3-factor, Carhart momentum factor, and Pastor and Stambaugh (2003) liquidity factor (FFCP5) model.

Panel A of Table 1.4 reports the performance of portfolios sorted by 1-month RNS (RNS1M). Portfolio returns illustrate a strong positive relation between 1-month RNS and future stock returns over the subsequent month. A zero-cost trading strategy that longs the highest quintile and shorts the lowest quintile portfolio exhibits significant positive alphas relative to the CAPM, FF3, FF5, FFC4 and FFCP5 models at the 1% level. In particular, the zero-cost high-low strategy has significantly positive monthly alphas relative to all benchmark models ranging from 0.83% (9.96% annualized) relative to FF3 model to 0.95% (11.4% annualized) relative to FFCP5 model. In addition, as we move from the lowest to highest RNS1M quintile portfolio, we find that there is a monotonic increase in abnormal performance. These results provide preliminary evidence that RNS calculated using the

short-term 1-month standardized options has the same predictability as the skewness measure documented in Xing et al. (2010) and Stilger et al. (2017). The positive predictive power for future abnormal returns suggests that our 1-month RNS might contain informed option investors' speculative or hedging demand.

Panel B of Table 1.4 reports the performance of portfolios sorted by 3-month RNS (RNS3M). Portfolio returns have a weak positive relation between 3-month RNS and future stock returns over the subsequent month. While the zero-cost trading strategy that longs the highest quintile and shorts the lowest quintile portfolio exhibits positive and significant alphas for some models, it is insignificant for others. In addition, the scale of alphas is much lower than that of alphas produced by 1-month RNS. These results show that as option maturity increases, the positive relation between RNS and future stock returns becomes weaker.

Panel C of Table 1.4 reports the performance of portfolios sorted by 6-month RNS (RNS6M). Portfolio returns exhibit a weak relation between 6-month RNS and future stock returns over the subsequent month. The zero-cost hedging strategy results in insignificant alphas for all models except the FF3. Thus, as the option maturity increases to 6 months, the positive relation between RNS and future stock returns disappears.

A notable reversal occurs in Panel D of Table 1.4. Here we report the performance of portfolios sorted by 9-month RNS (RNS9M). Portfolio returns show a negative relation between 9-month RNS and future stock returns. The zero-cost strategy that longs the highest quintile and shorts the lowest quintile portfolio exhibits negative alphas, significant for all models except the FF5. These results show that as the term increases to 9 months, the relation between RNS and future stock returns becomes negative.

Finally, Panel E of Table 1.4 reports the performance of portfolios sorted by 12-month RNS (RNS12M). Portfolio returns illustrate a strong negative relation between 12-month RNS and future stock returns over the subsequent month. The zero-cost trading strategy

that longs the highest and shorts the lowest quintile portfolio exhibits significantly negative alphas for all benchmark models, ranging from -0.46% (-5.52% annualized) at the 5% significance level relative to the FF5 model to -0.86% (-10.32% annualized) at the 1% significance level relative to the FF3 model.

This significant negative predictability is a sharp reversal from the positive predictability at the short end of the term structure of RNS and the insignificant predictability at its middle. Its significance is a proof that these results are not driven by data quality issues potentially introduced by the illiquidity of long-term option contracts. If the data were simply becoming less reliable for high option maturities, we would expect to see a continuation of insignificant predictive power at the long end of the term structure. These results also provide preliminary evidence that RNS calculated from 12-month standardized options is consistent with skewness preference.

Taken together, we find that short-term RNS positively predicts future stock returns, which is consistent with the prior empirical findings on skewness proxying for informed trading (Xing et al., 2010) and hedging demand (Stilger et al., 2017), while long-term RNS predicts negative future stock returns which matches the empirical findings on skewness preference (Conrad et al., 2013; Bali and Murray, 2013). The variability of the results one gets depending on the maturity of options one uses points to a potential resolution of the contradiction between these two sets of empirical findings. One potential explanation for this phenomenon is that investors use short-term options to hedge or speculate based on their information advantage. We will investigate the validity of this explanation in Section 1.6.

1.5 The Term Spread of RNS

Section 1.4 documents the different predictive directions of long- and short-term RNS for future stock returns. To capture these different sources of information from both long-

and short-term RNS, we construct a new variable, the term spread of RNS (RNSTS), which is defined as 12-month RNS minus 1-month RNS. As shown in Table 1.3, RNSTS is positively related with RNS12M and negatively related with RNS1M by construction. Combining the negative predictive power of RNS12M and the opposite of the positive predictive power of RNS1M for future returns as shown in Section 1.4, RNSTS should borrow information from both ends of the term structure and serve as a significantly negative predictor of future returns. In this section, we use both portfolio sorting and cross-sectional regression methodologies to show that the term spread possesses much stronger predictive power for future equity returns than either the short-term or the long-term RNS in isolation.

1.5.1 Portfolio Sorts

In this subsection, we test the ability of the term spread of RNS (RNSTS) to integrate information from both ends of the RNS term structure using a portfolio sorting approach. Each month we rank all sample firms in ascending order according to their RNSTS measured on the last trading day, and assign them into RNSTS quintiles. We then employ this ranking to construct an equal-weighted portfolio for each quintile over the subsequent month, forming 5 portfolios with returns sampled at the monthly frequency over the period February 1996 through December 2015. We fit the CAPM, FF3, FF5, FFC4, and FFCP5 benchmarks and compute alpha t-values using Newey-West standard errors with five lags to control for possible autocorrelation and conditional heteroscedasticity in returns.

In Table 1.5, we present the equal-weighted portfolio performance of monthly quintile portfolio based on RNSTS, the long-short term spread on RNS. From the table, Portfolio returns illustrate a strong negative relation between the term spread and future portfolio returns over the subsequent month. The zero-cost trading strategy that longs the highest quintile and shorts the lowest quintile portfolio exhibits negative alphas relative to all five

models which are significant at the 1% level. The zero-cost strategy has significantly negative monthly alphas ranging from -1.07% (-12.84% annualized) relative to the FF5 model to -1.33% (-15.96% annualized) relative to the FF3 model. As we move from the lowest to highest RNSTM quintile portfolio, we find that there is a monotonic decrease in performance. These results support our conjecture that the term spread of RNS combines price-relevant information from the short- and long-term RNS resulting in improved negative predictability on future stock returns. Consistent with this, the scale of the abnormal returns produced by this new anomaly variable is greater than that of the 1-month RNS and 12-month RNS individually. Notably, they are also greater than most existing anomalies in the general asset pricing literature.

1.5.2 Fama-MacBeth Regression

Next, we conduct Fama and MacBeth (1973) cross-sectional regressions to confirm the return predictability of RNSTS, defined as the 1-month to 12-month term spread of RNS, while controlling for other confounding variables including market beta, firm size, book-to-market ratio, momentum, reversal, idiosyncratic volatility and illiquidity. We also control for characteristics of the underlying stock, its lagged price per share and return, as well as option liquidity characteristics, its volume and open interest. Table 1.6 reports the cross-sectional coefficients for monthly excess stock returns on lagged term spread of RNS and a set of firm characteristics during the period 1996-2015.

Model (1) regresses the cross-section of monthly returns only on the term spread of RNS, RNSTS. Consistent with prior results, the term spread has a cross-sectional coefficient of -0.0100 which is significant at the 1% level, confirming the previously observed negative predictability. To control for RNSTS incorporating the effects of other known predictive variables, model (2) controls for market beta, firm size, book-to-market ratio, momentum, reversal and the Amihud (2002) illiquidity measure. The magnitude of the

coefficient on the RNSTS term spread becomes smaller at -0.0071 but still remains significant at the 1% level. This result further confirms the unique information content of the term spread of RNS in predicting stock returns relative to known predictive variables.

Model (3) further controls for trading characteristics of the underlying, its lagged price per share, return and idiosyncratic volatility. Model (4) controls for option liquidity by including option volume and open interest over the past month. The magnitudes of the coefficients of the term spread RNSTS become somewhat smaller still at -0.0066, but remain highly significant at the 1% level.

To summarize, both the portfolio sorting and cross-sectional regression strategies demonstrate robust negative predictability of returns from the term spread of RNS. Furthermore, this predictive effect is much stronger than that of using only short- or long-term RNS, indicating that the divergent information in two RNS measures is integrated by the term spread. In the next section, we further examine the firm-specific information that drives these patterns.

1.6 The Information Content of the RNS Term Structure

Given the opposite directions of return predictability stemming from short- and long-term risk neutral skewness, we next consider how this predictability may come about. In this section we examine the relationship between these two RNS measures and firms' earning surprises, likelihood of price crashes, and investors hedging demand. These results, taken with those in Section 1.4 and Section 1.5, help to complete the explanation we advance for the difference in return predictability across the RNS term structure. Specifically, these results all point to it being caused by differences in information sets of customers that drive demand for options at different points of the maturity continuum, resulting in differential return predictability across the RNS term structure.

1.6.1 Earnings Surprises and the Term Structure of RNS

The predictability of stock returns from short-term RNS is consistent with the informed trading argument in Xing et al. (2010). We explore whether option traders' superior information about firm fundamentals becomes impounded into the short-term RNS and thereby causes the positive predictive relationship between short-term RNS and firm performance. To do this, we follow Xing et al. (2010) and conduct cross-sectional regressions to test whether short-term RNS is a reliable predictor of earnings surprises, since this is a common and frequent source of news about the firm.

We use standardized unexpected earnings (SUE) to measure earnings surprises. SUE is defined as actual earnings minus the most recent analysts' forecast all scaled by stock price following Livnat and Mendenhall (2006). Since the earnings data usually becomes available within the next quarter, at each month, we regress the cross-section of next quarter's SUEs on short-term RNS after controlling for long-term RNS and other variables. We then aggregate all firm-specific coefficients of each month following the Fama and MacBeth (1973) procedure and compute Newey-West standard errors with five lags.

Table 1.7 reports the cross-sectional coefficients for short-term RNS in explaining the cross-section of SUEs over the next quarter, controlling for long-term RNS and a set of firm characteristics, during the period 1996-2015. Model (1) regresses quarterly SUE on long- and short-term RNS without controls. Consistent with Xing et al. (2010), the short-term RNS has a positive cross-sectional coefficient of 0.0010 at the 5% significance level. To isolate the potential effects of other predictive variables, model (2) adds market beta, firm size, book-to-market ratio, momentum, reversal and the Amihud (2002) illiquidity measure as controls. The coefficient on short-term RNS remains the same in both magnitude and significance. Model (3) and Model (4) add stock and option trading characteristics respectively. For both models, the coefficients of the short-term of RNS remain unchanged and significant at 1% level. This positive predictive relationship suggests that option informed

traders with private information about an upcoming negative SUE hedge this downside risk (Stilger et al., 2017) or speculate (Xing et al., 2010) by buying short-term OTM puts or selling short-term OTM calls. This increases the slope of the implied volatility function, and therefore decreases the short-term RNS causing a positive relationship with SUEs.

In addition, Table 1.7 shows that coefficients of long-term RNS for all regression models are significantly negative, which suggests that negative long-term skewness predicts higher future SUEs. This predictability is similar in direction to that of future stock returns from long-term RNS, consistent with the skewness preference theory that implies a negative risk premium for positive skewness. The long-term RNS's similar predictabilities on both future stock returns and earnings surprises is consistent with comovement in these two quantities. In other words, it is evidence that the negative risk premium theorized by skewness preference is driven by firm fundamentals.

1.6.2 Future Price Crashes and the Term Structure of RNS

We next examine the different information sets in long- and short-term RNS by considering their ability to predict the probability of a price crash. To do this we construct a monthly price crash dummy for each firm, an indicator variable that equals one for a firm-month that contains one or more crash days, and zero otherwise. Following Hutton et al. (2009), Kim et al. (2011a) and Kim et al. (2011b), we define crash days as those in which the firm experiences daily returns that are 3.09 (0.1% for normal distribution) standard deviations below the mean daily return over the prior year.[3]

We again use the cross-sectional regression approach by first conducting a monthly logistic regression of the future monthly price crash dummy on current short- and long-term RNS, controlling for a set of firm characteristics. We then aggregate coefficients across all months and compute the Newey-West standard errors with five lags for each coefficient.

[3] See Appendix 1.A for details.

In Table 1.8, Column (1) reports the cross-sectional coefficients for the next month's price crash indicator on current month short- and long-term RNS.

Consistent with prior results, the coefficient of short-term RNS is significantly negative at the 1% level. This suggests that expectations of more negative news by informed traders impounded in a more negative short-term RNS predicts that future price crashes happen with greater probability. In addition, the coefficient of long-term RNS is significantly positive at the 1% level. This is consistent with skewness preference, according to which investors require lower return for holding stocks with higher skewness. Given the mechanical relationship of lower returns with higher probability of price crashes, the positive relation between long-term RNS and future price crashes is as expected.

To examine how long these predictabilities on price crash will hold, we perform the Fama and MacBeth (1973) cross-sectional regression of price crash indicator variables two through six months ahead on short- and long-term RNS in the current month in Columns (2) through (6) respectively. Among all these regressions, the coefficients of short-term RNS remain significantly negative, indicating that the predictive power of short-term RNS for avoiding price crashes persists for at least 6 months. The coefficients on long-term RNS become insignificant, suggesting that the skewness preference effect of low expected returns only persists for one month.

These results are consistent with Bates (1996), confirming the relation between short-term RNS and jump processes. As emphasized by Cont and Tankov (2003) (Ch. 15.6), strong skewness and smiles at short maturities can be generated by jump processes. We next turn to the information content of long-term RNS regarding the underlying return processes.

1.6.3 Hedging Demand and the Term Structure of RNS

The prior results demonstrate that short-term RNS contains unique information about future firms' stock and fundamental performance, which suggests that informed traders express their beliefs about underlying stocks primarily in the short-term option market. In this section, following Stilger et al. (2017), we provide direct evidence that investors' hedging demand for short-term options is reflected in the short-term RNS. This isolates hedging demand as one of the drivers of the positive predictability of stock returns from short-term RNS.

Following Bollen and Whaley (2004) and Garleanu et al. (2009), Stilger et al. (2017) conjecture a mechanism by which hedging demand for options results in the positive relationship between their RNS estimate and future stock returns. They provide some tests for the validity of this channel, the first of which is to consider whether stocks characterized by higher hedging demand exhibit a more negative RNS value. The intuition is that higher hedging demand for downside risk pushes up the price of the OTM put option (Garleanu et al., 2009), which results in a more negatively skewed risk-neutral density. The second test is whether the underperformance of the portfolio with the lowest RNS stocks is driven by stocks that are relatively overpriced, which would be another driver of hedging or speculative demand. The third test is whether the the underperformance of the portfolio with the lowest RNS stocks is driven by stocks that are too hard to sell short, also driving demand for options as an alternative to shorting. In this section, we conduct these tests for both short- and long-term RNS measure.

Table 1.9 tests whether stocks characterized by higher hedging demand exhibit more negative RNS values. Following Stilger et al. (2017), three measures are used as hedging demand proxies: the ratio between aggregate put option volume and total option volume (PAOV) (Taylor et al., 2009), the aggregate open interest across all options (AOI) (Hong and Yogo, 2012), and the Z-score of Zmijewski (1984) (ZD) capturing default risk. In

order to match the 1-month maturity of short-term RNS, only options with maturity from 10 to 45 days are used to calculate the PAOV and AOI. Analogously, in order to match the 12-month maturity of long-term RNS only options with maturity from 319 to 456 days are used to calculate these two measures. Panel A of Table 1.9 reports the time-series average of 1-month RNS for quintile portfolios sorted by investor hedging demand. As each of the three hedging demand measures increases, short-term RNS decreases monotonically.

Panel B of Table 1.9 reports the time-series average of the 12-month RNS for quintile portfolios sorted by investor hedging demand. As each of the three hedging demand measures increases, both short- and long-term RNS decrease monotonically. This pattern is statistically significant, as the average short- and long-term RNS in highest hedging demand quintile is lower than that in lowest quintile at the 1% significance level. This confirms that options with higher hedging demand have more negative RNS values as suggested by Stilger et al. (2017).

Panel A-1 of Table 1.10 tests whether the underperformance of stocks with the lowest 1-month RNS (RNS1M) is driven by relative overpricing. It reports the performance of double sorted portfolios by 1-month RNS and proxies for overvaluation for the sample period from 1996 to 2015. We use the maximum daily stock returns over the previous month (MAX) (Bali et al., 2011) and the expected idiosyncratic skewness (EIS) (Boyer et al., 2010) as the overvaluation proxies. At the end of each month, we sort all stocks into tercile portfolios in ascending order by RNS1M. Within each RNS1M tercile portfolio, we create another set of tercile portfolios in ascending order based on the overvaluation proxy. We find that among three portfolios of stocks with the lowest 1-month RNS, the portfolios with highest MAX (EIS) underperform the portfolio with lowest MAX (EIS) by 1.0012 (0.9030)% per month at the 1% significance level. The underperformance of the portfolio with the lowest 1-month RNS stocks is driven by the stocks exhibiting the highest degree of overpricing.

Panel A-2 of Table 1.10 tests whether short-sale constraints drive the underperformance of the low 1-month RNS stocks. It reports the performance of double sorted portfolios by 1-month RNS and a proxy for short-selling constraint for the sample period from 1996 to 2015. The short-selling constraint is proxied by idiosyncratic volatility (IVOL) following Wurgler and Zhuravskaya (2002). At the end of each month, we sort stocks into tercile portfolios in ascending order by RNS1M. Within each RNS1M tercile portfolio, we further sort the constituents into tercile portfolios in ascending order based on the short-selling constraint. We find that among three portfolios of stocks with the lowest 1-month RNS, the portfolio with highest short-selling constraint underperforms the portfolio with lowest maximum return by 0.9498% per month at the 1% significance level. This indicates the underperformance of the portfolio with the lowest 1-month RNS stocks is also driven by stocks that are hard to short.

The results of these three tests in panel A of Table 1.9 and panel A of Table 1.10 show that hedging demand and short-sale constraint drive the return predictability of short-term RNS. Combined with the findings in previous two subsections, we have established evidence that short-term RNS contains both predictive information about the performance of the firm, and is positively related to hedging demand. This supports the conclusion that informed traders use short-term options to hedge downside risks or speculate on underlying stocks that are relatively overpriced and hard to short.

Although the long-term RNS decreases with measures of hedging demand in Panel B of Table 1.9, its behavior is inconsistent with hedging demand as shown in Panel B of Table 1.10. The hedging demand interpretation implies a positive relation between RNS and future stock return, inconsistent with the negative relation observed for long-term RNS. To further investigate the relation between long-term RNS and overvaluation as well as short-sale constraint, Panel B-1 of the Table 1.10 reports the performance of double sorted portfolios by 12-month RNS and overvaluation proxies (MAX and EIS), while Panel B-2 reports that for double sorts by 12-month RNS and short-selling constraint (IVOL). We find

the underperformance of the highest long-term RNS portfolio is mainly caused by stocks that are overpriced and hard to short. For example, within the tercile portfolios with highest MAX, EIS, and IVOL, the highest 12-month RNS tercile portfolio underperforms the lowest 12-month RNS tercile portfolio by 1.0015%, 0.7335%, and 0.9257%, respectively.

These results indicate that investors rarely use long-term options to hedge risk, which is consistent with long-term options being inappropriate hedging or speculative instruments if overpricing is corrected in the short term (Bali et al., 2011). Another possible reason for hedgers' reluctance in using long-term options is that long-term options have lower delta than short-term options do, which make them provide less downside protection to hedgers and less exposure to the underlying for speculators. Finally, investors face more trading costs when hedging through long-term options, which are usually less liquid than the their short-term counterparts.

1.6.4 Skewness Preference and Informed Trading

Under the assumption of common information across the stock and option markets and the consequent absence of informed speculators and hedgers, both the short-term and long-term RNS would reflect the equity market participants' expected risk-neutral skewness for the stock. The RNS across all maturities would thus bear the negative risk premium implied by skewness preference. The significance of hedging demand and short-sale constraint proxies in the short-term RNS portfolio performance is consistent with the activities of informed hedgers and speculators. The positive relationship between short-term RNS and future returns suggests that their participation in the short-term option market impounds new material information in the short-term RNS resulting in different information sets and risk premia across the RNS term structure.

The results in Panel E of Table 1.4, Table 1.7 and Table 1.8 all suggest that long-term RNS carries a negative risk premium, consistent with skewness preference. This provides

indirect evidence that long-term RNS is a good proxy of the underlying stocks' expected skewness. Panel B-1 of Table 1.10 provides additional evidence. The maximum daily return over the previous month (MAX) and expected idiosyncratic skewness (EIS) can also be interpreted as two physical skewness measures which proxy for lottery-like payoffs and bear negative risk premium implied by skewness preference theory. Panel B-1 of Table 1.10 shows these two measures are negatively priced in the cross-section of stock returns, consistent with Bali et al. (2011) and Boyer et al. (2010). These results also show that the underperformance of the highest physical skewness portfolio, whether in terms of MAX or EIS, is concentrated in stocks with the highest long-term RNS.

For example, in the tercile portfolios with the highest MAX and EIS, the highest 12-month RNS portfolio underperforms the lowest 12-month RNS portfolio by 1.0015% and 0.7335%, respectively. The double-sorted highest MAX (EIS) and highest long-term RNS portfolio underperform the double-sorted lowest MAX (EIS) and lowest long-term RNS portfolio by 1.301% (0.9487%) per month. The performance of double-sorted portfolios shows that the physical skewness measure and long-term risk-neutral skewness measure not only have the same function in pricing stock returns, but also complement each other. By combining both long-term risk-neutral and physical skewness measures, we construct the portfolio that carries the most negative risk premium consistent with skewness preference for its lottery-like payoffs.

To further demonstrate the relation between the term structure of RNS and the physical skewness measure, Panels A and B of Table 1.11 show the average MAX and EIS of quintile portfolios sorted by short-term and long-term RNS. These two panels show both long- and short-term RNS have positive relation with physical skewness measure; however, sorts on long-term RNS produce a greater variation in physical skewness. For example, the quintile portfolio with the highest 12-month RNS has 0.0485 (t-statistic=33.12) higher average MAX and 0.5810 (t-statistic=13.78) higher average EIS than the quintile portfolio with the lowest 12-month RNS, while the corresponding MAX and EIS spreads for 1-month RNS

are only 0.0099 and 0.2225 with lower t-statistics. This is consistent with the patten observed in Table 1.3: as the maturity increases, the Pearson correlation between RNS and MAX (EIS) increases from 0.05 (0.14) to 0.28 (0.35). These results are consistent with the interpretation of long-term RNS as the more accurate representation of the underlying stocks' expected skewness. This difference between short-term and long-term RNS underscores the importance of stochastic volatility and volatility asymmetries in underlying return processes necessary to represent a term structure of the volatility surface and long-term skewness (Bates, 1996; Barndorff-Nielsen, 1997; Barndorff-Nielsen and Shephard, 2001; Carr et al., 2003; Nicolato and Venardos, 2003).

1.7 The Factor Structure of the RNS Term Structure

The difference in predictive coefficients between short-term and long-term RNS for the cross-section of returns observed in the preceding analysis implies that the term structure of RNS itself contains information about the future distribution of the underlying asset. To map this information content more formally, we conduct a factor analysis on the RNS term structure to reduce its dimensionality and to identify the number of distinct informative signals it contains. In doing so, we rely on prior insights from the interest rate term structure literature.

1.7.1 The RNS Slope Factor and the Cross-section of Returns

Significant works in this literature, such as Nelson and Siegel (1987), Litterman and Scheinkman (1991) and Christensen et al. (2011), find that yield curves are usually explained by the level, slope, and curvature factors. In the same spirit, we perform a factor analysis on RNS measures across five fixed maturities at the 1, 3, 6, 9, and 12-month horizons of all firm-month observations to check whether a similar factor structure exists.

We present the loadings of three extracted factors on five RNS measures in Figure 1.5.

The first factor can be explained as the level factor of the RNS term structure, as it loads positively on RNS of all terms. That is, an increase in the first factor tends to push up the level of RNS of all maturities, though it affects the long-term RNS more. The second factor has a positive loading on long-term RNS and a negative loading on short-term RNS, thus it can be treated as the slope factor, which has a similar meaning to the term spread of RNS. The increase of this slope factor tends to push up the long-term RNS and push down the short-term RNS, creating the term spread of RNS identified earlier. The third factor indicates the curvature of the RNS term structure because its loading on RNS is positive only when the horizon of RNS reaches 6 month. The increase of third factor tends to push up the middle-term RNS. We observe that the first two factors capture a total of 79.19% of the variation of the RNS term structure, explaining 68.16% and 11.03% of it respectively. The third factor explains only 1.71% of the variation in RNS term structure, indicating it is unlikely to be meaningful.

We next explore how prior-month values of the RNS term structure factors affect the current month's cross-sectional excess underlying returns, summarizing the outcome in Table 1.12. We consider several specifications, each with additional levels of controls. Model (1) considers the explanatory power of the factors in isolation. Model (2) controls for firms' beta (BETA), market value (MV), book-to-market ratio (BM), momentum (MOM), one-month reversal (REV),stock illiquidity proxied by Amihud (2002) price impact ratio (ILLIQ). Model (3) additionally controls for lagged stock's return (RET), price per share (PRICE), and idiosyncratic volatility (IVOL). Model (4) additionally controls for option trading volume (OPVOL) and open interest (OPEN).

Consistent with prior results, we find that the values of the level and slope factors from the preceding month have opposite and significant coefficients in the cross-section of excess returns at the 10% and 1% levels respectively. This explanatory power is robust to the inclusion of size, value, systematic risk, liquidity, momentum, and reversal controls defined above. The level factor has positive loadings on short-term RNS and long-term

RNS, which have opposite pricing effects. The positive coefficient of the level factor on future stock returns, significant at the 10% level, suggests that the short-term RNS's positive effect weakly dominates the long-term RNS's negative effect. The negative cross-sectional coefficient of the slope factor, significant at the 1% level, further confirms the similarity between itself and the term spread of RNS. The curvature factor does not appear to be priced in the cross-section of excess returns, which is consistent with its insignificant contribution in explaining the variability of the RNS term structure and the negligible effect of middle-term RNS on future equity returns. Among the three factors, the slope factor exhibits the most significant predictive power on the cross-section of stock returns, indicating that the slope factor captures the majority of the price information in the RNS term structure. This analysis further confirms the importance of the term spread measure of RNS in explaining the cross-section of equity returns.

1.7.2 An Economic State Variable Interpretation of the RNS Slope Factor

The results in Table 1.12 above suggest that the RNS term structure slope factor contains information about future stock returns similar to the RNS term spread. In this section we establish the economic foundation for this factor using a vector autoregression (VAR) analysis of macroeconomic state variables following the approach of Petkova (2006). We include macroeconomic state variables that have a relation to the equity premium as described in Welch and Goyal (2008).[4] The VAR model uses monthly values of the equal-weighted average of SLOPE,[5] the RNS term structure slope factor across all optionable stocks, MKTRP, the market risk premium as the S&P 500 return net of the risk-free rate, EP, the log ratio of trailing 12-month S&P 500 earnings to current S&P price, TERM,

[4]We are grateful to Amit Goyal for providing these data on his website at http://www.hec.unil.ch/agoyal/.

[5]Substituting a value-weighted version of SLOPE in the analysis produces similar results, which we omit for brevity.

the term spread as the yield difference between long-term Treasury bonds and short-term bills, and DEF, the default spread as the yield difference between BAA and AAA-related corporate bond yields. We present the output of the VAR model in Table 1.13.

We observe that SLOPE is negatively related to last month's MKTRP with a coefficient of -0.0503, and positively related to the last month's TERM and DEF spreads with coefficients of 0.1845 and 1.1063, all significant at the 1% level. It is furthermore weakly related to last month's EP ratio with a coefficient of 0.0037 significant at the 10% level, and autocorrelated with a coefficient of 0.5653, statistically significant at the 1% level. Last month's SLOPE is also a predictor of both TERM and DEF spreads with coefficients of 0.0494 and 0.0173, both significant at the 1% level. These results suggest that the SLOPE factor only reacts to last month's market returns, but both predicts and is predicted by last month's bond term and default spreads.

To understand the economic magnitude, we estimate the implied risk premium for the SLOPE factor. Based on the time series of monthly SLOPE, the standard deviation is 0.0187. According to Model (4) in Table 1.12, the coefficient of the SLOPE factor in predicting next month return is -0.0742. Therefore, the estimated risk premium for a one standard deviation in SLOPE is -1.67% per year ($= -0.0742 \times 0.0187 \times 12$).

Furthermore, we can estimate the impact of each economic factor on the SLOPE risk premium based on Table 1.13. In particular, one standard deviation's increase of MKTRP (0.0426) results in a change of -0.0021 (-0.0503×0.0426) in SLOPE. From Model (4) in Table 1.12, the estimated risk premium for a one standard deviation in the MKTRP factor is 0.19% ($-0.0021 \times (-0.0742) \times 12$). Similarly, we estimate the risk premiums caused by a one standard deviation in the TERM and DEF factors to be -0.21% and -0.42% per year, respectively.

To better understand which components of the SLOPE factor drive its relation with the Welch and Goyal (2008) state variables, we also estimate VAR models with equal-weighted

RNS at each of our five constant maturities in Tables 1.14 through 1.18. Since the SLOPE factor is a linear combination of RNS at these maturities, this allows us to see which part of the term structure of RNS drives the factor's sensitivity to macroeconomic state variables.

The results in these tables show that the one-month (12-month) RNS is positively (negatively) related to last month's MKTRP at the 5% statistical significance level, suggesting that short-term option investors bet on continuation of trends whereas long-term ones bet on reversals. Last month's values of TERM have a relation to current short-term 1-month and 3-month RNS, with positive coefficients with statistical significance at the 5% level. This is consistent with informed traders in the short-term market taking bullish positions due to a positive signal about future economic growth. In contrast, only long-term 6-, 9-, and 12-month RNS have a relation to future TERM spreads with positive coefficients significant at the 1% level. Consistent with skewness preference theory, positive skewness expectations imply a high demand for stocks. This shift away from long-term bonds to stocks leads to an increase in the long-term bond yield and subsequently a high TERM yield spread. Furthermore, only the one-month RNS component of SLOPE is significantly related to the DEF spread. A high credit risk environment appears to lead short-term option investors to form a bearish market expectation, as indicated by the negative coefficient of DEF in predicting 1-month RNS at the 1% significance level. On the other hand, one-month RNS can negatively predict the DEF spread at the 5% significance level, consistent with previous evidence that short-term option traders may have superior information about the future.

These results suggest that the SLOPE factor of the RNS term structure, and therefore the RNS term spread itself, have a statistically significant relation to macroeconomic state variables that provides intuition for its ability to explain cross-sectional and time-series equity returns.

1.8 Conclusion

This paper contributes to the ongoing debate in the skewness pricing literature about the direction of the relationship between individual stock risk-neutral skewness (RNS) and future underlying asset returns. Specifically, we identify differences in the information content across the term structure of RNS.

Using a large sample of stock and options data from 1996 to 2015, we document positive predictability of future stock returns from short-term RNS, which is consistent with the informed trading and hedging demand literature (Xing et al., 2010; Stilger et al., 2017; Bollen and Whaley, 2004; Garleanu et al., 2009), and negative predictability from long-term RNS, which supports the skewness preference theory (Brunnermeier et al., 2007; Mitton and Vorkink, 2007; Barberis and Huang, 2008; Bali and Murray, 2013; Conrad et al., 2013).

Using this information we create a new return predictor, the term spread of RNS, which is defined as the long-term RNS minus short-term RNS. This predictor is constructed to capture information sets at both ends of the RNS term structure. The quintile portfolio with the highest RNS term spread underperforms the quintile portfolio with the lowest spread by 19.32% per year after controlling for common risk factors. The magnitude and robustness of this anomalous return suggests that the RNS term spread serves its designed purpose of integrating information distributed across the RNS term structure.

We further test the information differences across the RNS term structure by providing evidence that the short-term RNS is a positive predictor of future firms' earnings surprise and a negative predictor of future stock price crashes. The long-term RNS reverses the direction of predictability.

Additionally, we find that the positive predictability of equity returns from the short-term RNS is strongest for stocks that have high hedging or speculative demand from informed option traders consistent with Stilger et al. (2017). This evidence suggests that these

informed market participants mainly trade short-term options, which produces the different (similar) information sets between the short-term (long-term) skewness expectations in the option and equity markets. As a result, the short-term RNS impounds more informed trades and thereby positively predicts stock returns, while the long-term RNS carries the negative risk premium associated with the more accurate measure of expected underlying asset skewness as implied by skewness preference.

To provide more direct evidence that long-term RNS proxies for the underlying stocks' expected skewness, we compare it with two well-known physical skewness measures bearing negative risk premia. We find that the long-term RNS measure has a strong positive correlation with these two measures. In addition, both physical and long-term RNS measures complement each other in identifying stocks with the most negative risk premium for lottery-like payoffs.

A factor analysis of the RNS term structure, inspired by prior work in the factor structure of bond yields curves by Nelson and Siegel (1987), Litterman and Scheinkman (1991) and Christensen et al. (2011), confirms the existence of two distinct informational components priced in the cross-section of excess returns. We find a level factor that is priced positively consistent with our findings for the short-term RNS, and a slope factor that is priced negatively consistent with our findings for the RNS term spread. We find that the RNS term structure slope factor, which is most significantly related to both cross-sectional and time-series stock returns, is significantly related to macroeconomic state variables for the equity premium.

Our finding of the maturity-varying directionality of return predictability from RNS helps resolve the ongoing debate between two strands of the skewness pricing literature: one documenting the positive relationship between risk-neutral skewness and future stock returns following the informed trading and hedging literature, and the other documenting a negative relationship following the skewness preference theory. Our results confirm the

validity of both hypotheses, with the RNS from short-term options producing a positive relationship with future returns consistent with superior information, and the RNS from long-term options producing a negative one consistent with skewness preference.

Appendix

1.A Definitions of Variables

The definitions of the variables are detailed as follows. The corresponding summary statistics are presented in Table 1.2.

- BKM1M: Risk-neutral (option-implied) skewness with 1 month to expiration. With standardized OTM options maturing in 30 days of firm i on the last day of month t, BKM1M is estimated using the model-free methodology of Bakshi et al. (2003) and the trapezoidal rule (see section III.A in Bali and Murray, 2013).

- BKM3M: Risk-neutral (option-implied) skewness with 3 month to expiration. With standardized OTM options maturing in 91 days of firm i on the last day of month t, BKM3M is estimated using the model-free methodology of Bakshi et al. (2003) and the trapezoidal rule (see section III.A in Bali and Murray, 2013).

- BKM6M: Risk-neutral (option-implied) skewness with 6 month to expiration. With standardized OTM options maturing in 152 days of firm i on the last day of month t, BKM6M is estimated using the model-free methodology of Bakshi et al. (2003) and the trapezoidal rule (see section III.A in Bali and Murray, 2013).

- BKM9M: Risk-neutral (option-implied) skewness with 9 month to expiration. With standardized OTM options maturing in 273 days of firm i on the last day of month t, BKM9M is estimated using the model-free methodology of Bakshi et al. (2003) and the trapezoidal rule (see section III.A in Bali and Murray, 2013).

- BKM12M: Risk-neutral (option-implied) skewness with 12 month to expiration. With standardized OTM options maturing in 365 days of firm i on the last day of month t, BKM12M is estimated using the model-free methodology of Bakshi et al. (2003) and the trapezoidal rule (see section III.A in Bali and Murray, 2013).

- BKMTS: The term spread of risk-neutral skewness, which is defined as the difference between long-term skewness (BKM12M) and short-term skewness (BKM1M).

- BETA: The coefficient on market risk premium from the regression of excess monthly stock returns on market risk premium over last 60 months.

- MV: The market cap. The market cap is computed as the closing share price times the number of shares outstanding (in thousands).

- BM: The book to market ratio. Here the annual book value of the latest available is employed.

- MOM: Momentum for firm i is calculated as its cumulative stock return from the end of month $t-12$ to the end of month $t-1$.

- REV: Reversal for firm i is calculated as its stock return from the end of month $t-1$ to the end of month t.

- IVOL: Idiosyncratic volatility is defined as the standard deviation of residuals of daily firm-level residuals of the Fama and French (1993) three-factor model regression over the past 60 months.

- SUE: The standardized earnings surprise variable, SUE, is defined actual earning minus analysts' forecast, scaled by stock price, based on Livnat and Mendenhall (2006).

- CRASH: The monthly price crash measure is defined as the indicator variable that equals one for a firm-year that experience one or more crash days during the month,

and zero otherwise. Based on Hutton et al. (2009), Kim et al. (2011a) and Kim et al. (2011b), crash days in a given month are days in which the firm experiences firm-specific daily returns 3.09 (0.1% for normal distribution) standard deviation below the mean firm-specific daily returns over the entire year. Here the firm-specific daily return is defined as the natural log of one plus the residual return from the regression, $r_{i,t} = a_i + b_{1i}r_{m,t-2} + b_{2i}r_{m,t-1} + b_{3i}r_{m,t} + b_{4i}r_{m,t+1} + b_{5i}r_{m,t+2} + \varepsilon_{i,t}$, where $r_{i,t}$ is the return on stock i on day t and $r_{m,t}$ is the return on the CRSP value-weighted market index on day t.

- MAX: The maximum of daily returns for firm i during the month t.

- OPVOL: The total volumes of traded options for the underlying firm i on the last trading day of month t.

- OPEN: The total open interests of traded options for the underlying firm i on the last trading day of month t.

- PAOV: The put-to-all option volume ratio on a given trading day is the ratio of the total volume across all put options for a given maturity divided by the total volume across all options for a given maturity. We use 1-month PAOV to proxy hedging demand for short-term options. And traded options with maturity from 10 to 45 days are used to compute 1-month PAOV. We use 12-month PAOV to proxy hedging demand for long-term options. And traded options with maturity from 319 to 456 days are used to compute 12-month PAOV.

- EIS: Expected idiosyncratic skewness for firm i in the end of the month t is the forecast of expected idiosyncratic skewness observed at the end of month t for the distribution of daily returns over months $t + 1$ through $t + 60$, calculated using the same method in Boyer, Mitton, and Vorkink (2010). We first compute idiosyncratic skewness, ISKEW, for each firm-month observation by calculating the skewness of

residuals of daily firm-level residuals of the Fama and French (1993) three-factor model regression over the past 60 months. The variable $\text{ISKEW}_{i,t}$ is set to be missing at the end of month t if the number of observable returns is less than 250. We then estimate cross-sectional regressions separately at the end of each month t in our sample, $\text{ISKEW}_{i,t} = \beta_0^t + \beta_1^t \text{ISKEW}_{i,t-60} + \beta_1^t \text{IVOL}_{i,t-60} + \gamma^t X_{i,t-60} + \varepsilon_{i,t}$, where $X_{i,t-60}$ is a vector of additional firm-specific variables observable at the end of month $t-60$. These variables include the momentum from the end of month $t-60-12$ through the end of month $t-60-1$, the sum of daily turnover for firm i over the month $t-60-12$, dummy variable indicating firm i in the bottom tercile ranked by size at the end of month $t-60$, dummy variable indicating firm i in the middle tercile ranked by size at the end of month $t-60$, and dummies for 16 of the 17 industries defined by Ken French to create the "17 Industry Portfolios" on his website. We then use the regression parameters from the above regression, along with information observable at the end of each month t, to estimate expected idiosyncratic skewness for firm i, $E_t[\text{ISKEW}_{i,t+60}] = \beta_0^t + \beta_1^t \text{ISKEW}_{i,t} + \beta_1^t \text{IVOL}_{i,t} + \gamma^t X_{i,t}$.

- AOI: The aggregate open interest ratio of firm i on a given trading day is the ratio of the sum of open interests across all firm i's options for a given maturity divided by the sum of open interest across all firms with the same maturity on that day. We use 1-month AOI to proxy hedging demand for short-term options. And traded options with maturity from 10 to 45 days are used to compute 1-month AOI. We use 12-month AOI to proxy hedging demand for long-term options. And traded options with maturity from 319 to 456 days are used to compute 12-month AOI.

- ZD: Zmijewski (1984) Z-score, which measures the default risk of firm i, is computed as $Z = -4.3 - 4.5 \frac{\text{Net Income}}{\text{Total Asset}} + 5.7 \frac{\text{Total Debt}}{\text{Total Asset}} - 0.004 \frac{\text{Current Asset}}{\text{Current Liability}}$. ZD is used as one proxy of hedging demand for short-term options.

Table 1.1: Model Parameter Values

This table shows the parameters we use to solve the numerical solutions of our theoretical equilibrium model. Among them, we use the same parameters of the risk-aversion and skewness preference parameters (τ, ϕ) and the covariance matrix $(\mathbf{V})$ elements as in Mitton and Vorkink (2007).

Parameter	Variable	Value
Risk-aversion coefficient	τ	2.50
Skewness-preference coefficient	ϕ	2.50
Variance of Asset 1 returns	σ_1^2	0.20
Variance of Asset 2 returns	σ_2^2	0.35
Variance of Asset 3 returns	σ_3^2	0.25
Correlation coefficient, Assets 1 and 2	$\rho_{1,2}$	0.08
Correlation coefficient, Assets 1 and 3	$\rho_{1,3}$	0.15
Correlation coefficient, Assets 2 and 3	$\rho_{2,3}$	0.10
Number of periods	n	10
Total number of investors	N	300
Total investment on each asset at time 0	D	100
The proportion of traditional investors	P_T	1/2
The default proportion of informed lotto investors	P_{IL}	1/4
The default proportion of uninformed lotto investors	P_{UL}	1/4

Table 1.2: Descriptive Statistics

This table provides the descriptive statistics of risk-neutral skewness with different maturities, the term spread of risk-neutral skewness, as well as of the firm-specific variables that are used in subsequent analysis. The sample consists of 358,974 firm-month combinations based on the information in OptionMetrics, Compustat and CRSP from Jan 1996 through December 2015. The definitions for these variables are introduced in Appendix 1.A.

Variables	N	P5	P50	P95	Mean	STD
RNS_1M	358,974	-0.7279	-0.3357	0.1951	-0.3119	0.2784
RNS_3M	358,974	-0.7796	-0.4461	-0.1381	-0.4512	0.1915
RNS_6M	358,974	-0.8905	-0.4955	-0.2443	-0.5232	0.1937
RNS_9M	358,974	-1.0040	-0.5210	-0.2380	-0.5599	0.2299
RNS_12M	358,974	-1.1137	-0.5381	-0.2064	-0.5878	0.2720
RNS_TS	358,974	-0.9063	-0.2269	0.2339	-0.2759	0.3475
BETA	288,446	0.2611	1.1412	2.6880	1.2614	0.7190
MV	358,974	164,348	1,342,039	26,650,990	6,908,144	14,789,417
BM	284,960	0.0718	0.3737	1.2991	0.5041	0.4020
MOM	349,259	-0.5031	0.0949	1.1231	0.1858	0.5019
REV	284,748	-0.6250	0.4621	4.5214	1.0741	1.8103
IVOL	358,818	0.0119	0.0258	0.0518	0.0282	0.0121
SUE	106,045	-0.0070	0.0005	0.0078	0.0001	0.0057
CRASH	354,986	0.0000	0.0000	1.0000	0.1004	0.3005
MAX	358,843	0.0171	0.0467	0.1389	0.0589	0.0387
EIS	270,289	-0.3331	0.2803	1.2306	0.3363	0.4610
OPVOL	358,974	0	66	7,026	1,738	3,975
OPEN	358,974	126	3,740	173,143	39,759	87,253
ZD	282,978	-3.9591	-1.6712	0.7976	-1.6251	1.4717

Table 1.3: In-Sample Cross-Sectional Correlations

This table reports the time-series average of cross-sectional correlation coefficients between risk-neutral skewness for different maturities, the term spread of risk-neutral skewness, and some selected firm-specific variables that are used in my analysis. The lower triangular matrix presents the Pearson correlation matrix; the upper triangular matrix presents the non-parametric Spearman correlation matrix. The sample consists of 358,974 firm-month combinations from Jan 1996 through December 2015 using data from OptionMetrics, Compustat and CRSP. The definitions for these variables are introduced in Appendix 1.A.

	(1)	(2)	(3)	(4)	(5)	(6)	(7)	(8)	(9)	(10)	(11)	(12)	(13)	(14)
(1)RNS1M	1.00	0.54	0.42	0.35	0.30	-0.65	0.12	-0.28	0.10	-0.09	-0.07	0.22	0.13	0.18
(2)RNS3M	0.50	1.00	0.78	0.67	0.61	-0.04	0.24	-0.43	0.08	-0.12	-0.07	0.41	0.29	0.31
(3)RNS6M	0.36	0.78	1.00	0.94	0.88	0.23	0.34	-0.54	0.04	-0.12	-0.07	0.57	0.42	0.39
(4)RNS9M	0.29	0.68	0.95	1.00	0.97	0.35	0.39	-0.58	0.03	-0.12	-0.07	0.65	0.48	0.43
(5)RNS12M	0.25	0.61	0.88	0.96	1.00	0.41	0.42	-0.61	0.02	-0.13	-0.08	0.70	0.52	0.46
(6)RNSTS	-0.66	0.03	0.34	0.46	0.53	1.00	0.20	-0.19	-0.08	-0.01	0.02	0.30	0.27	0.15
(7)BETA	0.08	0.19	0.27	0.31	0.32	0.17	1.00	-0.27	0.01	-0.07	-0.06	0.57	0.39	0.31
(8)MV	-0.11	-0.17	-0.20	-0.21	-0.20	-0.05	-0.12	1.00	-0.24	0.20	0.20	-0.64	-0.38	-0.56
(9)BM	0.09	0.08	0.06	0.06	0.06	-0.03	0.01	-0.10	1.00	-0.35	-0.35	-0.10	-0.06	0.12
(10)MOM	-0.05	-0.06	-0.03	-0.03	-0.03	0.02	-0.00	0.02	-0.27	1.00	-0.06	-0.05	-0.09	-0.27
(11)REV	-0.03	-0.00	0.02	0.03	0.03	0.05	0.05	0.03	-0.21	-0.05	1.00	-0.05	-0.04	-0.07
(12)IVOL	0.14	0.29	0.41	0.47	0.50	0.24	0.55	-0.24	-0.05	0.10	0.12	1.00	0.57	0.57
(13)MAX	0.05	0.15	0.22	0.26	0.28	0.16	0.28	-0.12	0.01	-0.02	0.04	0.42	1.00	0.33
(14)EIS	0.14	0.25	0.30	0.33	0.35	0.12	0.29	-0.17	0.14	-0.24	0.03	0.60	0.27	1.00

Table 1.4: Portfolios Formed on Risk-Neutral Skewness of Different Maturities

Panels A, B, C, D and E present abnormal return over the following month of quintile portfolios sorted by 1-, 3-, 6-, 9-, and 12-month risk neutral skewness, respectively. 5 standard asset pricing models are used as benchmarks, which include Capital Asset Pricing Model (CAPM), Fama and French (1993) 3-factor model (FF3), Fama and French (2015) 5-factor model (FF5), Fama and French (1993) 3 factors plus Carhart (1997) momentum factor 4-factors model (FFC4) and Fama and French (1993) 3 factors, Carhart (1997) momentum factor plus Pastor and Stambaugh (2003) liquidity factor 5-factor model (FFCP5). In each panel, alphas of equal-weighted portfolios are reported. All returns are monthly based estimates without annualization. T-statistics computed using Newey-West standard errors with five lags are in parentheses. ***, ** and * indicate 1%, 5%, and 10% significance levels, respectively.

Panel A: Alpha of Portfolios Sorted by 1-month RNS

Quintile	CAPM Alpha	FF3 Alpha	FF5 Alpha	FFC4 Alpha	FFCP5 Alpha
Low	-0.33	-0.46	-0.61	-0.40	-0.40
2	-0.20	-0.31	-0.40	-0.23	-0.23
3	-0.00	-0.11	-0.19	-0.02	-0.01
4	0.06	-0.08	-0.18	0.04	0.04
High	0.54	0.37	0.23	0.55	0.55
High-Low	0.87***	0.83***	0.85***	0.95***	0.95***
t-stat.	(5.03)	(5.32)	(4.86)	(5.79)	(5.78)

Panel B: Alpha of Portfolios Sorted by 3-month RNS

Quintile	CAPM Alpha	FF3 Alpha	FF5 Alpha	FFC4 Alpha	FFCP5 Alpha
Low	-0.00	-0.12	-0.30	-0.09	-0.09
2	-0.06	-0.19	-0.34	-0.10	-0.10
3	-0.11	-0.22	-0.30	-0.13	-0.13
4	-0.03	-0.15	-0.22	-0.03	-0.03
High	0.27	0.09	0.00	0.31	0.31
High-Low	0.27	0.21	0.31*	0.40**	0.40**
t-stat.	(1.29)	(1.23)	(1.67)	(2.30)	(2.31)

Panel C: Alpha of Portfolios Sorted by 6-month RNS

Quintile	CAPM Alpha	FF3 Alpha	FF5 Alpha	FFC4 Alpha	FFCP5 Alpha
Low	0.11	0.00	-0.22	0.02	0.02
2	0.12	-0.02	-0.24	0.05	0.05
3	0.05	-0.09	-0.21	-0.00	-0.00
4	0.00	-0.12	-0.13	0.01	0.01
High	-0.20	-0.37	-0.35	-0.12	-0.12
High-Low	-0.32	-0.37**	-0.13	-0.14	-0.14
t-stat.	(-1.25)	(-2.09)	(-0.70)	(-0.74)	(-0.75)

Panel D: Alpha of Portfolios Sorted by 9-month RNS

Quintile	CAPM Alpha	FF3 Alpha	FF5 Alpha	FFC4 Alpha	FFCP5 Alpha
Low	0.18	0.07	-0.16	0.09	0.09
2	0.18	0.05	-0.20	0.09	0.09
3	0.19	0.04	-0.10	0.12	0.12
4	-0.02	-0.16	-0.20	-0.03	-0.03
High	-0.44	-0.59	-0.49	-0.31	-0.31
High-Low	-0.62**	-0.67***	-0.32	-0.40*	-0.40*
t-stat.	(-2.01)	(-3.14)	(-1.63)	(-1.91)	-1.94)

Panel E: Alpha of Portfolios Sorted by 12-month RNS

Quintile	CAPM Alpha	FF3 Alpha	FF5 Alpha	FFC4 Alpha	FFCP5 Alpha
Low	0.22	0.12	-0.14	0.13	0.13
2	0.23	0.10	-0.17	0.14	0.14
3	0.22	0.07	-0.10	0.14	0.14
4	0.01	-0.13	-0.16	-0.01	-0.01
High	-0.60	-0.75	-0.59	-0.43	-0.43
High-Low	-0.82***	-0.86***	-0.46**	-0.56***	-0.56***
t-stat.	(-2.43)	(-3.63)	(-2.12)	(-2.47)	(-2.52)

Table 1.5: Portfolios Formed on the Term Spread of Risk-Neutral Skewness

Panel A, B, C, D and E present abnormal return over the following month of quintile portfolios sorted by the difference between 12- and 1-month risk neutral skewness, respectively. 5 standard asset pricing models are used as benchmarks, which include Capital Asset Pricing Model (CAPM), Fama and French (1993) 3-factor model (FF3), Fama and French (2015) 5-factor model (FF5), Fama and French (1993) 3 factors plus Carhart (1997) momentum factor 4-factors model (FFC4) and Fama and French (1993) 3 factors, Carhart (1997) momentum factor plus Pastor and Stambaugh (2003) liquidity factor 5-factor model (FFCP5). In each panel, alphas of equal-weighted portfolios are reported. All returns are monthly based estimate without annualization. T-statistics computed using Newey-West standard errors with five lags are in parentheses. ***, ** and * indicate 1%, 5%, and 10% significance levels, respectively.

Alpha of Portfolios Sorted by Term Spread of RNS

Quintile	CAPM Alpha	FF3 Alpha	FF5 Alpha	FFC4 Alpha	FFCP5 Alpha
Low	0.57	0.42	0.19	0.52	0.52
2	0.36	0.23	0.02	0.30	0.30
3	0.13	0.01	-0.14	0.08	0.09
4	-0.22	-0.34	-0.35	-0.24	-0.24
High	-0.75	-0.91	-0.87	-0.70	-0.70
High-Low	-1.32***	-1.33***	-1.07***	-1.22***	-1.22***
t-stat.	(-5.69)	(-7.21)	(-6.56)	(-6.52)	(-6.61)

Table 1.6: Fama-MacBeth Cross-Sectional Regressions of Monthly Excess Stock Returns on Lagged Term Spread of RNS

This table reports the Fama-MacBeth coefficients of cross-sections of monthly excess stock returns on lagged term spread of risk-neutral skewness (RNSTS) and a set of firm characteristics during the period 1996-2015. RNSTS is calculated as the difference between long-term (12-month) and short-term (1-month) risk-neutral skewness. Models (2) controls for firms' beta (BETA), market value (MV), book-to-market ratio (BM), momentum (MOM), one-month reversal (REV),stock illiquidity proxied by Amihud (2002) price impact ratio (ILLQ). Model (3) additionally controls for lagged stock's return (RET), price per share (PRICE), and idiosyncratic volatility (IVOL). Model (4) additionally controls for option trading volume(OPVOL) and open interest(OPEN). T-statistics computed using Newey-West standard errors with five lags are in parentheses. ***, ** and * indicate 1%, 5%, and 10% significance levels, respectively.

	(1)	(2)	(3)	(4)
INTERCEPT	0.0062	0.0239 ***	0.0213 *	0.0244 **
	(1.45)	(2.37)	(1.79)	(2.13)
RNSTS	-0.0100***	-0.0071***	-0.0065***	-0.0066***
	(-3.83)	(-4.43)	(-4.40)	(-4.38)
BETA		0.0005	0.0004	0.0004
		(0.23)	(0.22)	(0.22)
log(MV)		-0.0011*	-0.0008	-0.0010*
		(-1.91)	(-1.40)	(-1.79)
BM		0.0004	-0.0002	-0.0002
		(0.28)	(-0.11)	(-0.15)
MOM		0.0001	-0.0004	-0.0004
		(0.05)	(-0.19)	(-0.17)
REV		-0.0002	-0.0003	-0.0003
		(-0.81)	(-1.07)	(-1.03)
ILLIQ*10^4		-0.4827*	-0.4665*	-0.4463
		(-1.69)	(-1.66)	(-1.50)
RET			-0.0219***	-0.0211***
			(-4.35)	(-4.23)
PRICE*10^{-2}			-0.0035	-0.0036
			(-1.34)	(-1.33)
IVOL			0.0078	-0.0078
			(0.06)	(-0.06)
OPVOL*10^{-4}				-0.0015
				(-1.20)
OPEN*10^{-4}				0.0002 *
				(1.91)
R-squared	0.0069	0.0740	0.0886	0.0912
Observations	358,802	235,652	235,652	234,418

Table 1.7: Fama-MacBeth Cross-Sectional Regressions of Quarterly SUE on Lagged RNS of Different Maturities

This table reports the Fama-MacBeth coefficients of cross-sections of the quarterly standardized earnings surprise (SUE) on lagged short-term(1 month) risk-neutral skewness(RNS1M), long-term(12 month) risk-neutral skewness(RNS12M), and a set of firm characteristics during the period 1996-2015. RNSTS is calculated as the difference between long-term (12-month) and short-term (1-month) risk-neutral skewness. Models (2) controls for firms' beta (BETA), market value (MV), book-to-market ratio (BM), momentum (MOM), one-month reversal (REV),stock illiquidity proxied by Amihud (2002) price impact ratio (ILLQ). Model (3) additionally controls for lagged stock's return (RET), price per share (PRICE), and idiosyncratic volatility (IVOL). Model (4) additionally controls for option trading volume (OPVOL) and open interest (OPEN). T-statistics computed using Newey-West standard errors with five lags are in parentheses. ***, ** and * indicate 1%, 5%, and 10% significance levels, respectively.

	(1)	(2)	(3)	(4)
INTERCEPT	-0.0028***	0.0022	0.0069 **	0.0067 **
	(-3.14)	(1.17)	(2.20)	(1.96)
RNS1M	0.0010 **	0.0011 ***	0.0011 ***	0.0011 ***
	(2.07)	(2.36)	(2.50)	(2.51)
RNS12M	-0.0052***	-0.0033***	-0.0026***	-0.0027***
	(-3.43)	(-2.89)	(-2.55)	(-2.63)
BETA		-0.0001	0.0003 *	0.0003 **
		(-0.44)	(1.87)	(2.10)
log(MV)		-0.0001	-0.0002*	-0.0002
		(-1.02)	(-1.74)	(-1.42)
BM		-0.0042**	-0.0045**	-0.0045**
		(-2.32)	(-2.28)	(-2.26)
MOM		0.0002	0.0007 ***	0.0008 ***
		(0.81)	(3.70)	(3.65)
REV		-0.0001	0.0000	0.0000
		(-1.28)	(0.51)	(0.51)
ILLIQ*10^4		-0.0030	0.0071	-0.0274
		(-0.02)	(0.05)	(-0.20)
RET			0.0028 ***	0.0029 ***
			(3.72)	(3.77)
PRICE*10^{-2}			-0.0017***	-0.0018***
			(-2.89)	(-3.02)
IVOL			-0.0998***	-0.1022***
			(-3.07)	(-3.08)
OPVOL*10^{-4}				-0.0001
				(-0.90)
OPEN*10^{-4}				-0.0000
				(-0.24)
R-squared	0.0066	0.0415	0.0491	0.0510
Observations	313,726	210,267	210,267	209,383

Table 1.8: Fama-MacBeth Cross-Sectional Logistic Regressions of Monthly Stock Price Crash on Lagged RNS of Different Maturities

This table reports the Fama-MacBeth coefficients of cross-sectional logistic regressions of monthly price crash on lagged 1 month risk-neutral skewness (RNS1M), 12 month risk-neutral skewness (RNS12M), and a set of firm characteristics during the period 1996-2015. RNSTS is calculated as the difference between long-term (12 month) and short-term (1 month) risk-neutral skewness. Model (1), (2), ..., and (6) regress 1-, 2-, ..., and 6-month ahead price crash dummy on independent variables, respectively. T-statistics computed using Newey-West standard errors with five lags are in parentheses. ***, ** and * indicate 1%, 5%, and 10% significance levels, respectively.

	(1)	(2)	(3)	(4)	(5)	(6)
INTERCEPT	-1.3512***	-1.3701***	-1.4917***	-1.5043***	-1.4829***	-1.3554***
	(-6.86)	(-6.99)	(-7.89)	(-8.10)	(-6.92)	(-6.48)
RNS_1M	-0.1048***	-0.0926***	-0.0866***	-0.0981***	-0.1124***	-0.0958***
	(-4.08)	(-3.49)	(-2.72)	(-2.98)	(-3.36)	(-2.87)
RNS_12M	0.2181 ***	0.0904	0.0663	0.0584	0.0622	-0.0005
	(3.95)	(1.38)	(1.18)	(1.08)	(1.09)	(-0.01)
BETA	-0.0362*	-0.0215	-0.0242	-0.0200	-0.0203	-0.0186
	(-1.89)	(-1.09)	(-1.44)	(-1.03)	(-1.09)	(-1.03)
log(MV)	-0.0418***	-0.0505***	-0.0469***	-0.0494***	-0.0509***	-0.0593***
	(-3.19)	(-4.04)	(-3.88)	(-4.01)	(-3.81)	(-4.22)
BM	-0.2443***	-0.2520***	-0.2502***	-0.2441***	-0.2348***	-0.2468***
	(-7.29)	(-7.60)	(-7.09)	(-7.33)	(-6.95)	(-7.31)
MOM	0.0951 ***	0.0450 *	-0.0011	-0.0110	-0.0184	-0.0520***
	(3.86)	(1.89)	(-0.05)	(-0.49)	(-1.02)	(-2.38)
REV	0.0013	-0.0036	-0.0074	-0.0121*	-0.0109*	-0.0095
	(0.19)	(-0.49)	(-1.12)	(-1.95)	(-1.68)	(-1.32)
ILLIQ*10^6	-0.6637***	-0.7444***	-0.6917***	-0.7648***	-0.8078***	-0.8891***
	(-4.63)	(-5.84)	(-4.95)	(-5.68)	(-6.48)	(-5.44)
RET	-0.4508***	-0.0330	0.1539	-0.0442	0.1876 **	0.1374
	(-4.17)	(-0.43)	(1.60)	(-0.49)	(2.25)	(1.56)
PRICE*10^{-2}	-0.0182	0.0587	0.0838	0.1144 *	0.1145 *	0.1046
	(-0.30)	(1.05)	(1.41)	(1.87)	(1.76)	(1.55)
IVOL	-3.4572***	-1.0521	0.8302	2.2693	2.3300	1.7347
	(-2.38)	(-0.74)	(0.55)	(1.52)	(1.51)	(1.16)
OPVOL*10^{-4}	0.1100 *	-0.3021***	-0.1945***	-0.2159**	-0.3850***	-0.3328***
	(1.93)	(-2.73)	(-3.25)	(-2.23)	(-2.93)	(-2.71)
OPEN*10^{-4}	-0.0131***	-0.0016	-0.0040	-0.0062	-0.0034	-0.0036
	(-3.39)	(-0.61)	(-1.11)	(-1.16)	(-0.68)	(-0.97)
Observations	232,506	231,038	229,499	227,795	226,154	224286

Table 1.9: Average Short- and Long-term Risk-Neutral Skewness of Quintile Portfolios Sorted by Hedging Demand

This table reports the time-series average of the average RNS for quintile portfolios sorted by investor hedging demand. Three measures are used as hedging demand proxies, including the ratio of aggregate put option volume to total option volume (PAOV), the aggregate open interest across all options (AOI), and the Z-score of Zmijewski (1984) (ZD) to capture default risk. In order to match 1 month maturity of short-term RNS, only options with maturity from 10 to 45 days are used to calculate the PAOV and AOI. Correspondingly, in order to match 12 month maturity of long-term RNS, only options with maturity from 319 to 456 days are used to calculate these two measures. The difference in average RNS between highest and the lowest hedging demand quintile portfolios are presented in the second to last line. T-statistics computed using Newey-West standard errors with five lags are in parentheses. ***, ** and * indicate 1%, 5%, and 10% significance levels, respectively.

Panel A: Short-term RNS and hedging demand

Quintile	Put-to-all Volume Ratio	Aggregate Open Interest	Z score Default Risk
Low	-0.3012	-0.2503	-0.2878
2	-0.3433	-0.2954	-0.3037
3	-0.3623	-0.3257	-0.3190
4	-0.3750	-0.3495	-0.3310
High	-0.3671	-0.3750	-0.3235
Q5-Q1	-0.0658***	-0.1247***	-0.0358***
T	(-17.31)	(-13.18)	(-11.11)

Panel B: Long-term RNS and hedging demand

Quintile	Put-to-all Volume Ratio	Aggregate Open Interest	Z score Default Risk
Low	-0.5702	-0.5938	-0.5296
2	-0.5963	-0.6049	-0.5636
3	-0.5934	-0.6164	-0.6034
4	-0.6161	-0.6221	-0.6459
High	-0.6216	-0.6395	-0.6142
Q5-Q1	-0.0514***	-0.0456***	-0.0845***
T	(-5.26)	(-2.68)	(-8.01)

Table 1.10: Double Sorted Portfolios by Hedging Demand and RNS of Different Terms

In this table, Panels A and B report the performance of double sorted portfolios by 1-month Risk-Neutral Skewness and 12-month Risk-Neutral Skewness respectively with overvaluation and short-sale constraint proxies for the sample period from 1996 to 2015. Stock overvaluation is proxied by the maximum daily stock returns over the last month (MAX) and expected idiosyncratic skewness (EIS). Short-sale constraint is proxied by idiosyncratic volatlity (IVOL). In the end of each month, stocks are sorted into tercile portfolios in ascending order by RNS. Within each RNS tercile portfolio, stocks are further sorted to tercile portfolios in ascending order based on the overvaluation or short-sale constraint proxies. We report abnormal returns relative to the Fama and French (1993) model. T-statistics computed using Newey-West standard errors with five lags are in parentheses. ***, ** and * indicate 1%, 5%, and 10% significance levels, respectively.

Panel A: Short-term RNS

Panel A-1: Stock Overvaluation

	MAX low	MAX medium	MAX high	Difference
RNS1M low	0.0265	-0.2370**	-0.9747***	-1.0012***
	(0.24)	(-1.96)	(-6.28)	(-5.54)
RNS1M medium	0.2063*	-0.0927	-0.6049***	-0.8112***
	(1.68)	(-0.63)	(-3.29)	(-4.10)
RNS1M high	0.6129***	0.2044	-0.1857	-0.7986***
	(4.14)	(1.18)	(-0.98)	(-4.65)
Difference	0.5864***	0.4414***	0.7890***	
	(5.14)	(3.10)	(5.14)	
	EIS low	EIS medium	EIS high	Difference
RNS1M low	0.1384	-0.1986	-0.7646***	-0.9030***
	(1.29)	(-1.51)	(-4.31)	(-4.86)
RNS1M medium	0.2697**	0.0147	-0.4366**	-0.7063***
	(2.06)	(0.10)	(-2.29)	(-3.52)
RNS1M high	0.4841***	0.3557**	0.1408	-0.3433*
	(3.46)	(2.11)	(0.74)	(-1.81)
Difference	0.3457***	0.5542***	0.9054***	
	(3.17)	(4.06)	(4.77)	

Panel A-2: Short-selling Constraint

	IVOL low	IVOL medium	IVOL high	Difference
RNS1M low	0.0430	-0.3288***	-0.9068***	-0.9498***
	(0.42)	(-2.62)	(-5.49)	(-5.01)
RNS1M medium	0.2723**	-0.1077	-0.6559***	-0.9282***
	(2.33)	(-0.74)	(-3.51)	(-4.69)
RNS1M high	0.4527***	0.3098*	-0.1317	-0.5844***
	(3.33)	(1.83)	(-0.60)	(-2.84)
Difference	0.4098***	0.6387***	0.7751***	
	(3.99)	(4.70)	(4.50)	

Panel B: Long-term RNS

Panel B-1: Stock Overvaluation

	MAX low	MAX medium	MAX high	Difference
RNS12M low	0.2995***	0.0800	-0.0110	-0.3105***
	(2.60)	(0.70)	(-0.08)	(-3.03)
RNS12M medium	0.3008**	-0.0259	-0.2003	-0.5010***
	(2.20)	(-0.18)	(-1.36)	(-3.81)
RNS12M high	0.0425	-0.5328***	-1.0125***	-1.0550***
	(0.23)	(-2.47)	(-3.73)	(-4.98)
Difference	-0.2570	-0.6129***	-1.0015***	
	(-1.40)	(-2.76)	(-3.64)	
	EIS low	EIS medium	EIS high	Difference
RNS12M low	0.2152**	0.0290	0.1269	-0.0883
	(2.25)	(0.24)	(0.87)	(-0.66)
RNS12M medium	0.4113***	0.0003	-0.0224	-0.4337***
	(2.89)	(0.00)	(-0.16)	(-2.86)
RNS12M high	0.0876	-0.2413	-0.6066***	-0.6942***
	(0.45)	(-1.33)	(-2.68)	(-3.72)
Difference	-0.1275	-0.2704	-0.7335***	
	(-0.60)	(-1.38)	(-3.66)	

Panel B-2: Short-selling Constraint

	IVOL low	IVOL medium	IVOL high	Difference
RNS12M low	0.2567***	0.0964	0.0143	-0.2424**
	(2.44)	(0.76)	(0.11)	(-2.07)
RNS12M medium	0.1932	-0.0118	-0.1064	-0.2996*
	(1.51)	(-0.08)	(-0.70)	(-1.93)
RNS12M high	-0.1346	-0.4556*	-0.9114***	-0.7768***
	(-0.66)	(-1.93)	(-3.39)	(-2.89)
Difference	-0.3913**	-0.5519**	-0.9257***	
	(-2.16)	(-2.29)	(-3.40)	

Table 1.11: Average Physical Skewness Measure of Quintile Portfolios Sorted by Short- and Long-term RNS

This table reports the time-series average of the average Physical Skewness measure for quintile portfolios sorted by short- and long-term RNS. We measure physical skewness using maximum daily return over the last month (MAX) and expected idiosyncratic skewness (EIS). The differences in average physical skewness between the highest and the lowest RNS portfolios are presented in the second to last line. T-statistics computed using Newey-West standard errors with five lags are in parentheses. ***, ** and * indicate 1%, 5%, and 10% significance levels, respectively.

Panel A: Short-term RNS and Physical Skewness Measure

RNS1M Quintile	Max Daily Return	Expected Idiosyncratic Skewness
Low	0.0524	0.2485
2	0.0582	0.2871
3	0.0621	0.3248
4	0.0638	0.3956
High	0.0623	0.4710
Q5-Q1	0.0099***	0.2225***
T	(11.91)	(12.02)

Panel B: Long-term RNS and Physical Skewness Measure

RNS12M Quintile	Max Daily Return	Expected Idiosyncratic Skewness
Low	0.0382	0.1077
2	0.0479	0.1981
3	0.0575	0.3022
4	0.0687	0.4301
High	0.0866	0.6887
Q5-Q1	0.0485***	0.5810***
T	(33.12)	(13.78)

Table 1.12: Fama-MacBeth Cross-Sectional Regressions of Monthly Excess Stock Returns on Lagged RNS Term Structure Factors

This table reports the Fama-MacBeth coefficients of cross-sectional regressions of monthly excess stock returns on lagged factors of the RNS term structure during the period 1996-2015. We perform a factor analysis of the RNS term structure across five fixed maturities at the 1, 3, 6, 9, and 12-month horizons for each firm-month observation. Model (1) considers the explanatory power of the factors in isolation. Model (2) controls for firms' beta (BETA), market value (MV), book-to-market ratio (BM), momentum (MOM), one-month reversal (REV),stock illiquidity proxied by Amihud (2002) price impact ratio (ILLIQ). Model (3) additionally controls for lagged stock's return (RET), price per share (PRICE), and idiosyncratic volatility (IVOL). Model (4) additionally controls for option trading volume (OPVOL) and open interest (OPEN). T-statistics computed using Newey-West standard errors with five lags are in parentheses. ***, ** and * indicate 1%, 5%, and 10% significance levels, respectively.

	(1)	(2)	(3)	(4)
INTERCEPT	0.0101	0.0239 ***	0.0228 *	0.0254 **
	(1.59)	(2.42)	(1.93)	(2.24)
Factor 1	0.0189 *	0.0128	0.0132 *	0.0134 *
	(1.89)	(1.57)	(1.70)	(1.74)
Factor 2	-0.1063***	-0.0786***	-0.0745***	-0.0742***
	(-3.33)	(-3.99)	(-4.30)	(-4.24)
Factor 3	0.2775	0.1493	0.1668	0.1635
	(1.48)	(1.25)	(1.57)	(1.54)
BETA		0.0000	0.0002	0.0001
		(0.02)	(0.10)	(0.08)
log(MV)		-0.0007	-0.0006	-0.0007*
		(-1.23)	(-1.01)	(-1.29)
BM		0.0004	-0.0001	-0.0001
		(0.27)	(-0.06)	(-0.09)
MOM		0.0004	-0.0003	-0.0003
		(0.17)	(-0.13)	(-0.11)
REV		-0.0002	-0.0003	-0.0003
		(-0.85)	(-1.05)	(-1.00)
ILLIQ*10^4		-0.5456*	-0.5341*	-0.5058*
		(-1.90)	(-1.89)	(-1.69)
RET			-0.0204***	-0.0196***
			(-4.04)	(-3.90)
PRICE*10^{-2}			-0.0027	-0.0027
			(-1.01)	(-1.01)
IVOL			-0.0011	-0.0172
			(-0.01)	(-0.15)
OPVOL*10^{-4}				-0.0017
				(-1.35)
OPEN*10^{-4}				0.0002 *
				(1.86)
R-squared	0.0243	0.0795	0.0927	0.0953
Observations	358,802	235,652	235,652	234,418

Table 1.13: RNS Term Structure Slope Factor and Macroeconomic Variables

This table reports coefficients from a monthly vector autoregressive model of the slope factor of the RNS term structure (SLOPE) along with macroeconomic variables related to equity expected returns. Here MKTRP is the S&P 500 return net of the T-bill rate, EP is the log ratio of trailing 12-month S&P 500 earnings to current S&P price, TERM is the term spread as the difference between long-term T-Bonds and short-term T-Bills, and DEF is the default spread as the difference between long-term corporate bonds and T-Bonds. T-statistics are in parentheses. ***, ** and * indicate 1%, 5%, and 10% significance levels, respectively.

	SLOPE	MKTRP	EP	TERM	DEF
$SLOPE_{t-1}$	0.5653 ***	-0.2273	0.2894	0.0494 ***	0.0173 ***
	(9.92)	(-0.91)	(0.67)	(3.02)	(2.81)
$MKTRP_{t-1}$	-0.0503***	0.0611	0.3624 ***	0.0029	-0.0094***
	(-3.35)	(0.92)	(3.17)	(0.67)	(-5.83)
EP_{t-1}	0.0037 *	0.0055	0.9304 ***	-0.0010*	0.0005 **
	(1.91)	(0.63)	(62.32)	(-1.83)	(2.46)
$TERM_{t-1}$	0.1845 ***	0.1733	1.5078 ***	0.9385 ***	-0.0077
	(3.13)	(0.67)	(3.36)	(55.59)	(-1.21)
DEF_{t-1}	1.1063 ***	0.2494	-10.5121***	-0.0745	0.9321 ***
	(4.44)	(0.23)	(-5.54)	(-1.04)	(34.73)
INTERCEPT	0.0152 ***	0.0256	-0.1654 ***	-0.0031*	0.0019 ***
	(2.70)	(1.04)	(-3.87)	(-1.92)	(3.07)
Observations	238	238	238	238	238

Table 1.14: One-Month RNS and Macroeconomic State Variables

This table reports coefficients from a vector autoregressive model of equal-weighted average RNS along with macroeconomic state variables related to equity expected returns. Here MKTRP is the S&P 500 return net of the T-bill rate, EP is the log ratio of trailing 12-month S&P 500 earnings to current S&P price, TERM is the term spread as the difference between long-term T-Bonds and short-term T-Bills, and DEF is the default spread as the difference between long-term corporate bonds and T-Bonds. T-statistics are in parentheses. ***, ** and * indicate 1%, 5%, and 10% significance levels, respectively.

	RNS1M	MKTRP	EP	TERM	DEF
$RNS1M_{t-1}$	0.5473 ***	0.07167	-0.0360	-0.0009	-0.0030**
	(9.70)	(1.43)	(-0.41)	(-0.27)	(-2.40)
$MKTRP_{t-1}$	0.1881 **	0.0635	0.3600 ***	0.0024	-0.0096***
	(2.54)	(0.96)	(3.14)	(0.55)	(-5.91)
EP_{t-1}	-0.0085	0.0048	0.9320 ***	-0.0007	0.0006 ***
	(-0.90)	(0.56)	(63.57)	(-1.23)	(2.90)
$TERM_{t-1}$	0.6256 **	-0.0357	1.6865 ***	0.9607 ***	0.0043
	(2.23)	(-0.14)	(3.90)	(57.93)	(0.70)
DEF_{t-1}	-3.0290***	0.2085	-9.9785***	0.0619	0.9567 ***
	(-2.92)	(0.23)	(-6.23)	(1.01)	(42.04)
INTERCEPT	-0.1530***	0.0414	-0.1689***	-0.0021	0.0014 **
	(-4.83)	(1.47)	(-3.45)	(-1.12)	(2.02)
Observations	238	238	238	238	238

Table 1.15: Three-Month RNS and Macroeconomic State Variables

This table reports coefficients from a vector autoregressive model of equal-weighted average RNS along with macroeconomic state variables related to equity expected returns. Here MKTRP is the S&P 500 return net of the T-bill rate, EP is the log ratio of trailing 12-month S&P 500 earnings to current S&P price, TERM is the term spread as the difference between long-term T-Bonds and short-term T-Bills, and DEF is the default spread as the difference between long-term corporate bonds and T-Bonds. T-statistics are in parentheses. ***, ** and * indicate 1%, 5%, and 10% significance levels, respectively.

	RNS3M	MKTRP	EP	TERM	DEF
$RNS3M_{t-1}$	0.8402 ***	0.0741	-0.1887 **	0.0046	-0.0005
	(22.85)	(1.51)	(-2.23)	(1.42)	(-0.40)
$MKTRP_{t-1}$	0.0656	0.0655	0.3539 ***	0.0026	-0.0096***
	(1.33)	(0.99)	(3.12)	(0.59)	(-5.85)
EP_{t-1}	-0.0069	0.0053	0.9286 ***	-0.0006	0.0006 ***
	(-1.09)	(0.63)	(63.73)	(-1.04)	(2.99)
$TERM_{t-1}$	0.4774 **	-0.1740	2.2710 ***	0.9435 ***	0.0012
	(2.21)	(-0.60)	(4.57)	(49.18)	(0.17)
DEF_{t-1}	-0.7976	0.0619	-10.8816***	0.0997	0.9795 ***
	(-1.22)	(0.07)	(-7.25)	(1.72)	(44.97)
INTERCEPT	-0.0966***	0.0589	-0.2577 ***	0.0006	0.0020 *
	(-3.67)	(1.67)	(-4.26)	(0.26)	(2.32)
Observations	238	238	238	238	238

Table 1.16: Six-Month RNS and Macroeconomic State Variables

This table reports coefficients from a vector autoregressive model of equal-weighted average RNS along with macroeconomic state variables related to equity expected returns. Here MKTRP is the S&P 500 return net of the T-bill rate, EP is the log ratio of trailing 12-month S&P 500 earnings to current S&P price, TERM is the term spread as the difference between long-term T-Bonds and short-term T-Bills, and DEF is the default spread as the difference between long-term corporate bonds and T-Bonds. T-statistics are in parentheses. ***, ** and * indicate 1%, 5%, and 10% significance levels, respectively.

	RNS6M	MKTRP	EP	TERM	DEF
$RNS6M_{t-1}$	0.9592 ***	0.0436	-0.1369**	0.0070 ***	0.0005
	(41.46)	(1.14)	(-2.09)	(2.82)	(0.49)
$MKTRP_{t-1}$	-0.0047	0.0662	0.3504 **	0.0029	-0.0100***
	(-0.12)	(1.00)	(3.09)	(0.68)	(-5.81)
EP_{t-1}	-0.0033	0.0043	0.9310 ***	-0.0006	0.0006 **
	(-0.65)	(0.51)	(64.17)	(-1.09)	(3.08)
$TERM_{t-1}$	0.1257	-0.1878	2.4628 ***	0.9165 ***	-0.0033
	(0.63)	(-0.57)	(4.33)	(42.30)	(-0.40)
DEF_{t-1}	0.0080	-0.3478	-9.8772***	0.0808	0.9833 ***
	(0.02)	(-0.43)	(-7.04)	(1.51)	(48.34)
INTERCEPT	-0.0339	0.0495	-0.2514***	0.0030	0.0026 ***
	(-1.58)	(1.40)	(-4.15)	(1.29)	(2.98)
Observations	238	238	238	238	238

Table 1.17: Nine-Month RNS and Macroeconomic State Variables

This table reports coefficients from a vector autoregressive model of equal-weighted average RNS along with macroeconomic state variables related to equity expected returns. Here MKTRP is the S&P 500 return net of the T-bill rate, EP is the log ratio of trailing 12-month S&P 500 earnings to current S&P price, TERM is the term spread as the difference between long-term T-Bonds and short-term T-Bills, and DEF is the default spread as the difference between long-term corporate bonds and T-Bonds. T-statistics are in parentheses. ***, ** and * indicate 1%, 5%, and 10% significance levels, respectively.

	RNS9M	MKTRP	EP	TERM	DEF
$RNS9M_{t-1}$	0.9843 ***	0.0320	-0.0770	0.0066 ***	0.0005
	(51.46)	(1.05)	(-1.47)	(3.35)	(0.73)
$MKTRP_{t-1}$	-0.0465	0.0666	0.3515 **	0.0032	-0.0095***
	(-1.12)	(1.01)	(3.08)	(0.73)	(-5.80)
EP_{t-1}	-0.0025	0.0037	0.9328 ***	-0.0007	0.0006 **
	(-0.47)	(0.44)	(64.07)	(-1.30)	(3.05)
$TERM_{t-1}$	-0.0322	-0.1883	2.2700 ***	0.9043 ***	-0.0050
	(-0.15)	(-0.54)	(3.80)	(40.24)	(-0.58)
DEF_{t-1}	0.0635	-0.5170	-9.4206***	0.0489	0.9809 ***
	(0.12)	(-0.63)	(-6.65)	(0.92)	(48.03)
INTERCEPT	-0.0151	0.0443	-0.2171***	0.0032	0.0027 **
	(-0.72)	(1.33)	(-3.78)	(1.50)	(3.28)
Observations	238	238	238	238	238

Table 1.18: Twelve-Month RNS and Macroeconomic State Variables

This table reports coefficients from a vector autoregressive model of equal-weighted average RNS along with macroeconomic state variables related to equity expected returns. Here MKTRP is the S&P 500 return net of the T-bill rate, EP is the log ratio of trailing 12-month S&P 500 earnings to current S&P price, TERM is the term spread as the difference between long-term T-Bonds and short-term T-Bills, and DEF is the default spread as the difference between long-term corporate bonds and T-Bonds. T-statistics are in parentheses. ***, ** and * indicate 1%, 5%, and 10% significance levels, respectively.

	RNS12M	MKTRP	EP	TERM	DEF
$RNS12M_{t-1}$	0.9885 ***	0.0255	-0.0487	0.0057 ***	0.0006
	(54.61)	(1.03)	(-1.14)	(3.55)	(0.83)
$ofMKTRP_{t-1}$	-0.1063**	0.0664	0.3536 **	0.0032	-0.0095***
	(-2.19)	(1.00)	(3.09)	(0.74)	(-5.80)
EP_{t-1}	-0.0018	0.0033	0.9336 ***	-0.0008	0.0006 ***
	(-0.29)	(0.39)	(63.87)	(-1.47)	(3.00)
$TERM_{t-1}$	-0.0621	-0.1843	2.1304 ***	0.9008 ***	-0.0057
	(-0.24)	(-0.53)	(3.55)	(40.10)	(-0.66)
DEF_{t-1}	-0.0259	-0.6123	-9.2889***	0.0259	0.9787 ***
	(-0.04)	(-0.73)	(-6.42)	(0.48)	(47.01)
INTERCEPT	-0.0085	0.0410	-0.1985***	0.0029	0.0027 ***
	(-0.37)	(1.30)	(-3.65)	(1.42)	(3.48)
Observations	238	238	238	238	238

Figure 1.1: Asset Returns and Demands when there is No Informed Trading

This figure plots asset returns and demands of each type of investor when there is no informed trading. In this case, uninformed lotto investors and informed ones are classified as the same type of investors. We set $\hat{M}_{222} = M_{222}$.

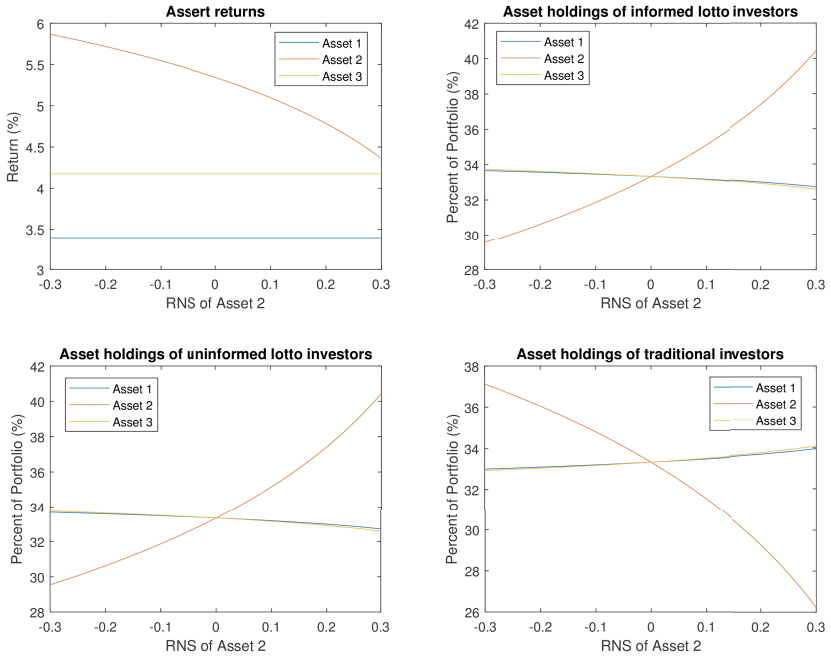

Figure 1.2: Asset Returns and Demands when RNS is Driven by the Expected Skewness of Uninformed Lotto Investors

This figure plots asset returns and demands when RNS is driven by the expected skewness of uninformed lotto investors. We set $M_{222} = 0.1$ and let $\hat{M}_{222}^{(0)}$ vary from -0.3 to 0.3.

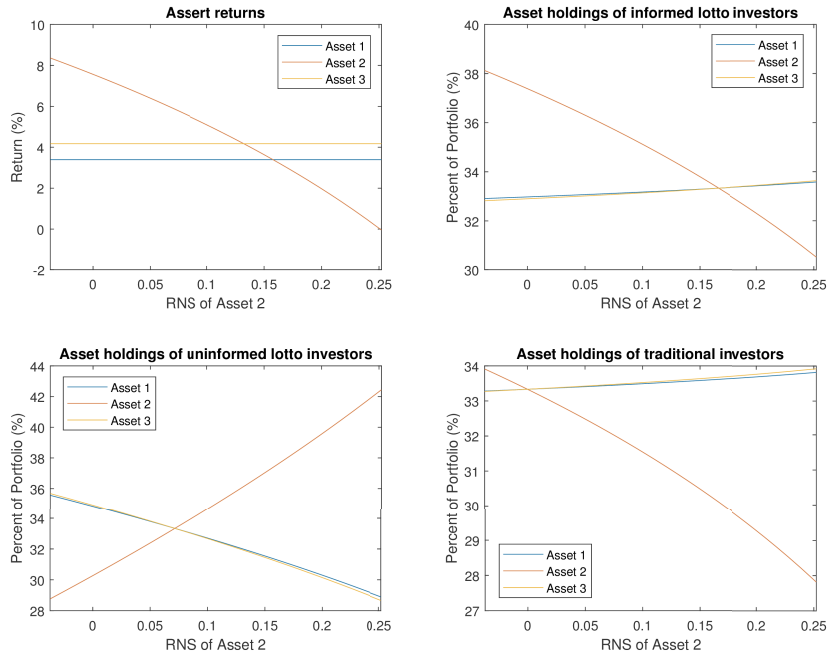

Figure 1.3: Asset Returns and Demands when RNS is Driven by the True Value of Skewness

This figure plots asset returns and demands when RNS is driven by the true value of skewness. We set $\hat{M}_{222} = 0.1$ and let M_{222} vary from -0.3 to 0.3.

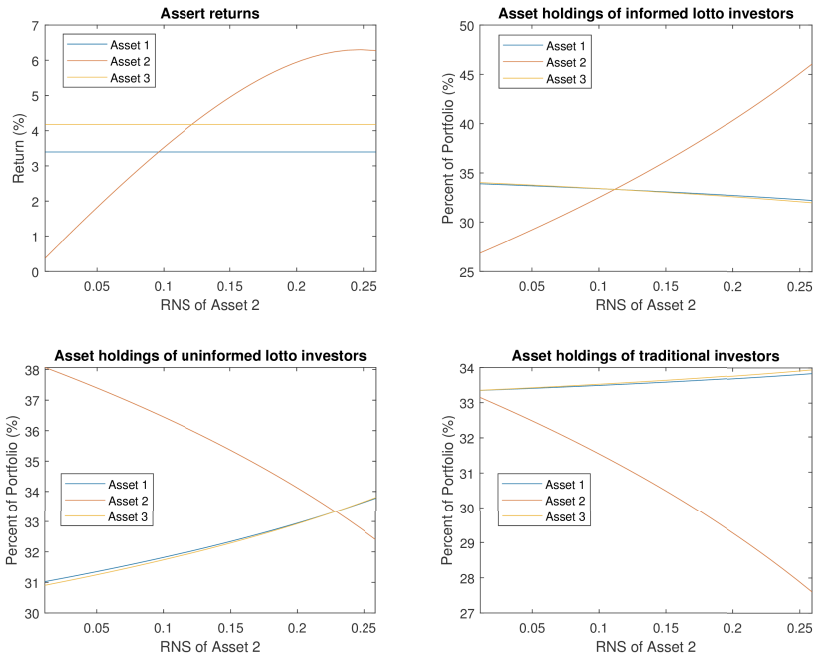

Figure 1.4: Correlation between RNS and Subsequent Asset Returns

This figure plots the correlation between RNS and subsequent asset returns given different proportion of informed lotto investors over all lotto investors.

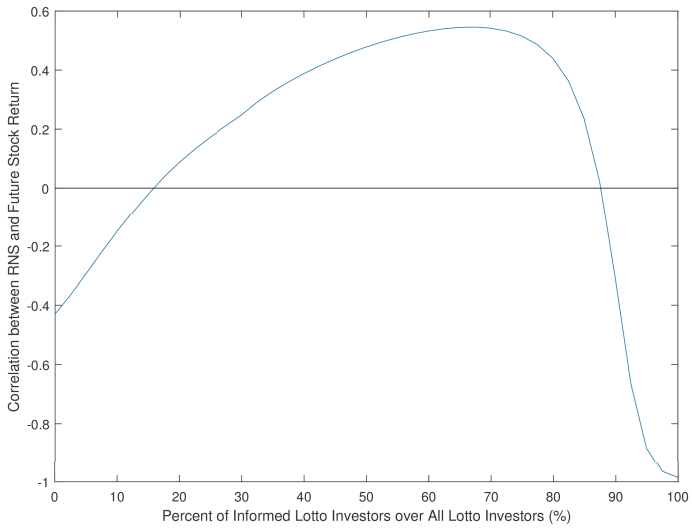

Figure 1.5: Factor Analysis of RNS across Different Maturities

This figure shows the loadings of three factors obtained from the factor analysis of RNS with five maturities. All firm-month observations are used for factor analysis. The blue, orange and green solid line indicates the loadings on 1-month RNS, 3-month RNS, 6-month RNS, 9-month RNS and 12-month RNS of the first, second, and third factor, respectively. The percentage of variance explained by each factor is presented in the legend.

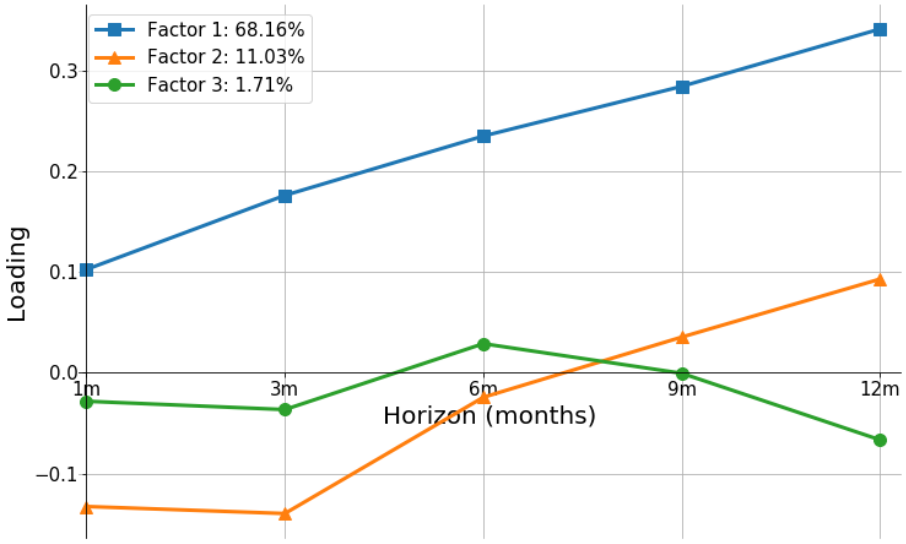

Chapter 2

Estimating Periodically Collapsing Rational Bubbles with the Mixture Kalman Filter

(Jointly with Rong Chen, Liang Wang and Yangru Wu)

2.1 Introduction

Bubbles have long intrigued people and gained growing interests. Many economists believe that stock prices are too volatile to be attributed to market fundamentals, connecting the unexplained term to bubbles has become one practical and reasonable way of modeling (Shiller, 1981; Tirole, 1982; Diba and Grossman, 1988; Campbell and Shiller, 1988; Froot and Obstfeld, 1991). A speculative bubble refers to the deviation of an asset's price from its fundamental value because the holders believe that they can resell the asset at an even higher price in the future. One type of bubbles which is extensively studied in the literature is rational bubbles, which assume that investors have rational expectations, identical information and homogeneous beliefs. Bubbles are often accompanied with periodically bursts, typically followed by dramatic price increases (Brunnermeier, 2009).

The literature has discussed econometric detection of rational bubbles with one important testable implication that bubbles should exhibit explosive behavior. To be specific, bubbles have to grow in expectations at the required rate of return of the asset, as is implied by the rational expectations assumption. One strand of literature utilizes cointegration and unit-root tests to examine whether the stock price is more explosive than its fundamental (Hamilton and Whiteman, 1985; Diba and Grossman, 1988). Evans (1991) criticizes this approach by arguing that it fails to detect the explosive bubbles with periodical collapses.

This issue is resolved by Phillips et al. (2011), who propose a recursive testing procedure. Another strand, which this research belongs to, is to directly formulate the existence of bubbles (West, 1987) and estimate bubbles as a latent variable in a state-space model using Kalman filter Wu (1997). However, the linear specification implies a constant growth, a pattern which is inconsistent with the inherent non-linear characteristics of the real-world data. This non-linearity is believed to origin from the periodical switching regimes of the underlying economic conditions.

This research adopts a conditional dynamic linear system (Harrison and West, 1999) to directly study the bubble process with regime-switching. We allow two or three regimes that switch by Markovian transition probability matrices while keeping the system conditionally linear and Gaussian given a regime. With a two-regime model, we specify an explosive regime in which a bubble grows faster than the asset's required rate of return, and a collapsing regime in which the bubble bursts. With a three-regime specification, we add a benchmark regime in which a bubble grows at the discount rate. In order to satisfy the rational expectations condition, the bubble process is required to grow unconditionally at the required rate of return. The regime-switching bubble has also been studied by Al-Anaswah and Wilfling (2011), but our model specification is different from and more realistic than theirs. Al-Anaswah and Wilfling (2011) generates bubbles' periodically collapsing patterns by assuming the asset's required rate of return to follow a Markov-switching process and constraining the growth rate of bubbles equal to the required rate of return under either regime. In reality, bubbles' growth rate is much more volatile than the required rate of return, as advocated by Blanchard and Watson (1982) and Evans (1991), both of whom assume a constant required rate of return and a stochastic bubble component. Therefore, we formulate the bubble's growth rate as a Markov-switching process while fixing the discount rate. Furthermore, the estimated required rate of return in Al-Anaswah and Wilfling (2011) is unrealistic, i.e., the rate can either exceed 100% when bubbles grow or fall into the negative territory when bubbles collapse. However, with our model specification, the

estimated rate lies in a plausible region.

Our asset-bubble system is expressed as a state-space model with regime switching and estimated by a novel sequential Monte Carlo (SMC) method, the mixture Kalman filter (MKF), proposed by Chen and Liu (2000). This methodology is advantageous over the existing estimation methods that have been applied to estimate the state space model with regime switching in the finance and economics literature. The first existing method is the Markov Chain Monte Carlo (MCMC) Gibbs sampling method (Kim and Nelson, 1999), with applications such as Xiang and Zhu (2013). Different from this method, our MKF is not subject to Bayesian bias from the prior belief of the unknown parameters. Second, the MKF is a likelihood-based approach so the associated model selection rules such as AIC, BIC and likelihood ratio tests can be implemented to test whether our model performs better than linear model. Third, MCMC-based algorithms are prohibitively costly when performing online estimation of states and parameters (Gamerman and Lopes, 2006). The second existing method is the approximate MLE method (see Chapter 5 of Kim and Nelson (1999) for details), which approximately collapses the mixture of $M \times M$ Gaussian densities into a mixture of M Gaussian densities at the end of each iteration (M is the number of regimes), with applications include Chauvet (1998) and Al-Anaswah and Wilfling (2011). The inaccuracy of their likelihood estimate increases since the approximation error accumulates as time steps increase. As an SMC method, our MKF has been proved theoretically to return an unbiased likelihood estimate, making the parameter estimation more reliable.

We first examine the efficacy of our method by applying it to artificial stock and periodically collapsing bubble data simulated by Evans (1991) model. Then the method is applied to the U.S. stock market indices including the S&P 500 and the NASDAQ. With the associated likelihood-based model selection techniques, the proposed model with regime-switching fit the bubble process more accurately, which indicates a Markov-switching structure in the actual stock bubbles. Furthermore, the estimated model provides a filtered

probability series of different regimes, among which the filtered probability of collapsing regime can be used to date stamp major historical bubble collapses successfully for the last three decades.

In addition to the literature about bubble testing and estimation of state space model with regime switching, we also contribute to another strand of literature, which uses the SMC method (particle filter) to estimate flexible asset pricing models. The particle filter methodology can be used for filtering and estimation of non-linear non-Gaussian state space models and are becoming increasingly popular in asset pricing. For example, Li and Zinna (2018) and Bardgett et al. (2018) use the particle filter to estimate derivative pricing models with jumps. However, high computational cost of the particle filter in general hinders its broad application. As a special type of particle filter, the MKF marginalizes out the linear component of the state variable and focuses its full attention on the space of the regime indicator. By performing importance sampling for the regime indicator and running Kalman filter given the regime, the MKF updates the posterior distribution of state variable sequentially. By combining the merits of the general particle filter and the traditional Kalman filter, the MKF exhibits both estimation accuracy and computational efficiency. To our knowledge, our paper is the first work that applies MKF in finance and this method can be broadly used in estimating latent-factor asset pricing models that are partially linear and conditionally Gaussian.

The remainder of this article is organized as follows. Section 2.2 reviews the classic rational bubble model with the specification of a linear state-space form and its estimation method, the Kalman filter. Section 2.3 is devoted to the elaboration of the rational stock bubble model with periodically collapsing. 2.4 introduces the mixture Kalman filtering technique, a parameter estimation strategy for the state-space model with regime switching. Section 2.5 reports the estimation results in both simulated and actual data. Section 2.6 extends the model to a three-regime version and discuss its implications. Section 2.7 concludes.

2.2 Classic Rational Bubble Model

In this section, we first introduce the classic model for the joint dynamics of a stock and its bubble component, based on the rational bubble theory. Then we provide its linear state-space form and review the corresponding estimation strategy, the Kalman filter.

2.2.1 Model Specification

Consider the standard linear rational expectations model of stock price determination,

$$\left[\mathrm{E}_t(P_{t+1} + D_{t+1}) - P_t\right] / P_t = r, \tag{2.2.1}$$

where P_t is the real stock price at the beginning of period t, D_{t+1} is the real dividend paid from the beginning to the end of period t, E_t is the mathematical expectations conditional on information available at time t, and r is the required real rate of return, $r > 0$. The market-fundamentals solution to (2.2.1) is

$$P_t^f = \sum_{j=1}^{\infty} (1+r)^{-j} \, \mathrm{E}_t D_{t+j}. \tag{2.2.2}$$

The entire class of solutions is given by $P_t = P_t^f + B_t$, where B_t is the rational bubble that satisfies the rational expectation condition

$$B_t = (1+r)^{-1} \, \mathrm{E}_t B_{t+1} \tag{2.2.3}$$

To avoid the problem of obtaining negative theoretical stock prices, in line with Wu (1997), we express the above present value model in terms of natural logarithms of price and dividend. After transforming the model in natural logarithm terms and taking linear

approximation (Campbell and Shiller, 1988), equation (2.2.1) can be written as,

$$q = \kappa + \rho \mathrm{E}_t p_{t+1} + (1-\rho)\mathrm{E}_t d_{t+1} - p_t, \tag{2.2.4}$$

where q is the required log gross return rate and ρ is the average ratio of the stock price to the sum of the stock price and the dividend, $0 < \rho < 1$. In addition, $\kappa = -\log(\rho) - (1-\rho)\log(1/\rho - 1)$, $p_t = \log(P_t)$, and $d_t = \log(D_t)$.

The unique forward-looking and no-bubble solution to (2.2.4), denoted by p_t^f, is given by

$$p_t^f = (\kappa - q)/(1-\rho) + (1-\rho)\sum_{i=1}^{\infty} \rho^{i-1}\mathrm{E}_t(d_{t+i}), \tag{2.2.5}$$

provided that the following transversality condition holds,

$$\lim_{i\to\infty} \rho^i \mathrm{E}_t(p_{t+i}) = 0. \tag{2.2.6}$$

Equation (2.2.5) is the present value relation which states that the log stock price is equal to the present value of expected future log dividend streams. Notice that if the transversality condition is violated, then (2.2.5) is only a particular solution to (2.2.4). Nevertheless, the transversality is usually hard to be satisfied in the real market. To fill this gap, a general solution to (2.2.4) brings in a bubble term which represents the difference between the stock price and its fundamental value,

$$p_t = (\kappa - q)/(1-\rho) + (1-\rho)\sum_{i=1}^{\infty} \rho^{i-1}\mathrm{E}_t(d_{t+i}) + b_t = p_t^f + b_t, \tag{2.2.7}$$

where $b_t = \lim_{i\to\infty} \rho^i \mathrm{E}_t(p_{t+i})$, which satisfies the rational expectations condition,

$$\mathrm{E}_t(b_{t+1}) = \frac{1}{\rho} b_t = (1+g)b_t, \tag{2.2.8}$$

where $g = \frac{1}{\rho} - 1 = \exp(\overline{d-p}) > 0$ is the growth rate of the bubble component in the

log stock price. Here $\overline{d-p}$ is the average log dividend-price ratio. In equation (2.2.7), the no-bubble solution p_t^f is exclusively determined by dividends and is often called the market-fundamental solution, while b_t can be driven by events extraneous to the market and is referred to as a rational speculative bubble component in the log stock price. The existence of a bubble causes the actual stock price to deviate from its market-fundamental value. Under the rational expectation condition (2.2.8), the bubble component in the log stock price, b_t, exhibits explosive behavior with a non-negative expected growth rate of g, which implies that the bubble in the original stock price, B_t, grows in expectation at the required rate of return, which is shown in (2.2.3).

It is well-known that the log dividends are non-stationary, we specify the model in its difference form. Taking the first difference of (2.2.7) yields

$$\Delta p_t = (1-\rho)\sum_{i=1}^{\infty}\rho^{i-1}\left[\mathrm{E}_t(d_{t+i}) - \mathrm{E}_{t-1}(d_{t-1+i})\right] + \Delta b_t = \Delta p_t^f + \Delta b_t. \tag{2.2.9}$$

To obtain a parsimonious specification, the log dividends can be assumed to follow an ARIMA(h,1,0) process as,

$$\Delta d_t = \mu + \sum_{j=1}^{h}\varphi_j \Delta d_{t-j} + \delta_t, \tag{2.2.10}$$

where δ_t is an i.i.d. error term and is distributed as $N(0,\sigma_\delta^2)$. The autoregressive order h in (2.2.10) is to be determined by the data.

Equation (2.2.10) can be written in the companion form,

$$Y_t = U + AY_{t-1} + \nu_t, \tag{2.2.11}$$

where $Y_t = (\Delta d_t, \Delta d_{t-1}, ..., \Delta d_{t-h+1})'$, $U = (\mu, 0, 0, ..., 0)'$, and $\nu_t = (\delta_t, 0, 0, ..., 0)'$ are

all h-vectors. In addition, $A = \begin{bmatrix} \varphi_1 & \varphi_2 & \cdots & \varphi_{h-1} & \varphi_h \\ 1 & 0 & \cdots & 0 & 0 \\ 0 & 1 & \cdots & 0 & 0 \\ \vdots & \vdots & \vdots & \vdots & \vdots \\ 0 & 0 & \cdots & 1 & 0 \end{bmatrix}$ is a $h \times h$ matrix. Therefore, equation (2.2.9) becomes

$$\Delta p_t = \Delta d_t + M \Delta Y_t + \Delta b_t, \tag{2.2.12}$$

where $M = fA(I - A)^{-1}[I - (1 - \rho)A(I - \rho A)^{-1}]$ is an h-row vector. Here $f = (1, 0, 0, ..., 0)$ is an h-row vector and I is an $h \times h$ identity matrix.

When estimating the stock price equation (2.2.12), we are confronted with the problem that the bubble component b_t is unobservable. In fact, b_t is also the only one unobserved series. Instead of directly estimating the bubble using equation (2.2.12), a more efficient way is to build up a state-space model which utilizes both the information from the measurement equation (2.2.12) and the stochastic dynamics of the bubble series.

A linear rational speculative bubble is assumed to have an AR(1) process,

$$b_t = \frac{1}{\rho} b_{t-1} + \eta_t, \tag{2.2.13}$$

where the innovation η_t is serially uncorrelated and have zero mean and finite variance σ_η^2. It is also assumed that η_t is uncorrelated with the dividend innovation, δ_t in equation (2.2.10). The above process is a straightforward and parsimonious specification satisfying the rational expectations condition (2.2.8). The AR(1) coefficient, $1/\rho$, is larger than 1 since it is equal to 1 plus the non-negative growth rate, g. The randomness of the bubble process is exclusively driven by the Gaussian innovation η_t.

2.2.2 The Linear State-space Form and the Kalman Filter

In a companion form, the above bubble-dividend-stock system can be written as the following state space model,

$$x_t = Hx_{t-1} + Ww_t, \tag{2.2.14}$$

$$z_t = Gx_t + Dg_t + Vv_t, \tag{2.2.15}$$

where

$x_t = (b_t, b_{t-1})'$ is the 2×1 vector of unobserved variable referred to as state variables;

$z_t = (\Delta d_t, \Delta p_t)'$ is the 2×1 vector of observable output variables;

$g_t = (1, \Delta d_t, \Delta d_{t-1}, ..., \Delta d_{t-h})'$ is $(h+1) \times 1)$ vector of observable input variables;

$H = \begin{bmatrix} 1/\rho & 0 \\ 1 & 0 \end{bmatrix}, G = \begin{bmatrix} 0 & 0 \\ 1 & -1 \end{bmatrix}, W = \begin{bmatrix} \sigma_\eta & 0 \\ 0 & 0 \end{bmatrix}, V = \begin{bmatrix} \sigma_\delta & 0 \\ 1 & 0 \end{bmatrix};$

$D = \begin{bmatrix} \mu & 0 & \varphi_1 & \varphi_2 & \cdots & \varphi_{h-1} & \varphi_h \\ 0 & 1+m_1 & m_2 - m_1 & m_3 - m_2 & \cdots & m_h - m_{h-1} & -m_h \end{bmatrix}$, where m_i is the i-th component of the $h \times 1$ vector M; and

w_t and v_t are i.i.d 2×1 standard normal random vectors.

The above model is linear and Gaussian with one regime, thus it is referred to as the one-regime model in subsequent analysis. Given observed stock prices and dividends, latent bubbles can be filtered by the Kalman filter (Kalman, 1960). Let $x_{t|\tau}$ denote the best linear mean-squared estimate of x_t given all observed data up to time τ, we obtain $x_{t|\tau}$ and its covariance matrix via the following equations,

$$
\begin{aligned}
x_{t+1|t} &= Hx_{t|t}, \\
P_{t+1|t} &= HP_{t|t}H' + WW', \\
S_{t+1|t} &= GP_{t+1|t}G' + VV', \\
x_{t+1|t+1} &= x_{t+1|t} + P_{t+1|t}G'S^{-1}_{t+1|t}(z_{t+1} - Gx_{t+1|t} - Dg_{t+1}), \\
P_{t+1|t+1} &= P_{t+1|t} - P_{t+1|t}G'S^{-1}_{t+1|t}Gx_{t+1|t},
\end{aligned}
\tag{2.2.16}
$$

where $P_{t+1|t} = E[(x_{t+1} - x_{t+1|t})(x_{t+1} - x_{t+1|t})']$ and $P_{t+1|t+1} = E[(x_{t+1} - x_{t+1|t+1})(x_{t+1} - x_{t+1|t+1})']$ are the error covariance matrices for $0 \leqslant t \leqslant T-1$.

The unknown parameters θ, $\theta = [\rho, \mu, \varphi, \sigma_\eta, \sigma_\delta]'$, can be estimated by maximizing the following log likelihood function,

$$
L(\theta|\mathbf{z}, \mathbf{g}) = -\frac{T}{2}\log(2\pi) - \frac{1}{2}\sum_{t=1}^{T}\log|S_{t|t-1}| - \frac{1}{2}\sum_{t=1}^{T}(z_t - Gx_{t|t-1} - Dg_t)'S^{-1}_{t|t-1}(z_t - Gx_{t|t-1} - Dg_t). \tag{2.2.17}
$$

2.3 Rational Bubble Model with Regime Switching

Many economic and financial data exhibit non-linear features with multiple regimes. This is also the case for stock bubbles. Economists characterize rational asset bubbles as those generated by extraneous events or rumors and driven by self-fulfilling expectations. One important implication of a bubble is that once it is initiated, it will grow, rapidly explode and eventually collapse, as described by Blanchard (1979), Blanchard and Watson (1982) and Evans (1991). Because the linear process in equation (2.2.13) does not capture the changing dynamics of observed data, we consider the following two-regime specification to describe the evolution of the bubble process.

2.3.1 A Two-regime Model

In this subsection, we introduce the model with two regimes. The bubble process is given by,

$$b_{t+1} = \begin{cases} (1+g_1)b_t + \eta_t^{(1)}, & \eta_t^{(1)} \sim N(0, \sigma_{\eta_1}^2) \quad \text{if } \lambda_t = 1, \\ (1+g_2)b_t + \eta_t^{(2)}, & \eta_t^{(2)} \sim N(0, \sigma_{\eta_2}^2) \quad \text{if } \lambda_t = 2, \end{cases} \tag{2.3.1}$$

where the regime-indicator λ_t ($\lambda_t = 1, 2$) is specified by a first-order Markov-process with the time-invariant transition-probability matrix

$$P = \begin{bmatrix} p_{11} & 1-p_{11} \\ 1-p_{22} & p_{22} \end{bmatrix}. \tag{2.3.2}$$

Here the transition probability from regime i to j is given by $p_{ij} = Pr[\lambda_t = j | \lambda_{t-1} = i]$.

The above transitional probability matrix implies that the unconditional probabilities of the two regimes are given by

$$\pi_1 = \frac{1-p_{22}}{2-p_{11}-p_{22}}, \ \pi_2 = \frac{1-p_{11}}{2-p_{11}-p_{22}}. \tag{2.3.3}$$

To satisfy the rational expectations condition (2.2.8), we impose the following constraint on the parameters

$$(1+g_1)\pi_1 + (1+g_2)\pi_2 = (1+g) = 1/\rho, \ g_2 < g < g_1. \tag{2.3.4}$$

The unknown parameters include μ, φ, σ_η,σ_δ,ρ, g_2, p_{11} and p_{22}. By (2.3.3) and (2.3.4), given ρ, g_2, p_{11} and p_{22}, g_1 can be uniquely determined.

Regime 1 is defined as the explosive regime since its growth rate g_1 is greater than g, which implies that the bubble component in the stock price, B_t, grows at a rate higher than the stock's required rate of return r. Regime 2 is defined as the collapsing regime since

its growth rate g_2 is less than g, which implies that B_t grows at a rate lower than r. In this two-regime Markov-switching system, the collapsing regime captures the downward shift of the bubble process. The conditional volatilities of b_t under different regimes can be different. However, for parameter parsimony, we assume that they are the same in the subsequent analysis.

Our model specification is different from and more realistic than that in Al-Anaswah and Wilfling (2011), who generate the periodically collapsing pattern of bubbles by making $1/\rho$ vary under different regimes. This implies that the asset's required rate of return switches across regimes. In the real world, asset bubbles exhibit much higher volatilities than the discount rate, as pointed out by Blanchard and Watson (1982) and Evans (1991). These researchers assume a constant discount rate while allowing the bubble process changes over time. Thus we model the bubble's growth rate as a Markov-switching process while assuming a constant required rate of return.

Empirically, Al-Anaswah and Wilfling (2011)'s estimated $1/\rho$ can sometimes be smaller than 0.5 for the U.S. market and larger than 2 for Japan, Indonesia and Malaysia, implying a negative required rate of return for the U.S. market and rates larger than 100% for the other three markets, respectively. In fact, as the average ratio of stock price to the sum of stock price and dividend, ρ should be close to but a little smaller than 1 (Campbell and Shiller, 1988), implying an expected $1/\rho$ slightly larger than 1. To get a reasonable estimate, we restrict ρ in a region, of which the lower and upper bounds are equal to the 75% and the 125% of the average ratio of the stock price to the sum of the stock price and the dividend in the full sample, respectively. Then we estimate the model parameters by Maximaum Likelihood.

2.3.2 The Piecewise Linear State-space Form with Regime Switching

The periodically collapsing bubble-dividend-stock system can be expressed as the following state space model with regime switching,

$$x_t = H_{\lambda_t} x_{t-1} + W_{\lambda_t} w_t, \tag{2.3.5}$$

$$z_t = G x_t + D g_t + V v_t, \tag{2.3.6}$$

where

$x_t = (b_t, b_{t-1})'$ is the 2×1 vector of unobserved variable referred to as state variables;

$z_t = (\Delta d_t, \Delta p_t)'$ is the 2×1 vector of observable output variables;

$g_t = (1, \Delta d_t, \Delta d_{t-1}, ..., \Delta d_{t-h})'$ is the $(h+1) \times 1$ vector of observable input variables;

$H = \begin{bmatrix} a_{\lambda_t} & 0 \\ 1 & 0 \end{bmatrix}, G = \begin{bmatrix} 0 & 0 \\ 1 & -1 \end{bmatrix}, W = \begin{bmatrix} \sigma_{\eta_{\lambda_t}} & 0 \\ 0 & 0 \end{bmatrix}, V = \begin{bmatrix} \sigma_\delta & 0 \\ 1 & 0 \end{bmatrix}$; and

$$D = \begin{bmatrix} \mu & 0 & \varphi_1 & \varphi_2 & \cdots & \varphi_{h-1} & \varphi_h \\ 0 & 1+m_1 & m_2 - m_1 & m_3 - m_2 & \cdots & m_h - m_{h-1} & -m_h \end{bmatrix}.$$

2.4 Estimation with the Mixture Kalman Filter

2.4.1 States Filtering

The state-space model with regime switching poses a significant change for states filtering and parameter estimation. According to the state transition equation (2.3.5) with regime switching, the state distribution is now a mixture of Gaussian. $p(x_t|\boldsymbol{z}_t)$ can no longer be calculated in closed form as in Kalman filter. Numerical methods, such as Monte Carlo approximation techniques, will be needed to estimate $p(x_t|\boldsymbol{z}_t)$. Chen and Liu (2000) propose a Rao-Blackwellised sequential Monte Carlo method, called the mixture Kalman

filter (MKF), and demonstrate the consistency and efficiency in dealing with the conditional dynamic linear system. The MKF marginalizes out the linear state variables and uses the sequential Monte Carlo method to approximate the regime indicator. Then given a trajectory of regime indicators, the Kalman filter can be implemented to filter the linear state variables. By doing so, the MKF can achieve a much smaller Monte Carlo variation than that of a sequential Monte Carlo method applied directly to the full state space. Furthermore, the MKF provides an unbiased estimate of the likelihood function, which is used for parameter estimation and model evaluation.

The MKF goes as follows: Let $\boldsymbol{z}_t = (z_1, ..., z_t)$ be the sequence of observations and $\boldsymbol{\Lambda}_t = (\Lambda_1, ..., \Lambda_t)$ be the sequence of regime indicators. Let $\boldsymbol{\lambda}_t$ and λ_s be realizations of $\boldsymbol{\Lambda}_t$ and Λ_s, respectively. We observe that

$$p(x_t|\boldsymbol{z}_t) = \int p(x_t|\boldsymbol{\lambda}_t, \boldsymbol{z}_t) p(\boldsymbol{\lambda}_t|\boldsymbol{z}_t) d\boldsymbol{\lambda}_t, \tag{2.4.1}$$

where $p(x_t|\boldsymbol{\lambda}_t, \boldsymbol{z}_t) \sim N\{\boldsymbol{\mu}_t(\boldsymbol{\lambda}_t), \boldsymbol{\Sigma}_t(\boldsymbol{\lambda}_t)\}$, in which $\{\boldsymbol{\mu}_t(\boldsymbol{\lambda}_t), \boldsymbol{\Sigma}_t(\boldsymbol{\lambda}_t)\}$ can be obtained by running the Kalman filter with a given trajectory $\boldsymbol{\Lambda}_t$. The main idea of the MKF is to use a weighted Monte Carlo sample of the indicators,

$$\boldsymbol{S}_t = \{(\boldsymbol{\lambda}_t^{(1)}, w_t^{(1)}), ..., (\boldsymbol{\lambda}_t^{(m)}, w_t^{(m)})\}, \tag{2.4.2}$$

to represent the distribution $p(\boldsymbol{\Lambda}_t|\boldsymbol{z}_t)$. In detail, we sample $\boldsymbol{\lambda}_t^{(j)},\ j = 1, ..., m$ from a preselected trial distribution $q(\boldsymbol{\lambda}_t|\boldsymbol{z}_t, \boldsymbol{x}_t)$ and assign $w_t^{(j)} = p(\boldsymbol{\lambda}_t|\boldsymbol{z}_t)/q(\boldsymbol{\lambda}_t|\boldsymbol{z}_t, \boldsymbol{x}_t)$. The target distribution $p(x_t|\boldsymbol{z}_t)$ is approximated by the mixture of Gaussian distribution

$$\frac{1}{W_t} \sum_{j=1}^{m} w_t^{(j)} N\{\boldsymbol{\mu}_t(\boldsymbol{\lambda}_t^{(j)}), \boldsymbol{\Sigma}_t(\boldsymbol{\lambda}_t^{(j)})\}, \tag{2.4.3}$$

where $W_t = \sum_{j=1}^{m} w_t^{(j)}$. For any integrable function $h(\cdot)$, we can estimate the quantity of

interest $E\{h(x_t)|\boldsymbol{z}_t\}$ as

$$\hat{E}\{h(x_t)|\boldsymbol{z}_t\} = \frac{1}{W_t}\sum_{j=1}^{m} w_t^{(j)} \int h(x)\phi\{x; \boldsymbol{\mu}_t(\boldsymbol{\lambda}_t^{(j)}), \boldsymbol{\Sigma}_t(\boldsymbol{\lambda}_t^{(j)})\}dx, \tag{2.4.4}$$

where ϕ is the Gaussian density function.

Let $\text{KF}_t^{(j)} = (\boldsymbol{\mu}_t(\boldsymbol{\lambda}_t^{(j)}), \boldsymbol{\Sigma}_t(\boldsymbol{\lambda}_t^{(j)}))$ record the posterior mean and covariance matrix of x_t, conditional on $\boldsymbol{z}_t$ and a given trajectory $\boldsymbol{\lambda}_t^{(j)}$, which can be obtained by the Kalman filter. Then the MKF updating scheme consists of recursive applications of the following steps.

For $j = 1, ..., m$:

(a) generate $\lambda_{t+1}^{(j)}$ from its predicative distribution $p(\lambda_{t+1}|\boldsymbol{\lambda}_t^{(j)}, \text{KF}_t^{(j)}, y_{t+1})$;

(b) obtain $\text{KF}_{t+1}^{(j)}$ by a one-step Kalman filter, conditional on $\{\text{KF}_t^{(j)}, z_{t+1}, \lambda_{t+1}^{(j)}\}$,

$$\begin{aligned}
P_{t+1} &= H_{\lambda_{t+1}}\Sigma_t H'_{\lambda_{t+1}} + W_{\lambda_{t+1}}W'_{\lambda_{t+1}}, \\
S_{t+1} &= GP_{t+1}G' + VV', \\
\mu_{t+1} &= H_{\lambda_{t+1}}\mu_t + P_{t+1}G'S_{t+1}^{-1}(z_{t+1} - GH_{\lambda_{t+1}}\mu_t - Dg_{t+1}), \\
\Sigma_{t+1} &= P_{t+1} - P_{t+1}G'S_{t+1}^{-1}GP_{t+1};
\end{aligned} \tag{2.4.5}$$

(c) update the new weight as $w_{t+1}^{(j)} = w_t^{(j)} \times u_{t+1}^{(j)}$, where

$$\begin{aligned}
u_{t+1}^{(j)} &= \frac{p(\boldsymbol{\lambda}_t^{(j)}, \lambda_{t+1}^{(j)}|\boldsymbol{z}_{t+1})}{p(\boldsymbol{\lambda}_t^{(j)}|\boldsymbol{z}_t)p(\lambda_{t+1}^{(j)}|\boldsymbol{\lambda}_t^{(j)}, \text{KF}_t^{(j)}, y_{t+1})} \\
&\propto p(z_{t+1}|\text{KF}_t^{(j)}) \\
&= \sum_{i\in I} p(z_{t+1}|\Lambda_{t+1} = i, \text{KF}_t^{(j)})p(\Lambda_{t+1} = i|\boldsymbol{\lambda}_t^{(j)}).
\end{aligned} \tag{2.4.6}$$

Here I is the set of possible values of Λ_t, i.e., $I = \{1, 2\}$ for the two-regime model. Specifically, the MKF updating step (c) can be implemented by the following steps:

(c.1) for each $\Lambda_{t+1} = i,\ i \in I$, run the Kalman filter to obtain

$$v_i^{(j)} \propto p(z_{t+1}|\Lambda_{t+1} = i, \mathrm{KF}_t^{(j)}) p(\Lambda_{t+1} = i|\boldsymbol{\lambda}_t^{(j)}), \tag{2.4.7}$$

where $p(\Lambda_{t+1} = i|\boldsymbol{\lambda}_t^{(j)})$ is the prior transition probability for the indicator and $p(z_{t+1}|\Lambda_{t+1} = i, \mathrm{KF}_t^{(j)})$ is a by-product of the Kalman filter

$$p(z_{t+1}|\boldsymbol{z}, \boldsymbol{\lambda_t}, \lambda_{t+1}) \sim N(GH_{\lambda_{t+1}}\mu_t + Dg_{t+1}, S_{t+1}), \tag{2.4.8}$$

(c.2) sample a $\lambda_{t+1}^{(j)}$ from the set I, with probability proportional to $v_t^{(j)}$,

(c.3) let $\mathrm{KF}_{t+1}^{(j)}$ be the one with $\Lambda_{t+1} = \lambda_{t+1}^{(j)}$,

(c.4) the new weight is $w_{t+1}^{(j)} = w_t^{(j)} \sum_{i\in\{1,2\}} v_i^{(j)}$.

(d) (resampling-rejuvenation) if the coefficient of variance of the w_{t+1} exceeds a threshold value, resample a new set of KF_{t+1} from $\{\mathrm{KF}_t^{(1)}, ..., \mathrm{KF}_t^{(m)}\}$ with probability proportional to the weights $w_{t+1}^{(j)}$.

2.4.2 Parameter Estimation

Given all parameters and times series of observable input and output variables, the log likelihood of a state-space model with regime switching is obtained by runing the MKF. It has an explicit formula as follows,

$$\hat{l}(\theta|\mathbf{z}, \mathbf{g}) = \log\Big(\sum_{j=1}^{m} w_T^{(j)}\Big), \tag{2.4.9}$$

where θ is the vector including all parameters. Therefore, we can estimate θ by maximizing this function.

The above objective function is discontinous and noisy since it is calculated based on simulation. So the traditional gradient-based method can not be used for optimization. We

adopt the Covariance Matrix Adaptation Evolution Strategy (CMA-ES)[1] (Hansen, 2006), an evolutionary algorithm for difficult non-linear non-convex black-box optimisation problems in continuous domain, to do maximum likelihood estimation. This method is feasible on non-smooth and even non-continuous problems, as well as on multimodal and/or noisy problems. Compared with other optimization methods that handle non-continuous and noisy problems, such as stochastic approximation, one advantage of the CMA-ES is that it fast converges to the global optimal solution.

2.4.3 Model Evaluation

The log-likelihood can be used to compute several criteria for model selection, for example, Akaike information criterion (AIC) (Akaike, 1974) given by

$$\text{AIC} = 2k - 2\hat{l}, \tag{2.4.10}$$

where k is the number of parameters. AIC can be directly used to measure the goodness of fit for a model. The smaller AIC, the better the model fits the data. Another tool of model evaluation is Bayesian Information Criterion (BIC) (Schwarz, 1978), which is defined as

$$\text{BIC} = \log(n)k - 2\hat{l}, \tag{2.4.11}$$

where n is the number of data points. When fitting models, it is possible to increase the likelihood by adding parameters, but doing so may result in overfitting. Both BIC and AIC attempt to resolve this problem by introducing a penalty term for the number of parameters in the model. The penalty term is larger in BIC than in AIC when the sample size is larger than 7.

[1]The matlab, python, C++ and R source codes can be downloaded from Nikolaus Hansen's website: http://cma.gforge.inria.fr/cmaesintro.html.

In addition, we can also use the likelihood ratio test (LR test) for comparing the goodness of fit of two models —- a null model against an alternative model. Suppose model M_1 has parameters $\theta = (\theta^{(1)}, \theta^{(2)})$ while its subset model M_0 has parameters $\theta = (\mathbf{0}, \theta^{(2)})$. $l_0(M_0)$ and $l_1(M_1)$ are their maximums of log likelihood. Then the α level test to reject M_0 in favor of M_1 is $D = 2\{l_1(M_1) - l_0(M_0)\} > c_\alpha$, where c_α is the $(1-\alpha)$ quantile of χ^2_k.

2.5 Estimation Results and Empirical Analysis

In this section we apply both the one-regime model with the Kalman filter and our proposed two-regime model with the MKF to both simulated observations and actual US stock data. In order to obtain the former, we simulate the stock price, dividend, and bubble observations following Evans (1991). For the latter, we study the S&P-500 and the NASDAQ indices for the past three decades.

2.5.1 Bubble Estimation for the Simulated Data

2.5.1.1 Simulation by the Evans (1991) Process

We follow Evans (1991) to simulate periodically collapsing bubbles and the associated stock price and dividend series. Bubbles are assumed to follow the process,

$$B_{t+1} = \begin{cases} (1+r)B_t u_{t+1}, & \text{if } B_t \leq \alpha, \\ \left[\delta + \frac{1+r}{\pi}(B_t - \frac{\delta}{1+r})\xi_{t+1}\right] u_{t+1}, & \text{if } B_t > \alpha, \end{cases} \tag{2.5.1}$$

where δ and α are positive parameters such that $0 < \delta < (1+r)\alpha$. $\{u_t\}$ is a sequence of non-negative exogenous i.i.d lognormal variables with $E_t(u_{t+1}) = 1$. Here we assume $\{u_t\}$ to be i.i.d. lognormally distributed and scaled to have unit mean, i.e., $u_t = \exp(y_t - \frac{\tau^2}{2})$ with $\{y_t\}$ being i.i.d. $N(0, \tau^2)$. $\{\xi_t\}$ is an exogenous i.i.d Bernoulli process independent of $\{u_t\}$ with $Pr(\xi_t = 0) = 1 - \pi$ and $Pr(\xi_t = 1) = \pi$ for $0 < \pi < 1$. The data-generating

process for the dividend follows a pure random walk, $D_t = D_{t-1} + \epsilon_t$, where $\{\epsilon_t\}$ is a Gaussian white-noise process with mean zero and variance σ_ϵ^2. Thus the fundamental stock price is $P_t^F = \sum_{j=1}^{\infty} (1+r)^{-j} \, \mathrm{E}_t D_{t+j} = D_t/r$, and the stock price is $P_t = P_t^F + B_t$.

Table 2.1 lists three sets of parameters for simulating the Evans (1991)'s data. The first set of parameters in column 1 is identical to that in Evans (1991). When we simulate the bubble process, B_t is scaled up by a factor of 20 in order to make the simulated bubbles generate about 75% of the variance of stock price changes, in line with Evans (1991). The second set of parameters in column 2 is equal to the first set except that π is 0.6, decreasing from 0.85 in the first set. A smaller π means a higher probability for bubbles to collapse in each period. The third set of parameters in column 3 is the same as the first set except that α is 0.5, decreasing from 1 in the first set. A smaller value of α relative to δ generates more frequent eruptions. For each parameter specification, we simulate one trajectory for model comparison.

2.5.1.2 Bubble Estimation

The left, central and right panels in Figure 2.1 show the estimated bubbles B_t in three stock price series simulated by the Evans model with the first, second and third parameter specifications, respectively. The B_t estimated by the one-regime switching model (in dashed red line) and that estimated by the two-regime model (in dashed blue line) are shown in the upper part of each panel. B_t is transformed from b_t, which is the filtered bubble component in the log simulated stock price. The simulated stock price (P), real fundamental price (dividend divided by the discount rate, D/r), and bubbles ($B \times 20$) are presented in green, magenta and black solid lines, respectively. The lower part of each panel shows the filtered probabilities of the collapsing regime (in blue solid line) estimated from the two-regime model.

Using our mixture Kalman filter, we can filter out the bubble series and estimate the

probability of bubble collapsing. For all three simulated series, we can see that the estimated bubbles of the two-regime model track the simulated bubbles fairly well during most of the sample period. Furthermore, we superimpose bubbles estimated by the one-regime model and find that the two-regime model estimates bubbles more accurately than the one-regime model. Because of the nature of filtering methods, both models estimate bubbles with relatively large tracking errors in the early part of sample. Take the first Evans process as an example. During the first 30 time periods, bubbles estimated by both models deviate from the simulated bubbles by relatively big margin. After that, bubbles estimated by the two-regime model are very close to the simulated bubbles. In contrast, the estimated bubbles of the one-regime model tend to overshoot the actual bubbles when bubbles explode and undershoot when bubbles collapse. The fundamental reason behind this is that our specification of the regime-switching bubble process is more consistent with the nature of the periodically collapsing one.

To formally conduct the comparison of two models, we compute the Root Mean Square Error (RMSE) between simulated bubbles and the estimated bubbles for each simulated Evans process (see Table 2.8). We can see that the RMSE of the two-regime model is much lower than that of the one-regime model, suggesting that our regime-switching model can estimate bubbles more accurately.

When major bubbles collapse, the filtered probability of collapsing (in solid blue line) increases dramatically from 0 to nearly 1, suggesting that it can be used as a powerful tool to judge whether a collapse happens. In practise, this insight is useful to understand the current state of the market and update our belief about future based on the estimated transition probability. However, the one-regime model does not provide such important information.

One feature of the simulated Evans bubble series, which aligns the equation (2.5.1), is that collapses are relatively sudden and strong. The Evans process approximates the reality

by creating a threshold (α), under which the bubble is rationally growing. However once the bubble grows out of the threshold, it starts to explode faster than the rational growing speed and be accompanied with a probability (1-π) to collapse to a certain low level, after which the bubble continues to survive again. From the first parameter specification to the second one, we reduce π from 0.85 to 0.60, which implies that the probability of collapsing increases. Consistent with this model setup, we can observe that there are more frequent collapses in the central panel than in the left panel. The same pattern is also observed when we reduce the threshold α from 1 (in the left panel) to 0.5 (in the right panel).

Table 2.2, 2.3 and 2.4 show the model evaluation statistics, estimated parameters and implied parameters of the one-regime and two-regime models for the simulated data series using the first, second, and third model specifications of the Evans process, respectively. The upper panel of each table includes several model evaluation criteria, including the log likelihood, AIC and BIC, for each model. In addition, we report the likelihood ratio tests (LRT) of the two-regime model over the one-regime model. The $p-$value of LRT is presented in parentheses. For the parameter estimation, we report both the estimated parameter and standard errors (in parentheses) in the middle panel. Moreover, some implied parameters, which are helpful for us to understand the bubble process, are presented in the bottom panel. The parameters include the expected growth rate of b_t (g), the growth rate of b_t under two regimes (g_1 and g_2), as well as the steady probabilities of two two regimes (π_1 and π_2).

A quick glance at the model selection criteria reveals that the model with two regimes are more preferable. For example, for the process 1 in Table 2.2, after the number of regimes increase from 1 to 2, the log likelihood increases from 388.21 to 646.04, while the AIC (BIC) decreases from -764.42 (-744.69) to -1274.08 (-1244.48). The LRT of the two-regime model over the one-regime model is significant at the 1% level. Based on the estimated and implied parameters, we find that the estimated growth rate in the collapsing state (g_2 in the two-regime model) is very negative and close to -100% for three simulated

series, which are consistent with the fact that a bubble in the Evans process drops to a constant value only in one step when it collapses. Both the transition probability from the collapsing state to itself and the unconditional probability of the collapsing state are small, suggesting that the collapsing state is temporary for the Evans process.

2.5.2 Bubble Estimation for the U.S. Data

2.5.2.1 Data

The data we use for estimating stock bubbles are the U.S. stock market indices including the S&P 500 and NASDAQ indices along with their corresponding dividend series. We obtain the monthly real S&P 500 and its dividend yield series from the online data of Robert Shiller [2]. We acquire the monthly nominal NASDAQ index and its dividend series from DataStream, then obtain the real counterparts by adjusting them with the CPI Index, which is also from the online data of Robert Shiller. Our sample period starts from January 1985 to August 2018, which covers several recent major financial crisis (the 1987 Black Monday, 2000-2002 Dot-com bubble and 2007-2009 financial crisis) in the past three decades. We choose 1985 as the beginning of the sample period, because at that time the US aggregated stock price is close to its fundamental value according to Wu (1997).

2.5.2.2 Evidence from the S&P 500 Index

The upper left panel in Figure 2.2 shows the estimated bubbles (in dashed green lines) in monthly SP500 index, B_t, from 1985.1 to 2018.8 by the two-regime model. B_t is transformed from b_t, which is the filtered bubble component in the log real stock price. We normalize the real stock price and real dividend to 1 in the beginning of the sample period and present them in green and magenta solid lines. The bottom left panel shows the filtered

[2] see http://www.econ.yale.edu/ shiller/data.htm

probabilities of the collapsing regime (in blue solid line) estimated from the two-regime model.

From the filtered probabilities of the collapsing states of the two-regime model, we can see that they successfully date stamps major crisis since 1985, including the Black Monday in 1987, the Dot-com bubble from 2000 to 2002, and the global financial crisis from 2007 to 2009, when there are several jumps towards 1 for filtered probabilities of the collapsing state, while for most of the sample period, the probabilities remain close to 0.

Table 2.5 shows the summary for estimating the one-regime and two-regime models using the real price and dividend data of the SP500 index, including model evaluation, estimated parameters and implied parameters. The structure of the tables is similar to that of previous Table. By checking the model selection criteria, we can conclude that the two-regime model outperforms the one-regime model. For example, after the number of regimes increase from 1 to 2, the log likelihood increases from 2388.32 to 2399.66, while the AIC (BIC) decreases from -4764.63 (-4740.67) to -4781.31 (-4745.37). The LRT of the two-regime model over the one-regime model is significant at the 1% level. We find that the estimated growth rate in the collapsing state (g_2 in the two regime model) here is milder than that of the three Evans processes (-6.5% vs nearly -100%). This indicates that in reality the crash of bubbles is less abrupt and rapid than that implied by the Evans process.

2.5.2.3 Evidence from the NASDAQ Index

The upper right and lower right panels in Figure 2.4 show the bubble estimation results of the two-regime model for the NASDAQ index. Similar to the S&P 500, we can see that filtered probabilities of the collapsing state can also detect three major crises successfully over the sample periodt. There appears to be more bubble crashes from 2000 to 2003 for the NASDAQ index than for the S&P 500. This is consistent with the fact that the NASDAQ

index includes more small-cap and high-tech stocks, whose prices drop more dramatically and frequently during the internet bubble period.

Table 2.6 shows the summary for estimating the one-regime and two-regime models using the real price and dividend data of the NASDAQ index, including model evaluation, estimated parameters and implied parameters. According to the model selection criteria, the two-regime model beats the one-regime model. For example, after switching from the one-regime model to the two-regime model, the log likelihood increases from 750.34 to 767.71, while the AIC (BIC) decreases from -1488.68 (-1464.71) to -1517.42 (-1481.48). The LRT rejects the one-regime model at the 1% level in flavor of the two-regime model. We find that the NASDAQ bubbles burst more rapidly than the S&P 500 bubbles in the collapsing state (g_2 is -13.5% instead of -6.5%), which is consistent with a higher volatility and risk level of the NASDAQ index.

2.6 Extension

The bubble dynamics can be quite complex. Whether the two-regime specification is sufficient to fully capture its evolution is an empirical issue. In this section, we extend the model to a three-regime version and discuss its implications.

2.6.1 A Three-regime Model

It might be more realistic to consider a model with three regimes to depict the bubble dynamics. In the real world, a bubble may start with a period that most investors are rational and correspondingly it grows with the stock's required rate of return. Then gradually the bubble grows out of control with an "explosive" growth rate larger than the discount rate, until it breaks down with a "collapsing" growth rate smaller than than the discount rate. In addition, according to Brunnermeier (2009), after a bubble collapses, it typically

recovers quickly, with a growth rate probabily greater than the discount rate. In order to accommodate these patterns, we specify our model as follows,

$$b_{t+1} = \begin{cases} (1+g_1)b_t + \eta_t^{(1)}, & \eta_t^{(1)} \sim N(0, \sigma_{\eta_1}^2) \quad \text{if } \lambda_t = 1, \\ (1+g_2)b_t + \eta_t^{(2)}, & \eta_t^{(2)} \sim N(0, \sigma_{\eta_2}^2) \quad \text{if } \lambda_t = 2, \\ (1+g_3)b_t + \eta_t^{(3)}, & \eta_t^{(3)} \sim N(0, \sigma_{\eta_3}^2) \quad \text{if } \lambda_t = 3, \end{cases} \tag{2.6.1}$$

where $g_1 = g = 1/\rho - 1$ and $g_3 < g < g_2$.

Regime 1 is the normal regime since the b_t's growth rate g_1 is identical to g, which implies that the bubble component in the stock price, B_t, grows at the stock's required rate of return r. Regime 2 is the exploding regime under which the b_t's growth rate g_2 is greater than g, implying that B_t grows at a rate higher than r. Under Regime 3, B_t grows at a rate lower than r, implying a bubble is bursting, and this is regarded as a collapsing regime. In addition, conditional volatilities of b_t under different regimes can be different. However, for parsimony purpose, we assume they are the same in the subsequent analysis.

The transition probability matrix of the three-regime model is

$$P = \begin{bmatrix} p_{11} & p_{12} & 1 - p_{11} - p_{12} \\ p_{21} & p_{22} & 1 - p_{21} - p_{22} \\ p_{31} & p_{32} & 1 - p_{31} - p_{32} \end{bmatrix}. \tag{2.6.2}$$

Following Kim and Nelson (1999), the unconditional probabilities for three regimes are

$$\begin{bmatrix} \pi_1 & \pi_2 & \pi_3 \end{bmatrix}' = (Q'Q)^{-1} Q' \begin{bmatrix} 0_{3\times 1} \\ 1 \end{bmatrix}, \quad Q = \begin{bmatrix} I_{3\times 3} - P' \\ 1_{1\times 3} \end{bmatrix}. \tag{2.6.3}$$

To satisfy the rational expectation condition (2.2.8), we constraint the parameters as

follows,

$$g\pi_1 + g_2\pi_2 + g_3\pi_3 = 1/\rho - 1 = g. \tag{2.6.4}$$

In estimation, the unknown parameters include μ, φ, σ_η, σ_δ, ρ, g_3, p_{11}, p_{12}, p_{21}, p_{22}, p_{31} and p_{32}. By (2.6.3) and (2.6.4), given ρ, g_3 and the transition probability matrix P, g_2 can be uniquely determined.

We use the above model to estimate the bubbles of the U.S. stock market and let the data determine the optimal parameters. However, when we use this model to estimate the simulated data, the model can be parsimoniously reduced to a simpler version based on the characteristics of the underlying structure, with the transition probability matrix as

$$P = \begin{bmatrix} p_{11} & 1-p_{11} & 0 \\ 0 & p_{22} & 1-p_{22} \\ 1-p_{33} & 0 & p_{33} \end{bmatrix}. \tag{2.6.5}$$

The unconditional probabilities of three regimes can be calculated as follows,

$$\pi_1 = \frac{q_{11}^{-1}}{q_{11}^{-1}+q_{22}^{-1}+q_{33}^{-1}},\ \pi_2 = \frac{q_{22}^{-1}}{q_{11}^{-1}+q_{22}^{-1}+q_{33}^{-1}},\ \pi_3 = \frac{q_{33}^{-1}}{q_{11}^{-1}+q_{22}^{-1}+q_{33}^{-1}}, \tag{2.6.6}$$

where $q_{ii} = 1 - p_{ii},\ i = 1, 2, 3$. Based on the rational expectation condition (2.6.4), we can derive the following parameter constraint,

$$q_{22}(a_1 - a_3) = q_{33}(a_2 - a_1). \tag{2.6.7}$$

2.6.2 Empirical Results

The left, central and right panels in Figure 2.3 show the estimated bubbles B_t (in dashed blue lines) by the three-regime model in three simulated data series. The lower part of each panel shows the filtered probabilities of the collapsing regime (in blue solid line) and the

exploding regime (in red dashed line) estimated from the three-regime model. Similar to the two-regime model, our three-regime model can estimate bubbles that track the simulated bubbles fairly well during most of the sample period. To formally conduct the comparison of two models, (Add RMSE and DM test here.). One advantage of the three-regime model over the two-regime one is that it provides the filtered probability of the exploding state. It increases from 0 to 1 gradually before bubbles suddenly collapse, after which it drops to zero immediately. This phenomenon is consistent with the nature of the Evans process.

Table 2.7 shows the model evaluation statistics, parameter estimation and implied parameters of the 3-regime models for the three simulated data series. The model selection criteria reveals that the three-regime model outperforms the two-regime model. For example, for the first simulated data, after the number of regimes increase from 2 to 3, the log likelihood increases from 646.04 to 666.01, while the AIC (BIC) decreases from -1274.08 (-1244.48) to -1312.02 (-1279.14). The LRT of the three-regime model over the two-regime model is significant at the 1% level. The predominance of the three-regime model stems from the fact that the the state transitional process is consistent with that of the simulated data, which recursively follows the order of rational surviving, exploding, and collapsing.

The left and right panels in Figure 2.4 show the estimated B_t (in dashed blue lines) as well as the filtered probabilities of the collapsing (in blue solid line) and exploding states (in red dashed line) in the monthly SP500 and NASDAQ indices by the three-regime model, respectively. Based on these probabilities, we can observe that bubbles not only collapse after it explodes, but also burst more unexpectedly in real life. More often a crisis happens while the bubble is still rationally growing. Before the major collapses except Black Monday, most periods are considered as the normal regime. Therefore, the model that forces the bubble to collapse only after exploding may be too restricted. Furthermore, the estimation based on the U.S. stock data shows that bubbles can also explode immediately after collapsing, which is consistent with Brunnermeier (2016), who states that periodically bursts of bubbles are typically followed by dramatic price increases.

Table 2.9 shows the model evaluation statistics, parameter estimation and implied parameters of the 3-regime models for the S&P 500 and NASDAQ indices. After switching from the two-regime model to the three-regime one, the log likelihood increases and AIC decreases. The LRT rejects the two-regime model in favor of the three-regime model at the conventional significance levels. However, BIC increases from -4745.37 (-1481.48) to -4733.03 (-1476.00) for the S&P 500 (NASDAQ) index, indicating some evidence of model over-fitting.

2.7 Conclusion

The article proposes a new framework for modeling the rational stock bubble process with periodically collapsing. A set of discrete conditional dynamic linear models is introduced to capture the regime-switching characteristics of speculative bubbles. We formulate the joint process of stock prices and dividends as well as latent bubbles as a state-space model with regime-switching. We employ a sequential Monte Carlo method, called the mixture Kalman Filter, to estimate the model parameters and the unobservable bubble process. To our knowledge, our paper is the first to implement this novel methodology in finance.

Using both simulated observations as well as the U.S. stock data, we demonstrate the superiority of our state-space model with regime switching over the traditional model without regime change. Specifically, our model exhibits substantial enhancement in the goodness-of-fit measured by standard model evaluation criteria. Second, the formal likelihood ratio test all rejects the traditional model without regime-switching at conventional significance levels in favor of our models with regime switching. Third, our model tracks the actual bubble process more accurately than the traditional model. The DM test demonstrates that our models outperforms the traditional model in terms of the RMSE of the bubble estimation. Finally, our model exhibits a strong capability in date stamping of the

bubble collapsing periods. In particular, our model can successfully capture the major financial crises over the past three decades.

Table 2.1: Parameter Specifications for the Evans Bubble Process

	Process 1	Process 2	Process 3
B_0	0.5000	0.5000	0.5000
τ^2	0.0025	0.0025	0.0025
r	0.0500	0.0500	0.0500
δ	0.5000	0.5000	0.5000
D_0	1.3000	1.3000	1.3000
σ_ϵ^2	0.1574	0.1574	0.1574
α	1.0000	1.0000	0.5000
π	0.8500	0.6000	0.8500
Scaling factor of the bubble	20	20	20
Number of observations	100	100	100

Table 2.2: Estimation Summary of the One-Regime and Two-Regime Models for the Evans Process 1

This table shows the model evaluation statistics, estimated parameters and implied parameters of the one-regime and two-regime models for the simulated data series using the first specification of the Evans process. The upper panel of each table includes several model evaluation criteria, including the log likelihood, AIC and BIC, for each model. In addition, we report the likelihood ratio tests (LRT) of the two-regime model over the one-regime model. The $p-$value of LRT is presented in parentheses. For the parameter estimation, we report both the estimated parameter and standard errors (in parentheses) in the middle panel. Moreover, some implied parameters, which are helpful for us to understand the bubble process, are presented in the bottom panel. The parameters include the expected growth rate of b_t (g), the growth rate of b_t under two regimes (g_1 and g_2), as well as the steady probabilities of two two regimes (π_1 and π_2).

	1-Regime			2-Regimes		
Model	loglike	388.21		loglike	646.04	
Evaluation	AIC	-764.42		AIC	-1274.08	
	BIC	-744.69		BIC	-1244.48	
				LRT over 1R	515.66	(0.0000)
Estimated	μ	0.0061	(0.0046)	μ	0.0036	(0.0067)
Parameters	ψ_1	0.0347	(0.0173)	ψ_1	-0.0526	(0.0128)
	ψ_2	-0.1474	(0.0212)	ψ_2	-0.0615	(0.0116)
	σ_δ	0.0926	(0.0027)	σ_δ	0.0937	(0.0047)
	σ_η	0.0885	(0.0016)	σ_η	0.0202	(0.0011)
	ρ	0.9702	(0.0081)	ρ	0.9702	(0.0023)
				$1+g_2$	0.0000	(0.0243)
				p_{11}	0.9437	(0.0016)
				p_{22}	0.5952	(0.0359)
Implied	r	0.0307		r	0.0307	
Parameters	g_1			g_1	0.1741	
	g_2			g_2	-1.0000	
	π_1			π_1	0.8778	
	π_2			π_2	0.1222	

Table 2.3: Estimation Summary of the One-Regime and Two-Regime Models for the Evans Process 2

This table shows the model evaluation statistics, estimated parameters and implied parameters of the one-regime and two-regime models for the simulated data series using the second specification of the Evans process. The upper panel of each table includes several model evaluation criteria, including the log likelihood, AIC and BIC, for each model. In addition, we report the likelihood ratio tests (LRT) of the two-regime model over the one-regime model. The $p-$value of LRT is presented in parentheses. For the parameter estimation, we report both the estimated parameter and standard errors (in parentheses) in the middle panel. Moreover, some implied parameters, which are helpful for us to understand the bubble process, are presented in the bottom panel. The parameters include the expected growth rate of b_t (g), the growth rate of b_t under two regimes (g_1 and g_2), as well as the steady probabilities of two two regimes (π_1 and π_2).

	1-Regime			2-Regimes		
Model	loglike	328.45		loglike	530.47	
Evaluation	AIC	-644.90		AIC	-1042.95	
	BIC	-625.17		BIC	-1013.35	
				LRT over 1R	404.05	(0.0000)
Estimated	μ	0.0094	(0.0068)	μ	0.0135	(0.0068)
Parameters	ψ_1	0.0402	(0.0455)	ψ_1	-0.0590	(0.0202)
	ψ_2	-0.0535	(0.0437)	ψ_2	-0.0018	(0.0179)
	σ_δ	0.0957	(0.0051)	σ_δ	0.0960	(0.0048)
	σ_η	0.1159	(0.0092)	σ_η	0.0349	(0.0010)
	ρ	0.9695	(0.0443)	ρ	0.9694	(0.0160)
				$1+g_2$	0.0278	(0.0280)
				p_{11}	0.8391	(0.0123)
				p_{22}	0.4137	(0.0144)
Implied	r	0.0314		r	0.0315	
Parameters	g_1			g_1	0.3069	
	g_2			g_2	-0.9722	
	π_1			π_1	0.7847	
	π_2			π_2	0.2153	

Table 2.4: Estimation Summary of the One-Regime and Two-Regime Models for the Evans Process 3

This table shows the model evaluation statistics, estimated parameters and implied parameters of the one-regime and two-regime models for the simulated data series using the third specification of the Evans process. The upper panel of each table includes several model evaluation criteria, including the log likelihood, AIC and BIC, for each model. In addition, we report the likelihood ratio tests (LRT) of the two-regime model over the one-regime model. The $p-$value of LRT is presented in parentheses. For the parameter estimation, we report both the estimated parameter and standard errors (in parentheses) in the middle panel. Moreover, some implied parameters, which are helpful for us to understand the bubble process, are presented in the bottom panel. The parameters include the expected growth rate of b_t (g), the growth rate of b_t under two regimes (g_1 and g_2), as well as the steady probabilities of two two regimes (π_1 and π_2).

	1-Regime			2-Regimes		
Model	loglike	369.33		loglike	549.58	
Evaluation	AIC	-726.65		AIC	-1081.16	
	BIC	-706.92		BIC	-1051.57	
				LRT over 1R	360.51	(0.0000)
Estimated	μ	0.0123	(0.0073)	μ	-0.0036	(0.0075)
Parameters	ψ_1	-0.1366	(0.0497)	ψ_1	-0.0822	(0.0175)
	ψ_2	-0.0056	(0.0419)	ψ_2	-0.0579	(0.0181)
	σ_δ	0.1032	(0.0056)	σ_δ	0.1056	(0.0053)
	σ_η	0.0873	(0.0030)	σ_η	0.0297	(0.0016)
	ρ	0.9692	(0.2973)	ρ	0.9619	(0.0128)
				$1+g_2$	0.1265	(0.0374)
				p_{11}	0.9241	(0.0020)
				p_{22}	0.2300	(0.1420)
Implied	r	0.0318		r	0.0396	
Parameters	g_1			g_1	0.1297	
	g_2			g_2	-0.8735	
	π_1			π_1	0.9102	
	π_2			π_2	0.0898	

Table 2.5: Estimation Summary of the One-Regime and Two-Regime Models for the S&P 500 Index

This table shows the model evaluation statistics, estimated parameters and implied parameters of the one-regime and two-regime models for the S&P 500 Index. The upper panel of each table includes several model evaluation criteria, including the log likelihood, AIC and BIC, for each model. In addition, we report the likelihood ratio tests (LRT) of the two-regime model over the one-regime model. The $p-$value of LRT is presented in parentheses. For the parameter estimation, we report both the estimated parameter and standard errors (in parentheses) in the middle panel. Moreover, some implied parameters, which are helpful for us to understand the bubble process, are presented in the bottom panel. The parameters include the expected growth rate of b_t (g), the growth rate of b_t under two regimes (g_1 and g_2), as well as the steady probabilities of two two regimes (π_1 and π_2).

		1-Regime			2-Regimes	
Model	loglike	2388.32		loglike	2399.66	
Evaluation	AIC	-4764.63		AIC	-4781.31	
	BIC	-4740.67		BIC	-4745.37	
				LRT over 1R	22.68	(0.0000)
Estimated	μ	0.0008	(0.0002)	μ	0.0008	(0.0002)
Parameters	ψ_1	0.7616	(0.0189)	ψ_1	0.7021	(0.0379)
	ψ_2	-0.0575	(0.0189)	ψ_2	0.0010	(0.0181)
	σ_δ	0.0041	(0.0001)	σ_δ	0.0041	(0.0001)
	σ_η	0.0369	(0.0013)	σ_η	0.0317	(0.0012)
	ρ	0.9986	(0.0017)	ρ	0.9985	(0.0019)
				$1+g_2$	0.9349	(0.0044)
				p_{11}	0.9500	(0.0034)
				p_{22}	0.3100	(0.1085)
Implied	r	0.0014		r	0.0014	
Parameters	g_1			g_1	0.0063	
	g_2			g_2	-0.0651	
	π_1			π_1	0.9324	
	π_2			π_2	0.0676	

Table 2.6: Estimation Summary of the One-Regime and Two-Regime Models for the NASDAQ Index

This table shows the model evaluation statistics, estimated parameters and implied parameters of the one-regime and two-regime models for the NASDAQ Index. The upper panel of each table includes several model evaluation criteria, including the log likelihood, AIC and BIC, for each model. In addition, we report the likelihood ratio tests (LRT) of the two-regime model over the one-regime model. The $p-$value of LRT is presented in parentheses. For the parameter estimation, we report both the estimated parameter and standard errors (in parentheses) in the middle panel. Moreover, some implied parameters, which are helpful for us to understand the bubble process, are presented in the bottom panel. The parameters include the expected growth rate of b_t (g), the growth rate of b_t under two regimes (g_1 and g_2), as well as the steady probabilities of two two regimes (π_1 and π_2).

		1-Regime			2-Regimes	
Model	loglike	750.34		loglike	767.71	
Evaluation	AIC	-1488.68		AIC	-1517.42	
	BIC	-1464.71		BIC	-1481.48	
				LRT over 1R	34.74	(0.0000)
Estimated	μ	0.0142	(0.0047)	μ	0.0140	(0.0046)
Parameters	ψ_1	-0.7483	(0.0394)	ψ_1	-0.7532	(0.0069)
	ψ_2	-0.4969	(0.0391)	ψ_2	-0.5110	(0.0385)
	σ_δ	0.0935	(0.0033)	σ_δ	0.0929	(0.0032)
	σ_η	0.0964	(0.0034)	σ_η	0.0839	(0.0006)
	ρ	0.9994	(0.0032)	ρ	0.9994	(0.0036)
				$1+g_2$	0.8653	(0.0100)
				p_{11}	0.9253	(0.0037)
				p_{22}	0.2790	(0.1334)
Implied	r	0.0006		r	0.0006	
Parameters	g_1			g_1	0.0146	
	g_2			g_2	-0.1347	
	π_1			π_1	0.9061	
	π_2			π_2	0.0939	

Table 2.7: Estimation Summary of the Three-Regime Model for Three Evans Processes

This table shows the model evaluation statistics, estimated parameters and implied parameters of the three-regime models for the three simulated data series using the three specifications of the Evans process, respectively. The upper panel of each table includes several model evaluation criteria, including the log likelihood, AIC and BIC, as well as the likelihood ratio tests (LRT) of over the one-regime model and over the two-regime model. The $p-$value of LRT is presented in parentheses. For the parameter estimation, we report both the estimated parameter and standard errors (in parentheses) in the middle panel. Moreover, some implied parameters, which are helpful for us to understand the bubble process, are presented in the bottom panel. The parameters include the expected growth rate of b_t (g), the growth rate of b_t under three regimes (g_1, g_2 and g_3), as well as the steady probabilities of three regimes (π_1, π_2 and π_3).

	The Evans 1 Process			The Evans 2 Process			The Evans 3 Process		
Model	loglike	666.01		loglike	560.34		loglike	565.04	
Evaluation	AIC	-1312.02		AIC	-1100.68		AIC	-1110.08	
	BIC	-1279.14		BIC	-1067.80		BIC	-1077.20	
	LRT over 1R	555.60	(0.0000)	LRT over 1R	463.79	(0.0000)	LRT over 1R	391.43	(0.0000)
	LRT over 2R	39.94	(0.0000)	LRT over 2R	59.74	(0.0000)	LRT over 2R	30.92	(0.0000)
Estimated	μ	0.0044	(0.0067)	μ	0.0161	(0.0069)	μ	-0.0047	(0.0076)
Parameters	ψ_1	-0.0561	(0.0120)	ψ_1	-0.0720	(0.0182)	ψ_1	-0.0907	(0.0000)
	ψ_2	-0.0656	(0.0108)	ψ_2	-0.0018	(0.0159)	ψ_2	-0.0468	(0.0000)
	σ_δ	0.0937	(0.0047)	σ_δ	0.0975	(0.0049)	σ_δ	0.1066	(0.0054)
	σ_η	0.0183	(0.0009)	σ_η	0.0291	(0.0015)	σ_η	0.0275	(0.0000)
	ρ	0.9699	(0.0002)	ρ	0.9681	(0.0001)	ρ	0.9647	(0.0001)
	$1+g_3$	0.0001	(0.0128)	$1+g_3$	0.0419	(0.0267)	$1+g_3$	0.1213	(0.0333)
	p_{11}	0.9261	(0.0942)	p_{11}	0.8518	(0.0100)	p_{11}	0.8911	(0.0001)
	p_{22}	0.8617	(0.0002)	p_{22}	0.6244	(0.0000)	p_{22}	0.8580	(0.0001)
	p_{33}	0.1119	(0.0688)	p_{33}	0.1270	(0.0519)	p_{33}	0.0231	(0.1085)
Implied	r	0.0311		r	-0.0319		r	0.0366	
Parameters	g_1	0.0311		g_1	-0.0319		g_1	0.0366	
	g_2	0.1916		g_2	0.3666		g_2	0.1696	
	g_3	-0.9999		g_3	-0.9581		g_3	-0.8787	
	π_1	0.6182		π_1	0.6393		π_1	0.5324	
	π_2	0.3304		π_2	0.2522		π_2	0.4083	
	π_3	0.0514		π_3	0.1085		π_3	0.0593	

Table 2.8: RMSE of Estimated Bubbles of Three Evans Processes

This table shows the Root Mean Square Error (RMSE) of the one-regime model, two-regime model and three-regime model in estimating bubbles for three Evans processes. RMSE is computed as the root mean square deviation from the simulated bubbles to the estimated bubbles.

	The One-regime Model	The Two-regime Model	The Three-regime Model
The Evans 1 Process	7.0097	3.4249	4.7360
The Evans 2 Process	13.1544	4.6211	4.5836
The Evans 3 Process	18.9142	4.6854	4.6929

Table 2.9: Estimation Summary of the Three-Regime Model for the S&P 500 and NASDAQ Indices

This table shows the model evaluation statistics, estimated parameters and implied parameters of the three-regime models for the S&P 500 and NASDAQ Indices, respectively. The upper panel of each table includes several model evaluation criteria, including the log likelihood, AIC and BIC, as well as the likelihood ratio tests (LRT) of over the one-regime model and over the two-regime model. The $p-$value of LRT is presented in parentheses. For the parameter estimation, we report both the estimated parameter and standard errors (in parentheses) in the middle panel. Moreover, some implied parameters, which are helpful for us to understand the bubble process, are presented in the bottom panel. The parameters include the expected growth rate of b_t (g), the growth rate of b_t under three regimes (g_1, g_2 and g_3), as well as the steady probabilities of three regimes (π_1, π_2 and π_3).

		S&P 500			NASDAQ	
Model	loglike	2405.48		loglike	776.96	
Evaluation	AIC	-4784.95		AIC	-1527.93	
	BIC	-4733.03		BIC	-1476.00	
	LRT over 1R	34.32	(0.0000)	LRT over 1R	53.25	(0.0000)
	LRT over 2R	11.64	(0.0202)	LRT over 2R	18.51	(0.0010)
Estimated	μ	0.0010	(0.0002)	μ	0.0137	(0.0047)
Parameters	ψ_1	0.6951	(0.0185)	ψ_1	-0.7600	(0.0395)
	ψ_2	-0.0006	(0.0185)	ψ_2	-0.4873	(0.0392)
	σ_δ	0.0041	(0.0001)	σ_δ	0.0941	(0.0034)
	σ_η	0.0319	(0.0001)	σ_η	0.0800	(0.0030)
	ρ	1.0014	(0.0013)	ρ	1.0007	(0.0047)
	$1+g_3$	0.9267	(0.0026)	$1+g_3$	0.9172	(0.0328)
	p_{11}	0.9750	(0.0012)	p_{11}	0.9704	(0.0188)
	p_{12}	0.0000	(0.0007)	p_{12}	0.0002	(0.0061)
	p_{21}	0.0000	(0.0000)	p_{21}	0.0040	(0.0912)
	p_{22}	0.9088	(0.0455)	p_{22}	0.3958	(0.1616)
	p_{31}	0.4233	(0.0983)	p_{31}	0.3208	(0.1331)
	p_{33}	0.3996	(0.0765)	p_{33}	0.2423	(0.0822)
Implied	r	0.0014		r	0.0007	
Parameters	g_1	0.0014		g_1	0.0007	
	g_2	0.0399		g_2	0.1155	
	g_3	-0.0733		g_3	-0.0828	
	π_1	0.8519		π_1	0.8638	
	π_2	0.0978		π_2	0.0573	
	π_3	0.0503		π_3	0.0789	

Figure 2.1: Bubbles of the Three Evans Process Estimated by the One-regime and Two-regime Models

The left, central and right panels show the estimated bubbles B_t in three stock price series simulated by the Evans model with the first, second and third parameter specifications, respectively. The B_t estimated by the one-regime switching model (in dashed red line) and that estimated by the two-regime model (in dashed blue line) are shown in the upper part of each panel. B_t is transformed from b_t, which is the filtered bubble component in the log simulated stock price. The simulated stock price (P), real fundamental price (dividend divided by the discount rate, D/r), and bubbles ($B \times 20$) are presented in green, magenta and black solid lines, respectively. The lower part of each panel shows the filtered probabilities of the collapsing regime (in blue solid line) estimated from the two-regime model.

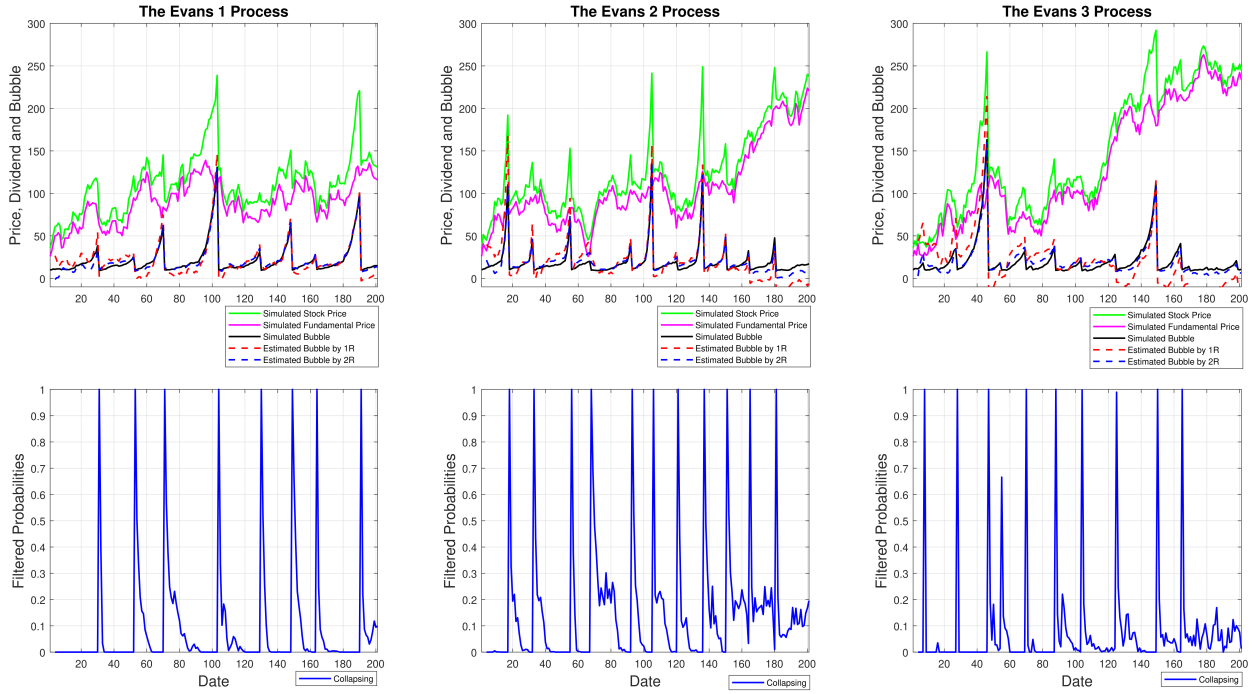

Figure 2.2: Bubbles of the S&P 500 and NASDAQ Indices Estimated by the One-Regime and Two-Regime Models

The left and right panels show the estimated bubbles B_t in the S&P 500 and NASDAQ Indices, respectively. The B_t estimated by the one-regime switching model (in dashed red line) and that estimated by the two-regime model (in dashed blue line) are shown in the upper part of each panel. B_t is transformed from b_t, which is the filtered bubble component in the log simulated stock price. We normalize the real stock price and real dividend to 1 in the beginning of the sample period and present them in green and magenta solid lines. The lower part of each panel shows the filtered probabilities of the collapsing regime (in blue solid line) estimated from the two-regime model.

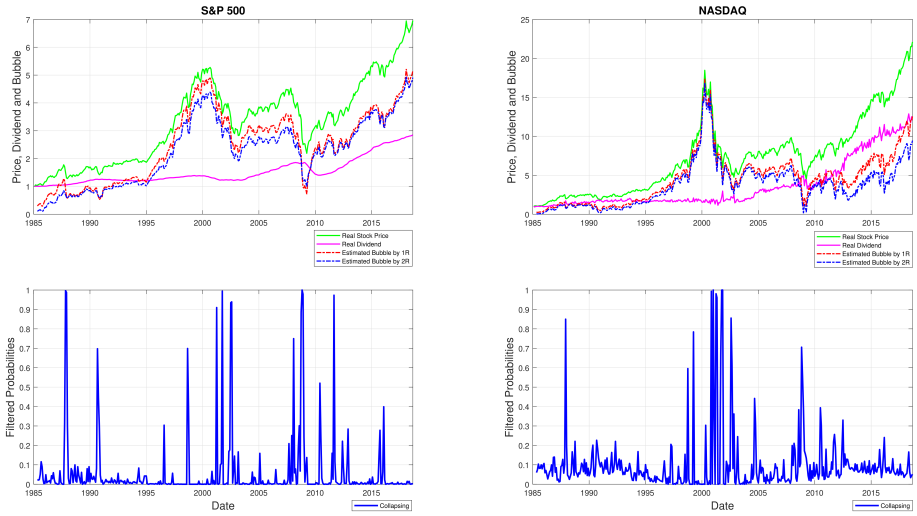

Figure 2.3: Bubbles of the Three Evans Process Estimated by the Three-Regime Model

The left, central and right panels show the estimated bubbles B_t in three stock price series simulated by the Evans model with the first, second and third parameter specifications, respectively. The B_t estimated by the one-regime switching model (in dashed red line) and that estimated by the three-regime model (in dashed blue line) are shown in the upper part of each panel. B_t is transformed from b_t, which is the filtered bubble component in the log simulated stock price. The simulated stock price (P), real fundamental price (dividend divided by the discount rate, D/r), and bubbles ($B \times 20$) are presented in green, magenta and black solid lines, respectively. The lower part of each panel shows the filtered probabilities of the collapsing regime (in blue solid line) and the exploding regime (in red dashed line) estimated from the three-regime model.

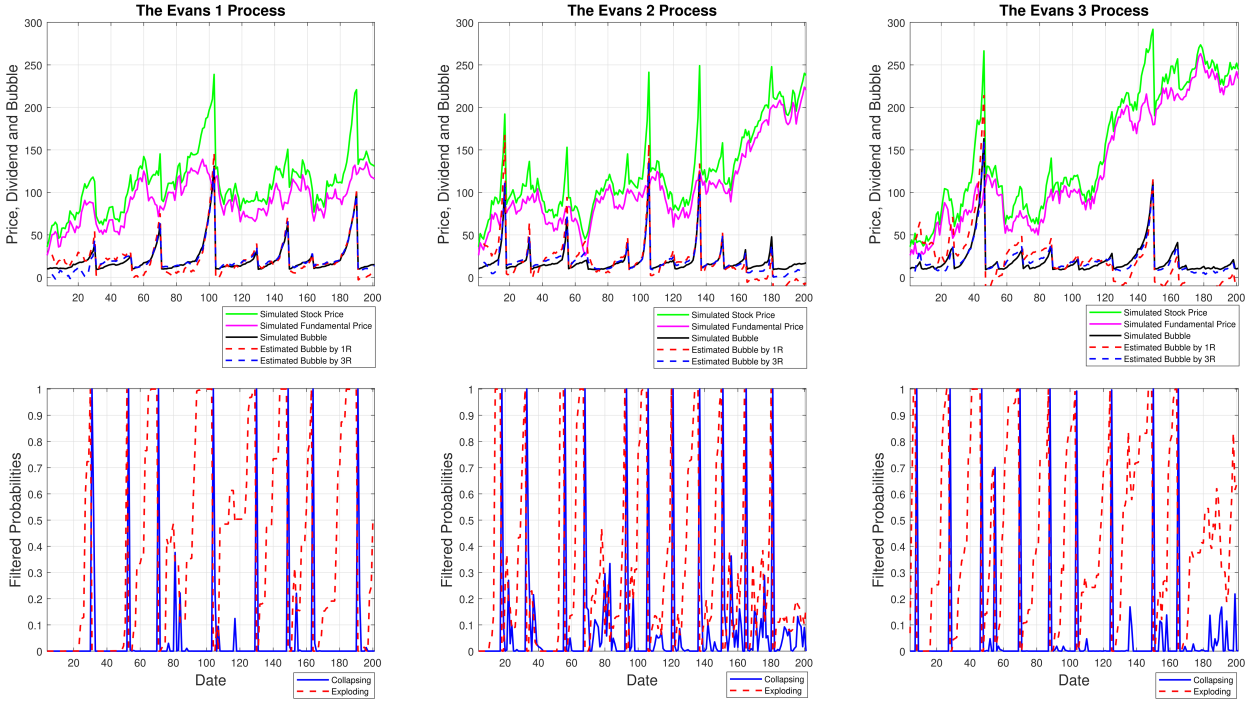

Figure 2.4: Bubbles of the S&P 500 and NASDAQ Indices Estimated by the Three-Regime Model

The left and right panels show the estimated bubbles B_t in the S&P 500 and NASDAQ Indices, respectively. The B_t estimated by the one-regime switching model (in dashed red line) and that estimated by the three-regime model (in dashed blue line) are shown in the upper part of each panel. B_t is transformed from b_t, which is the filtered bubble component in the log simulated stock price. We normalize the real stock price and real dividend to 1 in the beginning of the sample period and present them in green and magenta solid lines. The lower part of each panel shows the filtered probabilities of the collapsing regime (in blue solid line) and the exploding regime (in red dashed line) estimated from the three-regime model.

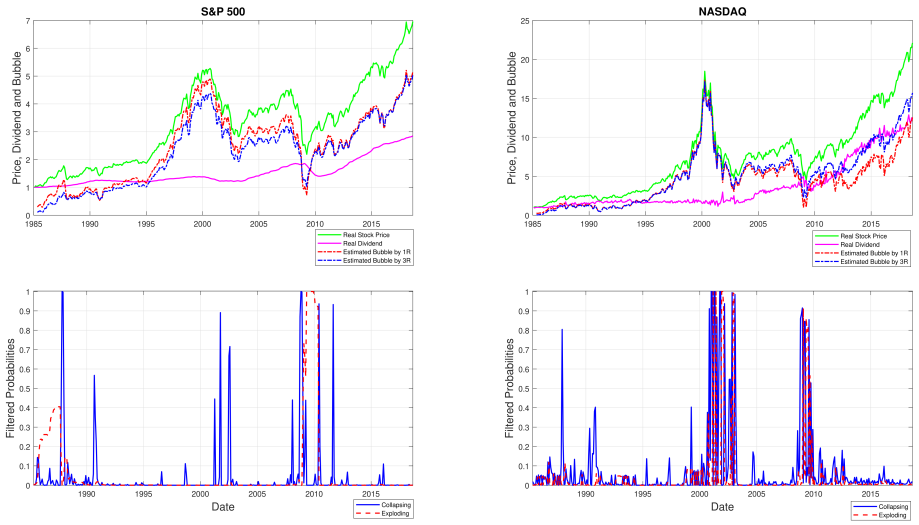

Chapter 3

Oil and Inflation Compensation: Evidence from Treasury Inflation-Protected Security Prices

3.1 Introduction

Since 2008, oil prices and market measures of long-term inflation compensation, such as 10-year Treasury Inflation-Protected Security (TIPS) Break-even Inflation (BEI), have moved together much more than they did previously, as can be seen in Figure 3.1. Defined as the spread between yields on nominal Treasury securities and on TIPS of comparable maturities, TIPS BEI is often used as a real-time proxy for market participants' inflation expectations (IE). Although lower oil prices today may result in lower inflation over the next several months or even one year, a current decline in oil prices should not reduce inflation five years or more in the future. It is puzzling that the huge increase of the correlation with oil prices after the financial crisis is in fact a robust pattern for TIPS BEI at all horizons from 5 years to 20 years. We provide both empirical and theoretical support to show that this phenomenon results from nominal interest rates being constrained by the zero lower bound (ZLB) after crisis.

To begin with, we first explore potential interpretations of the puzzle by performing a preliminary analysis for the TIPS BEI and oil price data. One possible explanation for the question is related to the public's doubt about the effectiveness of monetary policy around the ZLB. As mentioned by Sussman and Zohar (2015), after financial crisis the Federal Reserve rapidly cut its target for the short interest rate to near zero to combat the economic recession; therefore, monetary policy that is constrained by the zero lower

bound deteriorates the public's belief in the central bank's ability to stabilize inflation at middle- and even long-term horizons. We support this interpretation by documenting the asymmetric correlation between TIPS BEI and oil prices — TIPS BEI moves more often with oil prices if oil prices go down than if they go up — when the nominal short rate is near ZLB. This suggests that the lift of inflation led by the increase of oil prices is rapidly stabilized by the monetary policy that raises the fed funds rate, thereby the long-term IE is less affected by instantaneous oil price shocks; however, the decline of inflation caused by the drop of oil prices can not be mitigated sufficiently because there is no room for the Federal Reserve to reduce the nominal short rate further as long as it binds at ZLB. As a result, investors quickly lower their long-term inflation expectations after negative oil price changes.

Although TIPS BEI is often used as a market measure of IE, it sometimes may not give a clean read on investors' inflation expectations as it also reflects the compensations that risk-averse investors demand for bearing the uncertainty risks of future inflation dynamics. The risk premiums, also called inflation risk premiums (IRP), are related to the market's changing perceptions about the balance of inflation risks or changes in investor risk aversion. Moreover, TIPS yields often exceed risk-free real yields. The spread predominantly reflects the TIPS liquidity risk premiums (LRP) for TIPS investors to hold securities with poor liquidity relative to nominal Treasury securities. The combination of IRP and LRP could potentially drive a notable wedge between TIPS BEI and true IE. Thus the preliminary analysis based on TIPS BEI data and oil prices is not sufficient to conclude.

To estimate the clean measure of IE, we propose a shadow rate no-arbitrage four factor term structure model with the following two features. First, we follow D'Amico et al. (2018) to construct a joint no-arbitrage term structure model for nominal yields and TIPS yields with a TIPS liquidity specific factor, which helps us to infer liquidity risk premiums priced in TIPS as a side-product. Second, we follow Wu and Xia (2016) to posit the existence of a shadow nominal rate that is linear in Gaussian factors, with the actual short-term

nominal interest rate as the maximum of the shadow rate and zero. Including the ZLB constraint helps to estimate the IE more accurately, as suggested by Aruoba (2019). We estimate the model by jointly fitting nominal yields, TIPS yields, inflation rate and survey-based inflation forecasts at all horizons. We then tease out the liquidity effects of TIPS and extract the whole term structure of the clean measures of IE and IRP.

We obtain three main findings about the oil price effects on the model-implied IE and IRP. First, oil prices play a notably positive influence on the whole term structure of IE only when the nominal short rate is near ZLB. Second, the oil price shocks on IE under the ZLB regime predominantly stems from negative oil price changes — the oil prices exhibit asymmetric effects on IE, i.e., IE moves more often with oil prices when oil prices decrease than when they increase. Third, oil prices have a significantly positive impact on IRP only when oil prices decrease in an ZLB environment. Accompanied by the fact that the whole term structure of IRP often remains negative after financial crisis, we conclude that market participants would like to pay higher premiums for hedging deflation risks when they expect the monetary policy to be less effective around the ZLB.

Finally, we use a small-scale, closed-economy and new Keynesian dynamical stochastic general equilibrium (DSGE) model augmented with an oil sector and d a Taylor rule with the ZLB constraint to study the theoretical effects of ZLB on the relationship between oil prices and the term structure of IE. We simulate the model to show the correlation increases when the shadow interest rate decreases. To understand the underlying mechanisms, we analyze the impulse response functions (IRFs) of oil supply and oil demand shocks on all macro variables when the nominal short rate binds at ZLB. The IRFs exhibit notable asymmetric behaviors — both the positive shocks of oil supply and the negative shocks of oil demand, which result in the decline of oil prices, play a more influential role on the whole economy than their opposite counterparts do. Both supply-driven oil prices and demand-driven oil prices exhibit asymmetric and stronger effects under the ZLB regime. The comparison between the IRFs with ZLB and the counterparts without ZLB illustrates

that the ZLB is the predominate driver for the strikingly different effects of oil prices on IE in normal times versus when the nominal interest rate is near its lower bound.

Our contribution is to accomplish the first comprehensive analysis of the oil shocks on the term structure of IE under the ZLB and the No-ZLB regimes using both a no-arbitrage term structure model and a DSGE model with the same occasionally binding ZLB constraint. We are first to provide both empirical and theoretical evidence to explain different oil price effects on long-term IE before and after financial crisis. Naturally, our work contributes to three strands of the literature.

First, our paper expands the literature about the effects of oil related shocks on asset prices. Most papers in this strand mainly discuss the relation between oil and equity returns, such as Kilian and Park (2009), Chiang et al. (2015), Chiang and Hughen (2017) and Hitzemann (2016). Our research shows that oil shocks are also priced in Treasury bond markets — oil price changes drive a large part of the variation of the spread between nominal and TIPS yields after financial crisis, and provides sufficient empirical evidence and theoretical analysis to support our explanation.

Second, our paper extends the literature that employs the no-arbitrage term structure models to extract useful information such as IE, IRP, and nominal and real term premiums from nominal and TIPS yields. Examples are Kim and Wright (2005), Abrahams et al. (2013), D'Amico et al. (2018) and Christensen et al. (2010). However, all these research use the Gaussian affine term structure model (Duffie and Kan, 1996 and Dai and Singleton, 2000), which potentially allows nominal interest rates to go negative and faces real difficulties in capturing the structural breaks in the ZLB environment. The term structure models with the ZLB has been rapidly growing recently, such as Bauer and Rudebusch (2016), Christensen and Rudebusch (2016), Ichiue and Ueno (2007), Kim and Singleton (2012), Krippner (2012), Kim and Priebsch (2013) and Wu and Xia (2016). However, these models are mainly applied to fit nominal yields or future short rates only. Our term structure

model is the first joint model of nominal and TIPS yields with the ZLB constraint and it can be used to obtain more realistic estimation of variables that are potentially sensitive to the ZLB.

Finally, the paper fits within the rapidly expanding literature that uses fully nonlinear New Keynesian DSGE models with an occasionally ZLB binding constraint to analyze the implications of ZLB constraint on a set of variables, including macroeconomic variables (Fernández-Villaverde et al., 2015; Gavin et al., 2015; Gust et al., 2017; Nakata, 2017), the term structure of interest rates (Nakata and Tanaka, 2016), oil shocks on equity returns (Datta et al., 2018) and oil shocks on economic activity (Bodenstein et al., 2013). Our work expands the literature by using the New Keynesian model with the ZLB constraint to study how ZLB exaggerates the effects of oil shocks on the whole term structure of inflation expectations.

The remainder of this paper is organized as follows. Section 3.2 provides preliminary empirical evidence showing that the stronger positive effects of oil prices on TIPS BEI after crisis are caused by the market's doubt about the effectiveness of monetary policy when the nominal short rate is around the zero lower bound. Section 3.3 proposes a no-arbitrage term structure model that describes the joint dynamics of nominal yields, real yields, TIPS yields, inflation forecasts and show how to use the model to tease out the TIPS liquidity effects and then extract the clean measure of IE and IRP. Section 3.4 empirically studies the role of the ZLB in driving the effects of oil prices on IE and IRP. Section 3.5 uses a small-scale, closed-economy and new-Keynesian dynamical stochastic general equilibrium model augmented with an oil sector and a Taylor rule with the ZLB constraint to support our empirical findings. Section 3.6 concludes.

3.2 Preliminary Empirical Evidence

3.2.1 The Correlation between Oil Prices and TIPS BEI before and after Crisis

Many researchers and practitioners find that both middle-term (around 5 years) and long-term (10 years and more) market measures of IE have a strong positive correlation with oil prices since the onset of the global financial crisis, while the correlation had been weaker previously. For example, Sussman and Zohar (2015) show that the correlation between 5-year TIPS BEI and annual rates of oil price changes increases from 0.19 before crisis to 0.54 after crisis. Badel and McGillicuddy (2015) document a similar pattern for the correlation between 5-year TIPS BEI and oil price levels. The results keep robust if the inflation swap rate is employed as the market measure of IE. Elliott et al. (2015) show a 10% fall in oil prices is associated with a fall of approximately 4 basis points in 5-year inflation swap rate 5 years from now (5y5y IE) using daily data from January 2009 to July 2015. Darvas and Hüttl (2016) find a 10% increase in oil prices lifts 10-year inflation swap rates 10 years from now (10y10y IE) by 10 basis points using the weekly data from July 2007 to January 2016.

We use TIPS BEI as the market measure of IE in this paper. To begin our empirical analysis, we first present the daily dynamics of 10-year TIPS BEI and log oil price for the pre-crisis sample and post-crisis sample periods in Figure 3.1. We use WTI index to proxy the oil price level. The pre-crisis sample (upper left panel) starts from January 4, 1999, when TIPS is initially launched, to September 14, 2008. The post-crisis sample (upper right panel) begins from September 15, 2008, when the market value of global stock markets evaporated dramatically after Lehman Brothers filed for the biggest bankruptcy in history, to May 31, 2017. Although 10-year TIPS BEI shows some co-movement with oil prices before crisis, this pattern is much weaker than that after crisis, when TIPS BEI

mirrors moves in oil prices. The bottom left panel and bottom right panel show the scatter plots and OLS regression lines between changes of 10-year TIPS BEI and changes of log oil price before and after crisis, respectively. It can be easily observed visually that the positive relationship between two variables is more notable after crisis.

Panel A (Panel B) of Table 3.1 presents how oil price changes affect on TIPS BEI for 5-, 10-, 15-, and 20-year horizons before (after) financial crisis. To avoid the possibility of spurious regression caused by non-stationary processes, we regress the daily changes of TIPS BEI on the daily changes of log oil price because their change series are more stationary than their level series. The regression is as follows,

$$\Delta Y_t = \gamma_0 + \gamma_1 \Delta \left(\log WTI_t\right) + \epsilon_t. \tag{3.2.1}$$

Here we use TIPS BEI on t-th day as Y_t and it can be replaced by different variables in the following part of this paper. We employ the Newly-West standard errors to compute T statistics in this regression and all following regressions to overcome the autocorrelation and heteroskedasticity in the error terms in the models.

Comparing Panel A and Panel B, we find that by switching the sample period from pre-crisis to post-crisis, the coefficient and T-statistic of log oil price changes are more than doubled, and the adjusted R square becomes more than quintupled on average across regressions for all horizons. Take the regression for 10-year TIPS BEI as an example. The slope of log oil price change is 0.0022 with a T-statistic of 5.5 before crisis, but after crisis, it increases to 0.0054 with a T-statistic of 17.17. The corresponding adjusted R square increases from 2.05% to 9.8%. A 1% increase in oil prices lifts 5-, 10-, 15- and 20-year TIPS BEI by 0.66, 0.54, 0.45 and 0.39 bps after crisis, while previously the corresponding increase of TIPS BEI are 0.33, 0.22, 0.19 and 0.16 bps. Moreover, the strengthening of these oil effects right after crisis is greater for TIPS BEI with longer horizons.

To formally test the impact of financial crisis on the relationship between oil prices and

TIPS BEI, we conduct the following regression, with estimation results shown in Panel C of Table 3.1.

$$\Delta Y_t = \gamma_0 + \gamma_1 \Delta \left(\ln WTI_t \right) + \gamma_2 1_{Post} + \gamma_3 \Delta \left(\ln WTI_t \right) \cdot 1_{Post} + \epsilon_t, \tag{3.2.2}$$

where 1_{Post} is the post-crisis dummy variable that is 0 before September 15, 2008 and 1 afterwards, and Y_t is TIPS BEI for different terms as before. Our interest is the coefficient of the interaction term $\Delta \left(\ln WTI_t \right) \cdot 1_{Post}$, which identifies the additional effect of post-crisis oil price changes. Consistent with previous findings, the regressions for all maturities have positive coefficients for the interaction term at the significance level 1%.

3.2.2 Potential Explanations and Hypotheses

It makes sense for changes in oil and energy prices to influence short-term IE since they are obviously an important determinant of inflation in the near term such as the following several months or 1 year. But why do changes in oil prices have a strong and persistent impact on the market measure of IE for 5- to 20-year horizons? Researchers have given some possible interpretations for this question, although none of them provides direct evidence. The first explanation is that the market measures of IE, such as inflation swap rates and TIPS BEI, don't provide a clean read on investors' forecasts on future inflation (Elliott et al., 2015). In addition to IE, these measures reflect IRP, which is the compensation that risk-averse investors demand for bearing the uncertainty risks of future inflation dynamics. Based on this explanation, we propose the following hypothesis:

Hypothesis 1 (H1)**.** *The stronger positive effects of oil prices on the long-term market measure of IE after crisis result from the expansion of oil prices' impact on the market's long-term IRP, not IE.*

The second interpretation relates to the public's doubt about the effectiveness of monetary policy around the zero lower bound (ZLB) (Elliott et al., 2015; Sussman and Zohar,

2015). Sussman and Zohar (2015) show that both oil prices and inflation reacted quite strongly to global demand and oil supply shocks. They argue these shocks should not affect long-term IE in the normal times because central banks can, in principle, use standard monetary policy tools to offset the effect of these shocks on inflation. But after financial crisis, the Federal Reserve rapidly cut its target for the short interest rate to near zero to combat economic recession, thus the monetary policy constrained by the zero lower bound deteriorates the public's belief in the ability of monetary authorities to stabilize inflation at middle- and even long-term horizons. Based on this explanation, we propose the following hypothesis:

Hypothesis 2 (H2)**.** *The stronger positive effects of oil prices on the long-term market measure of IE after crisis are caused by the public's doubt about the effectiveness of monetary policy when the nominal short rate is around the zero lower bound.*

3.2.3 The Role of Zero Lower Bound

The Hypothesis 1 will be examined in section 3.4, after we obtain clean measures of IE and IRP in section 3.3 by estimating a joint no-arbitrage term structure model for Treasury nominal yields, TIPS yields and survey-based inflation forecasts. In this subsection, we assume TIPS BEI is able to reflect the market's IE and then conduct econometric tests for TIPS BEI and oil price data to test Hypothesis 2.

One natural way to test Hypothesis 2 is to examine asymmetric correlations between oil prices and TIPS BEI — whether TIPS BEI moves more often with oil prices when oil prices go down than when they go up — when the nominal short rate is close to the ZLB. Under the ZLB regime, the drop of oil prices leads to the decline of inflation, while the monetary authorities lose the ability to stabilize long-run inflation because there is no room for the Fed to further reduce the fed funds rate. Therefore, the oil price effects are transmitted to the market measure of long-term IE. However, this is not the case when oil prices increase

because the Fed is capable to raise Fed funds rate to mitigate the increase of inflation. Thus if Hypothesis 2 holds, when the nominal short rate binds at the ZLB, the escalation of TIPS BEI caused by the increase of oil prices should be less the the decline of TIPS BEI caused by the same amount of decrease of oil prices.

Table 3.2 conducts the regression between daily changes of TIPS BEI on daily changes of log oil price, the dummy variable indicating negative oil price change, and their interaction term, for pre-crisis and post-crisis samples.

$$\Delta Y_t = \gamma_0 + \gamma_1 \Delta \left(\ln WTI_t\right) + \gamma_2 1_{Neg} + \gamma_3 \Delta \left(\ln WTI_t\right) \cdot 1_{Neg} + \epsilon_t. \tag{3.2.3}$$

Here the dummy variable 1_{Neg} is 1 when $\Delta \left(\ln WTI_t\right)$ is negative and 0 when positive. Y_t is TIPS BEI for 5, 10, 15, or 20 years. Our interest is the coefficient of the interaction term $\Delta \left(\ln WTI_t\right) \cdot 1_{Neg}$, which identifies the additional effects of oil price changes on TIPS BEI when oil prices decrease. For the post-crisis sample, the coefficients for the interaction term are significantly positive for 10, 15 and 20 years at the significance level 5%, and significantly postive for 5 years at the significance level 10%. This justifies the asymmetric effects of oil prices on TIPS BEI after crisis. A 1% drop of oil prices leads to a decline of 0.84, 0.67, 0.66, and 0.51 bps of TIPS BEI for next 5, 10, 15, and 20 years; however, the corresponding lift of TIPS BEI rates caused by a 1% increase of oil prices are only 0.51, 0.38, 0.27, and 0.20 bps, suggesting that as term increases, the asymmetry of oil effects is more salient. For the pre-crsis sample, the coefficients of the interaction term turn to be negative. The notable structural difference between regression results in two periods suggests that investors expect that the Fed loses the effective tools to stabilize inflation when oil prices decrease after financial crisis, during which period the nominal short rate keeps close to the ZLB in most times.

To clearly estimate the oil price shock on TIPS BEI under different scenarios, we conduct regressions with two-way and three-way interactions for the whole sample in Table

3.3. We create a ZLB dummy 1_{ZLB}, which is equal to 1 when the contemporaneous 3-month nominal interest rate is smaller than 1% and 0 otherwise. The ZLB dummy is 1 for 9.47% observations in the pre-crisis sample, and for 99.77% observations in the post-crisis sample. To save space, only regression results for 10-year (Panel A) and 20-year (Panel B) TIPS BEI are presented. Column (1) regresses the daily changes of TIPS BEI on daily changes of log oil price. Consistent with previous results, the coefficient of oil shock is significantly positive. Column (2) conducts a regression with two-way interactions between log oil price change and the ZLB dummy,

$$\Delta Y_t = \gamma_0 + \gamma_1 \Delta \left(\ln WTI_t\right) + \gamma_2 1_{ZLB} + \gamma_3 \Delta \left(\ln WTI_t\right) \cdot 1_{ZLB} + \epsilon_t. \tag{3.2.4}$$

As the ZLB dummy and post-crisis dummy are equal in 94.95% of the whole sample, we can expect that the regression results should be similar to those in Panel C of Table 3.2. The coefficient of the interaction term is significantly positive at 1% level, suggesting that the oil's positive shocks on TIPS BEI is much stronger under the ZLB regime. Column (3) conducts a regression with two-way interactions between log oil price change and the negative change dummy, described in equation (3.2.3). The coefficient of the interaction term is not significant, which is consistent with the opposite asymmetric effects of oil shocks before and after crisis. Column (4) conducts a regression with three-way interactions among log oil price change, negative change dummy and ZLB dummy.

$$\begin{aligned}\Delta Y_t = {} & \gamma_0 + \gamma_1 \Delta \left(Oil_t\right) + \gamma_2 1_{ZLB} + \gamma_3 \Delta \left(Oil_t\right) \cdot 1_{ZLB} + \gamma_4 1_{Neg} + \gamma_5 \Delta \left(Oil_t\right) \cdot 1_{Neg} \\ & + \gamma_6 1_{ZLB} \cdot 1_{Neg} + \gamma_7 \Delta \left(Oil_t\right) \cdot 1_{ZLB} \cdot 1_{Neg} + \epsilon_t.\end{aligned} \tag{3.2.5}$$

The coefficient of the three-variable interaction term is significantly positive at 10% level for 10 years and at 5% for 20 years, which suggests that the oil's positive effects on TIPS BEI is strongest when oil prices drop under the ZLB regime.

The take-away of this section is that if we assume that TIPS BEI is a reasonable estimate of the market's IE, Hypothesis 2 holds. To examine hypothesis 1, we estimate clean measures of Inflation Expectations (IE) and Inflation Risk Premium (IRP) in next section and then perform similar econometric tests.

3.3 Estimating Inflation Expectation and Risk Premium

3.3.1 The Model

In this subsection, we propose a no-arbitrage term structure model that describes the joint dynamics of nominal yields, real yields, TIPS yields, inflation and inflation forecasts. We then show how to use the model to tease out the TIPS liquidity effects and extract the clean measure of IE and IRP. This model inherits the merits from the liquidity-adjusted TIPS pricing model (D'Amico et al., 2018) and the shadow rate term structure model (SRTSM) (Black, 1995 and Wu and Xia, 2016). The model employs uses a liquidity factor to capture liquidity risk priced in TIPS, and includes the ZLB constraint for nominal interest rates.

3.3.1.1 State Factors and Nominal Yields

The Gaussian affine term structure model (GATSM) specifies interest rates as affine functions of Gaussian state factors (Duffie and Kan, 1996 and Dai and Singleton, 2000), which potentially allows interest rates to go negative and faces real difficulties in the zero lower bound (ZLB) environment, i.e., when modeling nominal yields. Both fed funds rate and most of the nominal yield curve had been constrained at a certain point during the 2009-2015 period. Furthermore, the recent studies by Aruoba and Schorfheide (2015) and Aruoba (2019) suggest that the real data of inflation dynamics and the estimation of IE using term structure model is sensitive to ZLB. To capture the structural breaks in the data

and estimate IE more accurately, we follow Black (1995) and Wu and Xia (2016) to posit the existence of a shadow nominal rate that is linear in Gaussian factors, with the actual short-term nominal interest rate the maximum of the shadow rate and zero.

We assume that the nominal short rate $r^N(X_t)$ is

$$r_t^N = \max\left(r_t^{NS}, 0\right), \tag{3.3.1}$$

where 0 is the lower bound of nominal interest rate, and r_t^{NS} is the shadow rate that is defined as an affine function of the Gaussian state variables,

$$r^{NS}(X_t) = \rho_0^{NS} + \rho_1^{NS\prime} X_t. \tag{3.3.2}$$

If the shadow rate r_t^{NS} is greater than the lower bound, then r_t^{NS} is the nominal short rate; if the shadow rate r_t^{NS} is smaller than the lower bound, the nominal short rate is zero. Under the physical (P) measure, we assume three state variables have the following dynamics,

$$dX_t = \kappa(\mu - X_t)dt + \Sigma dW_t. \tag{3.3.3}$$

Following D'Amico et al. (2018), we employ the following normalization, which are necessary for achieving identification to allow a maximally flexible correlation structure between the factors

$$\mu = 0_{3\times 1},\ \kappa = \begin{bmatrix} \kappa_{11} & 0 & 0 \\ 0 & \kappa_{22} & 0 \\ 0 & 0 & \kappa_{33} \end{bmatrix},\ \Sigma = \begin{bmatrix} 0.01 & 0 & 0 \\ \Sigma_{21} & 0.01 & 0 \\ \Sigma_{31} & \Sigma_{32} & 0.01 \end{bmatrix}. \tag{3.3.4}$$

The nominal pricing kernel takes the form,

$$dM_t^N/M_t^N = -r^N(X_t)dt - \lambda^N(X_t)'dW_t, \tag{3.3.5}$$

where the vector of nominal prices of risk, λ^N is also assumed to be essentially affine form (Duffee, 2002),

$$\lambda^N(X_t) = \lambda_0^N + \Lambda^N X_t, \tag{3.3.6}$$

where λ_0^N is a 3×1 vector and Λ^N is a 3×3 matrix, without any specification.

If there is no ZLB, the shadow rate $r^{NS}(X_t)$ is the nominal short rate and the implied nominal yield has the standard closed form solution of GATSM proposed in Duffie and Kan (1996) and Dai and Singleton (2000). The closed-form solution for shadow rate implied $\tau-$maturity nominal yield at time t is a linear function of state factors,

$$y_{t,\tau}^{NS} = a_\tau^{NS} + b_\tau^{NS\prime} X_t, \;\; a_\tau^{NS} = -A_\tau^{NS}/\tau, \;\; b_\tau^{NS} = -B_\tau^{NS}/\tau, \tag{3.3.7}$$

where A_τ^{NS} and B_τ^{NS} are given by equations (3.A.4) and (3.A.5) in Appendix 3.A.

When considering ZLB, the equation (3.3.1) brings nonlinearity into an otherwise linear system. A closed-form pricing formula for the SRTSM is not available beyond one factor. Wu and Xia (2016) propose a simple analytical representation for bond prices in the multifactor SRTSM that provides an excellent approximation and can be applied directly-time data. Following Wu and Xia (2016), we discretize our model with sampling period h, construct the nominal forward rate curve $f_{t,kh,(k+1)h}^N$ (the forward rate for a loan starting at $t + kh$ and maturing at $t + (k+1)h$, where $0 \leqslant k \leqslant n-1$) at time t, and then compute $\tau-$maturity nominal yield $y_{t,\tau}^N$, where $\tau = nh$. Wu and Xia (2016) discretize the continuous system at monthly frequency, while we adopt the weekly frequency, $h = \frac{1}{52}$, to reduce the sampling bias and match the weekly data we use.

Following Wu and Xia (2016), we derive the forward rate at time t for a loan starting at $t + nh$ and maturing at $t + (n+1)h$ as

$$f_{t,nh,(n+1)h}^N = \frac{1}{h}\sigma_{nh}^{Q,N} g\left(\frac{\alpha_{nh}^N + \beta_{nh}^{N\prime} X_t}{\sigma_{nh}^{Q,N}}\right), \tag{3.3.8}$$

where the expressions of $\left(\sigma_{nh}^{Q,N}\right)$, α_{nh}^{N} and β_{nh}^{N} are given in Appendix 3.A. The function $g\left(z\right) \equiv z\Phi\left(z\right) + \phi\left(z\right)$ consists of a normal cumulative distribution function $\Phi\left(.\right)$ and normal probability density function $\phi\left(.\right)$. All derivations are deferred to Appendix 3.A.

Given the forward rates, the nominal yield $y_{t,\tau}^{N}$ with maturity $\tau = nh$ at time t can be easily computed as

$$y_{t,\tau=nh}^{N} = \frac{1}{n}\sum_{k=0}^{n-1} f_{t,kh,(k+1)h}^{N} = \frac{1}{nh}\sum_{k=0}^{n-1} \sigma_{kh}^{Q,N} g\left(\frac{\alpha_{kh}^{N} + \beta_{kh}^{N\prime} X_t}{\sigma_{kh}^{Q,N}}\right). \tag{3.3.9}$$

3.3.1.2 Inflation Dynamics and Real Yields

Price level is assumed to follow the log-normal process,

$$dQ_t/Q_t = r^I(X_t)dt + \sigma_q' dW_t + \sigma_q^{\perp} dW_t^{\perp}, \tag{3.3.10}$$

where the instantaneous inflation rate $r^I(X_t)$ is an affine function of the state variables:

$$r^I(X_t) = \rho_0^I + \rho_1^{I\prime} X_t. \tag{3.3.11}$$

Following D'Amico et al. (2018), the inflation innovation loads not only on shocks that drive risk factors dW_t, but also on an orthogonal shock that is unspanned by yield curve dynamics $dW_t^{\perp}$.

At time t, a real bond paying 1 unit of the consumption basket at time T can be deemed as a nominal asset paying the price level, Q_T, upon maturity. Therefore, no-arbitrage condition requires the following linkage between the real and nominal pricing kernels,

$$M_t^R = M_t^N Q_t, \tag{3.3.12}$$

based on which the instantaneous inflation rate and nominal market price of risks can be derived.

The real pricing kernel takes the form,

$$dM_t^R/M_t^R = -r^R(X_t)dt - \lambda^R(X_t)'dW_t, \tag{3.3.13}$$

where the vector of real prices of risk, λ_t^R, is further assumed to be essentially affine form, $\lambda^R(X_t) = \lambda_0^R + \Lambda^R X_t$, as suggested in Duffee (2002). The coefficient of real market price of risks are derived as equations (3.B.2) and (3.B.3). The instantaneous real interest rate is derived as

$$r^R(X_t) = r^N(X_t) - r^{BEI}(X_t) = r^N(X_t) - \rho_0^{BEI} - \rho_1^{BEI\prime} X_t, \tag{3.3.14}$$

where ρ_0^{BEI} and ρ_1^{BEI} are derived as equations (3.B.7) and (3.B.8), respectively. Here $r^{BEI}(X_t) = \rho_0^{BEI} + \rho_1^{BEI\prime} X_t$ is defined as the instantaneous break-even inflation (BEI) rate.

If there is no ZLB, the shadow rate $r^{NS}(X_t)$ is the nominal short rate and the corresponding real rate is the real shadow rate, defined as $r^{RS}(X_t) = r^{NS}(X_t) - r^{BEI}(X_t)$. It is an affine function of the state variables, $r^{RS}(X_t) = \rho_0^{RS} + \rho_1^{RS\prime} X_t$, where $\rho_0^{RS} = \rho_0^{NS} - \rho_0^{BEI}$ and $\rho_1^{RS} = \rho_1^{NS} - \rho_1^{BEI}$. The closed-form solution for shadow rate implied $\tau-$maturity real yield at time t is a linear function of state factors,

$$y_{t,\tau}^{RS} = a_\tau^{RS} + b_\tau^{RS\prime} X_t, \;\; a_\tau^{RS} = -A_\tau^{RS}/\tau, \;\; b_\tau^{RS} = -B_\tau^{RS}/\tau, \tag{3.3.15}$$

where A_τ^{RS} and B_τ^{RS} are given by equations (3.B.13) and (3.B.14) in Appendix 3.B.

When considering ZLB, we derive the forward real rate at time t for a loan starting at $t + nh$ and maturing at $t + (n+1)h$ as

$$f^R_{t,nh,(n+1)h} \approx -\frac{\alpha^{BEI}_{nh}}{h} - \rho_1^{BEI\prime} h C^{Q,R}_{nh} \rho_1^{BEI} - \frac{\beta^{BEI\prime}_{nh}}{h} X_t + \frac{1}{h}\sigma^{Q,N,R}_{nh} g\left(\frac{\alpha^{N,R}_{nh} + \beta^{N,R\prime}_{nh} X_t}{\sigma^{Q,N,R}_{nh}}\right) + \rho_1^{NS\prime} C^{Q,R}_{nh} \rho_1^{BEI} h \Phi\left(\frac{\bar{\alpha}^{N,R}_{nh} + \beta^{N,R\prime}_{nh} X_t}{\sigma^{Q,N,R}_{nh}}\right), \tag{3.3.16}$$

where the expressions of all coefficients are given in Appendix 3.B. All derivations are deferred to Appendix 3.B.

Given the forward real rates, the real yield $y^N_{t,\tau}$ with maturity $\tau = nh$ at time t can be easily computed as

$$\begin{aligned} y^R_{t,\tau=nh} \approx & -\frac{1}{nh}\sum_{k=0}^{n-1} \alpha^{BEI}_{kh} - \frac{h}{n}\rho_1^{BEI\prime} \sum_{k=0}^{n-1} C^{Q,R}_{kh} \rho_1^{BEI} - \frac{1}{nh}\sum_{k=0}^{n-1} \beta^{BEI\prime}_{kh} X_t \\ & + \frac{1}{nh}\sum_{k=0}^{n-1} \sigma^{Q,N,R}_{kh} g\left(\frac{\alpha^{N,R}_{kh} + \beta^{N,R\prime}_{kh} X_t}{\sigma^{Q,N,R}_{kh}}\right) \\ & + \frac{h}{n}\rho_1^{NS\prime} \sum_{k=0}^{n-1} C^{Q,R}_{kh} \rho_1^{BEI} \Phi\left(\frac{\bar{\alpha}^{N,R}_{kh} + \beta^{N,R\prime}_{kh} X_t}{\sigma^{Q,N,R}_{kh}}\right). \end{aligned} \tag{3.3.17}$$

3.3.1.3 TIPS Liquidity Effects

In this subsubsection, we introduce how we take TIPS liquidity effects into account so as to price TIPS accurately. Existing research (Gürkaynak et al., 2010; Abrahams et al., 2013; D'Amico et al., 2018; Grishchenko and Huang, 2013) provides adequate evidence on the existence of a TIPS liquidity factor, which pushes TIPS yields to deviate from the underlying real yields. The liquidity premium that investors demand for holding TIPS is mainly captured by the spread between the TIPS yield and the real yield as

$$L_{t,\tau} = y^{TIPS}_{t,\tau} - y^R_{t,\tau}. \tag{3.3.18}$$

Following D'Amico et al. (2018), we assume that the instantaneous rate investors require to price TIPS is the sum of the instantaneous real short rate and a positive spread, l_s. As a result, the liquidity risk premium can be written as,

$$L_{t,\tau} = -\frac{1}{\tau}\log E_t^Q\left(\exp\left(-\int_t^{t+\tau}(r_s^R + l_s)ds\right)\right) - y_{t,\tau}^R. \tag{3.3.19}$$

The instantaneous spread l_s is assumed to load on not only three risk factors X_t, but also a TIPS-specific factor, $\widetilde{X}_t$, i.e., $l_t = \beta' X_t + \widetilde{\beta}\widetilde{X}_t$, where $\widetilde{\beta}$ is a constant and β is a 3×1 constant vector. The TIPS-specific factor, $\widetilde{X}_t$, is assumed to be orthogonal to X_t and follow an independent Vasicek (1977) process,

$$d\widetilde{X}_t = \widetilde{\kappa}(\widetilde{\mu} - \widetilde{X}_t)dt + \widetilde{\sigma}d\widetilde{W}_t, \tag{3.3.20}$$

with $dW_t d\widetilde{W}_t = 0_{3\times 1}$. For identification, we set $\widetilde{\sigma} = 0.01$. By construction, $\widetilde{\beta}\widetilde{X}_t$ captures the TIPS-idiosyncratic component that is contemporaneous orthogonal to the systematic state variables in the economy. In the end, $\widetilde{X}_t$ is assumed to bear a market price of risk as $\widetilde{\lambda}_t = \widetilde{\lambda}_0 + \widetilde{\lambda}_1\widetilde{X}_t$.

The instantaneous TIPS rate is $r_t^{TIPS} = r_t^R + l_t = r_t^N - r_t^{BEI} + \beta' X_t + \widetilde{\beta}\widetilde{X}_t = r_t^N - \rho_0^{BEI} - (\rho_1^{BEI} - \beta)' X_t + \widetilde{\beta}\widetilde{X}_t$. The instantaneous TIPS BEI rate is defined as $r^{TBEI} = r^N - r^{TIPS} = \rho_0^{BEI} + (\rho_1^{BEI} - \beta)' X_t - \widetilde{\beta}\widetilde{X}_t$. As detailed in Appendix 3.C, the forward TIPS rate at time t for a loan starting at $t + nh$ and maturing at $t + (n+1)h$ derived as

$$\begin{aligned} f_{t,nh,(n+1)h}^{TIPS} \approx & -\frac{\alpha_{nh}^{TBEIa}}{h} - \frac{\alpha_{nh}^{TBEIb}}{h} - \left(\rho_1^{BEI} - \beta\right)' h C_{nh}^{Q,R}\left(\rho_1^{BEI} - \beta\right) - \widetilde{\beta}' h \widetilde{C}_{nh}^{Q,R}\widetilde{\beta} \\ & - \frac{\beta_{nh}^{TBEIa\prime}}{h} X_t - \frac{\beta_{nh}^{TBEIb}}{h}\widetilde{X}_t + \frac{1}{h}\sigma_{nh}^{Q,N,R} g\left(\frac{\alpha_{nh}^{N,R} + \beta_{nh}^{N,R\prime} X_t}{\sigma_{nh}^{Q,N,R}}\right) \\ & + \rho_1^{NS\prime} C_{nh}^{Q,R}\left(\rho_1^{BEI} - \beta\right) h\Phi\left(\frac{\bar{\alpha}_{nh}^{N,R} + \beta_{nh}^{N,R\prime} X_t}{\sigma_{nh}^{Q,N,R}}\right). \end{aligned} \tag{3.3.21}$$

All coefficients are detailed in Appendix 3.C. Given the forward TIPS rates, the TIPS yield

$y_{t,\tau}^{TIPS}$ with maturity $\tau = nh$ at time t can be easily computed as

$$\begin{aligned} y_{t,\tau=nh}^{TIPS} \approx & -\frac{1}{nh}\sum_{k=0}^{n-1}\alpha_{kh}^{TBEIa} - \frac{1}{nh}\sum_{k=0}^{n-1}\alpha_{kh}^{TBEIb} - \frac{h}{n}\left(\rho_1^{BEI}-\beta\right)'\sum_{k=0}^{n-1}C_{kh}^{Q,R}\left(\rho_1^{BEI}-\beta\right) \\ & - \frac{h}{n}\widetilde{\beta}'\sum_{k=0}^{n-1}\widetilde{C}_{kh}^{Q,R}\widetilde{\beta} - \frac{1}{nh}\sum_{k=0}^{n-1}\beta_{kh}^{TBEIa\prime}X_t - \frac{1}{nh}\sum_{k=0}^{n-1}\beta_{kh}^{TBEIb}\widetilde{X}_t \\ & + \frac{1}{nh}\sum_{k=0}^{n-1}\sigma_{kh}^{Q,N,R}g\left(\frac{\alpha_{kh}^{N,R}+\beta_{kh}^{N,R\prime}X_t}{\sigma_{kh}^{Q,N,R}}\right) \\ & + \frac{h}{n}\rho_1^{NS\prime}\sum_{k=0}^{n-1}C_{kh}^{Q,R}\left(\rho_1^{BEI}-\beta\right)\Phi\left(\frac{\bar{\alpha}_{kh}^{N,R}+\beta_{kh}^{N,R\prime}X_t}{\sigma_{kh}^{Q,N,R}}\right). \end{aligned} \tag{3.3.22}$$

3.3.1.4 Break-even Inflation Rate Decomposition

We now introduce how to decompose BEI into IE and IRP. The τ-period BEI, also called τ-period inflation compensation, is defined as the difference between the τ-period nominal yield and real yield,

$$\text{BEI}_{t,\tau} = y_{t,\tau}^{N} - y_{t,\tau}^{R}. \tag{3.3.23}$$

In reality, the real yield can not be observed directly, so an empirical approximation of the τ-period BEI is the τ-period TIPS BEI, which is defined as the τ-period TIPS yield minus the τ-period nominal yield. Based on equation (3.3.18), the τ-period TIPS BEI equals the τ-period BEI minus the τ-period TIPS liquidity risk premium. By estimating our joint time structure model, we can remove the TIPS liquidity effects and then compute BEI over different horizons, which are the difference between nominal yields and real yields at corresponding maturities.

The τ-period BEI can then be decomposed into τ-period IRP and τ-period IE over the same horizon, i.e.,

$$\text{BEI}_{t,\tau} = \text{IE}_{t,\tau} + \text{IRP}_{t,\tau} = \frac{1}{\tau}\text{E}_t\left(\int_t^{t+\tau} r_s^I ds\right) + \text{IRP}_{t,\tau}. \tag{3.3.24}$$

The τ-period IE is the expectation of future inflation rates over the next τ-period, while the corresponding IRP is the premium investors require in order to bear the uncertainty risks of inflation dynamics over the same horizon.

Because the inflation rate r_t^I is an affine function of X_t. Therefore, inflation expectations $\text{IE}_{t,\tau} = \frac{1}{\tau}\text{E}_t\left(\int_t^{t+\tau} r_s^I ds\right)$ is also an affine function of X_t, with the closed-form solution detailed in Appendix 3.D.

3.3.2 Data

The data sample covers the period from January 1999 to May 2017. We collect nominal and TIPS zero-coupon yields from Gürkaynak et al.(2007; 2010) datasets which can be downloaded from the Federal Reserve Board of Governors research data page.[1]. The maturities of TIPS yields include 2, 3, 4, ..., 19 and 20 years, and those of nominal counterparts include 1, 2, 3, ..., 29 and 30 years. We expand the cross-section of nominal yields by adding 3- and 6- month T-bill yields obtained from the economic data website of Federal Reserve Bank of St. Louis. The large cross-section of zero-coupon yields, which consists of 32 maturities for nominal and 19 maturities for TIPS bonds, allows us to extract sufficient information from the yield curves. All yields are sampled at weekly frequency[2] for a total of T = 961 time-stamps.

We acquire monthly headline Consumer Price Index for all urban consumers (CPI-U) from the economic data website of Federal Reserve Bank of St. Louis. We choose seasonally-adjusted CPI inflation for estimation since our model does not take the seasonality into account. Because the CPI data is not released weekly, we assume CPI does not change during the same month and use monthly CPI as the observation for each week,

[1] See https://www.federalreserve.gov/pubs/feds/2006/200628/200628abs.html and https://www.federalreserve.gov/pubs/feds/2008/200805/200805abs.html.

[2] To get rid of weekend effects, we sample yields on each Wednesday. If data on Wednesday is missing, we replace it by that on Thursday or Tuesday.

without any forward-looking bias.

To reliably estimate the Inflation expectations (IE) and Inflation Risk Premium (IRP), one key dataset required to be fed into the models is the survey of inflation forecasts. We obtain 1-year inflation forecasts over the next 1, 5 and 10 years from the Survey of Professional Forecasters (SPF) dataset issued by the Federal Reserve Bank of Philadelphia. The survey data is released in the middle month of each quarter. We find the exact release date for each survey and use the corresponding data as the observations for the first Wednesday following the release. Consequently, there is only one week having the professional forecasts data during each quarter. For other weeks, we set the forecasts as missing data. All of these forecasts are available each quarter.

Another advantage of feeding the forecasts data into my models is that it helps to overcome the "small-sample problem", which means typical data sample used in a dynamic term structure estimation, for example, 5 to 15 years, results in unreliable estimate of physical dynamics of interest rate due to the trouble of observing a sufficient number of "mean-reversions". As suggested by Kim and Orphanides (2012), the supplement of the survey forecasts data of 3-month Tbill rates provides additional relevant information to effectively stabilize the estimation and pin down the P parameters. Therefore, we also add 3-month Tbill rate forecasts over the next 1 year and 10 years from the SPF dataset to our model. The first forecast is available each quarter, while second one are is only reported every first quarter.

For oil price data, we obtain weekly crude oil price by sampling the West Texas Intermediate (WTI) index on each Wednesday from the economic data website of Federal Reserve Bank of St. Louis.

3.3.3 Parameter Estimation and Model Fit

As detailed in Appendix 3.E, our joint model is reorganized as a nonlinear state-space model with Gaussian measurement errors, because some observable variables, including nominal yields, inflation forecasts and nominal rate forecasts are all nonlinear functions of state variables. We linearize these observable equations using the analytical first-order derivatives in spirit of Wu and Xia (2016), then estimate the system by maximum likelihood methodology using the extended Kalman Filter (EKF). All technical details are provided in Appendix 3.E. With 29 model parameters and 20 observation standard errors, the state-space model includes a 5-dimension state transition equation and a 21-dimension observation equation [3]. The large cross-section and time series of observations help to pin down parameters. We use a sufficient set of starting values for robustness checks to ensure the parameters we estimate arrives at the global optimum.

Survey forecasts are not available for each week during our sample period, which results in missing data in the observation equation. In order to handle this issue, we allow the dimension of the observation equation matches the actual number of observations at each time (see section 3.4.7 of Harvey (1989) for further details). For identification purpose, we impose the standard non-negative constraints on κ_{11}, κ_{22}, κ_{33}, $\tilde{\kappa}$, and λ. In addition, We normalize $\widetilde{\sigma}$ to be equal to 0.01.

Table 3.4 presents the log likelihood, estimated parameters and standard errors for our model. All parameters driving the dynamics of nominal yields, inflation and TIPS yields are significant at 1% level, which suggests our model is easy to be identified using the large cross-sectional data.

To assess the fitting performance of our model, in Figure 3.2, 3.3, 3.4 and 3.5, we plot the actual and fitted nominal yields, TIPS yields and survey forecasts of inflation and 3-month Till rates. The root mean squared errors (RMSEs) of the in-sample fitting are

[3]The first observable variable, the logarithm of CPI, is assumed to be observed without error.

shown in the title of each plot. These figures show that our model exhibits quite well overall fitting performance for nominal and TIPS yields given a large cross section of data for simultaneous fitting. As a real-time, model-free measure, survey forecasts data contain useful information for future dynamics and outperform the other forecasting methods including the term structure specification (Ang et al., 2007). A visual comparison between the model-implied expectations and survey-based counterparts show that our model capture the majority of information, given the large dispersion in survey forecasts.

In Figure 3.6, we also show shows the estimated nominal/real yields (in blue), which assume there is the ZLB constraint, and the shadow rate implied nominal/real yields yields (in dashed red), which relaxes the constraint, at maturities of 3 months, 6 months, 1 year, 3 years, 5 years and 10 years. Before the financial crisis, the shadow rate implied yields almost coincide with observed nominal yields, while after the financial crisis, the shadow rate implied yields deviates below the actual yields, especially for the short-term yields. These patterns suggests the necessity to include the ZLB constraint in our model.

3.3.4 TIPS BEI Decomposition

Figure 3.7 shows the decomposition of TIPS BEI, including IE, IRP and IRP, for 10 year, 15 year and 20 year. The upper three panels show IE (in blue), BEI (in red) and TIPS BEI (in yellow) of three maturities. The level of TIPS BEI is more volatile and often lower than BEI, indicating that it is not accurate to use TIPS BEI to approximate inflation compensation because of liquidity risk premium. The further comparison between IE and BEI shows that IE is stabler than BEI, reflecting the time-varying market prices of inflation risk.

The middle three panels show IRP of 10, 15 and 20 years. They keep positive in most of pre-crisis period, suggesting that investors usually demand premia for inflation risk. This is not the case for many days after financial crisis, when the IRP of all three horizons fall into

the negative horizon, suggesting that the market would like to pay for hedging deflation risks.

The bottom three panels show that LRP of 10, 15 and 20 years keep positive and relatively high for the period 1999-2003, 2008-2010, which suggests that investors needs to pay the price higher than the fair value of TIPS because they are illiquid during these periods. The high level of LRP in the beginning of the sample indicates the illiquidity of TIPS when they were just issued to the market. Its downward trend afterwards till 2004 reflects TIPS liquidity kept improving during this period. The sharp surge of the factor around 2009 suggests TIPS liquidity evaporated during the financial crisis.

3.4 Oil Shocks on IE and IRP

We now examine the Hypothesis 1 and 2 by analyzing oil price shocks on IE and IRP under ZLB and No-ZLB regimes.

3.4.1 Oil Shocks on IE

We start our analysis from studying the oil's different shocks on IE before and after financial crisis. Panel A (Panel B) of Table 3.5 regresses the weekly changes of IE of 5, 10, 15, and 20 years on the weekly changes of log oil price. The regression is described in equation (3.2.1), where Y_t is the IE estimate of each week. By comparing Panel A and Panel B, we find that before crisis, the coefficient of oil shocks is insignificant; however, after crisis, the coefficient becomes significant at level 1%, with dramatically increasing T-statistic and adjusted R square. Take the regression for 10-year IE as an example. The slope of log return of oil price is zero before crisis, but after crisis, it increases to 0.0016 with a t-statistic of 7.04. The corresponding adjusted R square increases from negative to 8.73%. A 1% increase in oil prices lifts 5-, 10-, 15- and 20-year IE by 0.19, 0.16, 0.13 and

0.11 bps after crisis, while the corresponding pre-crisis increases of IE are zero. As horizon increases, the difference between oil effects on IE before and after crisis becomes weaker.

To formally test the post-crisis oil shocks on IE, in Panel C of Table 3.5 we regress the weekly changes of IE on the weekly changes of log oil price, the post-crisis dummy and the interaction term, as described in equation (3.2.2), with Y_t standing for the IE estimate of each week. Our interest is the coefficient of the interaction term $\Delta(\ln WTI_t) \cdot 1_{Post}$, which identifies the additional effects of oil price changes after crisis. Consistent with our previous analysis, all regressions have significantly positive coefficients of the interaction term at level 1%. All these results reject Hypothesis 1, which states that oil shocks on IE plays no role in amplifying oil's positive effects on inflation compensation after crisis.

We then test Hypothesis 2 using the method in section 3.2.3, which examines the asymmetric effects of oil shocks on IE. Table 3.6 estimate oil shocks on IE under different scenarios by conducting regressions with two-way and three-way interactions for the whole sample. To save space, only regression results for 10-year (Panel A) and 20-year (Panel B) IE are presented. Column (1) regresses the weekly changes of IE on weekly changes of log oil price. Consistent with previous results, the coefficient of long oil price changes is significantly positive. Column (2) conducts a regression with two-way interactions between log oil price changes and the ZLB dummy, described in equation (3.2.4). The coefficient of the interaction term is significantly positive at the 1% level, showing the oil's positive effects on IE is much stronger under the ZLB regime. Column (3) conducts a regression with two-way interactions between log oil price changes and the negative change dummy, described in equation (3.2.3). The coefficient of the interaction term is not significant, which implies that oil shocks exhibit opposite asymmetric effects for the ZLB and No-ZLB sample points. Column (4) conducts a regression with three-way interactions among log oil price change, the negative change dummy and the ZLB dummy, as described in equation (3.2.5). The coefficient of the three-variable interaction term is significantly positive at the 5% level, which suggests that the oil's positive effects on IE arrive at the peak when oil

prices drop under the ZLB regime. In other words, when the nominal short rate is close to ZLB, IE moves more frequently with oil prices when the oil prices go down then when it go up. This provides the direct evidence to support Hypothesis 2.

3.4.2 Oil Shocks on IRP

Although we have demonstrated that the oil's positive effects on long-term IRP after crisis is due to the ZLB constraint of monetary policy, we are interested at how oil prices affect the investors' premium for bearing the inflation risks before and after crisis. Panel A (Panel B) of Table 3.7 regresses weekly changes of IRP of 5, 10, 15, and 20 years on weekly changes of log oil price. The regression is described in equation (3.2.1), where Y_t is the IRP estimate of each week. By comparing Panel A and Panel B, we find that before crisis, the coefficient of oil shocks is insignificantly negative; however, after crisis, the coefficient becomes positive at the significant level 1% except for 5 years, with dramatically increasing T-statistic and adjusted R square. Take the regression for 10-year IRP as an example. The slope of log return of oil price is -0.0003 with a t-statistic of -0.91 before crisis, but after crisis, it increases to 0.0009 with a t-statistic of 3.47. The corresponding adjusted R square increases from 0.06% to 3.18%. A 1% increase in oil prices lifts 5-, 10-, 15- and 20-year IRP by 0.04, 0.09, 0.11 and 0.13 bps after crisis, while the corresponding pre-crisis changes of IRP are negative and negligible. As horizon increases, the difference between oil effects on IRP before and after crisis becomes more notable.

To formally test the post-crisis oil shocks on IRP, in Panel C of Table 3.7 we regress the weekly changes of IRP on the weekly changes of log oil price, the post-crisis dummy and the interaction term, as described in equation (3.2.2), with Y_t standing for the IRP estimate of each week. Our interest is the coefficient of the interaction term $\Delta\left(\ln WTI_t\right) \cdot 1_{Post}$, which identifies the additional effects of oil price changes after crisis. Consistent with our previous analysis, all regressions have significantly positive coefficients for the

interaction term at the level 1% except for 5 years. These results demonstrate that before the financial crisis, oil prices have no influences on IRP; while after crisis, oil prices have notably positive effects on IRP, which helps to exaggerate the oil's effects on inflation compensation.

We further examine whether there exists asymmetric effects of oil shocks on IRP under ZLB and NO-ZLB regimes. Table 3.8 estimate the oil shocks on IRP under different scenarios by conducting regressions with two-way and three-way interactions for the whole sample. To save space, only regression results for 10-year (Panel A) and 20-year (Panel B) TIPS BEI are presented. Column (1) regresses the weekly changes of IRP on weekly changes of log oil price. Consistent with previous results, the coefficient of oil shocks is significantly positive. Column (2) conducts a regression with two-way interactions between log oil price changes and the ZLB dummy, described in equation (3.2.4). The coefficient of the interaction term is significantly positive at the 1% level, showing the oil's positive effects on IRP are much stronger under the ZLB regime. Column (3) conducts a regression with two-way interactions between log oil price changes and the dummy of negative oil price changes, described in equation (3.2.3). The coefficient of the interaction term is not significant, which implies that oil shocks don't exhibit asymmetric effects for the mixed ZLB and No-ZLB sample points. Column (4) conducts a regression with three-way interactions among log oil price change, the negative change dummy and ZLB dummy, as described in equation (3.2.5). The coefficient of the three-variable interaction term is significantly positive at the 5% level, which suggests that the oil prices' positive effects on IRP is strongest when oil prices drop under the ZLB regime. In other words, under the ZLB regime, IRP moves more often with oil prices when the oil price go down then when it go up. Therefore, the positive effects of oil shocks are asymmetric for both IE and IRP.

In summary, the oil's positive effects on IRP are only significant when oil prices decrease under the ZLB regime. Given the fact that IRP often keeps negative under the ZLB

regime, we conclude that investors would like to pay higher premiums for hedging long-term deflation risks when oil price decreases in an ZLB environment.

3.5 General Equilibrium Analysis

In this section we use a small-scale, closed-economy and new-Keynesian DSGE model augmented with an oil sector and the Taylor rule with the ZLB constraint to study the theoretical effects of ZLB on the relationship between oil prices and the term structure of IE.

3.5.1 A DSGE model with Oil and the ZLB Binding Constraint

3.5.1.1 Household

We consider an economy in which the representative household maximizes its utility at time t by deciding discrete streams of final goods consumption C_{t+k}, oil consumption C^O_{t+k}, labor services N_{t+k}, and real bond holdings B_{t+k}/P_{t+k}, where $k = 0, 1, 2, ..., \infty$. B_t is the holding of nominal risk-free bond and P_t is the price level of final goods. The agent's preferences are described by

$$\mathrm{E}_t \sum_{k=0}^{\infty} \beta^k \left[U\left(C_{t+k}, C^O_{t+k}, N_{t+k}, d^O_{t+k}\right) + s_{t+k}\lambda_{t+k} V\left(\frac{B_{t+k}}{P_{t+k}}\right)\right], \tag{3.5.1}$$

where β is the subjective discount factor, d^O_{t+k} is the oil demand shock that shifts the household's preferences for oil consumption, and s_{t+k} is the real bond demand shock that shifts the household's preferences for holding risk-free assets. Both d^O_{t+k} and s_{t+k} follow stochastic and exogenous processes.

We specify the function U by augmenting oil consumption to the GHH utility function

originally proposed by

$$U\left(C_{t+k}, C_{t+k}^{O}, N_{t+k}, d_{t+k}^{O}\right) = \log Q_t - \frac{N_t^{1+\chi}}{1+\chi}, \tag{3.5.2}$$

where Q_t is the consumption bondle

$$Q_t = \left[(1-\alpha_C)\, C_t^{1-\frac{1}{\rho_C}} + \alpha_C \left(\frac{C_t^O}{d_t^O}\right)^{1-\frac{1}{\rho_C}}\right]^{\frac{1}{1-\frac{1}{\rho_C}}}. \tag{3.5.3}$$

This preference is similar to those used in Bodenstein et al. (2013) and Datta et al. (2018). We specify the consumption bundle of general consumption good and oil as a CES function, where $\alpha_C \in (0,1)$ describes the relative importance of oil consumption in the economy, and $\rho_C \in (0,\infty)$ is the constant elasticity of substitution. Oil and the general consumption good are complements for ρ_C close to zero, while they are substitutes for large ρ_C. $\chi \in (0,1)$ is the inverse Frisch elasticity of labor supply.

We include the separable utility function $V(\cdot)$ for in the household's preference to generate the premium investors would like to pay for holding real bonds, following Smets and Wouters (2007), Fisher (2015) and Datta et al. (2018). $V(\cdot)$ is positive, increasing and concave. The stochastic and exogenous variable s_t capture the time-varying risk premium of risky assets over save and liquid assets such as treasuries.

The household maximizes (3.5.1) by choosing state contingent paths for C_{t+k}, C_{t+k}^O, N_{t+k} and B_{t+k} subject to the following sequences of flow budget constraints:

$$C_t + P_t^O C_t^O + B_t/P_t \leq W_t N_t + R_{t-1} B_{t-1}/P_t + T_t, \tag{3.5.4}$$

where P_t^O is the real price of oil, W_t is the real wage, R_t is the gross nominal one-period interest rate, and T_t denotes real lump-sum government taxes and transfers.

Following Datta et al. (2018), we define $\lambda_t = \partial U_t / \partial \bar{C}_t$, where $\bar{x}_t$ represents an aggregate quantity taken as given by the household. By normalizing $V(\cdot)$ and using the household's first order conditions, the intertemporal Euler equation is given by

$$1 = s_t + \mathrm{E}_t \left[M_{t+1} R_t \right], \tag{3.5.5}$$

where the nominal pricing kernel is

$$M_{t+1} = \beta \frac{\partial U_{t+1} / \partial C_{t+1}}{\partial U_t / \partial C_t} \frac{1}{\Pi_{t+1}} = \beta \left(\frac{C_{t+1}}{C_t} \right)^{-\frac{1}{\rho_C}} \left(\frac{Q_{t+1}}{Q_t} \right)^{-1+\frac{1}{\rho_C}} \frac{1}{\Pi_{t+1}}. \tag{3.5.6}$$

Here $\Pi_{t+1} \equiv \frac{P_{t+1}}{P_t}$ is the gross inflation of the price level of final goods. s_t is identical to the spread between the one-period risk-free bond and other assets and its stochastic property generates time-varying demand shocks for safe and liquid assets. For example, a flight to safety of investors during financial crisis periods push s_t to a large value.

In addition, the household's first order conditions implies the intratemporal conditions hold that the real price of oil is equal to the marginal rate of substitution between oil and the general consumption good, i.e.,

$$P_t^O = \frac{\partial U_t / \partial C_t^O}{\partial U_t / \partial C_t} = \frac{\alpha_C}{1 - \alpha_C} \left(\frac{C_t^O}{C_t} \right)^{-\frac{1}{\rho_C}} \left(d_t^O \right)^{-1+\frac{1}{\rho_C}}, \tag{3.5.7}$$

and the real wage rate of labor supply is equal to the negative marginal rate of substitution between labor and the general consumption good, i.e.,

$$W_t = -\frac{\partial U_t / \partial W_t}{\partial U_t / \partial C_t} = \frac{N_t^{\chi} Q_t^{1-\frac{1}{\rho_C}}}{(1 - \alpha_C) C_t^{-\frac{1}{\rho_C}}}. \tag{3.5.8}$$

3.5.1.2 Firms and Production

To produce the composite final goods Y_t, perfectly competitive firms aggregate a variety of intermediate goods $Y_t(i)$ using a CES production technology,

$$Y_t = \left(\int_0^1 Y_t\left(i\right)^{\frac{\theta-1}{\theta}} di \right)^{\frac{\theta}{\theta-1}},$$

where $\theta > 1$ and $i \in [0,1]$. To minimize the production cost, $\int_0^1 P_t\left(i\right) Y_t\left(i\right) di$, where $P(i)$ is the price of intermediate goods i, we can derive the demand curves for intermediate goods,

$$Y_t\left(i\right) = \left(\frac{P_t\left(i\right)}{P_t} \right)^{-\theta} Y_t. \tag{3.5.9}$$

The intermediate goods are produced by a continuum of monopolistic competitors indexed by $i \in [0,1]$. At time t, the producer i choose state contingent streams of $P_t\left(i\right)$ and $Y_t\left(i\right)$ to maximize the profit,

$$\mathrm{E}_t \sum_{k=0}^{\infty} M_{t,t+k} \left[\left(P_{t+k}\left(i\right) - MC_{t+k} P_{t+k} \right) Y_{t+k}(i) - \frac{\varphi}{2} \left(\frac{P_{t+k}\left(i\right)}{P_{t+k-1}\left(i\right) \bar{\Pi}} - 1 \right)^2 Y_{t+k} P_{t+k} \right], \tag{3.5.10}$$

where $M_{t,t+k} = \prod_{m=0}^{k} M_{t+m}$ is the stochastic discount factor that evaluates the period $t+k$ nominal profit flows at time t. MC_t is the real marginal cost function. The cost adjusting parameter $\varphi > 0$ determines the degree of price rigidity. As stressed by Rotemberg (1982), the quadratic adjustment cost $\frac{\varphi}{2} \left(\frac{P_t(i)}{P_{t-1}(i)\bar{\Pi}} - 1 \right)^2 Y_t$ accounts for the negative effects of price changes on the customer-firm relationship, which increases with the size of the price change and with the overall magnitude of economic output Y_t. Following Nakata and Tanaka (2016), we assume the firms use a simple price indexation on the central bank's inflation target $\bar{\Pi}$.

We use I_t^O to denote the aggregate oil inputs for production. The firm i combines the labor $N_t(i)$ and oil inputs $I_t^O(i)$ to produce the intermediate good i according to the

following technology,

$$Y_t(i) = A_t \left[(1-\alpha_Y) N_t(i)^{1-\frac{1}{\rho_Y}} + \alpha_Y \left(I_t^O(i) \right)^{1-\frac{1}{\rho_Y}} \right]^{\frac{1}{1-\frac{1}{\rho_Y}}}, \tag{3.5.11}$$

where $\alpha_Y \in (0,1)$ describes the relative importance of oil inputs in production, and $\rho_C \in (0,\infty)$ is the constant elasticity of substitution. Oil inputs and the labor are complements for ρ_Y close to zero, while they are substitutes for large ρ_Y. A_t is the stochastic productivity level. We assume it is stationary and exogenous, capturing stochastic technology shock. The first-order condition for minimizing production cost, $c(Y_t(i)) = W_t N_t(i) + P_t^O I_t^O(i)$, implies that the input ratio between oil and labor is

$$\frac{I_t^O}{N_t} = \frac{I_t^O(i)}{N_t(i)} = \left(\frac{1-\alpha_Y}{\alpha_Y} \frac{P_t^O}{W_t} \right)^{-\rho_Y} \tag{3.5.12}$$

and the real marginal cost $\partial c(Y_t(i))/\partial Y_t(i)$ is

$$MC_t = \frac{1}{A_t} \left[(1-\alpha_Y)^{\rho} W_t^{1-\rho_Y} + \alpha_Y^{\rho} \left(P_t^O \right)^{1-\rho_Y} \right]^{\frac{1}{1-\rho_Y}}. \tag{3.5.13}$$

All monopolists are identical and face the same problem, and thus choose the same price, use the same inputs of oil and labor, and produce the same quantity. In other words, the symmetric equilibrium holds, $P_t(i) = P_t$, $N_t(i) = N_t$, $I_t^O(i) = I_t^O$ and $Y_t(i) = Y_t$. Therefore, based on the first-order condition to maximize (3.5.10) and the symmetric equilibrium, we obtain

$$Y_t \left[\varphi \left(\frac{\Pi_t}{\bar{\Pi}} - 1 \right) \frac{\Pi_t}{\bar{\Pi}} - (1-\theta) - \theta MC_t \right] = \mathrm{E}_t \left[M_{t+1} \Pi_{t+1} Y_{t+1} \varphi \left(\frac{\Pi_{t+1}}{\bar{\Pi}} - 1 \right) \frac{\Pi_{t+1}}{\bar{\Pi}} \right]. \tag{3.5.14}$$

3.5.1.3 Monetary Policy

The central bank follows the Taylor rule with occasionally binding ZLB constraint to conduct monetary policy, setting the nominal one-period interest rate as,

$$R_t = \max\left[0, R_t^*\right], \tag{3.5.15}$$

where the nominal shadow rate R_t^* satisfies

$$R_t^* = \bar{R}\left(\frac{\Pi_t}{\bar{\Pi}}\right)^{\phi_\Pi}\left(\frac{Y_t}{\bar{Y}}\right)^{\phi_y}. \tag{3.5.16}$$

Here $\bar{R}$, $\bar{\Pi}$ and $\bar{Y}$ denote the steady state of R_t, Π_t and Y_t.

3.5.1.4 Market Clearing

In equilibrium, the clearing condition for final goods market is

$$Y_t = C_t + \frac{\varphi}{2}\left[\int_0^1\left(\frac{P_t(i)}{P_{t-1}(i)\bar{\Pi}} - 1\right)^2 di\right] Y_t = C_t + \frac{\varphi}{2}\left(\frac{\Pi_t}{\bar{\Pi}} - 1\right)^2 Y_t, \tag{3.5.17}$$

$$Y_t = A_t\left[(1-\alpha_Y)\, {N_t}^{1-\frac{1}{\rho_Y}} + \alpha_Y\left(I_t^O\right)^{1-\frac{1}{\rho_Y}}\right]^{\frac{1}{1-\frac{1}{\rho_Y}}}. \tag{3.5.18}$$

The aggregation condition in the oil market requires that the oil demand equals the oil supply in each period,

$$S_t^O = C_t^O + I_t^O, \tag{3.5.19}$$

where the oil supply S_t^O is exogenously determined and follows a stationary stochastic process.

3.5.1.5 Exogenous Stochastic Processes

The exogenous variables in our model include demand shock for real bond holdings s_t, oil demand shock d_t^O, oil supply shock S_t^O, and productivity shock A_t. We assume that each of them follows a log AR(1) process as follows,

$$\log x_t = (1-\rho_x)\log\bar{x} + \rho_x \log x_{t-1} + \varepsilon_{x,t}, \tag{3.5.20}$$

where $\varepsilon_{x,t}$ is i.i.d normal with standard deviation of σ_x and $\bar{x}$ represents the steady state value. We assume all process are independent with each other.

3.5.1.6 Equilibrium Characterization and Model Solution

Given the exogenous processes $\left\{s_t, d_t^O, S_t^O, A_t\right\}_{t\geq 0}$, a monopolistically competitive equilibrium is defined as a set of endogenous processes including $\{Q_t,\ U_t,\ C_t,\ N_t,\ M_t,\ R_t,\ \Pi_t,\ Y_t,\ W_t,\ C_t^O,\ I_t^O,\ P_t^O,\ MC_t\}_{t\geq 0}$ such that: (1) the household's problem satisfies the F.O.C. (3.5.5), (3.5.6), (3.5.7) and (3.5.8), given the specification of preferences (3.5.2) with (3.5.3); (2) the intermediate goods' producers' problem satisfies the F.O.C. (3.5.12), (3.5.13) and (3.5.14); (3) monetary policy follows the Taylor rule with ZLB binding constraint (3.5.15); (4) final goods market satisfies the clearing conditions (3.5.17) and (3.5.18), and oil market satisfies the clearing conditions (3.5.19). Given 13 equations and 13 endogenous variables, the equilibrium can be uniquely determined.

Adding the occasionally ZLB binding constraint to the monetary policy causes a strong non-linearity for the DSGE system, and researchers have adopted different methods to accommodate the constraint, Nakata and Tanaka (2016) and Datta et al. (2018) solve and simulate their DSGE models with ZLB constraint using a brute-force time (policy function) iteration method in the spirit of Bizer and Judd (1989) and Coleman (1991). The method's significant startup costs and a reliance on grid-based method lead to high computational costs and limits the number of state variables. Richter et al. (2014) advocate the

method with parallel computing and linear interpolation. Guerrieri and Iacoviello (2015) develop a computationally fast toolkit, "Occbin", which provides a piecewise perturbation solution that can handle a large number of state variables. However, the toolkit is not able to simulate state variables and capture the precautionary behavior caused by the possibility that a constraint may become binding in the future, as a result of shocks yet unrealized.

We employ the computationally efficient "dynareOBC" toolkit developed by Holden (2017) to solve and simulate our model. Holden (2016) derives the first necessary and sufficient conditions for the existence of a unique perfect-foresight solution to an otherwise linear dynamic model with occasionally binding constraints, given a fixed terminal condition, and Holden (2017) constructs the corresponding algorithm and extends it to consider the stochastic simulation and future uncertainty. We use the "Global" option of the toolkit to let the household and producers take into account the risk of hitting the bound at all horizons.

3.5.2 Baseline Model Simulation

In this section, we simulate the baseline model — the full model as outlined above — to generate data that can be used to study the correlation between oil prices and the term structure of inflation expectations given different level of interest rates. We first introduce the parameter choices and then analyze the simulation results.

3.5.2.1 Parameter Choices

Table 3.9 reports all parameters for simulating the baseline model. Most parameters for the household's preferences, goods production and monetary policy are in line with literature. The quarterly subjective discount factor β is fixed at 0.985 and the steady state for bond preference shock, $\bar{s}$, is set to be 0.01, in line with Datta et al. (2018). This implies a 2 percent risk-free real interest rate and a 4 percent annual premium on risky assets over

the risk-free bond in the steady state. We set the oil share in consumption bundle, α_C, to 0.05, and set the the elasticity of substitution ρ_C between oil and final goods to 0.25, in line with Ready (2018). Furthermore, we assume the inverse Frisch elasticity, χ, is 0.25, in line with Nakata and Tanaka (2016).

For production, we assume the oil share in production α_Y is 0.055 and the elasticity of substitution ρ_Y between oil and labor is 0.225, following Ready (2018). This suggests that firms use more oil as an input to production that households consume. The elasticity of substitution among intermediate goods θ, price adjustment cost φ, the steady state of gross inflation $\bar{\Pi}$, and the Taylor rule parameters ϕ_π are all in line with Nakata and Tanaka (2016). Moreover, all AR(1) coefficients and standard derivation of exogenous shocks are listed in the Panel D.

3.5.2.2 Simulation Results

Given the above parameters, we simulate our model to analyze the correlation between oil prices and the term structure of inflation expectations given different level of shadow interest rates. The simulated real bond preference shocks s_t play a predominate role in generating time-varying nominal interest rates with ZLB. Higher s_t makes the nominal interest rate lower and closer to ZLB. When s_t increases to a certain degree or more, the interest rate binds at ZLB. Using the baseline parameters, the probability that the nominal interest rate binds at zero, i.e., the shadow rate is lower than 0, is 18%. We compute the correlation between oil prices and inflation expectations local to a particular value of annualized shadow rate, $r^* = 400(R^* - 1)$, using the nonparametric kernel method. Then we can analyze how the correlation changes with the shadow rate. This method is in spirit of Datta et al. (2018), which uses the same methods to demonstrate ZLB causes the increased correlation between oil prices and equity returns.

We compute the mean of a variable x_t, which is the oil price or inflation expectations

with a specific term, local to a particular value of r^* based on

$$\mu_x(r^*) = \frac{\sum_i K_\lambda(r^*, r_i^*)\, x_i}{\sum_i K_\lambda(r^*, r_i^*)},$$

where we set the kernel function $K_\lambda(r^*, r_i^*)$ to be the standard normal density function of $\frac{r^* - r_i^*}{\lambda}$. λ is the bandwidth parameter. The local variance and covariances are given by

$$\sigma_x^2(r^*) = \frac{\sum_i K_\lambda(r^*, r_i^*)\,(x_i - \mu_x(r^*))^2}{\sum_i K_\lambda(r^*, r_i^*)},$$

$$\sigma_{xy}(r^*) = \frac{\sum_i K_\lambda(r^*, r_i^*)\,(x_i - \mu_x(r^*))\,(y_i - \mu_y(r^*))}{\sum_i K_\lambda(r^*, r_i^*)}.$$

Finally, we can calculate the local correlation as

$$corr_{xy}(r^*) = \frac{\sigma_{xy}(r^*)}{\sigma_x(r^*)\,\sigma_y(r^*)}.$$

Figure 3.8 shows the local correlation between oil real prices and the term structure of inflation expectations at different shadow nominal interest rate. The upper left, upper right, bottom left and bottom right panels shows the oil real prices' correlation with contemporaneous inflation rate, 1-year IE, 5-year IE, and 10-year IE local to different nominal shadow interest rates ranging from -5% to 5%. We choose the bandwidth parameter as $\lambda = 5$. The blue line in each figure shows the local correlation when the ZLB binding constraint is considered. We can see that when the shadow rate decreases, the local correlations monotonically increases. When the shadow rate changes from 5% to -5%, the local correlation between oil real price and 10-year IE increases monotonically from 0.35 to 0.7. This is consistent with the empirical pattern that oil prices have a larger impact on long-term IE when nominal interest rate is close to or binding at the ZLB. We can also infer that when nominal rate is at ZLB, the oil price changes should exhibit the asymmetric effects on the changes of IE at different horizons. As oil prices are an important component of inflation

and inflation is positively related to shadow rate according to Taylor rule, oil prices have a positive correlation with shadow interest rate. Therefore, the local correlation, or local beta between oil and IE is larger when oil prices decrease than that when oil prices increase. In other words, the decrease of IE caused by the negative change of oil price exceeds the increase of IE caused by the same positive change of oil price. Thus the simulation of our baseline model is consistant with the oil effects in empirical findings.

We also simulate the model ignoring the ZLB. That is, we treat the shadow interest rate as the nominal short rate. The red line in each panel shows the corresponding local correlation between oil prices and IE at different horizons. We can see all of them are lower than blue lines and keeps flat for different shadow rates. This further confirms that the ZLB is the only factor that amplify the oil's effect on IE and make the effect asymmetric.

3.5.3 Mechanisms

To understand the forces driving the oil prices' asymmetric effects on long-term IE at the ZLB, it is useful to perform impulse response function analysis of oil supply and demand factors, which are two exogenous variables affecting oil prices. By studying how oil prices and other macro variables such as output, consumption and inflation change with oil supply or demand factors, we can show the role of ZLB clearly. In our baseline model, the steady state of annualized nominal interest rate is 4%. In order to push nominal rate down to ZLB, we need to give an extremely positive impulse on oil supply factor or an extremely negative impulse on oil demand factor to push down the oil prices as well as inflation. In order to analyze oil shocks on economy around the ZLB, we create a virtual environment with steady nominal interest rate at 25 bps by fixing bond preference shock s_t at 0.01929, i.e., we set $\bar{s}$ and σ_s to 0.01929 and 0, respectively. All other parameters are still the same with those in the baseline model. We create this extended version of the baseline model to describe the temporal steady economy in financial crisis period with

nominal short rate extremely close to ZLB.

3.5.4 Supply-driven Oil Prices

Figure 3.9 shows the impulse responses of two standard deviation of oil supply shocks (10% change in level) on all macro variables and IE with different horizons. The red solid line indicates the impulse responses for the 10% positive change of oil supply and the blue solid line indicates that for the 10% negative change of oil supply. The red dashed line indicates the impulse responses for the 10% positive change of oil supply if we ignore ZLB binding constraint in the model. The percentage change of all variables except annualized nominal interest rate are plotted. For annualized nominal interest rate, we show its impulse response of level. All impulse responses are reported for horizons ranging from 0 to 5 years.

We first analyze the impulse response functions (IRF) of oil supply shock ignoring the ZLB constraint. In this case, the IRF of the 10% positive change of oil supply is symmetric to the IRF of the 10% negative change of oil supply with respect to the steady state because the model is symmetric around the steady state. When oil supply increases by 10%, both oil consumption and oil input for production increase. More oil consumption pushes down the elasticity of substitution between oil consumption and final goods consumption, thus the oil prices decrease by 20.73%. As oil input is a key component for production, the decreasing of oil prices reduces the real marginal cost as well as the price level of intermediate and final goods. Therefore, the inflation decreases. According to the Taylor rule, the Federal Reserve sets lower nominal short rate to mitigate the reduction of inflation. From Figure 3.9 we can see that the central bank decreases the nominal short rate from 25 bps to -2.09%, with the help of which the annualized inflation decreases by 47.14%, changing from the steady state's value 2% to 1.05%. Correspondingly, IE at different horizons decreases. Longer the term, less decreases for IE. The 10-year IE decreases only by 5.74%, changing

from 2% to 1.89%.

Now we discuss how ZLB amplifies the impact of positive changes of oil supply. As the above case without ZLB, the increases of oil supply pushes down the inflation. Because of the ZLB constraint, the central bank reduces the nominal short rate from 25 bps and to 0 instead of -2.09%. The deviation from the Taylor rule exacerbates the reduction of inflation and IE at all horizons. For example, the inflation decreases by 315.00%, changing from 2% to -4.3%, and the 10-year IE decreases by 23.69%. We should also notice that ZLB also exaggerates the reduction of oil prices. Instead of decreasing by 20.73% in above case, now oil real prices decrease by 37.71%. This is because with the ZLB constraint, the nominal short rate binds at 0, which is much higher than that without ZLB constraint. Higher nominal interest rate slows down the increase of final goods production as well as consumption. As a result, the elasticity of substitution between oil consumption and final goods consumption becomes lower than that without ZLB. The more decrease of IE than that of oil real prices makes the sensitivity of IE on oil real price higher that it is when we ignore the ZLB constraint.

According to the IRFs of oil supply shocks, we plot how inflation and IE of different terms changes with the supply-driven oil prices in Figure 3.10. The x-axis is the percentage change deviated from the steady state of oil real price and the y-axis is that of inflation or IE. The red dashed lines indicate the relation of the variables in our model with ZLB constraint, while the blue solid line indicates the relation of the variables without the ZLB constraint. The green solid vertical line indicates the threshold state where the ZLB binds. We can see that when we ignore the ZLB constraint, the relation between IE/inflation and oil prices is approximately linear with positive slope. Adding the ZLB constraint causes strong non-linearity of the relationship and the asymmetric effects of oil price changes on IE/inflation at the threshold state where the ZLB binds. An additional decrease in the supply-driven oil prices leads to larger declines in inflation/IE when the policy rate is constrained at the ZLB than when it is not.

3.5.5 Demand-driven Oil Prices

Oil demand has a weaker influence on the economy than oil supply does, because oil demand only affects the household's preference on oil consumption, while oil supply affects both oil consumption and the production of final goods. To better show the impact of oil demand shock, in Figure 3.11 we plot the impulse responses of four standard deviation of oil demand shocks (20% change in level) on all macro variables and IE with different horizons. The red solid line indicates the impulse responses for the 20% negative change of oil demand and the blue solid line indicates those for the 20% positive change of oil demand. The red dashed line indicates the impulse responses for the 20% positive change of oil demand if we ignore ZLB binding constraint in the model.

We first analyze the impulse response functions (IRF) of oil demand shock ignoring the ZLB constraint. In this case, the IRF of the 20% negative change of oil demand is exactly equal to the negative IRF of the 20% positive change of oil supply with respect to the steady state because the model is symmetric around the steady state. When oil demand decreases by 20%, oil consumption decreases by 8% and oil real prices decrease by 14%. The the decreasing of oil prices leads to decline of the inflation. According to the Taylor rule, the central bank reduces the nominal short rate from 25 bps to -1.1%, with the help of which the annualized inflation decreases by 25%, changing from the steady state's value 2% to 1.5%. Correspondingly, IE at different horizons decreases. Longer the term, less decreases for IE. The 10-year IE decreases only by 3%, changing from 2% to 1.94%.

Now we discuss how ZLB exaggerates the impact of positive changes of oil demand. As the above case without ZLB, the decrease of oil demand pushes down the inflation. Because of the ZLB constraint, the central bank reduces the nominal short rate from 25 bps and to 0 instead of -1.24%. The deviation from the Taylor rule exacerbates the reduction of inflation and IE at all horizons. For example, the inflation decreases by 110.00%, changing from 2% to -0.2%, and the 10-year IE decreases by 8%. We should also notice that ZLB

also exaggerate the reduction of oil prices. Instead of decreasing by 14% in above case, now oil real prices decreases by 20%. This is because with the ZLB constraint, the nominal short rate binds at 0, which is much higher than that without ZLB constraint. Higher nominal interest rate slows down the increase of final goods production as well as consumption. As a result, the elasticity of substitution between oil consumption and final goods consumption becomes lower than that without ZLB. The more decrease of IE than that of oil real price makes the sensitivity of IE on oil real prices higher that it is when we ignore the ZLB constraint.

According to the IRFs of oil demand shocks, we plot how inflation and IE in different terms changes with the demand-driven oil prices in Figure 3.12. We can see the demand-driven oil prices have a similar impact on inflation/IE as the supply-driven oil prices do. Without ZLB, the relation between IE/inflation and oil prices is approximately linear with a positive slope, while the relation exhibits strong non-linearity at the threshold state where the ZLB binds. When the interest rate arrives at zero, the declines in inflation/IE caused by the additional decrease in the demand-driven oil prices is larger than the increases in inflation/IE led by the additional increase in the demand-driven oil prices. We also notice that the effects of demand-driven oil prices are weaker than those of supply-driven oil prices in both ZLB and NO ZLB cases.

3.6 Conclusion

Starting from late 2008, oil prices have a much stronger co-movement with market measures of long-term inflation compensation, such as 10-year TIPS BEI, than before. Our main explanation for this phenomenon is that it results from the ZLB binding constraint of nominal short rate, which alters dynamic behaviors of the economy. Our argument is supported by the following observations. First, oil price shocks have a much higher positive impact on TIPS BEI, model-implied IE and model-implied IRP when the nominal short rate

is closer to ZLB. Second, the oil effects are strongest when oil prices decrease in a ZLB environment. These empirical findings suggest that when the monetary policy becomes less effective to stabilize the economy at ZLB, investors expect long-term inflation is more subject to short-term oil price changes and would like to pay higher premiums to hedge long-term deflation risks.

In addition to empirical findings, we also provide theoretical support for our argument by using a stylized new-Keynesian DSGE model augmented with an oil sector and the Taylor rule with the ZLB constraint. The model simulation is consistent with empirical observations. The impulse response functions (IRFs) of oil supply and oil demand shocks on macroeconomic variables and IE at all maturities clearly present the underlying mechanisms about how the ZLB amplifies the correlation between oil and IE.

Our paper links the literature about oil prices, inflation expectations and risk premiums, and the ZLB constraint of monetary policy. The simultaneous uses of the shadow-rate latent variable term structure model and the DSGE model with ZLB constraint help us to understand the oil effects on the term structure of IE more clearly. In the future, we are going to extend our DSGE model to calibrate the oil shocks on IRP under ZLB and No-ZLB regimes. As IRP is approximately equal to the difference between nominal term premium and real term premium, this future work will help us to understand the role of ZLB on the relationship between oil prices and on the nominal and real yield curves.

Appendix

3.A State Factors and Nominal Yields

Given the the state dynamics under the P measure (3.3.3) and the essentially affine form of the market prices of risks (3.3.6), we can derive the state dynamics under the risk neutral (Q) measure in the nominal world,

$$dX_t = \kappa^{Q,N}(\mu^{Q,N} - X_t)dt + \Sigma dW_t^Q, \tag{3.A.1}$$

where

$$\kappa^{Q,N} = \kappa + \Sigma\Lambda^N, \quad \mu^{Q,N} = \left(\kappa^{Q,N}\right)^{-1}\left(\kappa\mu - \Sigma\lambda_0^N\right). \tag{3.A.2}$$

If there is no ZLB, the shadow rate $r^{NS}(X_t)$ is the nominal short rate and the implied nominal yield has the standard closed form solution of GATSM proposed in Duffie and Kan (1996) and Dai and Singleton (2000). The closed-form solution for shadow rate implied $\tau-$maturity nominal bond at time t is

$$P_{t,\tau}^{NS} = \mathrm{E}_t^{Q,N}\left(\exp\left(-\int_t^{t+\tau} r_u^{NS}du\right)\right) = \exp(A_\tau^{NS} + B_\tau^{NS\prime}X_t), \tag{3.A.3}$$

where

$$\frac{dA_\tau^{NS}}{d\tau} = -\rho_0^{NS} + B_\tau^{NS\prime}(\kappa\mu - \Sigma\lambda_0^N) + \frac{1}{2}B_\tau^{NS\prime}\Sigma\Sigma^\prime B_\tau^{NS}, \tag{3.A.4}$$

$$\frac{dB_\tau^{NS}}{d\tau} = -\rho_1^{NS} - (\kappa + \Sigma\Lambda^N)^\prime B_\tau^{NS}, \tag{3.A.5}$$

with initial conditions $A_0^{NS} = 0$ and $B_0^{NS} = 0_{3\times1}$. Nominal yields therefore take the affine

form,

$$y_{t,\tau}^{NS} = a_\tau^{NS} + b_\tau^{NS\prime} X_t, \;\; a_\tau^{NS} = -A_\tau^{NS}/\tau, \;\; b_\tau^{NS} = -B_\tau^{NS}/\tau. \tag{3.A.6}$$

When considering ZLB, the equation (3.3.1) brings nonlinearity into an otherwise linear system. A closed-form pricing formula for the SRTSM is not available beyond one factor. Wu and Xia (2016) propose a simple analytical representation for bond prices in the multifactor SRTSM that provides an excellent approximation and can be applied directly-time data. Following Wu and Xia (2016), we discretize our model with sampling period h, construct the nominal forward rate curve $f_{t,kh,(k+1)h}^N$ (the forward rate for a loan starting at $t+kh$ and maturing at $t+(k+1)h$, where $0 \leqslant k \leqslant n-1$) at time t, and then compute $\tau-$maturity nominal yield $y_{t,\tau}^N$, where $\tau = nh$. Wu and Xia (2016) discretize the continuous system at monthly frequency, while we adopt the weekly frequency, $h = \frac{1}{52}$, to reduce the sampling bias and match the weekly data we use.

Under the discretized system, $r_t^{NS}h = \rho_0^{NS}h + \rho_1^{NS\prime}hX_t$ is the non-annualized shadow rate from time t to time $t+h$. The P dynamics for the state factors is

$$X_{t+h} = \kappa\mu h + \left(I_{3\times3} - \kappa h\right) X_t + \Sigma\sqrt{h}\epsilon_{t+h}, \tag{3.A.7}$$

and the Q dynamics for the state factors in the nominal world is

$$X_{t+h} = \kappa^{Q,N}\mu^{Q,N}h + \left(I_{3\times3} - \kappa^{Q,N}h\right) X_t + \Sigma\sqrt{h}\epsilon_{t+h}^Q, \tag{3.A.8}$$

where $\epsilon_{t+h} \sim N(0, I_{3\times3})$ and $\epsilon_{t+h}^Q \sim N(0, I_{3\times3})$. The log nominal pricing kernel is

$$\log M_{t+h}^N = -r_t^N h - \frac{1}{2}\lambda_t^{N\prime}\lambda_t^N h - \lambda_t^{N\prime}\sqrt{h}\epsilon_{t+h}. \tag{3.A.9}$$

Given the shadow rate implied nominal yield $y_{t,\tau}^{NS}$, the corresponding forward rate at

time t for a loan starting at $t+nh$ and maturing at $t+(n+1)h$ is

$$f^{NS}_{t,nh,(n+1)h} = (n+1)\, y^{NS}_{t,(n+1)h} - n y^{NS}_{t,nh}, \tag{3.A.10}$$

which is a linear function of state factors.

As derived in Wu and Xia (2016), the forward rate is

$$f^{N}_{t,nh,(n+1)h} = \frac{1}{h}\sigma^{Q,N}_{nh}\, g\left(\frac{\alpha^{N}_{nh} + \beta^{N\prime}_{nh} X_t}{\sigma^{Q,N}_{nh}}\right), \tag{3.A.11}$$

where $\left(\sigma^{Q,N}_{nh}\right)^2 \equiv \text{Var}^{Q,N}\left(r^{NS}_{t+nh}h\right)$. And $\text{E}^{Q,N}_t\left(r^{NS}_{t+nh}h\right) = \bar{\alpha}^{N}_{nh} + \beta^{N\prime}_{nh} X_t$. The function $g(z) \equiv z\Phi(z) + \phi(z)$ consists of a normal cumulative distribution function $\Phi(.)$ and normal probability density function $\phi(.)$. Its nonlinearity comes from moments of the truncated normal distribution. The expression for $\bar{\alpha}^{N}_{nh}$, α^{N}_{nh} and β^{N}_{nh} are

$$\bar{\alpha}^{N}_{nh} \equiv \rho^{N}_0 h + \rho^{N\prime}_1 h \left(\sum_{j=0}^{n-1}\left(\left(I_{3\times3} - \kappa^{Q,N}h\right)^j\right)\right)\kappa^{Q,N}\mu^{Q,N}h \tag{3.A.12}$$

$$\alpha^{N}_{nh} \equiv \bar{\alpha}^{N}_{nh} - \frac{1}{2}\rho^{N\prime}_1 h C^{Q,N}_{nh}\rho^{N}_1 h, \tag{3.A.13}$$

$$\beta^{N\prime}_{nh} \equiv \rho^{N\prime}_1 h\left(I_{3\times3} - \kappa^{Q,N}h\right)^n. \tag{3.A.14}$$

Here $C^{Q,N}_{nh}$ is the matrix driving the convexity effects of nominal yields,

$$C^{Q,N}_{nh} = \left(\sum_{j=0}^{n-1}\left(\left(I_{3\times3} - \kappa^{Q,N}h\right)^j\right)\right)\Sigma\Sigma' h\left(\sum_{j=0}^{n-1}\left(\left(I_{3\times3} - \kappa^{Q,N}h\right)^j\right)\right)'. \tag{3.A.15}$$

The expression for $\left(\sigma^{Q,N}_{nh}\right)^2$ is

$$\left(\sigma^{Q,N}_{nh}\right)^2 = \sum_{j=0}^{n-1}\rho^{N\prime}_1 h\left(I_{3\times3} - \kappa^{Q,N}h\right)^j \Sigma\Sigma' h\left(\left(I_{3\times3} - \kappa^{Q,N}h\right)'\right)^j \rho^{N}_1 h. \tag{3.A.16}$$

Given the forward rates, the nominal yield $y^N_{t,\tau}$ with maturity $\tau = nh$ at time t can be easily computed as

$$y^N_{t,\tau=nh} = \frac{1}{n}\sum_{k=0}^{n-1} f^N_{t,kh,(k+1)h} = \frac{1}{nh}\sum_{k=0}^{n-1} \sigma^{Q,N}_{kh}\, g\left(\frac{\alpha^N_{kh} + \beta^{N\prime}_{kh} X_t}{\sigma^{Q,N}_{kh}}\right). \tag{3.A.17}$$

3.B Inflation Dynamics and Real Yields

Applying Ito's lemma to equation (3.3.12), we have,

$$dM^R_t/M^R_t = dM^N_t/M^N_t + dQ_t/Q_t + (dM^N_t/M^N_t)\cdot(dQ_t/Q_t). \tag{3.B.1}$$

Plug equations (3.3.5), (3.3.10) and (3.3.13) into this equation, the instantaneous real rate and real market prices of risks can be derived. The coefficient of real market price of risks, $\lambda^R(X_t) = \lambda^R_0 + \Lambda^R X_t$, are

$$\lambda^R_0 = \lambda^N_0 - \sigma_q, \tag{3.B.2}$$

$$\Lambda^R = \Lambda^N. \tag{3.B.3}$$

Given the state dynamics under the P measure (3.3.3) and the above essentially affine form of the market prices of risks in the real world, we can derive the state dynamics under the risk neutral (Q) measure in the real world,

$$dX_t = \kappa^{Q,R}(\mu^{Q,R} - X_t)dt + \Sigma dW^Q_t, \tag{3.B.4}$$

where

$$\kappa^{Q,R} = \kappa + \Sigma\Lambda^R, \quad \mu^{Q,R} = \left(\kappa^{Q,R}\right)^{-1}\left(\kappa\mu - \Sigma\lambda^R_0\right). \tag{3.B.5}$$

The instantaneous real interest rate is derived as

$$r^R(X_t) = r^N(X_t) - r^I(X_t) + \lambda_0^{N\prime}\sigma_q + \left(\Lambda^{N\prime}\sigma_q\right)' X_t. \tag{3.B.6}$$

We define the instantaneous break-even inflation (BEI) rate as $r^{BEI}(X_t) = r^N(X_t) - r^R(X_t)$. So $r^{BEI}(X_t) = r^I(X_t) - \lambda_0^{N\prime}\sigma_q - \left(\Lambda^{N\prime}\sigma_q\right)' X_t = \rho_0^{BEI} + \rho_1^{BEI\prime} X_t$, where

$$\rho_0^{BEI} = \rho_0^I - \lambda_0^{N\prime}\sigma_q, \tag{3.B.7}$$

$$\rho_1^{BEI} = \rho_1^I - \Lambda^{N\prime}\sigma_q. \tag{3.B.8}$$

Thus the real interest rate is

$$r^R(X_t) = r^N(X_t) - \rho_0^{BEI} - \rho_1^{BEI\prime} X_t. \tag{3.B.9}$$

If there is no ZLB, the shadow rate $r^{NS}(X_t)$ is the nominal short rate and the corresponding real rate is the real shadow rate, defined as $r^{RS}(X_t) = r^{NS}(X_t) - r^{BEI}(X_t)$. It is an affine function of the state variables,

$$r^{RS}(X_t) = \rho_0^{RS} + \rho_1^{RS\prime} X_t, \tag{3.B.10}$$

where

$$\rho_0^{RS} = \rho_0^{NS} - \rho_0^{BEI}, \tag{3.B.11}$$

$$\rho_1^{RS} = \rho_1^{NS} - \rho_1^{BEI}. \tag{3.B.12}$$

The closed-form solution for shadow rate implied $\tau-$maturity real bond at time t is

$P_{t,\tau}^{RS} = \mathrm{E}_t^{Q,R}\left(\exp\left(-\int_t^{t+\tau} r_u^{RS} du\right)\right) = \exp(A_\tau^{RS} + B_\tau^{RS\prime} X_t)$, where

$$\frac{dA_\tau^{RS}}{d\tau} = -\rho_0^{RS} + B_\tau^{RS\prime}(\kappa\mu - \Sigma\lambda_0^R) + \frac{1}{2}B_\tau^{RS\prime}\Sigma\Sigma' B_\tau^{RS}, \tag{3.B.13}$$

$$\frac{dB_\tau^{RS}}{d\tau} = -\rho_1^{RS} - (\kappa + \Sigma\Lambda^R)' B_\tau^{RS}, \tag{3.B.14}$$

with initial conditions $A_0^{RS} = 0$ and $B_0^{RS} = 0_{3\times 1}$.

When considering ZLB, according to the equation $(A1)$ of Wu and Xia (2016), the non-annualized forward real rate between $t+nh$ and $t+(n+1)h$ at time t can be approximated as follows,

$$
\begin{aligned}
& f^{R}_{t,nh,(n+1)h}h \\
&= (n+1)\, y^{R}_{t,(n+1)h}h - n y^{R}_{t,nh}h \\
&= -\log\left(e^{-r^{R}_{t}h}E^{Q,R}_{t}\left[e^{-\Sigma_{j=1}^{n}r^{R}_{t+jh}h}\right]\right) + \log\left(e^{-r^{R}_{t}h}E^{Q,R}_{t}\left[e^{-\Sigma_{j=1}^{n-1}r^{R}_{t+jh}h}\right]\right) \\
&\approx \mathrm{E}^{Q,R}_{t}\left[\sum_{j=1}^{n} r^{R}_{t+jh}h\right] - \frac{1}{2}\mathrm{Var}^{Q,R}_{t}\left[\sum_{j=1}^{n} r^{R}_{t+jh}h\right] - \mathrm{E}^{Q,R}_{t}\left[\sum_{j=1}^{n-1} r^{R}_{t+jh}h\right] + \frac{1}{2}\mathrm{Var}^{Q,R}_{t}\left[\sum_{j=1}^{n-1} r^{R}_{t+jh}h\right] \\
&= \mathrm{E}^{Q,R}_{t}\left[r^{R}_{t+nh}h\right] - \frac{1}{2}\left(\mathrm{Var}^{Q,R}_{t}\left[\sum_{j=1}^{n} r^{R}_{t+jh}h\right] - \mathrm{Var}^{Q,R}_{t}\left[\sum_{j=1}^{n-1} r^{R}_{t+jh}h\right]\right) \\
&= \mathrm{E}^{Q,R}_{t}\left[r^{R}_{t+nh}h\right] - \frac{1}{2}\left(\mathrm{Var}^{Q,R}_{t}\left[\sum_{j=1}^{n} r^{R}_{t+jh}h\right] - \mathrm{Var}^{Q,R}_{t}\left[\sum_{j=1}^{n-1} r^{R}_{t+jh}h\right]\right) \\
&= \mathrm{E}^{Q,R}_{t}\left[r^{N}_{t+nh}h\right] - \mathrm{E}^{Q,R}_{t}\left[r^{BEI}_{t+nh}h\right] \\
&\quad - \frac{1}{2}\left(\mathrm{Var}^{Q,R}_{t}\left[\sum_{j=1}^{n} r^{N}_{t+jh}h\right] + \mathrm{Var}^{Q,R}_{t}\left[\sum_{j=1}^{n} r^{BEI}_{t+jh}h\right] - 2\mathrm{Cov}^{Q,R}_{t}\left[\sum_{j=1}^{n} r^{N}_{t+jh}h, \sum_{j=1}^{n} r^{BEI}_{t+jh}h\right]\right) \\
&\quad + \frac{1}{2}\left(\mathrm{Var}^{Q,R}_{t}\left[\sum_{j=1}^{n-1} r^{N}_{t+jh}h\right] + \mathrm{Var}^{Q,R}_{t}\left[\sum_{j=1}^{n-1} r^{BEI}_{t+jh}h\right] - 2\mathrm{Cov}^{Q,R}_{t}\left[\sum_{j=1}^{n-1} r^{N}_{t+jh}h, \sum_{j=1}^{n-1} r^{BEI}_{t+jh}h\right]\right) \\
&= \left(\mathrm{E}^{Q,R}_{t}\left[r^{N}_{t+nh}h\right] - \frac{1}{2}\left(\mathrm{Var}^{Q,R}_{t}\left[\sum_{j=1}^{n} r^{N}_{t+jh}h\right] - \mathrm{Var}^{Q,R}_{t}\left[\sum_{j=1}^{n-1} r^{N}_{t+jh}h\right]\right)\right) \\
&\quad - \left(\mathrm{E}^{Q,R}_{t}\left[r^{BEI}_{t+nh}h\right] - \frac{1}{2}\left(\mathrm{Var}^{Q,R}_{t}\left[\sum_{j=1}^{n} r^{BEI}_{t+jh}h\right] - \mathrm{Var}^{Q,R}_{t}\left[\sum_{j=1}^{n-1} r^{BEI}_{t+jh}h\right]\right)\right) \\
&\quad - \mathrm{Var}^{Q,R}_{t}\left[\sum_{j=1}^{n} r^{BEI}_{t+jh}h\right] + \mathrm{Var}^{Q,R}_{t}\left[\sum_{j=1}^{n-1} r^{BEI}_{t+jh}h\right] \\
&\quad + \mathrm{Cov}^{Q,R}_{t}\left[\sum_{j=1}^{n} r^{N}_{t+jh}h, \sum_{j=1}^{n} r^{BEI}_{t+jh}h\right] - \mathrm{Cov}^{Q,R}_{t}\left[\sum_{j=1}^{n-1} r^{N}_{t+jh}h, \sum_{j=1}^{n-1} r^{BEI}_{t+jh}h\right] \\
&= f^{N,R}_{t,nh,(n+1)h}h - f^{BEI}_{t,nh,(n+1)h}h - \left(\mathrm{Var}^{Q,R}_{t}\left[\sum_{j=1}^{n} r^{BEI}_{t+jh}h\right] - \mathrm{Var}^{Q,R}_{t}\left[\sum_{j=1}^{n-1} r^{BEI}_{t+jh}h\right]\right) \\
&\quad + \left(\mathrm{Cov}^{Q,R}_{t}\left[\sum_{j=1}^{n} r^{N}_{t+jh}h, \sum_{j=1}^{n} r^{BEI}_{t+jh}h\right] - \mathrm{Cov}^{Q,R}_{t}\left[\sum_{j=1}^{n-1} r^{N}_{t+jh}h, \sum_{j=1}^{n-1} r^{BEI}_{t+jh}h\right]\right). \qquad (3.B.15)
\end{aligned}
$$

Here $f^{N,R}_{t,nh,(n+1)h}$ is the nominal forward rate observed in the real world,

$$
f^{N,R}_{t,nh,(n+1)h} = \frac{1}{h}\sigma^{Q,N,R}_{nh}\, g\left(\frac{\alpha^{N,R}_{nh} + \beta^{N,R\prime}_{nh} X_t}{\sigma^{Q,N,R}_{nh}}\right), \qquad (3.B.16)
$$

where $\left(\sigma_{nh}^{Q,N,R}\right)^2 \equiv \text{Var}^{Q,R}\left(r_{t+nh}^{NS}h\right)$. And $\text{E}_t^{Q,R}\left(r_{t+nh}^{NS}h\right) = \bar{\alpha}_{nh}^{N,R} + \beta_{nh}^{N,R\prime}X_t$. Its nonlinearity comes from moments of the truncated normal distribution. The expression for $\bar{\alpha}_{nh}^{N,R}$, $\alpha_{nh}^{N,R}$ and $\beta_{nh}^{N,R}$ are

$$\bar{\alpha}_{nh}^{N,R} \equiv \rho_0^N h + \rho_1^{N\prime} h \left(\sum_{j=0}^{n-1}\left(\left(I_{3\times3} - \kappa^{Q,R}h\right)^j\right)\right)\kappa^{Q,R}\mu^{Q,R}h \tag{3.B.17}$$

$$\alpha_{nh}^{N,R} \equiv \bar{\alpha}_{nh}^{N,R} - \frac{1}{2}\rho_1^{N\prime}hC_{nh}^{N,R}\rho_1^N h, \tag{3.B.18}$$

$$\beta_{nh}^{N,R\prime} \equiv \rho_1^{N\prime}h\left(I_{3\times3} - \kappa^{Q,R}h\right)^n. \tag{3.B.19}$$

Here $C_{nh}^{Q,R}$ is the matrix driving the convexity effects of real yields,

$$C_{nh}^{Q,R} = \left(\sum_{j=0}^{n-1}\left(\left(I_{3\times3} - \kappa^{Q,R}h\right)^j\right)\right)\Sigma\Sigma'h\left(\sum_{j=0}^{n-1}\left(\left(I_{3\times3} - \kappa^{Q,R}h\right)^j\right)\right)'. \tag{3.B.20}$$

The expression for $\left(\sigma_{nh}^{Q,N,R}\right)^2$ is

$$\left(\sigma_{nh}^{Q,N,R}\right)^2 = \sum_{j=0}^{n-1}\rho_1^{N\prime}h\left(I_{3\times3} - \kappa^{Q,R}h\right)^j\Sigma\Sigma'h\left(\left(I_{3\times3} - \kappa^{Q,R}h\right)'\right)^j\rho_1^N h. \tag{3.B.21}$$

The non-annualized forward instantaneou BEI rate $f_{t,nh,(n+1)h}^{BEI}h$ is

$$f_{t,nh,(n+1)h}^{BEI}h = \alpha_{nh}^{BEI} + \beta_{nh}^{BEI\prime}X_t, \tag{3.B.22}$$

where α_{nh}^{BEI} and β_{nh}^{BEI} are

$$\alpha_{nh}^{BEI} \equiv \bar{\alpha}_{nh}^{BEI} - \frac{1}{2}\rho_1^{BEI\prime}hC_{nh}^{Q,R}\rho_1^{BEI}h, \tag{3.B.23}$$

$$\beta_{nh}^{BEI\prime} \equiv \rho_1^{BEI\prime}h\left(I_{3\times3} - \kappa^{Q,R}h\right)^n, \tag{3.B.24}$$

$$\bar{\alpha}_{nh}^{BEI} \equiv \rho_0^{BEI}h + \rho_1^{BEI\prime}h\left(\sum_{j=0}^{n-1}\left(\left(I_{3\times3} - \kappa^{Q,R}h\right)^j\right)\right)\kappa^{Q,R}\mu^{Q,R}h. \tag{3.B.25}$$

The third term of equation (3.B.15) is as follows,

$$\text{Var}_t^{Q,R}\left[\sum_{j=1}^{n} r_{t+jh}^{BEI}\right] - \text{Var}_t^{Q,R}\left[\sum_{j=1}^{n-1} r_{t+jh}^{BEI}\right] = \rho_1^{BEI\prime} h C_{nh}^{Q,R} \rho_1^{BEI} h. \tag{3.B.26}$$

Similar to the equation (A4) in Wu and Xia (2016), the fourth term of equation (3.B.15) is as follows,

$$\begin{aligned}
&\text{Cov}_t^{Q,R}\left[\sum_{j=1}^{n} r_{t+jh}^{N}, \sum_{j=1}^{n} r_{t+jh}^{BEI}\right] - \text{Cov}_t^{Q,R}\left[\sum_{j=1}^{n-1} r_{t+jh}^{N}, \sum_{j=1}^{n-1} r_{t+jh}^{BEI}\right] \\
&= \sum_{i=1}^{n-1} \text{Cov}_t^{Q,R}\left[r_{t+ih}^{N}, r_{t+nh}^{BEI}\right] + \sum_{j=1}^{n-1} \text{Cov}_t^{Q,R}\left[r_{t+nh}^{N}, r_{t+jh}^{BEI}\right] + \text{Cov}_t^{Q,R}\left[r_{t+nh}^{N}, r_{t+nh}^{BEI}\right] \\
&\approx \sum_{i=1}^{n-1} \text{Pr}_t^{Q,R}\left[r_{t+ih}^{NS} \geq 0\right] \text{Cov}_t^{Q,R}\left[r_{t+ih}^{NS}, r_{t+nh}^{BEI}\right] + \sum_{j=1}^{n-1} \text{Pr}_t^{Q,R}\left[r_{t+nh}^{NS} \geq 0\right] \text{Cov}_t^{Q,R}\left[r_{t+nh}^{NS}, r_{t+jh}^{BEI}\right] \\
&\quad + \text{Pr}_t^{Q,R}\left[r_{t+nh}^{NS} \geq 0\right] \text{Cov}_t^{Q,R}\left[r_{t+nh}^{NS}, r_{t+nh}^{BEI}\right] \\
&\approx \text{Pr}_t^{Q,R}\left[r_{t+nh}^{NS} \geq 0\right] \left(\text{Cov}_t^{Q,R}\left[\sum_{j=1}^{n} r_{t+jh}^{NS}, \sum_{j=1}^{n} r_{t+jh}^{BEI}\right] - \text{Cov}_t^{Q,R}\left[\sum_{j=1}^{n-1} r_{t+jh}^{NS}, \sum_{j=1}^{n-1} r_{t+jh}^{BEI}\right]\right) \\
&= \Phi\left(\frac{\bar{\alpha}_{nh}^{N,R} + \beta_{nh}^{N,R\prime} X_t}{\sigma_{nh}^{Q,N,R}}\right) \rho_1^{NS\prime} h C_{nh}^{Q,R} \rho_1^{BEI} h.
\end{aligned} \tag{3.B.27}$$

Plug equations (3.3.8), (3.B.22), (3.B.26) and (3.B.27) to equation (3.B.15), we can get

$$\begin{aligned}
f_{t,nh,(n+1)h}^{R} h \approx \sigma_{nh}^{Q,N,R} g\left(\frac{\alpha_{nh}^{N,R} + \beta_{nh}^{N,R\prime} X_t}{\sigma_{nh}^{Q,N,R}}\right) - \alpha_{nh}^{BEI} - \beta_{nh}^{BEI\prime} X_t - \rho_1^{BEI\prime} h C_{nh}^{Q,R} \rho_1^{BEI} h \\
+ \Phi\left(\frac{\bar{\alpha}_{nh}^{N,R} + \beta_{nh}^{N,R\prime} X_t}{\sigma_{nh}^{Q,N,R}}\right) \rho_1^{NS\prime} h C_{nh}^{Q,R} \rho_1^{BEI} h.
\end{aligned} \tag{3.B.28}$$

Therefore, the real forward rate at time t for a loan starting at $t + nh$ and maturing at

$t + (n+1)h$ is

$$f^R_{t,nh,(n+1)h} \approx -\frac{\alpha^{BEI}_{nh}}{h} - \rho_1^{BEI\prime} h C^{Q,R}_{nh} \rho_1^{BEI} - \frac{\beta^{BEI\prime}_{nh}}{h} X_t + \frac{1}{h}\sigma^{Q,N,R}_{nh} g\left(\frac{\alpha^{N,R}_{nh} + \beta^{N,R\prime}_{nh} X_t}{\sigma^{Q,N,R}_{nh}}\right) + \rho_1^{NS\prime} C^{Q,R}_{nh} \rho_1^{BEI} h \Phi\left(\frac{\bar{\alpha}^{N,R}_{nh} + \beta^{N,R\prime}_{nh} X_t}{\sigma^{Q,N,R}_{nh}}\right). \tag{3.B.29}$$

Given the real forward rates, the real yield $y^R_{t,\tau}$ with maturity $\tau = nh$ at time t can be easily computed as

$$\begin{aligned} y^R_{t,\tau=nh} \approx & -\frac{1}{nh}\sum_{k=0}^{n-1} \alpha^{BEI}_{kh} - \frac{h}{n}\rho_1^{BEI\prime} \sum_{k=0}^{n-1} C^{Q,R}_{kh} \rho_1^{BEI} - \frac{1}{nh}\sum_{k=0}^{n-1} \beta^{BEI\prime}_{kh} X_t \\ & + \frac{1}{nh}\sum_{k=0}^{n-1} \sigma^{Q,N,R}_{kh} g\left(\frac{\alpha^{N,R}_{kh} + \beta^{N,R\prime}_{kh} X_t}{\sigma^{Q,N,R}_{kh}}\right) \\ & + \frac{h}{n}\rho_1^{NS\prime} \sum_{k=0}^{n-1} C^{Q,R}_{kh} \rho_1^{BEI} \Phi\left(\frac{\bar{\alpha}^{N,R}_{kh} + \beta^{N,R\prime}_{kh} X_t}{\sigma^{Q,N,R}_{kh}}\right). \end{aligned} \tag{3.B.30}$$

3.C TIPS Liquidity Effects

The risk neutral (Q) dynamics of $\widetilde{X}_t$ in the real world can be derived as follows,

$$d\widetilde{X}_t = \widetilde{\kappa}^{Q,R}(\widetilde{\mu}^{Q,R} - \widetilde{X}_t)dt + \widetilde{\sigma} d\widetilde{W}^Q_t, \tag{3.C.1}$$

where

$$\widetilde{\kappa}^{Q,R} = \widetilde{\kappa} + \widetilde{\lambda}_1 \widetilde{\sigma}, \quad \widetilde{\mu}^{Q,R} = \left(\widetilde{\kappa}\widetilde{\mu} - \widetilde{\lambda}_0 \widetilde{\sigma}\right) / \widetilde{\kappa}^{Q,R}. \tag{3.C.2}$$

We can split $r^{TBEI} = r^N - r^{TIPS} = \rho_0^{BEI} + (\rho_1^{BEI} - \beta)' X_t - \widetilde{\beta}\widetilde{X}_t$ into two parts. One is the part that is explained by three common factors, $r^{TBEIa} = \rho_0^{BEI} + (\rho_1^{BEI} - \beta)' X_t$, and the other part is the TIPS liquidity specific part $r^{TBEIb} = \widetilde{\beta}\widetilde{X}_t$. Because r^{TBEIb} has no correlation with r^N_t and r^{TBEIa}, we can derive the non-annualized forward TIPS rate from nh to $(n+1)h$ at time t as follows,

$$
\begin{aligned}
& f^{TIPS}_{t,nh,(n+1)h}h \qquad (3.C.3)\\
&\approx \mathrm{E}^{Q,R}_t\left[r^{TIPS}_{t+nh}h\right] - \frac{1}{2}\left(\mathrm{Var}^{Q,R}_t\left[\sum_{j=1}^{n} r^{TIPS}_{t+jh}h\right] - \mathrm{Var}^{Q,R}_t\left[\sum_{j=1}^{n-1} r^{TIPS}_{t+jh}h\right]\right)\\
&= \mathrm{E}^{Q,R}_t\left[r^{N}_{t+nh}h\right] - \mathrm{E}^{Q,R}_t\left[r^{TBEIa}_{t+nh}h\right] - \mathrm{E}^{Q,R}_t\left[r^{TBEIb}_{t+nh}h\right]\\
&\quad - \frac{1}{2}\left(\mathrm{Var}^{Q,R}_t\left[\sum_{j=1}^{n} r^{N}_{t+jh}h\right] + \mathrm{Var}^{Q,R}_t\left[\sum_{j=1}^{n} r^{TBEIa}_{t+jh}h\right] - 2\mathrm{Cov}^{Q,R}_t\left[\sum_{j=1}^{n} r^{N}_{t+jh}h, \sum_{j=1}^{n} r^{TBEIa}_{t+jh}h\right]\right)\\
&\quad + \frac{1}{2}\left(\mathrm{Var}^{Q,R}_t\left[\sum_{j=1}^{n-1} r^{N}_{t+jh}h\right] + \mathrm{Var}^{Q,R}_t\left[\sum_{j=1}^{n-1} r^{TBEIa}_{t+jh}h\right] - 2\mathrm{Cov}^{Q,R}_t\left[\sum_{j=1}^{n-1} r^{N}_{t+jh}h, \sum_{j=1}^{n-1} r^{TBEIa}_{t+jh}h\right]\right)\\
&\quad - \frac{1}{2}\mathrm{Var}^{Q,R}_t\left[\sum_{j=1}^{n} r^{TBEIb}_{t+jh}h\right] + \frac{1}{2}\mathrm{Var}^{Q,R}_t\left[\sum_{j=1}^{n-1} r^{TBEIb}_{t+jh}h\right]\\
&= \left(\mathrm{E}^{Q,R}_t\left[r^{N}_{t+nh}h\right] - \frac{1}{2}\left(\mathrm{Var}^{Q,R}_t\left[\sum_{j=1}^{n} r^{N}_{t+jh}h\right] - \mathrm{Var}^{Q,R}_t\left[\sum_{j=1}^{n-1} r^{N}_{t+jh}h\right]\right)\right)\\
&\quad - \left(\mathrm{E}^{Q,R}_t\left[r^{TBEIa}_{t+nh}h\right] - \frac{1}{2}\left(\mathrm{Var}^{Q,R}_t\left[\sum_{j=1}^{n} r^{TBEIa}_{t+jh}h\right] - \mathrm{Var}^{Q,R}_t\left[\sum_{j=1}^{n-1} r^{TBEIa}_{t+jh}h\right]\right)\right)\\
&\quad - \left(\mathrm{E}^{Q,R}_t\left[r^{TBEIb}_{t+nh}h\right] - \frac{1}{2}\left(\mathrm{Var}^{Q,R}_t\left[\sum_{j=1}^{n} r^{TBEIb}_{t+jh}h\right] - \mathrm{Var}^{Q,R}_t\left[\sum_{j=1}^{n-1} r^{TBEIb}_{t+jh}h\right]\right)\right)\\
&\quad - \mathrm{Var}^{Q,R}_t\left[\sum_{j=1}^{n} r^{TBEIa}_{t+jh}h\right] + \mathrm{Var}^{Q,R}_t\left[\sum_{j=1}^{n-1} r^{TBEIa}_{t+jh}h\right]\\
&\quad + \mathrm{Cov}^{Q,R}_t\left[\sum_{j=1}^{n} r^{N}_{t+jh}h, \sum_{j=1}^{n} r^{TBEIa}_{t+jh}h\right] - \mathrm{Cov}^{Q,R}_t\left[\sum_{j=1}^{n-1} r^{N}_{t+jh}h, \sum_{j=1}^{n-1} r^{TBEIa}_{t+jh}h\right]\\
&\quad - \mathrm{Var}^{Q,R}_t\left[\sum_{j=1}^{n} r^{TBEIb}_{t+jh}h\right] + \mathrm{Var}^{Q,R}_t\left[\sum_{j=1}^{n-1} r^{TBEIb}_{t+jh}h\right]\\
&= f^{N,R}_{t,nh,(n+1)h}h - f^{TBEIa}_{t,nh,(n+1)h}h - f^{TBEIb}_{t,nh,(n+1)h}h\\
&\quad - \left(\mathrm{Var}^{Q,R}_t\left[\sum_{j=1}^{n} r^{TBEIa}_{t+jh}h\right] - \mathrm{Var}^{Q,R}_t\left[\sum_{j=1}^{n-1} r^{TBEIa}_{t+jh}h\right]\right)\\
&\quad + \left(\mathrm{Cov}^{Q,R}_t\left[\sum_{j=1}^{n} r^{N}_{t+jh}h, \sum_{j=1}^{n} r^{TBEIa}_{t+jh}h\right] - \mathrm{Cov}^{Q,R}_t\left[\sum_{j=1}^{n-1} r^{N}_{t+jh}h, \sum_{j=1}^{n-1} r^{TBEIa}_{t+jh}h\right]\right)\\
&\quad - \left(\mathrm{Var}^{Q,R}_t\left[\sum_{j=1}^{n} r^{TBEIb}_{t+jh}h\right] - \mathrm{Var}^{Q,R}_t\left[\sum_{j=1}^{n-1} r^{TBEIb}_{t+jh}h\right]\right). \qquad (3.C.4)
\end{aligned}
$$

Here $f^{TBEIa}_{t,nh,(n+1)h}h$ is

$$f^{TBEIa}_{t,nh,(n+1)h}h = \alpha^{TBEIa}_{nh} + \beta^{TBEIa\prime}_{nh} X_t, \tag{3.C.5}$$

where α^{TBEIa}_{nh} and β^{TBEIa}_{nh} are

$$\alpha^{TBEIa}_{nh} \equiv \bar{\alpha}^{TBEIa}_{nh} - \frac{1}{2}\left(\rho_1^{BEI} - \beta\right)' h C^{Q,R}_{nh} \left(\rho_1^{BEI} - \beta\right) h, \tag{3.C.6}$$

$$\beta^{TBEIa\prime}_{nh} \equiv \left(\rho_1^{BEI} - \beta\right)' h \left(I_{3\times 3} - \kappa^{Q,R} h\right)^n, \tag{3.C.7}$$

$$\bar{\alpha}^{TBEIa}_{nh} \equiv \rho_0^{BEI} h + \left(\rho_1^{BEI} - \beta\right)' h \left(\sum_{j=0}^{n-1} \left(\left(I_{3\times 3} - \kappa^{Q,R} h\right)^j\right)\right) \kappa^{Q,R} \mu^{Q,R} h. \tag{3.C.8}$$

The fourth term of equation (3.C.4) is as follows,

$$\text{Var}^{Q,R}_t \left[\sum_{j=1}^{n} r^{TBEIa}_{t+jh}\right] - \text{Var}^{Q,R}_t \left[\sum_{j=1}^{n-1} r^{TBEIa}_{t+jh}\right] = \left(\rho_1^{BEI} - \beta\right)' h C^{Q,R}_{nh} \left(\rho_1^{BEI} - \beta\right) h. \tag{3.C.9}$$

The fifth term of equation (3.C.4) is as follows,

$$\begin{aligned} &\text{Cov}^{Q,R}_t \left[\sum_{j=1}^{n} r^{N}_{t+jh}, \sum_{j=1}^{n} r^{BEI}_{t+jh}\right] - \text{Cov}^{Q,R}_t \left[\sum_{j=1}^{n-1} r^{N}_{t+jh}, \sum_{j=1}^{n-1} r^{BEI}_{t+jh}\right] \\ &= \Phi\left(\frac{\bar{\alpha}^{N,R}_{nh} + \beta^{N,R\prime}_{nh} X_t}{\sigma^{Q,N,R}_{nh}}\right) \rho_1^{NS\prime} h C^{Q,R}_{nh} \left(\rho_1^{BEI} - \beta\right)' h. \end{aligned} \tag{3.C.10}$$

The third term of equation (3.C.4) is

$$f^{TBEIb}_{t,nh,(n+1)h}h = \alpha^{TBEIb}_{nh} + \beta^{TBEIb\prime}_{nh} \widetilde{X}_t, \tag{3.C.11}$$

where α_{nh}^{TBEIb} and β_{nh}^{TBEIb} are

$$\alpha_{nh}^{TBEIb} \equiv \bar{\alpha}_{nh}^{TBEIb} - \frac{1}{2}\widetilde{\beta}' h \widetilde{C}_{nh}^{Q,R} \widetilde{\beta} h, \tag{3.C.12}$$

$$\beta_{nh}^{TBEIb\prime} \equiv \widetilde{\beta}' h \left(1 - \widetilde{\kappa}^{Q,R} h\right)^n, \tag{3.C.13}$$

$$\bar{\alpha}_{nh}^{TBEIb} \equiv \widetilde{\beta}' h \left(\sum_{j=0}^{n-1} \left(\left(1 - \widetilde{\kappa}^{Q,R} h\right)^j \right) \right) \widetilde{\kappa}^{Q,R} \widetilde{\mu}^{Q,R} h. \tag{3.C.14}$$

Here $\widetilde{C}_{nh}^{Q,R}$ is given by

$$\widetilde{C}_{nh}^{Q,R} = \left(\sum_{j=0}^{n-1} \left(\left(1 - \widetilde{\kappa}^{Q,R} h\right)^j \right) \right) \widetilde{\sigma}^2 h \left(\sum_{j=0}^{n-1} \left(\left(1 - \widetilde{\kappa}^{Q,R} h\right)^j \right) \right)'. \tag{3.C.15}$$

The last term of equation (3.C.4) is as follows,

$$\text{Var}_t^{Q,R}\left[\sum_{j=1}^{n} r_{t+jh}^{TBEIb}\right] - \text{Var}_t^{Q,R}\left[\sum_{j=1}^{n-1} r_{t+jh}^{TBEIb}\right] = \widetilde{\beta}' h \widetilde{C}_{nh}^{Q,R} \widetilde{\beta} h. \tag{3.C.16}$$

Plug equations (3.3.8), (3.B.22), (3.C.9) and (3.C.9) to equation (3.C.4), we can get

$$\begin{aligned} f_{t,nh,(n+1)h}^{TIPS} h \approx \sigma_{nh}^{Q,N,R} g \left(\frac{\alpha_{nh}^{N,R} + \beta_{nh}^{N,R\prime} X_t}{\sigma_{nh}^{Q,N,R}} \right) - \alpha_{nh}^{TBEIa} - \beta_{nh}^{TBEIa\prime} X_t \\ - \left(\rho_1^{BEI} - \beta\right)' h C_{nh}^{Q,R} \left(\rho_1^{BEI} - \beta\right) h \\ + \Phi \left(\frac{\bar{\alpha}_{nh}^{N,R} + \beta_{nh}^{N,R\prime} X_t}{\sigma_{nh}^{Q,N,R}} \right) \rho_1^{NS\prime} h C_{nh}^{Q,R} \left(\rho_1^{BEI} - \beta\right) h \\ - \alpha_{nh}^{TBEIb} - \beta_{nh}^{TBEIb\prime} \widetilde{X}_t - \widetilde{\beta}' h \widetilde{C}_{nh}^{Q,R} \widetilde{\beta} h. \end{aligned} \tag{3.C.17}$$

Therefore, the forward TIPS rate at time t for a loan starting at $t + nh$ and maturing at $t + (n+1)h$ is

$$
\begin{aligned}
f^{TIPS}_{t,nh,(n+1)h} \approx & -\frac{\alpha^{TBEIa}_{nh}}{h} - \frac{\alpha^{TBEIb}_{nh}}{h} - \left(\rho_1^{BEI} - \beta\right)' h C^{Q,R}_{nh} \left(\rho_1^{BEI} - \beta\right) - \widetilde{\beta}' h \widetilde{C}^{Q,R}_{nh} \widetilde{\beta} \\
& - \frac{\beta^{TBEIa\prime}_{nh}}{h} X_t - \frac{\beta^{TBEIb}_{nh}}{h} \widetilde{X}_t + \frac{1}{h} \sigma^{Q,N,R}_{nh} g\left(\frac{\alpha^{N,R}_{nh} + \beta^{N,R\prime}_{nh} X_t}{\sigma^{Q,N,R}_{nh}}\right) \\
& + \rho_1^{NS\prime} C^{Q,R}_{nh} \left(\rho_1^{BEI} - \beta\right) h \Phi\left(\frac{\bar{\alpha}^{N,R}_{nh} + \beta^{N,R\prime}_{nh} X_t}{\sigma^{Q,N,R}_{nh}}\right). \qquad \text{(3.C.18)}
\end{aligned}
$$

Given the forward TIPS rates, the TIPS yield $y^{TIPS}_{t,\tau}$ with maturity $\tau = nh$ at time t can be easily computed as

$$
\begin{aligned}
y^{TIPS}_{t,\tau=nh} \approx & -\frac{1}{nh} \sum_{k=0}^{n-1} \alpha^{TBEIa}_{kh} - \frac{1}{nh} \sum_{k=0}^{n-1} \alpha^{TBEIb}_{kh} - \frac{h}{n} \left(\rho_1^{BEI} - \beta\right)' \sum_{k=0}^{n-1} C^{Q,R}_{kh} \left(\rho_1^{BEI} - \beta\right) \\
& - \frac{h}{n} \widetilde{\beta}' \sum_{k=0}^{n-1} \widetilde{C}^{Q,R}_{kh} \widetilde{\beta} - \frac{1}{nh} \sum_{k=0}^{n-1} \beta^{TBEIa\prime}_{kh} X_t - \frac{1}{nh} \sum_{k=0}^{n-1} \beta^{TBEIb}_{kh} \widetilde{X}_t \\
& + \frac{1}{nh} \sum_{k=0}^{n-1} \sigma^{Q,N,R}_{kh} g\left(\frac{\alpha^{N,R}_{kh} + \beta^{N,R\prime}_{kh} X_t}{\sigma^{Q,N,R}_{kh}}\right) \\
& + \frac{h}{n} \rho_1^{NS\prime} \sum_{k=0}^{n-1} C^{Q,R}_{kh} \left(\rho_1^{BEI} - \beta\right) \Phi\left(\frac{\bar{\alpha}^{N,R}_{kh} + \beta^{N,R\prime}_{kh} X_t}{\sigma^{Q,N,R}_{kh}}\right). \qquad \text{(3.C.19)}
\end{aligned}
$$

3.D Inflation Expectation

Given the explicit conditional expectation of future state variables in Vasicek model, $\mathrm{E}_t\left(X_{t+\tau} \mid X_t\right) = \mu + e^{-\kappa\tau}\left(X_t - \mu\right)$, the closed-form formulas of inflation expectations, $\mathrm{IE}_{t,\tau} = a^{IE}_{\tau} + b^{IE\prime}_{\tau} dX_t$, over next τ period can be derived as,

$$
\frac{1}{\tau} \mathrm{E}_t\left(\int_t^{t+\tau} r^I_s ds\right) = a^{IE}_{\tau} + b^{IE\prime}_{\tau} X_t, \qquad \text{(3.D.1)}
$$

where the factor loadings a^{IE}_{τ} and b^{IE}_{τ} are given by

$$a_\tau^{IE} = \rho_0^I + \frac{1}{\tau}\rho_1^{I\prime}\int_0^\tau \left(I - e^{-\kappa s}\right)\mu ds, \tag{3.D.2}$$

$$b_\tau^{IE} = \frac{1}{\tau}\int_0^\tau e^{-\kappa' s}\rho_1^I ds. \tag{3.D.3}$$

3.E The Nonlinear State-Space Form and the Extended Kalman Filter

Let $q_t = \log Q_t$. By applying Ito's lemma to the equation (3.3.10), the log price level is given by

$$dq_t = \left(r^I(X_t) - \frac{1}{2}\left({\sigma_q}'\sigma_q + {\sigma_q^\perp}^2\right)\right)dt + \sigma_q' dW_t + \sigma_q^\perp dW_t^\perp. \tag{3.E.1}$$

We write our model as a nonlinear state space model with an augmented state vector $x_t = [q, X_t]$, which includes the log price level, three systematic state variables and one TIPS-specific factor. Expressed as the Euler discretization of equations (3.3.3), (3.3.20) and (3.E.1),, the state equation takes the affine form

$$x_t = A_h + B_h x_{t-h} + \varepsilon_t, \tag{3.E.2}$$

where

$$A_h = \begin{bmatrix} \left(\rho_0^I - \frac{1}{2}\left({\sigma_q}'\sigma_q + {\sigma_q^\perp}^2\right)\right)h \\ \kappa\mu h \\ \tilde{\kappa}\mu h \end{bmatrix},\ B_h = \begin{bmatrix} 1 & \rho_1^{I\prime}h & 0 \\ 0_{3\times1} & (I_{3\times3} - \kappa h) & 0_{1\times3} \\ 0 & 0_{1\times3} & 1 - \tilde{\kappa}h \end{bmatrix},$$

$$\text{and } \varepsilon_t = \begin{bmatrix} {\sigma_q}' & \sigma_q^\perp & 0 \\ \Sigma & 0 & 0_{3\times1} \\ 0_{1\times3} & 0 & \tilde{\sigma} \end{bmatrix} h\epsilon_t,\ \epsilon_t \sim N(0, I_{5\times5}).$$

Given the information at time t, the transition equation is deterministic and linear.

As we sample data at weekly frequency, h is set to be 1/52. we denote the series of nominal yields as $Y_t^N = \{y_{t,\tau_i}^N\}_{i=1}^{32}$, the series of TIPS yields as $Y_t^{TIPS} = \{y_{t,\tau_i}^{TIPS}\}_{i=1}^{19}$, the series of inflation forecasts as $IE_t = \{IE_{t,\tau_i}\}_{i=1}^{3}$, and the series of 3-month Tbill rate forecasts as $NE_t = \{NE_{t,\tau_i}\}_{i=1}^{2}$. Then the observable vector is written as $y_t = [q_t, Y_t^N, Y_t^{TIPS}, IE_t, NE_t]'$. The observation equation is not linear because Y_t^N, Y_t^{TIPS} and NE_t are nonlinear functions of state variables. These functions have closed-form formula and their analytic first-order derivatives can be easily derived, thus we can linearize the observation equation without any numerical approximation. Therefore, Assuming all observable variables are observed with Gaussian error, we use the extended Kalman filter, which applies the Kalman filter by linearizing the nonlinear observation equation at each step, to compute the log likelihood of the system given a set of parameters, and then find the optimal parameters by MLE.

Ignoring the measurement errors, the model has 29 unknown parameters. In the 57-dimension observation equation, all observable variables except log price level q_t are observed with error.

Table 3.1: Oil Price Effects on TIPS BEI before and after Crisis

Panel A (Panel B) regresses the daily changes of TIPS BEI on the daily changes of log oil price before (after) financial crisis. Panel C regresses the daily changes of TIPS BEI on the daily changes of log oil price, the post-crisis dummy, and their interaction term. The post-crisis dummy is set to be 0 before September 15, 2008 and 1 afterwards. We employ the Newly-West standard errors to compute T statistics to overcome the autocorrelation and heteroskedasticity in the error terms in the models.

	5 year	10 year	15 year	20 year
Panel A: Pre-crisis				
const	-0.0001	0.0002	0.0001	0.0000
	(-0.10)	(0.22)	(0.16)	(0.04)
$\Delta(\ln WTI_t)$	0.0033	0.0022	0.0019	0.0016
	(6.77)	(5.50)	(4.83)	(4.34)
Adjusted R^2	0.0370	0.0205	0.0149	0.0121
Panel B: Post-crisis				
const	0.0005	0.0001	0.0000	0.0000
	(0.52)	(0.16)	(-0.01)	(0.04)
$\Delta(\ln WTI_t)$	0.0066	0.0054	0.0045	0.0039
	(7.99)	(9.80)	(9.31)	(7.86)
Adjusted R^2	0.1443	0.1191	0.0846	0.0615
Panel C: Whole sample				
const	-0.0002	0.0001	0.0001	0.0000
	(-0.19)	(0.15)	(0.11)	(0.00)
$\Delta(\ln WTI_t)$	0.0033	0.0023	0.0019	0.0016
	(6.58)	(5.46)	(4.82)	(4.34)
1_{Post}	0.0007	0.0000	-0.0001	0.0000
	(0.52)	(0.03)	(-0.08)	(0.03)
$\Delta(\ln WTI_t) \cdot 1_{Post}$	0.0033	0.0031	0.0026	0.0023
	(3.31)	(4.54)	(4.24)	(3.72)
Adjusted R^2	0.0932	0.0713	0.0511	0.0394

Table 3.2: Oil Price Effects on TIPS BEI when Oil Prices Increase and Decrease

This table conducts the regression of daily changes of 5-, 10-, 15-, 20-year TIPS BEI on daily changes of log oil price, the dummy variable of negative daily changes of log oil price, and the interaction term for pre-crisis and post-crisis sample periods. We employ the Newly-West standard errors to compute T statistics to overcome the autocorrelation and heteroskedasticity in the error terms in the models.

	5-year Horizon		10 -year Horizon	
	Pre-crisis	Post-crisis	Pre-crisis	Post-crisis
const	0.0007	0.0032	0.0000	0.0032
	(0.42)	(2.12)	(0.03)	(2.42)
$\Delta(\ln WTI_t)$	0.0033	0.0051	0.0027	0.0038
	(3.97)	(6.31)	(3.47)	(6.13)
1_{Neg}	-0.0041	0.0004	-0.0030	-0.0010
	(-1.54)	(0.13)	(-1.24)	(-0.44)
$\Delta(\ln WTI_t) \cdot 1_{Neg}$	-0.0013	0.0033	-0.0017	0.0029
	(-1.03)	(1.66)	(-1.49)	(2.31)
Adjusted R^2	0.0380	0.1492	0.0218	0.1240
	15-year Horizon		20-year Horizon	
	Pre-crisis	Post-crisis	Pre-crisis	Post-crisis
const	-0.0003	0.0038	-0.0006	0.0041
	(-0.18)	(2.70)	(-0.40)	(2.56)
$\Delta(\ln WTI_t)$	0.0024	0.0027	0.0022	0.0020
	(3.21)	(4.26)	(3.10)	(2.48)
1_{Neg}	-0.0024	-0.0025	-0.0017	-0.0027
	(-1.01)	(-1.10)	(-0.73)	(-1.14)
$\Delta(\ln WTI_t) \cdot 1_{Neg}$	-0.0017	0.0029	-0.0016	0.0031
	(-1.55)	(2.23)	(-1.55)	(2.01)
Adjusted R^2	0.0161	0.0899	0.0129	0.0669

Table 3.3: Oil Price Effects on TIPS BEI under Different Regimes

Panel A (Panel B) conducts four different regressions between the daily changes of 10-year (20-year) TIPS BEI and the daily changes of log oil price with different controls. The zero lower bound (ZLB) dummy 1_{ZLB} is set to be 1 when the contemporaneous 3-month nominal interest rate is below 1% and 0 otherwise. The negative change dummay 1_{Neg} is set to be 1 when the $\Delta(\ln WTI_t)$ is negative and 0 otherwise. We employ the Newly-West standard errors to compute T statistics to overcome the autocorrelation and heteroskedasticity in the error terms in the models.

Panel A: 10 year Horizon				
	(1)	(2)	(3)	(4)
const	0.0000	-0.0004	0.0012	-0.0002
	(0.05)	(-0.53)	(1.21)	(-0.09)
$\Delta(\ln WTI_t)$	0.0039	0.0026	0.0033	0.0028
	(10.31)	(5.75)	(6.93)	(3.43)
1_{ZLB}		0.0009		0.0030
		(0.81)		(1.43)
$\Delta(\ln WTI_t) \cdot 1_{ZLB}$		0.0023		0.0009
		(3.42)		(0.92)
1_{Neg}			-0.0013	-0.0024
			(-0.70)	(-0.90)
$\Delta(\ln WTI_t) \cdot 1_{Neg}$			0.0007	-0.0010
			(0.76)	(-0.76)
$1_{ZLB} \cdot 1_{Neg}$				0.0015
				(0.42)
$\Delta(\ln WTI_t) \cdot 1_{Neg} \cdot 1_{ZLB}$				0.0032
				(1.81)
Adjusted R^2	0.0616	0.0668	0.0615	0.0678
Panel B: 20 year Horizon				
	(1)	(2)	(3)	(4)
const	0.0000	-0.0004	0.0016	-0.0010
	(-0.09)	(-0.64)	(1.40)	(-0.59)
$\Delta(\ln WTI_t)$	0.0028	0.0019	0.0021	0.0023
	(8.63)	(4.72)	(3.74)	(3.12)
1_{ZLB}		0.0008		0.0048
		(0.76)		(2.14)
$\Delta(\ln WTI_t) \cdot 1_{ZLB}$		0.0017		-0.0004
		(2.81)		(-0.40)
1_{Neg}			-0.0017	-0.0014
			(-1.02)	(-0.55)
$\Delta(\ln WTI_t) \cdot 1_{Neg}$			0.0009	-0.0013
			(0.90)	(-1.13)
$1_{ZLB} \cdot 1_{Neg}$				-0.0010
				(-0.29)
$\Delta(\ln WTI_t) \cdot 1_{Neg} \cdot 1_{ZLB}$				0.0039
				(2.14)
Adjusted R^2	0.0340	0.0368	0.0343	0.0390

Table 3.4: Parameter Estimates

This table presents all parameters and standard errors (in parenthese) for the model we use to describe the joint dynamics of nominal yields, inflation, real yields and TIPS yields. We compute standard errors by calculating the fishier information matrix numerically.

Log likelihood $= 276701.58$												
State Variables			Nominal Pricing Kernel						Price Level		TIPS Liquidity	
κ_{11}	0.3802	ρ_0^{NS}	0.0382	$\left[\Sigma\Lambda^N\right]_{11}$	-0.0098				ρ_0^I	0.0209	$\tilde{\beta}$	1.1621
	(0.0093)		(0.0016)		(0.0002)					(0.0004)		(0.0255)
κ_{22}	0.1067	$\rho_{1,1}^{NS}$	3.0663	$\left[\Sigma\Lambda^N\right]_{21}$	0.2648				$\rho_{1,1}^I$	0.0897	$\tilde{\kappa}$	0.5333
	(0.0039)		(0.0691)		(0.0187)					(0.0032)		(0.0058)
κ_{33}	0.8767	$\rho_{1,2}^{NS}$	0.5352	$\left[\Sigma\Lambda^N\right]_{31}$	0.1229				$\rho_{1,2}^I$	0.1932	$\tilde{\mu}$	0.0061
	(0.0147)		(0.0116)		(0.0031)					(0.0158)		(0.0001)
$\Sigma_{2,1}$	-0.0173	$\rho_{1,3}^{NS}$	0.6159	$\left[\Sigma\Lambda^N\right]_{12}$	-0.0159				$\rho_{1,3}^I$	-0.0962	$\tilde{\lambda}_0$	0.3511
	(0.0008)		(0.0135)		(0.0006)					(0.0050)		(0.0059)
$\Sigma_{3,1}$	-0.0292	$\lambda_{0,1}^N$	0.1088	$\left[\Sigma\Lambda^N\right]_{22}$	-0.1431				$\sigma_{q,1}$	-0.0024	$\tilde{\lambda}_1$	-0.4328
	(0.0010)		(0.0032)		(0.0038)					(0.0002)		(0.0085)
$\Sigma_{3,2}$	-0.0075	$\lambda_{0,2}^N$	-0.2262	$\left[\Sigma\Lambda^N\right]_{32}$	-0.0913				$\sigma_{q,2}$	0.0007	β_1	-0.5551
	(0.0003)		(0.0041)		(0.0026)					(0.0000)		(0.0539)
		$\lambda_{0,3}^N$	-0.9421	$\left[\Sigma\Lambda^N\right]_{13}$	0.0841				$\sigma_{q,3}$	0.0002	β_2	-0.0626
			(0.0385)		(0.0020)					(0.0000)		(0.0067)
				$\left[\Sigma\Lambda^N\right]_{23}$	0.2236				$\sigma_q^{\perp}$	0.0080	β_3	0.0119
					(0.0041)					(0.0011)		(0.0003)
				$\left[\Sigma\Lambda^N\right]_{33}$	-0.3834							
					(0.0125)							

Table 3.5: Oil Price Effects on IE before and after Crisis

Panel A (Panel B) regresses the weekly changes of IE on the weekly changes of log oil price before (after) financial crisis. Panel C regresses the weekly changes of IE on the weekly changes of log oil price, the post-crisis dummy, and their interaction term. The post-crisis dummy is set to be 0 before September 15, 2008 and 1 afterwards. T-statistic are reported in parentheses. We employ the Newly-West standard errors to compute T statistics to overcome the autocorrelation and heteroskedasticity in the error terms in the models.

	5 year	10 year	15 year	20 year
Panel A: Pre-crisis				
const	-0.0006	-0.0005	-0.0004	-0.0003
	(-0.52)	(-0.55)	(-0.55)	(-0.55)
$\Delta(\ln WTI_t)$	0.0000	0.0000	0.0000	0.0000
	(-0.13)	(-0.05)	(-0.02)	(-0.01)
Adjusted R^2	-0.0019	-0.0020	-0.0020	-0.0020
Panel B: Post-crisis				
const	-0.0008	-0.0007	-0.0006	-0.0005
	(-0.54)	(-0.53)	(-0.52)	(-0.52)
$\Delta(\ln WTI_t)$	0.0019	0.0016	0.0013	0.0011
	(7.11)	(7.04)	(6.97)	(6.93)
Adjusted R^2	0.0908	0.0873	0.0856	0.0848
Panel C: Whole sample				
const	-0.0004	-0.0004	-0.0003	-0.0003
	(-0.39)	(-0.43)	(-0.44)	(-0.44)
$\Delta(\ln WTI_t)$	0.0000	0.0000	0.0000	0.0000
	(0.13)	(0.20)	(0.22)	(0.23)
1_{Post}	-0.0004	-0.0003	-0.0003	-0.0002
	(-0.23)	(-0.21)	(-0.21)	(-0.20)
$\Delta(\ln WTI_t) \cdot 1_{Post}$	0.0018	0.0016	0.0013	0.0011
	(5.02)	(5.24)	(5.27)	(5.27)
Adjusted R^2	0.0526	0.0528	0.0522	0.0519

Table 3.6: Oil Price Effects on IE under Different Regimes

Panel A (Panel B) conducts four different regressions between the weekly changes of 10-year (20-year) IE on the weekly changes of log oil price with different controls. The zero lower bound (ZLB) dummy 1_{ZLB} is set to be 1 when the contemporaneous 3-month nominal interest rate is below 1% and 0 otherwise. The negative change dummay 1_{Neg} is set to be 1 when the $\Delta(\ln WTI_t)$ is negative and 0 otherwise. T-statistic are reported in parentheses. We employ the Newly-West standard errors to compute T statistics to overcome the autocorrelation and heteroskedasticity in the error terms in the models.

Panel A: 10 year Horizon				
	(1)	(2)	(3)	(4)
const	-0.0008	-0.0007	-0.0011	-0.0027
	(-0.96)	(-0.83)	(-0.86)	(-1.62)
$\Delta(\ln WTI_t)$	0.0008	0.0000	0.0009	0.0005
	(4.64)	(0.07)	(3.33)	(1.32)
1_{ZLB}		0.0003		0.0034
		(0.22)		(1.32)
$\Delta(\ln WTI_t) \cdot 1_{ZLB}$		0.0015		0.0006
		(5.24)		(1.12)
1_{Neg}			0.0010	-0.0003
			(0.43)	(-0.11)
$\Delta(\ln WTI_t) \cdot 1_{Neg}$			0.0001	-0.0011
			(0.13)	(-1.78)
$1_{ZLB} \cdot 1_{Neg}$				0.0016
				(0.38)
$\Delta(\ln WTI_t) \cdot 1_{Neg} \cdot 1_{ZLB}$				0.0020
				(2.33)
Adjusted R^2	0.0286	0.0515	0.0268	0.0524
Panel B: 20 year Horizon				
	(1)	(2)	(3)	(4)
const	-0.0005	-0.0005	-0.0008	-0.0017
	(-0.96)	(-0.76)	(-0.91)	(-1.48)
$\Delta(\ln WTI_t)$	0.0006	0.0000	0.0006	0.0004
	(4.68)	(0.10)	(3.35)	(1.22)
1_{ZLB}		0.0001		0.0020
		(0.14)		(1.11)
$\Delta(\ln WTI_t) \cdot 1_{ZLB}$		0.0011		0.0005
		(5.23)		(1.25)
1_{Neg}			0.0008	-0.0003
			(0.48)	(-0.16)
$\Delta(\ln WTI_t) \cdot 1_{Neg}$			0.0000	-0.0007
			(0.12)	(-1.73)
$1_{ZLB} \cdot 1_{Neg}$				0.0014
				(0.48)
$\Delta(\ln WTI_t) \cdot 1_{Neg} \cdot 1_{ZLB}$				0.0014
				(2.25)
Adjusted R^2	0.0283	0.0505	0.0265	0.0509

Table 3.7: Oil Price Effects on IRP when Oil Prices Increase and Decrease

Panel A (Panel B) regresses the weekly changes of IRP on the weekly changes of log oil price before (after) financial crisis. Panel C regresses the weekly changes of IRP on the weekly changes of log oil price, the post-crisis dummy, and their interaction term. The post-crisis dummy is set to be 0 before September 15, 2008 and 1 afterwards. T-statistic are reported in parentheses. We employ the Newly-West standard errors to compute T statistics to overcome the autocorrelation and heteroskedasticity in the error terms in the models.

	5 year	10 year	15 year	20 year
Panel A: Pre-crisis				
const	0.0004	0.0003	0.0002	0.0002
	(0.33)	(0.27)	(0.20)	(0.15)
$\Delta(\ln WTI_t)$	-0.0003	-0.0003	-0.0002	-0.0002
	(-0.91)	(-0.91)	(-0.88)	(-0.85)
Adjusted R^2	0.0005	0.0006	0.0005	0.0002
Panel B: Post-crisis				
const	-0.0002	-0.0004	-0.0005	-0.0006
	(-0.16)	(-0.32)	(-0.42)	(-0.47)
$\Delta(\ln WTI_t)$	0.0004	0.0009	0.0011	0.0013
	(1.52)	(3.47)	(4.76)	(5.42)
Adjusted R^2	0.0047	0.0318	0.0553	0.0671
Panel C: Whole sample				
const	0.0005	0.0005	0.0004	0.0003
	(0.43)	(0.39)	(0.34)	(0.29)
$\Delta(\ln WTI_t)$	-0.0002	-0.0002	-0.0002	-0.0002
	(-0.69)	(-0.65)	(-0.60)	(-0.57)
1_{Post}	-0.0007	-0.0009	-0.0009	-0.0009
	(-0.42)	(-0.51)	(-0.54)	(-0.54)
$\Delta(\ln WTI_t) \cdot 1_{Post}$	0.0006	0.0011	0.0013	0.0014
	(1.48)	(2.65)	(3.39)	(3.77)
Adjusted R^2	0.0012	0.0138	0.0252	0.0313

Table 3.8: Oil Price Effects on IRP under Different Regimes

Panel A (Panel B) conducts four different regressions between the weekly changes of 10-year (20-year) IRP on the weekly changes of log oil price with different controls. The zero lower bound (ZLB) dummy 1_{ZLB} is set to be 1 when the contemporaneous 3-month nominal interest rate is below 1% and 0 otherwise. The negative change dummay 1_{Neg} is set to be 1 when the $\Delta(\ln WTI_t)$ is negative and 0 otherwise. T-statistic are reported in parentheses. We employ the Newly-West standard errors to compute T statistics to overcome the autocorrelation and heteroskedasticity in the error terms in the models.

Panel A: 10 year Horizon				
	(1)	(2)	(3)	(4)
const	-0.0001	-0.0004	0.0006	-0.0038
	(-0.10)	(-0.30)	(0.33)	(-1.74)
$\Delta(\ln WTI_t)$	0.0003	-0.0002	0.0003	0.0006
	(1.75)	(-0.79)	(0.78)	(1.46)
1_{ZLB}		0.0008		0.0076
		(0.44)		(2.36)
$\Delta(\ln WTI_t) \cdot 1_{ZLB}$		0.0011		-0.0005
		(2.89)		(-0.76)
1_{Neg}			-0.0015	0.0011
			(-0.58)	(0.30)
$\Delta(\ln WTI_t) \cdot 1_{Neg}$			0.0000	-0.0015
			(-0.05)	(-1.69)
$1_{ZLB} \cdot 1_{Neg}$				-0.0045
				(-0.94)
$\Delta(\ln WTI_t) \cdot 1_{Neg} \cdot 1_{ZLB}$				0.0024
				(2.08)
Adjusted R^2	0.0040	0.0144	0.0023	0.0178
Panel B: 20 year Horizon				
	(1)	(2)	(3)	(4)
const	-0.0003	-0.0004	0.0000	-0.0039
	(-0.36)	(-0.39)	(-0.02)	(-1.84)
$\Delta(\ln WTI_t)$	0.0006	-0.0002	0.0005	0.0007
	(2.82)	(-0.73)	(1.78)	(1.58)
1_{ZLB}		0.0006		0.0070
		(0.35)		(2.32)
$\Delta(\ln WTI_t) \cdot 1_{ZLB}$		0.0014		-0.0001
		(4.01)		(-0.17)
1_{Neg}			-0.0008	0.0005
			(-0.32)	(0.15)
$\Delta(\ln WTI_t) \cdot 1_{Neg}$			-0.0001	-0.0016
			(-0.10)	(-1.94)
$1_{ZLB} \cdot 1_{Neg}$				-0.0026
				(-0.56)
$\Delta(\ln WTI_t) \cdot 1_{Neg} \cdot 1_{ZLB}$				0.0027
				(2.36)
Adjusted R^2	0.0121	0.0314	0.0101	0.0353

Table 3.9: Parameter for the Baseline Model

All parameters for the household's preferences, goods production and monetary policy are in line with literature.

Parameter	Description	Value
Panel A: Preferences		
β	Subjective discount factor	0.985
ρ_C	Elasticity of substitution for consumption bundle	0.25
α_C	Oil Share in consumption bundle	0.05
χ	Preference over consumption bundle vs leisure	0.25
Panel B: Production		
θ	Elasticity of substitution among intermediate goods	6
φ	Price adjustment cost	80
ρ_Y	Elasticity of substitution for production	0.225
α_Y	Oil Share in production	0.055
Panel C: Monetary Policy		
ϕ_π	Coefficient on inflation in the Taylor rule	2.5
$400\left(\bar{\Pi}-1\right)$	Annualized target rate of inflation	0.02
Panel D: Exogenous Shocks		
$\bar{s}$	Steady state for bond preference shock	0.01
ρ_s	AR(1) coefficient for bond preference shock	0.9
σ_s	Standard deviation for bond preference shock	0.25
ρ_{d^O}	AR(1) coefficient for oil demand shock	0.8
σ_{d^O}	Standard deviation for oil demand shock	0.05
ρ_{S^O}	AR(1) coefficient for oil supply shock	0.8
σ_{S^O}	Standard deviation for oil supply shock	0.05
ρ_A	AR(1) coefficient for productivity shock	0.9
σ_A	Standard deviation for productivity shock	0.001

Figure 3.1: 10-year TIPS BEI and Oil Prices before and after Financial Crisis

This upper left panel shows the daily dynamics of 10-year TIPS BEI and log oil price for the pre-crisis period (01/04/1999 to 09/14/2008) and the upper right panel shows the same for post-crisis period (09/15/2008 to 05/31/2017). The bottom left panel and bottom right panel shows the scatter plots and OLS regression lines between daily changes of two variables for the pre-crisis and post-crisis sample periods, respectively.

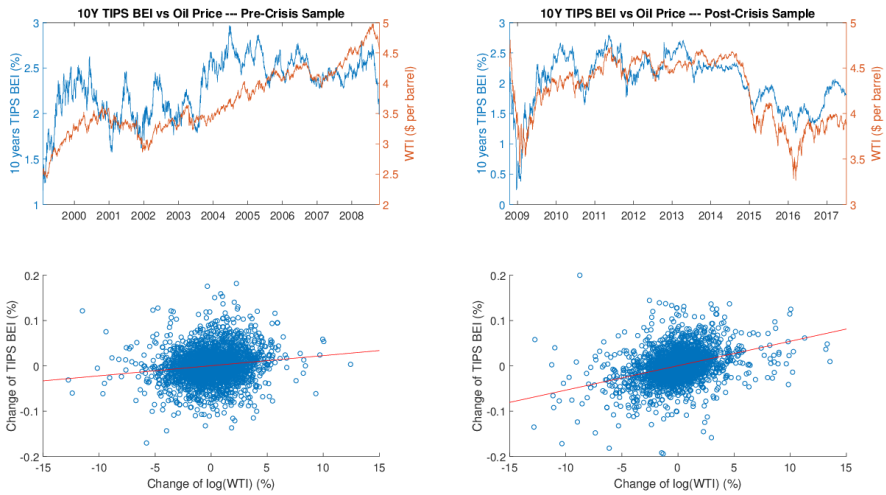

Figure 3.2: Nominal Yields Fitting

This figure shows the actual (in blue) and fitted (in red) nominal yields with maturities 3 and 6 month, as well as 1, 2, ... , 13 and 14 years. The RMSE of in-sample fitting (in bps) are shown in the title of each plot.

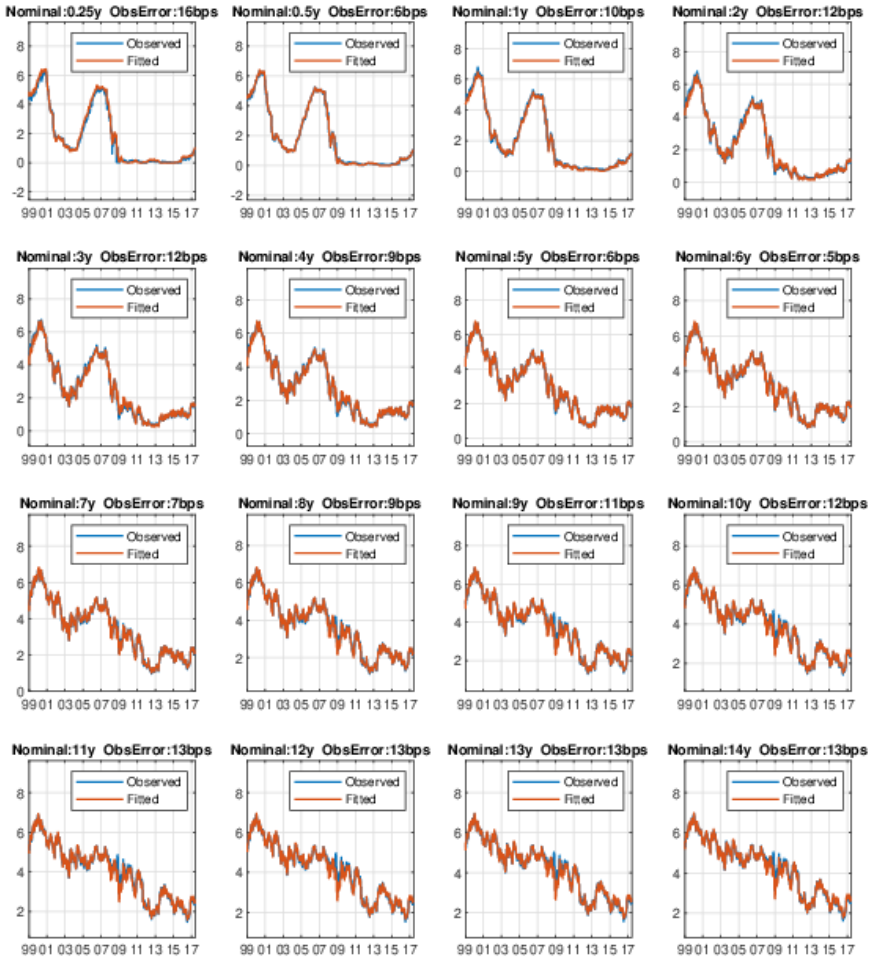

Figure 3.3: Nominal Yields Fitting

This figure shows the actual (in blue) and fitted (in red) nominal yields with maturities 15, 16, ..., 29 and 30 years. The RMSE of in-sample fitting (in bps) are shown in the title of each plot.

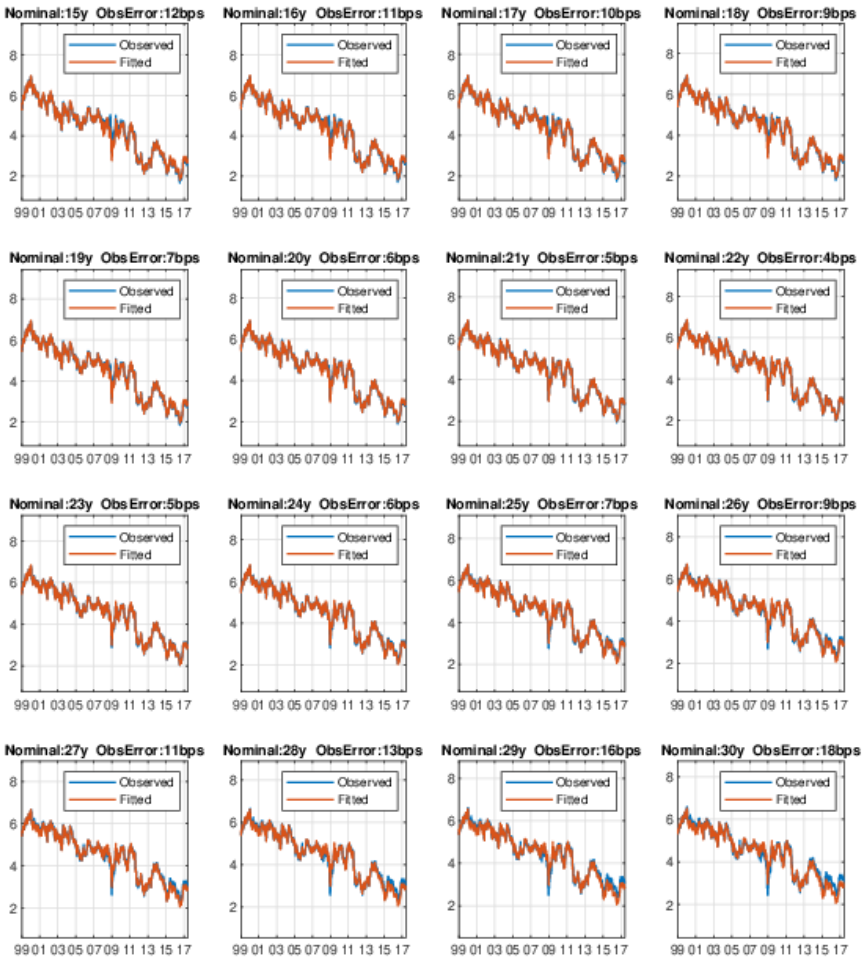

Figure 3.4: TIPS Yields

This figure shows the actual (in blue) and fitted (in red) TIPS yields with maturities 2, 3, ... , 12 and 13 years. The RMSE of in-sample fitting (in bps) of observation equations are shown in the title of each plot.

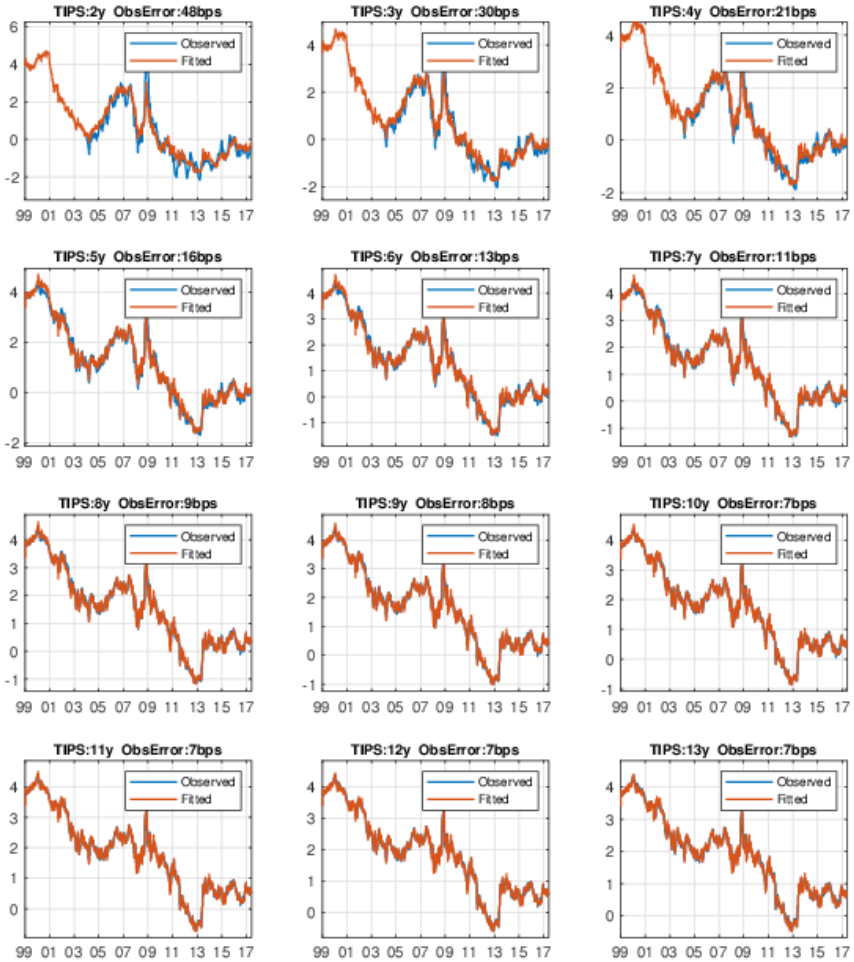

Figure 3.5: TIPS Yields and Survey Forecasts Fitting

This figure shows the actual (in blue) and fitted (in red) TIPS yields with maturities 14, 15, ... , 19 and 20 years, inflation forecasts with maturities 1, 5, and 10 years, and 3-month Tbill rates forecasts with 1 and 10 years. The RMSE of in-sample fitting (in bps) of observation equations are shown in the title of each plot.

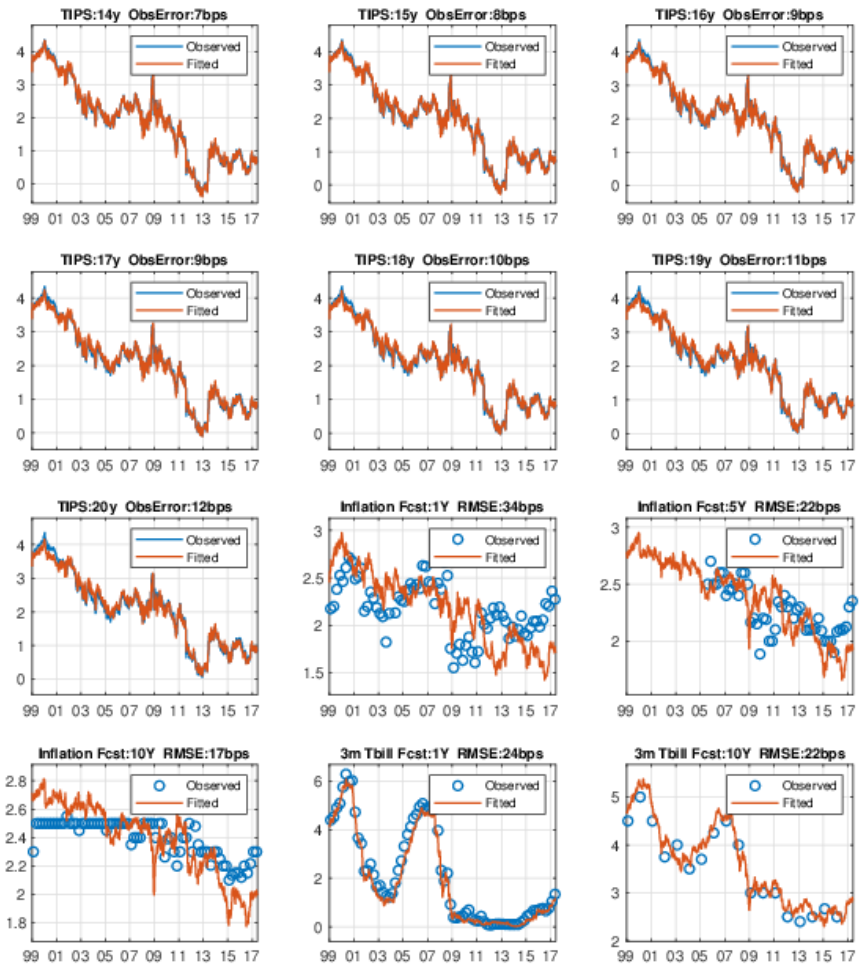

Figure 3.6: Shadow Rate Implied Nominal and Real Yields

This figure shows the estimated nominal/real yields (in blue), which assume there is the ZLB constraint, and the shadow rate implied nominal/real yields yields (in dashed red), which relaxes the constraint, at maturities of 3 months, 6 months, 1 year, 3 years, 5 years and 10 years.

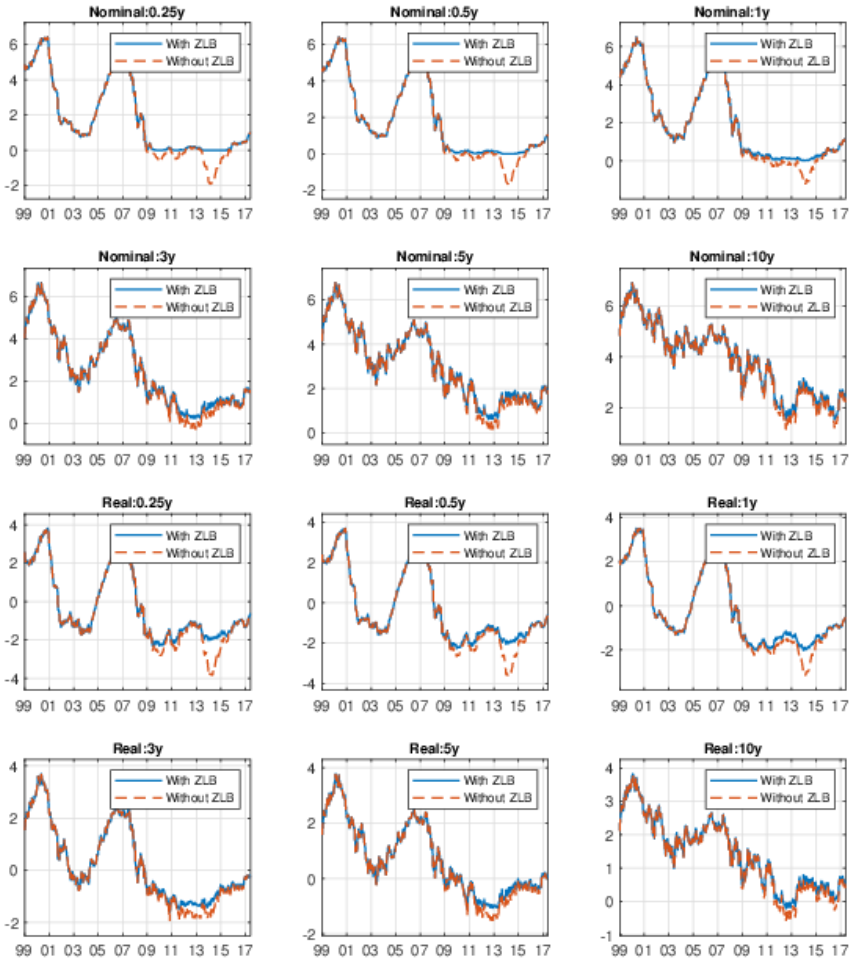

Figure 3.7: Decomposition of TIPS BEI

This figure shows the decomposition of TIPS BEI for 10 year, 15 year and 20 year. The upper three panels show IE (in blue), BEI (in red) and TIPS BEI (in yellow) of three maturities. The middle three panels show IRP of three maturities. And the bottom three panels show LRP of three maturities.

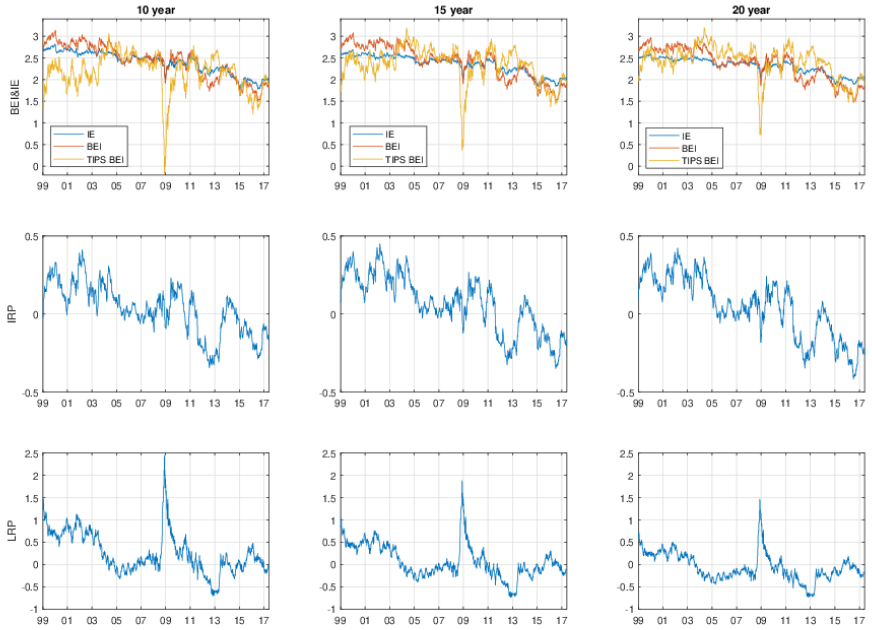

Figure 3.8: Local Correlation between Oil Real Prices and the Term Structure of Inflation Expectation

The upper left, upper right, bottom left and bottom right shows the oil real price's correlation with contemporaneous inflation rate, 1-year IE, 5-year IE, and 10-year IE local to different nominal shadow interest rates. The blue line shows the local correlation with ZLB constraint, while the red line shows the result without the binding constraint.

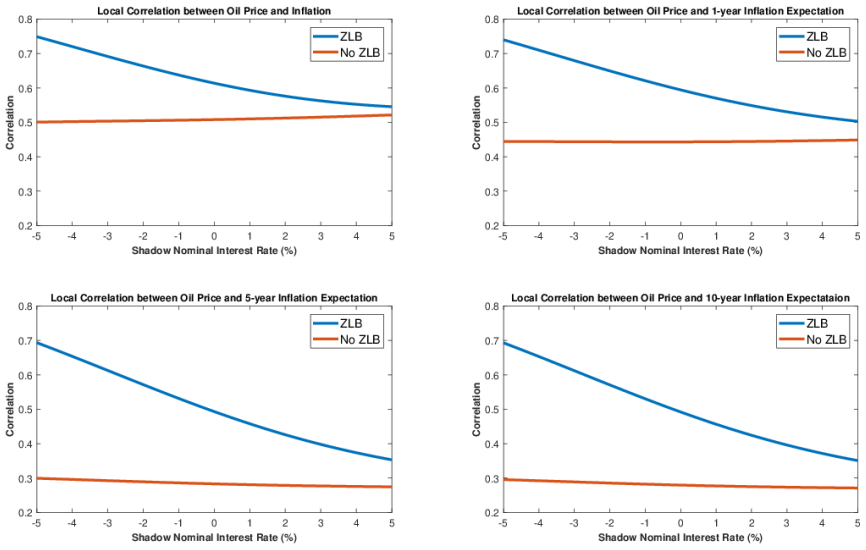

Figure 3.9: Impulse Response of Oil Supply

This figure shows the impulse responses of two standard deviation of oil supply shocks (10% change in level) on all macro variables and IE with different horizons. The red solid line indicates the impulse responses for the 10% positive change of oil supply and the blue solid line indicates that for the 10% negative change of oil supply. The red dashed line indicates the impulse responses for the 10% positive change of oil supply if we ignore ZLB binding constraint in the model. The percentage changes of all variables except annualized nominal interest rates are plotted. For annualized nominal interest rates, we show their impulse response function for levels. All impulse responses are reported for horizons ranging from 0 to 5 years.

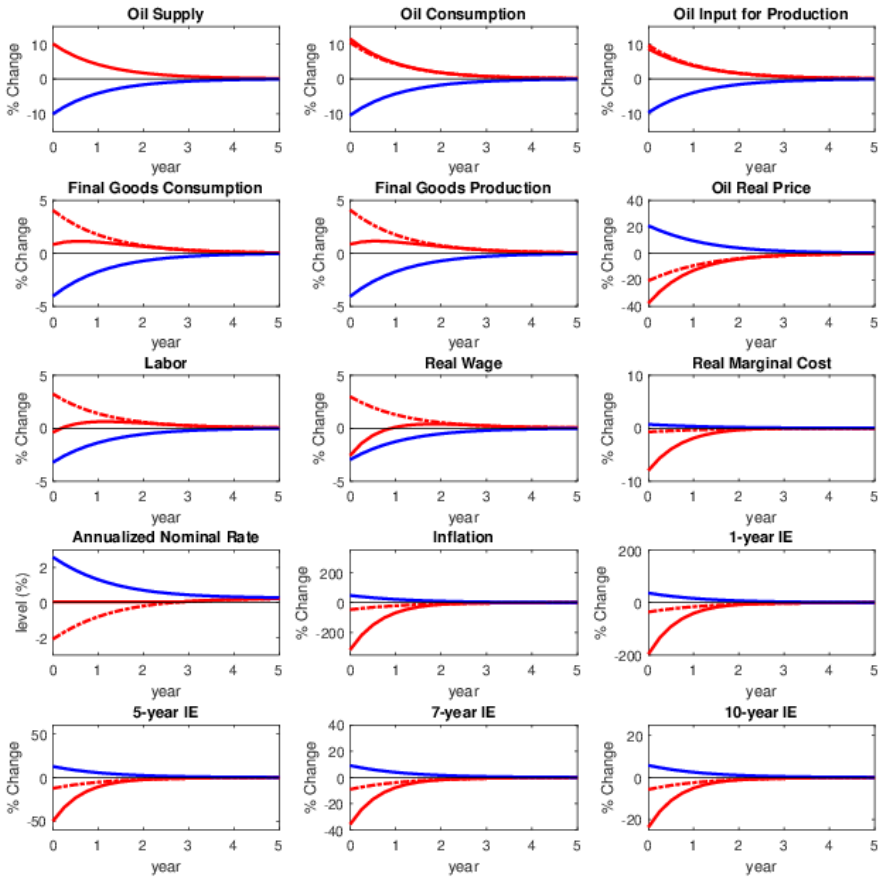

Figure 3.10: How Inflation and IE in Different Horizons Changes with Supply-Driven Oil Prices

This figure shows how inflation and IE in different horizons change with the supply-driven oil prices. The x-axis is the percentage change deviated from the steady state of oil real price and the y-axis is that of inflation or IE. The red dashed lines indicate the relation of the variables in our model with ZLB constraint, while the blue solid line indicate the relation of the variables without the ZLB constraint. The green solid vertical line indicates the threshold state where the ZLB binds.

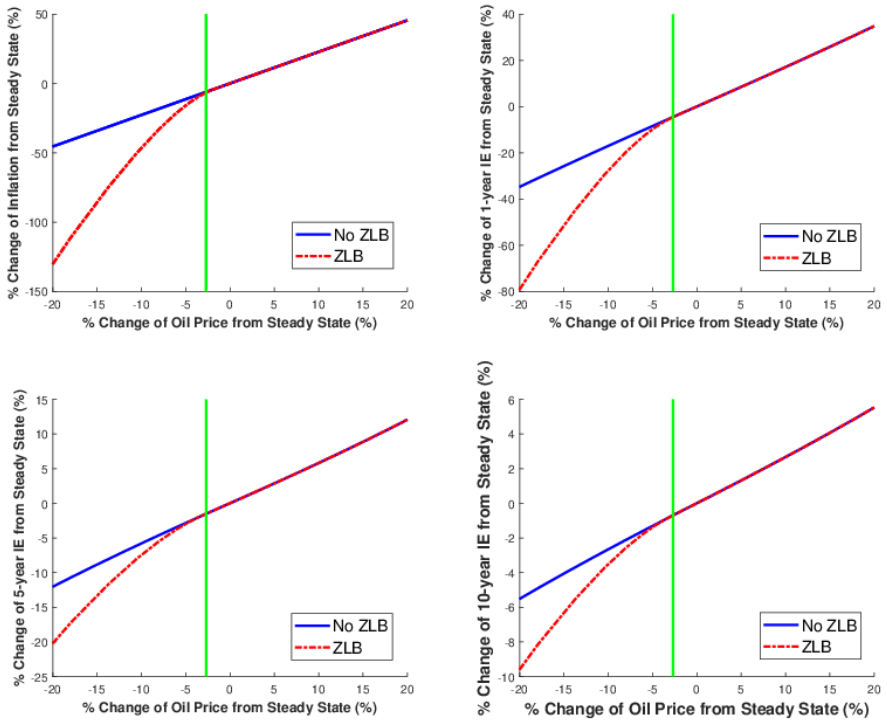

Figure 3.11: Impulse Response of Oil Demand

This figure shows the impulse responses of two standard deviation of oil demand shocks (10% change in level) on all macro variables and IE with different horizons. The red solid line indicates the impulse responses for the 10% negative change of oil demand and the blue solid line indicates that for the 10% positive change of oil demand. The red dashed line indicates the impulse responses for the 10% negative change of oil supply if we ignore ZLB binding constraint in the model. The percentage change of all variables except annualized nominal interest rates are plotted. For annualized nominal interest rates, we show their impulse response for levels. All impulse responses are reported for horizons ranging from 0 to 5 years.

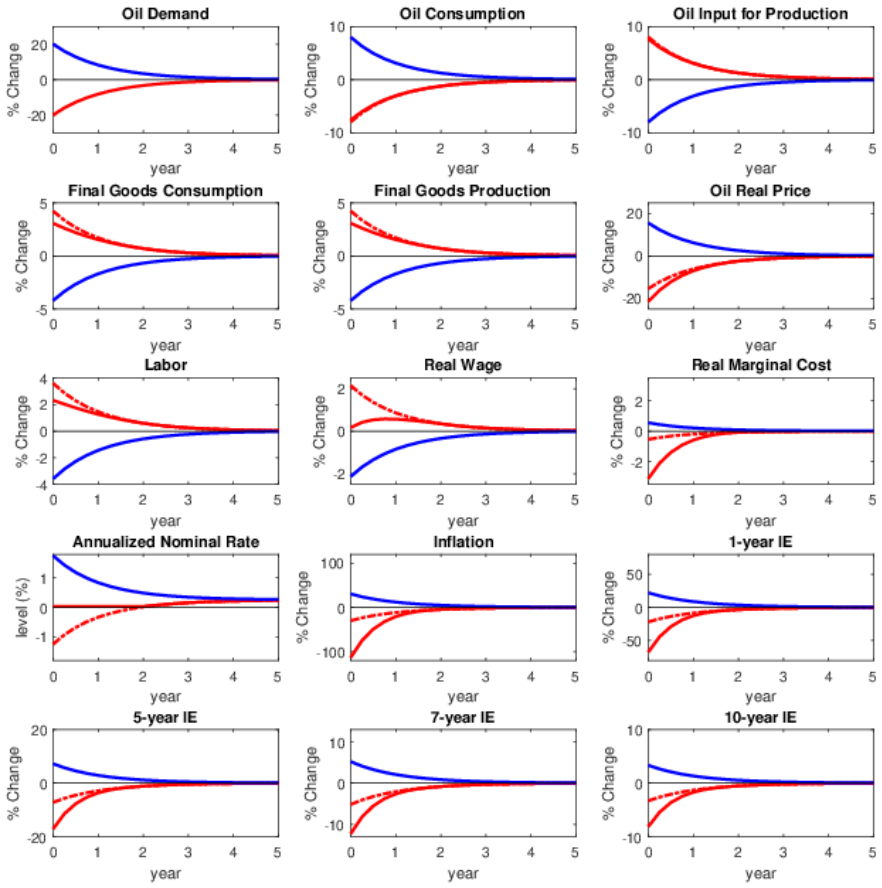

Figure 3.12: How Inflation and IE in Different Horizons Changes with Demand-Driven Oil Prices

This figure shows how inflation and IE in different horizons changes with the Demand-driven oil prices. The x-axis is the percentage change deviated from the steady state of oil real price and the y-axis is that of inflation or IE. The red dashed lines indicate the relation of the variables in our model with ZLB constraint, while the blue solid line indicate the relation of the variables without the ZLB constraint. The green solid vertical line indicates the threshold state where the ZLB binds.

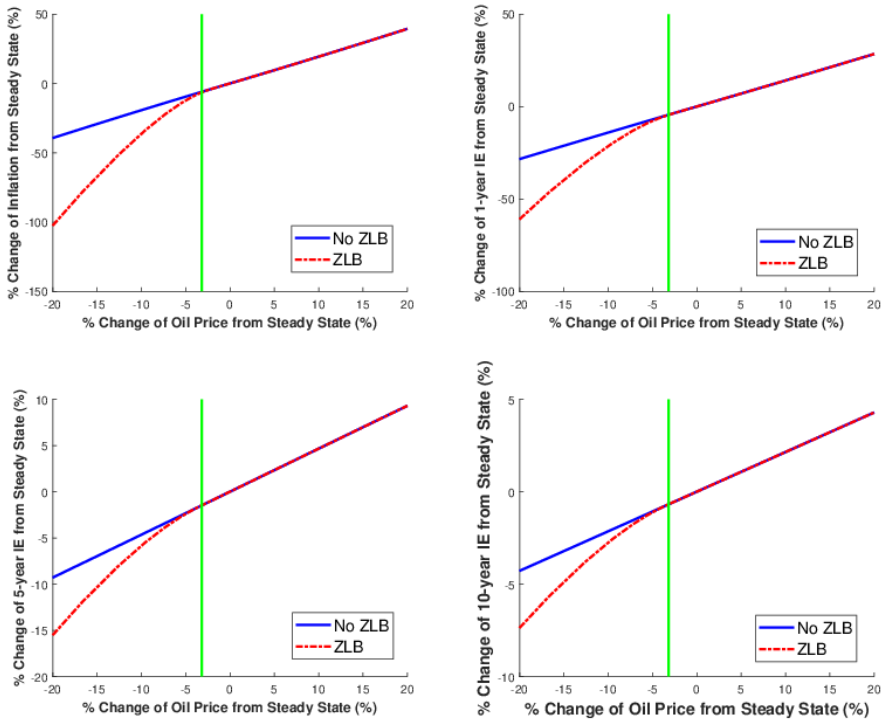

Chapter 4

The Information Content of Treasury Term Premium

(Jointly with Xiaoyang (Sean) Dong)

4.1 Introduction

As global economies are increasingly financially integrated, nowadays US Treasury (UST) dynamics are no longer dominated by US fundamentals, but are becoming more responsive to foreign monetary policies and institutional flows. One of the most striking puzzles in 2016 was the deep dive of UST term premium into negative territory while the Fed was raising rates in a tightening cycle. It was the first time in history that the entire treasury curve was priced with significantly negative term premium throughout short-end to long-end. Figure 4.1 plots popular measures of 10y zero-yield term premium by Adrian et al. (2013); Kim and Wright (2005) as well as from our model. The huge drop in early 2016 to deep negative zone is a robust pattern echoed by various model specifications. This raises the question: what crushed treasury term premium while there were no salient shocks to either US growth or US inflation? More broadly speaking, what're the information contents of modern treasury term premium?

In order to understand the economic drivers behind treasury term premium, we conduct three layers of decompositions. The first layer of decomposition is to break Nominal Term Premium (NTP) into Real Term Premium (RTP) and Inflation Term Premium (ITP), so that we can understand which of the two components dropped a lot. After that, the second layer of decomposition is to further identify what risks Real & Inflation TP are compensating for respectively. Based on the risk factor attribution from the second layer, we further delve

into their major drivers in the third step. To achieve these 3 goals, we need a model with the following features. First, as term premium is pinned down by yield minus expectation, we want the model to fit both yields and survey expectations jointly, so that both observables naturally pin down term premium and hence the estimates are more robust to model-misspecification. Second, the model is designed with similar Arbitrage-Free Nelson-Siegel (AFNS) structure as in Christensen et al. (2011), so that all factors have clear economic meanings. Level corresponds to duration risk; slope corresponds to steepener risk; and curvature corresponds to monetary policy risk - LSAP/QEs are all concentrated on 2$\sim$10y which matches with the hump-shape impacts of monetary shocks. On the real-side, we follow D'Amico et al. (2018) to augment the standard affine structure with a liquidity factor, which helps us to infer liquidity risk premium priced in TIPS as a side-product. Third, after we extract the factors, we further compare them with flows to reveal their true drivers in 2016.

There're three major findings from the decompositions. First, Real TP accounts for over three quarters of Nominal TP variations, while Inflation TP is a slow-moving component mostly driven by oil price. Second, duration factor is priced with significantly positive risk price, as investors demand premium for bearing duration risk. Yet monetary factor is priced with significantly negative risk price, as central banks are willing to pay to lower term premium. Steepener risk, on the other hand, is barely priced in the Real TP empirically, which is not too surprising as the slope factor is well-known to drive rates expectation rather than term premium. Last but not least, the duration factor dynamics have been driven by foreign flows from Japan and Europe due to monetary divergence during recent years. For instance, Figure 4.2 shows the striking co-movement between duration-attributed Real TP and JPY cross-currency basis (which measures foreign hedging demand of $-assets and hence Japanese flows). In other words, the information contents embedded in treasury term premium go beyond US fundamentals. The puzzles cannot be resolved if we focus exclusively on local macro variables but ignoring foreign demands. This explains why

structural macro models in the literature tend to fit poorly especially for recent samples.

To further demonstrate the role of foreign demand in driving treasury term premium, we estimate two versions of extended models on top of our Nelson-Siegel structure - one by adding a US-local macro factor (the Chicago Fed National Activity Index) and one with a foreign demand factor (JPY cross-currency basis). By comparing out-of-sample RMSE from 2015 to 2017, we show that the local macro factor model is dominated by the foreign demand model for maturity longer than 10y. Yet both models fail to beat the Nelson-Siegel benchmark on the short-end. The main insight from this study suggests that the prevalence of modern carry trades and cross-border investment flows are becoming an increasingly important driver of mid/long-end of treasury curves. It could be a bit ambitious for structural macro models to capture the fine structure of treasury term premium dynamics without the international flow component.

This paper contributes to three strands of literature. The first one is about the estimation of Nominal TP, Real TP, Inflation Risk Premium (IRP) and Inflation Expectation (IE) by using Gaussian affine term structure framework. Kim and Wright (2005) use a three-factor arbitrage-free term structure to estimate Nominal and Real TP with yields and survey forecasts data. By using computationally efficient regression method, Abrahams et al. (2013) estimate a seven-factor affine model that jointly price TIPS and treasury yields with controlling TIPS' liquidity effects. Different from these studies, several others mainly focus on the estimation of IRP and IE. D'Amico et al. (2018) models yields, inflation, and survey expectation jointly to extract IRP and IE after adjusting for the TIPS-specific liquidity factor, while Christensen et al. (2010) do similar work without survey forecasts by employing the AFNS structure. Inheriting all of their advantages, our model is designed to be able to jointly fit yields and survey forecasts, and grant each factor clear economic meaning. In addition, we unify the estimation of Nominal, Real and Inflation TP, as well as IRP and IE, under the same framework by clearly stating the relation between Inflation TP and IRP.

The second strand of literature this paper speaks to are macro-finance studies, in particular, estimating interest rate term structure by using macro factors. Ang and Piazzesi (2003) demonstrate the necessity of adding inflation and economic activity information in term structure estimation. Pioneered by this study, a number of papers model yield curves by local macro variables, such as Mönch (2008), Joslin et al. (2013) and Joslin et al. (2014). Our paper supplements this area by illustrating that in addition to local factors, international factors are also significantly priced in treasury yields. In particular, we find oil price, which is driven by global supply and demand shocks, performs as a predominant driver for IE, IRP, and Inflation TP. In addition, foreign monetary policies and capital flows are priced in Real TP. These evidences shed light on the necessity of including global macro information in modeling local yield curve dynamics.

Finally, the paper fits within the rapidly growing literature about the supply and demand effects on the government bond market. Several studies document that bond yields and future returns are positively related to the supply factor proxied by the maturity-weighted-debt-to-GDP ratio (Greenwood and Vayanos, 2014), and negatively associated with the demand factor resulting from investors' preferences for specific maturities (Vayanos and Vila, 2009; Kaminska et al., 2011), central banks' QE or foreign investor flows. Several theoretical (Eggertsson and Woodford, 2003) and empirical studies (Krishnamurthy and Vissing-Jorgensen, 2011) illustrate the positive effect of QE on asset prices and describe the corresponding channels. The recent study by Koijen et al. (2016) estimates the negative impact of the ECB's ongoing asset purchase program on bond yields. Using no-arbitrage model or regression based methods, a number of other papers (Bernanke et al., 2004; Rudebusch et al., 2006; Warnock and Warnock, 2009; Beltran et al., 2013; Sierra, 2014; Kohn, 2016; Yan, 2016) demonstrate the importance of the foreign reserve holdings in determining the US yield curves. Our study provides additional evidences through a novel exogenous natural experiment, BoJ's Negative Interest Rate Policies, which squeezed out Japanese investors from Japanese government bond market to US treasury market. Results

show that this inflow pushed down treasury yields and resulted in unconventional negative term premium in 2016.

The remainder of the paper is organized as follows. Section 4.2 introduces our joint model for pricing nominal, real, and TIPS yields, as well as how we decompose treasury term premium. Section 4.3 describes the data, estimation methodology, fitting performance and robustness checks. Section 4.4 digs into the information contents and economic drivers of treasury term premium by conducting three layers of decompositions. Section 4.5 further compares two extended models with the benchmark model and demonstrates that foreign demand indeed plays a vital role. Section 4.6 concludes.

4.2 The Model

In this section, we introduce the no-arbitrage affine term structure model that we employ to specify the joint dynamics of nominal yields, real yields, TIPS yields and inflation. Our model inherits the advantages from both Arbitrage-Free Nelson Siegel (AFNS) model (Christensen et al., 2011) and liquidity-adjusted TIPS pricing model (D'Amico et al., 2018). We then show how to use the model to decompose treasuries' Nominal Term Premium into Real TP and Inflation TP.

4.2.1 Economic Factors and Nominal Pricing

This subsection introduces the model we use to price the nominal bonds. Nominal yields are driven by three Nelson-Siegel factors - level, slope, and curvature - denoted by $X_t = [L_t, S_t, C_t]'$. The AFNS structure grants each factor clear economic meaning. The level factor captures duration risk of yield curve level shifts. The slope factor indicates the steepness of the yield curve. We interpret it as the steepener risk factor, as it characterizes the exposure to slope shifts. The curvature factor determines the hump shape of yield curves. As Large-Scale Asset Purchase (LSAP) or Quantitiative Easing (QE) mainly

focuses on the maturity 2$\sim$10 years, the curvature factor is mostly affected by monetary shocks post-crisis. Hence we interpret the curvature factor as the monetary policy risk factor.

Christensen et al. (2011) show that the AFNS structure implies that the nominal zero-coupon yield with maturity τ at time t, $y^N_{t,\tau}$, takes the analytical Nelson Siegel form,

$$y^N_{t,\tau} = 1 \cdot L_t + \frac{1 - e^{-\lambda\tau}}{\lambda\tau} S_t + \left(\frac{1 - e^{-\lambda\tau}}{\lambda\tau} - e^{-\lambda\tau} \right) C_t + a^N_\tau, \tag{4.2.1}$$

where the constant term a^N_τ is given by equation (4.A.7), and the the risk-neutral (Q) dynamics of three factors are detailed in (4.A.1) and (4.A.2) in Appendix 4.A.

Under the physical (P) measure, we assume the three state variables have the following dynamics,

$$dX_t = \kappa(\mu - X_t)dt + \Sigma dW_t, \tag{4.2.2}$$

where 3×3 matrices κ is diagonal, specified in equation (3.3.4) of Appendix 4.A.

The nominal pricing kernel takes the form,

$$dM^N_t / M^N_t = -r^N(X_t)dt - \lambda^N(X_t)' dW_t, \tag{4.2.3}$$

where the vector of nominal prices of risk, λ^N, is further assumed to be essentially affine form, $\lambda^N(X_t) = \lambda^N_0 + \Lambda^N X_t$, as suggested in Duffee (2002). Given the drift terms under P and Q measure, λ^N is uniquely determined. All technical details about the implied λ^N_0 and Λ^N are deferred to Appendix 4.A in equation (4.A.9).

4.2.2 Inflation and Real Yields

In this subsection, we present how we model the inflation dynamics so as to price real bonds. Price level is assumed to follow the log-normal process,

$$dQ_t/Q_t = r^I(X_t)dt + \sigma_q' dW_t + \sigma_q^\perp dW_t^\perp, \tag{4.2.4}$$

where the instantaneous inflation rate is linearly driven by the three risk factors, $r^I(X_t) = \rho_0^I + \rho_1^{I\prime} X_t$. The inflation innovation loads on not only shocks that drive risk factors dW_t, but also an orthogonal shock that is unspanned by yield curve dynamics $dW_t^\perp$.

At time t, a real bond paying 1 unit of the consumption basket at time T can be deemed as a nominal asset paying the price level, Q_T, upon maturity. Therefore, no-arbitrage condition requires the following linkage between the real and nominal pricing kernels,

$$M_t^R = M_t^N Q_t. \tag{4.2.5}$$

By Ito's lemma, the real pricing kernel is drived as

$$dM_t^R/M_t^R = -r^R(X_t)dt - \lambda^R(X_t)' dW_t - (\cdot)dW_t^\perp, \tag{4.2.6}$$

where $r^R(X_t) = \rho_0^R + \rho_1^{R\prime} X_t$ is the instantaneous real risk-free rate and $\lambda^R(X_t) = \lambda_0^R + \Lambda^R X_t$ is the vector of real prices of risk. The formulas of coefficients are provided in equations (4.B.4) to (4.B.7) deferred to Appendix 4.B.

As derived in Appendix 4.B, the zero-coupon real yield $y_{t,\tau}^N$ is given by

$$y_{t,\tau}^R = \rho_1^{R,1} L_t + \rho_1^{R,2} \frac{1-e^{-\lambda\tau}}{\lambda\tau} S_t + \left((\rho_1^{R,2} + \rho_1^{R,3}) \frac{1-e^{-\lambda\tau}}{\lambda\tau} - \rho_1^{R,2} e^{-\lambda\tau} \right) C_t + a_\tau^R, \tag{4.2.7}$$

where the constant term a_τ^R is given by equation (4.B.16).

4.2.3 TIPS Liquidity Effects

In this subsection, we introduce how our model takes TIPS liquidity effects into account so as to price TIPS accurately. Existing research (Gürkaynak et al., 2010; Abrahams et al., 2013; D'Amico et al., 2018; Grishchenko and Huang, 2013) presents sufficient evidences on the existences of a TIPS liquidity factor, which pushes the TIPS yield to deviate from the underlying real yield. The liquidity premium that investors demand for holding TIPS is mainly captured by the spread between the TIPS yield and the real yield as

$$L_{t,\tau} = y_{t,\tau}^{TIPS} - y_{t,\tau}^{R}. \tag{4.2.8}$$

Following D'Amico et al. (2018), we assume that the instantaneous rate investors require to price TIPS is the sum of the instantaneous real short rate and a positive spread, l_s. As a result, the liquidity risk premium can be written as,

$$L_{t,\tau} = -\frac{1}{\tau}\log E_t^Q\left(\exp\left(-\int_t^{t+\tau}(r_s^R + l_s)ds\right)\right) - y_{t,\tau}^R. \tag{4.2.9}$$

The instantaneous spread l_s is assumed to load on not only three risk factors X_t, but also a TIPS-specific factor, $\widetilde{X}_t$, i.e., $l_t = \beta' X_t + \widetilde{\beta}\widetilde{X}_t$, where $\widetilde{\beta}$ is a constant and β is a 3×1 constant vector. The TIPS-specific factor, $\widetilde{X}_t$, is assumed to be orthogonal to X_t and follow an independent Vasicek (1977) process,

$$d\tilde{x}_t = \widetilde{\kappa}(\widetilde{\mu} - \widetilde{X}_t)dt + \widetilde{\sigma}dB_t, \tag{4.2.10}$$

with $dB_t dW_t = 0_{3\times 1}$. By construction, $\widetilde{\beta}\widetilde{X}_t$ captures the TIPS-idiosyncratic component that is contemporaneous orthogonal to the systematic state variables in the economy. In the end, $\widetilde{X}_t$ is assumed to bear a market price of risk as $\tilde{\lambda}_t = \tilde{\lambda}_0 + \tilde{\lambda}_1\tilde{X}_t$.

As is detailed in Appendix 4.D, the liquidity risk premium $L_{t,\tau}$ has the form

$$L_{t,\tau} = \left[\widetilde{a}_\tau + (a_\tau^h - a_\tau^R)\right] + \begin{bmatrix} (a_\tau^h - a_\tau^R)' & \widetilde{b}_\tau \end{bmatrix} \begin{bmatrix} X_t \\ \widetilde{X}_t \end{bmatrix}. \tag{4.2.11}$$

Therefore, the TIPS yields can be computed by $y_{t,\tau}^{TIPS} = y_{t,\tau}^R + L_{t,\tau}$. We ignore the indexation lag of TIPS since D'Amico et al. (2018) demonstrate its effect is negligible. In fact, we find the indexation lag indeed makes almost no difference to our estimation results.

4.2.4 Theoretical Decomposition of Term Premium

Based on the above model, we now present how to decompose Nominal Term Premium (NTP) into Real Term Premium (RTP) and Inflation Term Premium (ITP). The Nominal TP is the compensation that investors require for bearing the risk that future path of the short-term nominal yield deviates from what they expect. At time t, τ-period NTP is measured by the spread between τ-period nominal yield, $y_{t,\tau}^N$, and the expected average future short nominal rate, $\frac{1}{\tau}E_t\left(\int_t^{t+\tau} r_s^N ds\right)$, i.e.,

$$NTP_{t,\tau} = y_{t,\tau}^N - \frac{1}{\tau}E_t\left(\int_t^{t+\tau} r_s^N ds\right). \tag{4.2.12}$$

Similarly, Real TP is the excess yield that investors require to hold a long-term real bond instead of rolling over the investments on short-term real bonds sequentially. Accordingly, Real TP is defined as,

$$RTP_{t,\tau} = y_{t,\tau}^R - \frac{1}{\tau}E_t\left(\int_t^{t+\tau} r_s^R ds\right). \tag{4.2.13}$$

We define Inflation TP as the part of Nominal TP that can not be explained by Real TP, i.e.,

$$ITP_{t,\tau} = NTP_{t,\tau} - RTP_{t,\tau}. \tag{4.2.14}$$

We now establish its relationship with the well-known concepts of Inflation Risk Premium (IRP) and Inflation Expectation (IE). The difference between the τ-period nominal yield and real yield is the so called Inflation Compensation, or Break-even Inflation (BEI), over next τ-period. The BEI can then be decomposed into IE and IRP over the same horizon, i.e.,

$$BEI_{t,\tau} = y^N_{t,\tau} - y^R_{t,\tau} = \frac{1}{\tau} E_t \left(\int_t^{t+\tau} r^I_s ds \right) + IRP_{t,\tau}. \tag{4.2.15}$$

When $\tau \to 0$, the equation (4.2.16) exhibits the relationship between instantaneous nominal rate, real rate, BEI, IE and IRP,

$$BEI_{t,0} = r^N_t - r^R_t = r^I_t + IRP_{t,0}. \tag{4.2.16}$$

Accordingly, using equations (4.2.12) to (4.2.16), we can derive the Inflation TP as

$$ITP_{t,\tau} = IRP_{t,\tau} - \frac{1}{\tau} E_t \left(\int_t^{t+\tau} IRP_{s,0} ds \right). \tag{4.2.17}$$

Therefore, Inflation TP is equal to the spread between IRP and expected future average instantaneous IRP, i.e., the term premium of IRP. As the term premium of IE is zero by design, Inflation TP can also be thought of as the term premium of Inflation Compensation or BEI.

The affine-Gaussian model provides analytical formulas to interest rate and inflation expectations, i.e., $\frac{1}{\tau} E_t \left(\int_t^{t+\tau} r^j_s ds \right) = a^j_\tau + b^{j\prime}_\tau X_t, \;\; j = N, R, I$, where the factor loadings a^j_τ and b^j_τ are detailed in Appendix 4.D. Thus we can use equations (4.2.12) and (4.2.14) to calculate Nominal, Real, and Inflation TP.

4.3 Data and Estimation Results

We start this section by introducing how we collect data and estimate the joint model. Next, we present the results about parameter estimates and overall fitting performance. Finally, to demonstrate the robustness of the estimation, we compare the filtered state variables with their observable counterparts and analyze their economic meanings by matching them with real economic events.

4.3.1 Data

Our data sample covers the period from January 1999 to November 2016. We collect nominal and TIPS zero-coupon yields with all maturities from Gürkaynak et al.(2007; 2010) (hereafter GSW) datasets which can be downloaded from the Federal Reserve Board of Governors research data page.[1]. The maturities of TIPS yields include 2, 3, 4, ..., 19, and 20 years, and those of nominal counterparts include 1, 2, 3, ..., 29, and 30 years. We expand the cross-section of nominal yields by adding 3- and 6- month yields obtained from the data website of Federal Reserve Bank of St. Louis. The huge cross-section of zero-coupon yields, which consists of 32 maturities for nominal and 19 maturities for TIPS bonds, allows us to extract full information from the yield curves. All yields are sampled at weekly frequency[2] for a total of $T = 933$ time-stamps.

We acquire monthly headline Consumer Price Index for all urban consumers (CPI-U) from the economic data website of Federal Reserve Bank of St. Louis. We choose seasonally-adjusted CPI inflation for estimation since our model does not take the seasonality into account. Because the CPI data is not released weekly, we assume CPI does not change during the same month and use monthly CPI as the observation for each week,

[1] See https://www.federalreserve.gov/pubs/feds/2006/200628/200628abs.html and https://www.federalreserve.gov/pubs/feds/2008/200805/200805abs.html.

[2] To get rid of weekend effects, we sample yields on each Wednesday. If data on Wednesday is missing, we replace it by that on Thursday or Tuesday.

without any forward-looking bias.

To reliably estimate the Nominal and Inflation Term Premium, two key datasets required to be fed into our model are short-term interest rate and inflation expectation. For the former, we use 3-month Tbill rate forecasts over the next 1 year and 10 years from the Survey of Professional Forecasters (SPF) dataset issued by the Federal Reserve Bank of Philadelphia. For the latter, we obtain 1-year inflation forecasts over the next 1, 5 and 10 years from the same dataset. The survey data is released in the middle month of each quarter. We find the exact release date for each survey and use the corresponding data as the observations for the first Wednesday following the release. Consequently, there is only one week having the professional forecasts data during each quarter. For other weeks, we set the forecasts as missing data. Among the five type of SPF data we select, all are available each quarter except for 3-month Tbill rate forecasts over the next 10 years, which are only reported every first quarter.

Another advantage of feeding the forecasts data into our model is that it helps to overcome the "small-sample problem", which means typical data sample used in a dynamic term structure estimation, for example, 5 to 15 years, results in unreliable estimate of physical dynamics of interest rate due to the trouble of observing a sufficient number of "mean-reversions". As suggested by Kim and Orphanides (2012), the supplement of the survey forecasts data of 3-month Tbill rates provides additional relevant information to effectively stabilize the estimation and pin down the P parameters.

To investigate the underlying drivers behind each component of treasury term premium, we collect a series of economic data, ranging from fundamental information to international capital flows. We obtain weekly crude oil price by sampling the West Texas Intermediate (WTI) index on each Wednesday from the economic data website of Federal Reserve Bank

of St. Louis. We use JPY cross-currency basis (JYBS) to measure Japanese investors' $-hedging demand. The daily data of JYBS from 2012 to 2016 is collected from Bloomberg[3]. In addition, we obtain monthly Japanese treasury holding data in 2016 from the home page of Treasury International Capital (TIC) System[4].

4.3.2 Estimation Strategy

As detailed in Appendix 4.E, our joint model is reorganized as a state-space model, which can be estimated by maximum likelihood methodology using the Kalman Filter. With 29 model parameters and 9 observation standard errors, the state-space model includes a 5-dimension state transition equation and a 57-dimension observation equation. The large cross-section and time series of observations help to pin down parameters. We use a sufficient set of starting values for robustness checks to ensure the parameters we estimate arrives at the global optimum.

Survey forecasts and 2-, 3-, and 4-year TIPS yields are not available for each week during our sample period, which results in missing data in the observation equation. In order to handle this issue, we allow the dimension of the observation equation matches the actual number of observations at each time (see section 3.4.7 of Harvey (1989) for details). For identification purpose, we impose some standard non-negative constraints on κ_{11}, κ_{22}, κ_{33}, $\tilde{\kappa}$, and λ. In addition, We normalize $\widetilde{\sigma}$ to be equal to 0.01.

4.3.3 Parameter Estimates and Model Fit

Table 4.1 presents the log likelihood, estimated parameters and standard errors for our model. Most of parameters driving the dynamics of nominal yields, inflation and TIPS

[3]The corresponding Ticker is JYBSC.

[4]See https://www.treasury.gov/resource-center/data-chart-center/tic/Pages/index.aspx.

yields are significant at 1% level, which suggests our model is easy to be identified using the large cross-sectional data.

To assess the fitting performance of our model, in Figure 4.7 to Figure 4.9, we plot the actual and fitted nominal yields, TIPS yields and survey forecasts. The root mean square of errors (RMSE) are shown in the upper right corner of each plot. The first number is the RMSE (in bps) for the sample period excluding the last half-year, while the second number is the RMSE (in bps) for last 26 weeks, which helps us to evaluate the recent fitting performance of our model out-of-sample. These figures show that our model exhibits quite well overall fitting performance given a large cross section of treasury yields for simultaneous estimation. For nominal and TIPS yields, one noticeable aspect is that as the maturity increase, the yields are more likely fitted with less pricing errors, which complies with the error structures we impose (see equation (4.E.4) and (4.E.5)) and the fact that short-term yields are more difficult to obtain decent fitting performance by Nelson-Siegel structures. We find our model fit TIPS yields with maturities larger than 5 years very well. Most of them have RMSE less than 3bps, which indicates the necessity of including TIPS liquidity factor into the model.

In Figure 4.9, we investigate how closely the model-implied inflation and short rate expectation mimic survey-based counterparts. As a real-time, model-free measure, survey forecasts data contain useful information for future dynamics and outperform the other forecasting methods including the term structure specification (Ang et al., 2007). A visual comparison between the model-implied expectations and survey-based counterparts show that our model capture the majority of information in survey forecasts. They exhibit the same overall trends over the sample period and the pricing errors are fairly small given the large noise and dispersion in survey forecasts.

4.3.4 Robustness Check and Factor Economic Meanings

In this subsection, we design two ways to demonstrate the robustness of our estimation results. The first way is to compare whether the filtered state variables have similar dynamics with their observable counterparts. The second way is to analyze their economic meanings by matching them with real economic events.

Figure 4.3 shows the dynamics of model-implied duration, steepener, monetary policy, and TIPS liquidity risk factors. In the upper left panel, the empirical level factor, 30-year treasury yield, is plotted to be compared with model-implied duration risk factor. The upper right panel plots both model-implied steepener risk and empirical slope factor, 3-month minus 30-year nominal yields. The filtered factors are in line with its empirical observables, which suggests the estimates are quite robust.

The monetary policy risk factor shown in the lower left panel is striking as its dynamics is thoroughly affected by monetary policies of major central banks in the world. Starting from November 2008, Fed undertook a form of "unconventional" monetary policy, LSAP, in three waves, commonly referred as QE1 (announced in late November 2008), OE2 (announced in November 2010), and QE3 (announced in September 2012). Correspondingly, from late 2008 to early 2013, the monetary factor dropped continuously, as the large purchase of $2\sim10$ years treasury bonds put down pressure on middle-term yields. However, in mid 2013, there was a sharp reversal of the monetary factor. During that period, Fed Chairman Ben Bernanke announced that Fed may taper the size of QE (Taper Tantrum), which imposed upward pressure on middle-term yields. In January 2015, European Central Bank also launched the asset purchase program. Afterwards European investors' capital inflows to UST drove a big drop of the curvature of yield curve in the first half of 2015. In January 2016, the Bank of Japan imposed the Negative Interest Rate Policies, which pushes another sharp decline of the curvature. All these major monetary events are fully priced in our monetary factor.

The lower right panel plots the TIPS liquidity factor, which captures the historical variation of illiquidity of TIPS market. The high level of liquidity risk factor in the beginning of the sample indicates the illiquidity of TIPS when they were just issued to the market. Its downward trend afterwards till 2004 reflects TIPS liquidity kept improving during this period. The sharp surge of the factor around 2009 suggests TIPS liquidity evaporated during the financial crisis. While the recent upward trend of the factor reflects that illiquidity of TIPS market has been exacerbated by banking regulations after the pass of the Dodd-frank Act.

The analysis of monetary policy and TIPS liquidity factors indicates that they have clear economic identification, which also illustrates the robustness of our model.

4.4 Empirical Decomposition of Treasury Term Premium

In this section, we conduct three layers of decompositions to understand the economic drivers behind treasury term premium. In 4.1, we conduct the first layer of decomposition, which is to break Nominal TP into Real TP and Inflation TP, by which we find Real TP has the main contribution to negative treasury term premium. In addition, we document the highly significant causality between oil price and Inflation TP. In 4.2, the second layer of decomposition is conducted to show that Real TP are mainly compensating for duration risk and monetary policy risk. In 4.3, we further delve into the underlying drivers of the duration factor.

4.4.1 Layer 1: Which TP Is The Major Driver of Nominal TP?

In this subsection, we decompose Nominal TP into Inflation TP and Real TP to examine which component drove most variations of Nominal TP and hence is the major contributor of the negative treasury term premium in 2016. In addition, we demonstrate that the main driver behind Inflation TP is oil price.

Figure 4.4 shows the dynamics of 10-year Nominal TP, Real TP and Inflation TP, which are indicated by blue, red, and black lines, respectively. We find that Nominal TP has much greater co-movement with Real TP rather than Inflation TP. Compared with Real TP, Inflation TP is a slow-moving component. During the first half of 2016, 10-year Nominal TP dropped 60bps. We find this dramatic decline was due to a fall in the Real TP, which dropped 50bps, while Inflation TP only moved 10bps.

Although Real TP is identified as the main contributor for variations of Nominal TP, before we move to the second layer of decomposition, we are eager to figure out the mechanism behind the movement of Inflation TP, which is an important economic indicator of uncertainty about future inflation. If Inflation TP is positive, investors demand compensation for bearing future inflation risk, while if it is negative, investors pay premium for hedging future deflation risk. Figure 4.4 shows Inflation TP remains positive or close to zero for most of periods before the financial crisis, while negative for majority of time after the crisis, especially after July 2011. This indicates investors' concern about deflation risk during recent five years. After Mr. Donald Trump was elected as the new US president on November 8, 2016, Inflation TP experienced a salient spike, reflecting investors' expectation that Trump's economic policies would stimulate inflation and Fed would raise fed funds rate in the future.

Lots of studies estimate Inflation Risk Premium (IRP) and inflation expectation (IE) with or without information in the TIPS market (i.e., Ang et al., 2008; Gürkaynak et al., 2010; Christensen et al. (2010); Haubrich et al., 2012; D'Amico et al., 2018). However, few of this studies document the economic drivers behind them. A recent study by Wong (2015) confirms IE is sensitive to oil price shock by using regression methods. Perez-Segura and Vigfusson (2016) establish the relationship between changes in TIPS Break-even Inflation (BEI)[5] and oil prices. These research enlighten us that oil price may be an potential driver

[5]TIPS BEI is defined as TIPS yield minus nominal yield, while BEI is defined as real yield minus nominal yield. Therefore, TIPS BEI equals BEI minus TIPS liquidity risk premium. TIPS BEI is an empirical

for IRP as well as Inflation TP.

To test oil shocks on Inflation TP before and after the financial crisis, we conduct the following regression as shown in Table 4.2. Let 1_{Post} be the post-crisis dummy variable that is 0 before December 2007 and 1 afterwards. We run the following regression,

$$\Delta Y_t = \gamma_0 + \gamma_1 \Delta \left(\ln WTI_t \right) + \gamma_2 1_{Post} + \gamma_3 \Delta \left(\ln WTI_t \right) \cdot 1_{Post} + \epsilon_t, \tag{4.4.1}$$

where Y_t is IE, IRP or Inflation TP for 5-, 10- or 30- years. Our interest is the coefficient of the interaction term $\Delta \left(\ln WTI_t \right) \cdot 1_{Post}$, which identifies the effect of post-crisis shocks of oil price change. For each regression, Newey-West standard errors with six lags are reported. Table 4.2 shows that all regressions obtain significantly positive coefficient of the interaction term at level 1%, which suggests a stronger effect of oil price on Inflation TP. According to the estimated coefficients, if log oil price decrease by 1%, the implied Inflation TP over 5-, 10-, and 30-year horizons dropped 0.07 bps, 0.11 bps and 0.24 bps, respectively. Simply put, we find sufficient evidences that Inflation TP have been mainly driven by oil price after financial crisis.

4.4.2 Layer 2: What Risk Is Real TP Compensating for?

The second layer of decomposition is to decipher what exact risk real TP is compensating for. Figure 4.5 decomposes the real TP, plotted in purple, into the three risk factors. First, the steenpener factor's contribution is almost zero over time, meaning this factor is not priced at all in Real TP. This result is not surprising as the slope is mostly about rates expectation rather than term premium. By symmetry, it makes sense that investors price zero premium for steepener/flattener risks. Regarding the two other factors, duration is priced with significantly positive risk price, as investors demand premium for bearing duration risk. Monetary factor on the other hand, is priced with significantly negative risk

approximation of BEI.

price, as central banks are willing to pay to lower TP, so as to stimulate investments and consumptions during recessions. If we zoom in to the dynamics in early 2016, we can see that real TP dropped around 50bps from peak to trough, where 25bps was coming from the monetary factor, and the other 25bps was contributed by duration factor.

The biggest monetary event happened in late January 2016 was Bank of Japan's Negative Interest Rate Policies (BoJ NIRP). It was the first time in history that a central bank pushes policy rate to negative zone. Although the initial move was only 0.1%, NIRP caught most market participants off guard. This monetary shock quickly spread across global bond yields, as European investors also started to worry about NIRP (although ECB was still under ZIRP). From our term premium decomposition, we can see a salient slump of the monetary factor on the NIRP announcement date, which is clearly unrelated to US fundamentals.

More interestingly, the 25bps duration move in early 2016 was at the same magnitude as the monetary shock, which is very sizeable. So now our question refines to what drove duration move at the time when there're no fundamental shocks to either US growth or inflation. This seems like a puzzle.

4.4.3 Layer 3: What Drove Duration in 2016?

The answer is revealed by the striking co-movement between duration and JPY cross-currency basis (JYBS), as shown earlier in Figure 4.2. Cross-currency basis measures foreign investors' $-hedging demand, which is to hedge $-asset purchases so as to reduce currency exposure. As treasury yield was commoving up and down along with cross-currency basis, it means that the $-asset they purchased was presumably US Treasury. Japan has become the largest holder of UST since late 2016, according to TIC monthly foreign holding releases. The two major players are Japanese banks and life insurers, who usually get rid of currency exposure by trading JYBS. So when Japanese treasury purchase

increases, hedging demand cranks up JYBS (more negative) and the treasury inflow pushes down yields. Therefore, JYBS serves as a perfect instrument to measure Japanese $-inflows to the treasury markets. In terms of maturities, Japanese investors usually focus on 10y treasury. They're not interested in 5y because the hedging cost is higher than 5y treasury yields. They're also not interested in 30y UST because Japanese Government Bond (JGB) 30y yields have always been positive, so it makes more sense to purchase 10y UST as 10y JGB had negative yields in 2016. If we regress UST 10y yield daily changes on JYBS daily changes over the past five years, the coefficient is significantly positive with Newey-West $t - stat = 2.10$. Quantitatively speaking, when JYBS widens 10bps (becomes more negative), Japanese inflows push down UST 10y yields by around 1.7bps.

$$\Delta Tsy10_t = -0.0005 + 0.1703\Delta JYBS_t + \epsilon_t.$$

In order to make sure Japanese flows' price impact is not through other indirect transmission mechanism, Figure 4.6 plots Japanese Treasury Holdings (source from TIC) versus 10y UST yields. In order to tease out clean demand impacts other than fundamental shifts, we use the trick of 5-10-30 fly[6] to track flows on 10y, as fly hedges out level & slope shifts by design. The massive Japanese inflows in early 2016 were due to investors' reach-for-yield after BoJ's NIRP announcement. The outflows in July[7] 2016 were triggered by $-liquidity squeeze due to the Money Market Reform. Figure 4.2 & 4.6 demonstrate that foreign flows play a central role in driving treasury yields. The deep-dive of treasury term premium to negative zone in early 2016 and its sharp reversal in summer 2016 was not about US fundamental shocks, but largely due to foreign flows. Structural models focusing on local US macro variables unfortunately won't be able to capture the fine structure of term premium dynamics. Therefore, the main takeaway of this paper is that the information

[6]The results for 10y raw yields are very similar.

[7]July was the last month to issue 3m CD/CP before the Oct Reform.

contents of treasury term premium go beyond US fundamentals.

4.5 Two Extended Models vs. Benchmark

In this section, we estimate two versions of extended models - one with a local macro factor, and one with a foreign demand measure. The former speaks to the strand of literature tracing back to Ang and Piazzesi (2003), while the latter is to incorporate the modern frictional view on supply-demand effects on asset prices (Greenwood and Vayanos, 2014; Krishnamurthy and Vissing-Jorgensen, 2011).

We follow the macro-term-structure literature to augment the latent Nelson-Siegel factors with an extra observable state variable. The first extended model adds Chicago Fed National Activity Index (CFNAI) as a US real-growth factor. CFNAI is a weighted average of 85 monthly indicators of US national economic activities drawn from four broad categories of data: production and income; employment, unemployment and hours; personal consumption and housing; and sales, orders and inventories. We use CFNAI to augment the CPI growth rate already incorporated in the benchmark model, so that the model captures observable shocks to both US real growth and inflation. In later discussions, we call this version "the extended model with US macro".

The second extended model adds JPY Cross-currency Basis (JYBS) as a foreign institutional demand factor. JYBS measures foreign demand [8] from both carry trades and cross-border real investments / corporate issuances hedging demand. The importance of its role has been clearly illustrated in Figure 4.2 and explained in subsection 4.4.3. In classical asset pricing theory, demand typically plays no role for no-arbitrage models. However, modern literature on institutional demand (Koijen et al., 2016; Greenwood and Vayanos, 2014) emphasizes its price impacts in real world due to frictions. So this "extended model

[8]Note that European demand is also priced in JYBS through no-arbitrage. Otherwise one can always swap Euro to JPY and then to USD.

with foreign demand" aims to test the key channel.

The reduced-form extension by adding a fourth factor to the same Gaussian Affine Term Structure framework is trivial technically. One nice thing about the extended model with foreign demand is that it could be endogenized by backward engineering an appropriate supply loading structure as in Vayanos and Vila (2009). So our reduced-form extended model with foreign demand is equivalent to a structural frictional model with preferred-habitat demand.

In order to judge whether the two extended models beat the benchmark Nelson-Siegel model, we compare their out-of-sample fitting performance (2015-2017) in Figure 4.10[9]. As one may expect following the discussions in subsection 4.4.3, the extended model with foreign demand dominates the other models on maturities longer than 10y, especially for the longend where it beat the benchmark model by 65demand plays a central role in driving treasury long-end in recent years due to monetary divergence. Interestingly, both extended models fail to outperform the benchmark on the short-end, meaning duration, steepener and monetary factors have already absorbed the macro information and foreign demand plays little role on short maturities. Recall that U-hedged US Treasury (UST) actually has lower yield (after hedging cost) than Japanese Government Bonds (JGB) for maturities shorter than 5y since 2016, as shown in Figure 4.11.

The nominal TP decomposition of the two extended models into real and inflation TP are very similar to Figure 4.4. However, the real TP factor attribution is quite different from Figure 4.5. Figure 4.12 plots the estimated decomposition of real TP into factors for the two extended models. In the left subfigure, we can see that the US macro factor cranks up real TP during the crisis due to high real uncertainty in 08-09. Yet this macro factor has been very stable after 2010, explaining little term premium variations since then. In the right subfigure, on the contrary, the foreign demand factor crushed real TP both during the

[9]CFNAI releases monthly. To make it comparable, we re-estimate the benchmark model as well as the two extended models using in-sample month-end data from January 1999 to January 2015.

crisis and in recent years. This international component works through the inflow channel via either flight-to-quality or reach-for-yield due to monetary divergence. According to our estimates shown in the right subfigure, the recent negative term premium is presumably linked to the foreign inflows thanks to the Zero Interest Rate Policies in Europe and Japan. Therefore, the main insight from this extension exercise is that foreign demand has been a key source of friction driving mid/long-end of treasury curves, while adding US-local macro factors would have little help in explaining the negative term premium puzzle in 2016.

4.6 Conclusions

Traditional structural term structure models often focus on US local macro state variables, which implicitly assumes that treasury term premium variations are mostly driven by US fundamentals. This paper delves into its fine structure and challenges this conventional wisdom by demonstrating that the information contents of treasury term premium is far richer than just US growth and inflation.

In order to show the full picture, we decompose treasury TP carefully layer by layer. The first layer of decomposition reveals that Inflation TP only accounts for a minority of Nominal TP variations and it's highly correlated with global oil prices. The second layer further decomposes Real TP into intuitive term structure factor risks: duration is priced with positive risk price, monetary factor has negative risk price, and yet steepener risk is barely priced. Finally, in the third layer, we further decipher the driver of the biggest risk factor (duration) and use cross-currency basis as a perfect instrument to measure foreign demand.

As a direct empirical application, our model resolves the negative term premium puzzle on why TP dropped an astonishing 60bps in early 2016 while Fed was actually in a tightening cycle. We demonstrate that Bank of Japan's NIRP and Japanese investors'

reach-for-yield were the true drivers which crushed 10y treasury term premium by around 50bps.

Simply put, treasury term premium is priced with rich information about monetary divergence, foreign demand as well as global oil price, which may not be embedded in US fundamental macro variables. This poses challenges to conventional structural macro term structure models where the above information is typically ignored.

Appendix

4.A State Variables, Nominal Pricing Kernel and Nominal Yields

The AFNS model assumes the level (duration risk), slope (steepener risk), and curvature (monetary policy risk) factors follows a multivariate Gaussian process under Q measure,

$$dX_t = \kappa^Q(\mu^Q - X_t)dt + \Sigma dW_t^Q, \tag{4.A.1}$$

where W_t^Q is an 3×1 vector of standard Brownian motion. 3×1 constant vector, μ^Q, κ^Q, and Σ are specified as,

$$\kappa^Q = \begin{bmatrix} 0 & 0 & 0 \\ 0 & \lambda & -\lambda \\ 0 & 0 & \lambda \end{bmatrix}, \mu^Q = \begin{bmatrix} 0 \\ 0 \\ 0 \end{bmatrix}, \Sigma = \begin{bmatrix} \sigma_{11} & 0 & 0 \\ \sigma_{12} & \sigma_{22} & 0 \\ \sigma_{13} & \sigma_{23} & \sigma_{33} \end{bmatrix}. \tag{4.A.2}$$

The AFNS model assumes the instantaneous nominal risk-free rate, $r^N(X_t)$, is the sum of the duration and steepener factors. Hence $r^N(X_t) = \rho_0^N + \rho_1^N X_t$, where $\rho_0^N = 0$ and $\rho_1^N = [1, 1, 0, 0]'$. Christensen et al. (2011) show that this structure implies that nominal zero-coupon yields with maturity τ at time t, $y_{t,\tau}^N$, take the analytical Nelson-Siegel form. In particular, the zero-coupon nominal bond prices are given by $P_{t,\tau}^N = E_t^Q\left(\exp\left(-\int_t^{t+\tau} r_s^N ds\right)\right) = \exp\left(A_\tau^N + B_\tau^{N\prime} X_t\right)$, where $B_\tau^N = [B_\tau^{N,1}, B_\tau^{N,2}, B_\tau^{N,3}]'$ is the vector of loadings on state variables and takes the form,

$$B_\tau^{N,1} = -\tau, \tag{4.A.3}$$

$$B_\tau^{N,2} = -\frac{1-e^{-\lambda\tau}}{\lambda}, \tag{4.A.4}$$

$$B_\tau^{N,3} = \tau e^{-\lambda\tau} - \frac{1-e^{-\lambda\tau}}{\lambda}, \tag{4.A.5}$$

and the constant term

$$A_\tau^N = \frac{1}{2}\int_0^\tau B_s^{N\prime}\Sigma\Sigma' B_s^N ds. \tag{4.A.6}$$

Therefore, nominal yields take the Nelson Siegel form, $y_{t,\tau}^N = -\frac{1}{\tau}\log\left(P_{t,\tau}^N\right) = a_\tau^N + L_t + \frac{1-e^{-\lambda\tau}}{\lambda\tau}S_t + \left(\frac{1-e^{-\lambda\tau}}{\lambda\tau} - e^{-\lambda\tau}\right)C_t$, where the constant term[10],

$$a_\tau^N = -\frac{1}{2\tau}\int_0^\tau B_s^{N\prime}\Sigma\Sigma' B_s^N ds. \tag{4.A.7}$$

In the P dynamics of nominal state variables shown in equation (4.2.2), 3×3 constant matrices κ and 3×1 constant vector μ are specified as

$$\kappa = \begin{bmatrix} \kappa_{11} & 0 & 0 \\ 0 & \kappa_{22} & 0 \\ 0 & 0 & \kappa_{33} \end{bmatrix},\ \mu = \begin{bmatrix} \mu_1 \\ \mu_2 \\ \mu_3 \end{bmatrix}. \tag{4.A.8}$$

Here we assume the diagonal structure for κ for the purpose of parsimony.

Given the essentially affine form of nominal market price of risk, $\lambda^N(X_t) = \lambda_0^N + \Lambda^N X_t$, and the relation between drift terms of Q and P dynamics, $\kappa^Q(\mu^Q - X_t) + \Sigma\lambda^N(X_t) = \kappa^P(\mu^P - X_t)$, the implied λ_0^N and Λ^N are derived as,

$$\lambda_0^N = \Sigma^{-1}(\kappa^P\mu^P - \kappa^Q\mu^Q),\ \Lambda^N = \Sigma^{-1}(\kappa^Q - \kappa^P). \tag{4.A.9}$$

[10]For analytical form, see Appendix 4.B of Christensen et al. (2011).

4.B Real Pricing Kernel and Real Yields

Using equations (4.2.3), (4.2.4), and applying Ito's lemma to equation (4.2.5), we derive the real pricing kernel as,

$$\begin{aligned} dM_t^R/M_t^R &= dM_t^N/M_t^N + dQ_t/Q_t + (dM_t^N/M_t^N)\cdot(dQ_t/Q_t) \\ &= -r^R(X_t)dt - \lambda^R(X_t)'dW_t - (\cdot)dW_t^{\perp}, \end{aligned} \tag{4.B.1}$$

where the real short rate takes the form

$$r^R(X_t) = \rho_0^R + \rho_1^{R\prime} X_t, \tag{4.B.2}$$

the real prices of risk takes the form

$$\lambda^R(X_t) = \lambda_0^R + \Lambda^R X_t, \tag{4.B.3}$$

and the coefficients are determined by their nominal counterparts by

$$\rho_0^R = \rho_0^N - \rho_0^I + \lambda_0^{N\prime}\sigma_q, \tag{4.B.4}$$

$$\rho_1^R = \rho_1^N - \rho_1^I + \Lambda^{N\prime}\sigma_q, \tag{4.B.5}$$

$$\lambda_0^R = \lambda_0^N - \sigma_q, \tag{4.B.6}$$

$$\Lambda^R = \Lambda^N. \tag{4.B.7}$$

Following Duffie and Kan (1996) and Dai and Singleton (2000), the closed-form solution for the $\tau-$maturity zero-coupon real bond at time t is $P_{t,\tau}^R = E_t^Q\left(\exp\left(-\int_t^{t+\tau} r_s^R ds\right)\right)$

$= \exp(A_\tau^R + B_\tau^{R\prime} X_t)$, where

$$\frac{dA_\tau^R}{d\tau} = -\rho_0^R + B_\tau^{R\prime}(\kappa\mu - \Sigma\lambda_0^R) + \frac{1}{2} B_\tau^{R\prime}\Sigma\Sigma' B_\tau^R, \tag{4.B.8}$$

$$\frac{dB_\tau^R}{d\tau} = -\rho_1^R - (\kappa + \Sigma\Lambda^R)' B_\tau^R, \tag{4.B.9}$$

with initial conditions $A_0^R = 0$ and $B_0^R = 0_{3\times 1}$.

Based on equation (4.B.7), we have $\kappa + \Sigma\Lambda^R = \kappa + \Sigma\Lambda^N = \kappa^Q$, so the ODE system (4.B.9) can be written as

$$\begin{pmatrix} \frac{dB_\tau^{R,1}}{d\tau} \\ \frac{dB_\tau^{R,2}}{d\tau} \\ \frac{dB_\tau^{R,2}}{d\tau} \end{pmatrix} = \begin{pmatrix} \rho_1^{R,1} \\ \rho_1^{R,2} \\ \rho_1^{R,2} \end{pmatrix} - \begin{pmatrix} 0 & 0 & 0 \\ 0 & \lambda & 0 \\ 0 & -\lambda & \lambda \end{pmatrix} \begin{pmatrix} B_\tau^{R,1} \\ B_\tau^{R,2} \\ B_\tau^{R,2} \end{pmatrix}. \tag{4.B.10}$$

One can easily check that the unique solution that satisfy this ODE system and its initial conditions is,

$$B_\tau^{R,1} = -\rho_1^{R,1}\tau, \tag{4.B.11}$$

$$B_\tau^{R,2} = -\rho_1^{R,2}\frac{1 - e^{-\lambda\tau}}{\lambda}, \tag{4.B.12}$$

$$B_\tau^{R,3} = \rho_1^{R,2}\tau e^{-\lambda\tau} - (\rho_1^{R,2} + \rho_1^{R,3})\frac{1 - e^{-\lambda\tau}}{\lambda}, \tag{4.B.13}$$

and the constant term,

$$A_\tau^R = -\rho_0^R\tau + \int_0^\tau B_s^{R\prime}(\kappa\mu - \Sigma\lambda_0^R)ds + \frac{1}{2}\int_0^\tau B_s^{R\prime}\Sigma\Sigma' B_s^R ds. \tag{4.B.14}$$

Finally, real yields therefore take the affine form,

$$\begin{aligned} y^R_{\{t,\tau\}} &= -\frac{1}{\tau}\log\left(P^R_{t,\tau}\right) \\ &= a^R_\tau + \rho^{R,1}_1 L_t + \rho^{R,2}_1 \frac{1-e^{-\lambda\tau}}{\lambda\tau} S_t + \left((\rho^{R,2}_1 + \rho^{R,3}_1)\frac{1-e^{-\lambda\tau}}{\lambda\tau} - \rho^{R,2}_1 e^{-\lambda\tau}\right) C_t, \end{aligned} \tag{4.B.15}$$

where

$$a^R_\tau = \rho^R_0 - \frac{1}{\tau}\int_0^\tau B^{R\prime}_s(\kappa\mu - \Sigma\lambda^R_0)ds - \frac{1}{2\tau}\int_0^\tau B^{R\prime}_s \Sigma\Sigma' B^R_s ds. \tag{4.B.16}$$

The analytical formula for a^R_τ can be derived in a similar way to Appendix 4.B of Christensen et al. (2011).

4.C TIPS Liquidity Risk Premium

The TIPS yield is given by

$$\begin{aligned} y^{TIPS}_{t,\tau} &= -\frac{1}{\tau}\log E^Q_t\left(\exp\left(-\int_t^{t+\tau}(r^R_s + l_s)ds\right)\right) \\ &= -\frac{1}{\tau}\log E^Q_t\left(\exp\left(-\int_t^{t+\tau}\widetilde{\beta}\widetilde{X}_s ds\right)\right) \\ &\quad -\frac{1}{\tau}\log E^Q_t\left(\exp\left(-\int_t^{t+\tau}(\rho^R_0 + (\rho^R_1 + \beta)' X_S)ds\right)\right). \end{aligned} \tag{4.C.1}$$

Based on the property of one-factor Vasicek model, the first component is derived to be

$$-\frac{1}{\tau}\log E^Q_t\left(\exp\left(-\int_t^{t+\tau}\widetilde{\beta}\widetilde{X}_s ds\right)\right) = \widetilde{a}_\tau + \widetilde{b}_\tau \widetilde{X}_t, \tag{4.C.2}$$

in which

$$\widetilde{a}_\tau = \left(\widetilde{\mu}^*\widetilde{\beta} - \frac{\widetilde{\beta}^2\widetilde{\sigma}^2}{2\widetilde{\kappa}^{*2}}\right)\left(1 - \frac{\widetilde{b}_\tau}{\widetilde{\beta}}\right) + \frac{\widetilde{\sigma}^2\tau}{4\widetilde{\kappa}^*}\widetilde{b}_\tau, \tag{4.C.3}$$

$$\widetilde{b}_\tau = \widetilde{\beta}\frac{1 - \exp(\text{-}\widetilde{\kappa}^*\tau)}{\widetilde{\kappa}^*\tau}. \tag{4.C.4}$$

Here, the risk-neutral $\widetilde{\mu}^*$and $\widetilde{\kappa}^*$ are given by

$$\widetilde{\mu}^* = (\widetilde{\kappa}\widetilde{\mu} - \widetilde{\sigma}\widetilde{\lambda}_0)/\widetilde{\kappa}^*, \quad \widetilde{\kappa}^* = \widetilde{\kappa} + \widetilde{\sigma}\widetilde{\lambda}_1. \tag{4.C.5}$$

The second component takes the form

$$-\frac{1}{\tau}\log E_t^Q\left(\exp\left(-\int_t^{t+\tau}(\rho_0^R + (\rho_1^R + \beta)')ds\right)\right) = a_\tau^h + b_\tau^{h\prime}X_t, \tag{4.C.6}$$

where a_τ^h and b_τ^h can be derived through replacing ρ_1^R to $\rho_1^R + \beta$ in equations (4.B.11) to (4.B.15).

Taken all together, we have

$$\begin{aligned} L_{t,\tau} &= y_{t,\tau}^{TIPS} - y_{t,\tau}^R \\ &= (\widetilde{a}_\tau + a_\tau^h) + \begin{bmatrix} b_\tau^{h\prime} & \widetilde{b}_\tau \end{bmatrix}\begin{bmatrix} X_t \\ \widetilde{X}_t \end{bmatrix} - a_\tau^R - b_\tau^{R\prime}X_t \\ &= \left[\widetilde{a}_\tau + (a_\tau^h - a_\tau^R)\right] + \begin{bmatrix} (b_\tau^h - b_\tau^R)' & \widetilde{b}_\tau \end{bmatrix}\begin{bmatrix} X_t \\ \widetilde{X}_t \end{bmatrix}. \end{aligned} \tag{4.C.7}$$

4.D Interest Rate and Inflation Expectation

As instantaneous nominal, real, and inflation rates all linearly load on state variables, given the explicit conditional expectation of future state variables in Vasicek model,

$$E_t\left(X_{t+\tau} \mid X_t\right) = \mu + e^{-\kappa\tau}\left(X_t - \mu\right),$$

the closed-form formulas of the expected future rates can be derived as,

$$\frac{1}{\tau}E_t\left(\int_t^{t+\tau} r_s^j ds\right) = a_\tau^j + b_\tau^{j\prime} X_t, \;\; j = N, R, I, \tag{4.D.1}$$

where the factor loadings a_τ^j and b_τ^j are given by

$$a_\tau^j = \rho_0^j + \frac{1}{\tau}\rho_1^{j\prime}\int_0^\tau \left(I - e^{-\kappa s}\right)\mu ds, \tag{4.D.2}$$

$$b_\tau^j = \frac{1}{\tau}\int_0^\tau e^{-\kappa' s}\rho_1^j ds. \tag{4.D.3}$$

4.E The Linear State-Space Form and the Kalman Filter

Let $q_t = \log Q_t$. By applying Ito's lemma to the equation (4.2.4), the log price level is given by

$$dq_t = \left(r^I(X_t) - \frac{1}{2}\left(\sigma_q{}'\sigma_q + \sigma_q^{\perp 2}\right)\right)dt + \sigma_q' dW_t + \sigma_q^\perp dW_t^\perp. \tag{4.E.1}$$

Denoted by $x_t = [q, X_t, \widetilde{X}_t]'$, the state vector in the state-space model includes the log price level, three systematic state variables and one TIPS-specific factor. Expressed as the Euler discretization of equations (4.A.1), (4.E.1), and (4.2.10), the state equation takes the form

$$x_t = A_h + B_h x_{t-h} + \varepsilon_t, \tag{4.E.2}$$

where

$$A_h = \begin{bmatrix} \left(\rho_0^I - \frac{1}{2}\left(\sigma_q{}'\sigma_q + \sigma_q^{\perp 2}\right)\right)h \\ \kappa\mu h \\ \tilde{\kappa}\mu h \end{bmatrix}, \; B_h = \begin{bmatrix} 1 & \rho_0^{I\prime}h & 0 \\ 0_{3\times 1} & (I_{3\times 3} - \kappa h) & 0_{1\times 3} \\ 0 & 0_{1\times 3} & 1 - \tilde{\kappa}h \end{bmatrix},$$

$$\text{and } \varepsilon_t = \begin{bmatrix} \sigma_q{}' & \sigma_q^{\perp} & 0 \\ \Sigma & 0 & 0_{3\times 1} \\ 0_{1\times 3} & 0 & \tilde{\sigma} \end{bmatrix} h\epsilon_t,\ \epsilon_t \sim N(0, I_{5\times 5}).$$

As we sample data at weekly frequency, h is set to be 1/52. We denote the series of nominal yields as $Y_t^N = \{y_{t,\tau_i}^N\}_{i=1}^{32}$, the series of TIPS yields as $Y_t^{TIPS} = \{y_{t,\tau_i}^{TIPS}\}_{i=1}^{19}$, the series of inflation forecasts as $IE_t = \{IE_{t,\tau_i}\}_{i=1}^{3}$, and the series of 3-month Tbill rate forecasts as $TE_t = \{TE_{t,\tau_i}\}_{i=1}^{2}$. Then the observable vector is written as $y_t = [q_t, Y_t^N, Y_t^{TIPS}, IE_t, TE_t]'$. Assuming all observable variables are observed with Gaussian error, we write the observation equation as,

$$y_t = C + Dx_t + \eta_t, \tag{4.E.3}$$

where

$$C = \begin{bmatrix} 0 \\ a^N \\ a^{TIPS} \\ a^{IE} \\ a^{TE} \end{bmatrix},\ D = \begin{bmatrix} 1 & 0_{1\times 3} & 0 \\ 0_{32\times 1} & b^{N\prime} & 0_{32\times 1} \\ 0_{19\times 1} & b^{TIPS\prime} & \\ 0_{3\times 1} & b^{IE\prime} & 0_{3\times 1} \\ 0_{2\times 1} & b^{TE\prime} & 0_{2\times 1} \end{bmatrix},\ \text{and } \eta_t = \begin{bmatrix} 0 \\ \eta_t^N \\ \eta_t^{TIPS} \\ \eta_t^{IE} \\ \eta_t^{TE} \end{bmatrix}.$$

Ignoring the measurement errors, the model has 29 unknown parameters. In the 57-dimension observation equation, 56 observable variables are observed with error. If we assume an i.i.d structure for the all measurement errors, the number of parameters would increase to 85, which magnifies the difficulty of parameter estimation. In order to overcome

this issue, we use the cross-sectional measurement error structures for Y_t^N and Y_t^{TIPS} as

$$\eta_{t,\tau_i}^N \sim N\left(0, \delta_{\tau_i}^{N\,2}\right), \text{ with } \delta_{\tau_i}^N = \exp(\log(0.0015 - \alpha_1 - \gamma_1\tau_i)), \tag{4.E.4}$$

$$\eta_{t,\tau_i}^{TIPS} \sim N\left(0, \delta_{\tau_i}^{TIPS\,2}\right), \text{ with } \delta_{\tau_i}^{TIPS} = \exp(\log(0.0015 - \alpha_2 - \gamma_2\tau_i)), \tag{4.E.5}$$

where α_i and β_i ($i = 1, 2$) are positive. These structures conform to the fact that compared with long-term counterparts, short-term yields are more difficult to obtain decent fitting performance by Gaussian affine model. In addition, the standard deviations of all errors are bounded by 15bps.

For survey forecasts, the measurement errors, $\eta_{t,\tau_i}^{IE} \sim N\left(0, \delta_{\tau_i}^{IE\,2}\right)$ and $\eta_{t,\tau_i}^{TE} \sim N\left(0, \delta_{\tau_i}^{TE\,2}\right)$ are assumed to follow an i.i.d structure. When maximizing log likelihood, we set up the upper bounds of δ_τ^{IE} and δ_τ^{TE} as 15bps and 25bps, respectively. In total, the state-space model includes 38 parameters, among which 9 parameters specify the measurement errors.

Table 4.1: Parameter Estimates

This table presents all parameters and standard errors (in parenthese) for the model we use to specify the dynamics of nominal yields, inflation and TIPS yields. Standard errors are computed by numerically calculating fishier information matrix.

Panel A								
State Variable Q Parameters			State Vriable P parameters			Price Level Parameters		
λ	0.2874	(0.0105)	κ_{11}	0.0952	(0.0330)	ρ_0^I	0.0174	(0.0014)
$\sigma_{1,1}$	0.0109	(0.0004)	κ_{22}	0.2830	(0.1099)	$\rho_{1,1}^I$	0.1430	(0.0190)
$\sigma_{1,1}$	0.0089	(0.0029)	κ_{33}	0.6358	(0.1106)	$\rho_{1,2}^I$	0.1128	(0.0335)
$\sigma_{1,2}$	0.0258	(0.0042)	μ_1	0.1076	(0.0137)	$\rho_{1,3}^I$	-0.0247	(0.0519)
$\sigma_{2,2}$	-0.0042	(0.0023)	μ_2	-0.0433	(0.0068)	$\sigma_{q,1}$	0.0285	(0.0041)
$\sigma_{2,3}$	-0.0310	(0.0017)	μ_3	-0.0121	(0.0027)	$\sigma_{q,2}$	0.0215	(0.0021)
$\sigma_{3,3}$	-0.0225	(0.0030)				$\sigma_{q,3}$	-0.0192	(0.0030)
						$\sigma_q^{\perp}$	0.0157	(0.0134)
Panel B								
TIPS Liquidity Premium			Measurement Error Parameters			Log likelihood		
β_1	0.0068	(0.0219)	α_1	0.0000	(Inf)	258,908.5025		
β_2	-0.1895	(0.0424)	γ_1	0.0136	(0.0083)			
β_3	0.4596	(0.0552)	α_2	0.0000	(Inf)			
$\widetilde{\beta}$	0.2272	(0.0256)	γ_2	0.1391	(0.0196)			
$\widetilde{\kappa}$	1.2556	(0.0127)	δ_{1y}^{IE}	0.0015	(0.0032)			
$\widetilde{\mu}$	0.0282	(0.0003)	δ_{5y}^{IE}	0.0014	(0.0046)			
$\widetilde{\lambda}_0$	3.7349	(0.0386)	δ_{10y}^{IE}	0.0010	(0.0024)			
$\widetilde{\sigma}\widetilde{\lambda}_1$	-1.3102	(0.0204)	δ_{1y}^{TE}	0.0025	(0.0060)			
			δ_{10y}^{TE}	0.0025	(0.0115)			

Table 4.2: Oil Shocks on IE, IRP and ITP

This table presents all parameters and standard errors for the regression of weekly change of IE/IRP/ITP on the contemporaneous weekly log WTI return $\Delta(\ln WTI_t)$, dummy variable for post-crisis (Post), and the interaction of these two variables. 1_{Post} is a dummy variable that is 1 if the date is later than November 1, 2007, and 0 otherwise. The standard error computed using Newey-West standard errors with six lags are provided in parentheses.

Panel A: 5-year Horizon						
	ΔIE		ΔIRP		ΔITP	
$\Delta(\ln WTI_t)$	0.0001	(0.0002)	-0.0004	(0.0001)	-0.0004	(0.0001)
1_{Post}	-0.0078	(0.0011)	-0.0131	(0.0011)	-0.0052	(0.0004)
$\Delta(\ln WTI_t) \cdot 1_{Post}$	0.0012	(0.0003)	0.0029	(0.0003)	0.0011	(0.0001)
Intercept	0.0237	(0.0008)	0.0019	(0.0005)	0.0018	(0.0002)
Panel B: 10-year Horizon						
	ΔIE		ΔIRP		ΔITP	
$\Delta(\ln WTI_t)$	-0.0001	(0.0001)	-0.0010	(0.0002)	-0.0008	(0.0001)
1_{Post}	-0.0075	(0.0008)	-0.0150	(0.0011)	-0.0089	(0.0008)
$\Delta(\ln WTI_t) \cdot 1_{Post}$	0.0013	(0.0002)	0.0033	(0.0003)	0.0020	(0.0002)
Intercept	0.0253	(0.0005)	0.0045	(0.0006)	0.0035	(0.0004)
Panel C: 30-year Horizon						
	ΔIE		ΔIRP		ΔITP	
$\Delta(\ln WTI_t)$	-0.0002	(0.0001)	-0.0015	(0.0002)	-0.0014	(0.0002)
1_{Post}	-0.0044	(0.0004)	-0.0202	(0.0015)	-0.0172	(0.0013)
$\Delta(\ln WTI_t) \cdot 1_{Post}$	0.0009	(0.0001)	0.0044	(0.0004)	0.0038	(0.0003)
Intercept	0.0271	(0.0002)	0.0024	(0.0008)	0.0006	(0.0007)

Figure 4.1: Term Premium Drop in 2016 while in Absence of US Fundamental Shocks

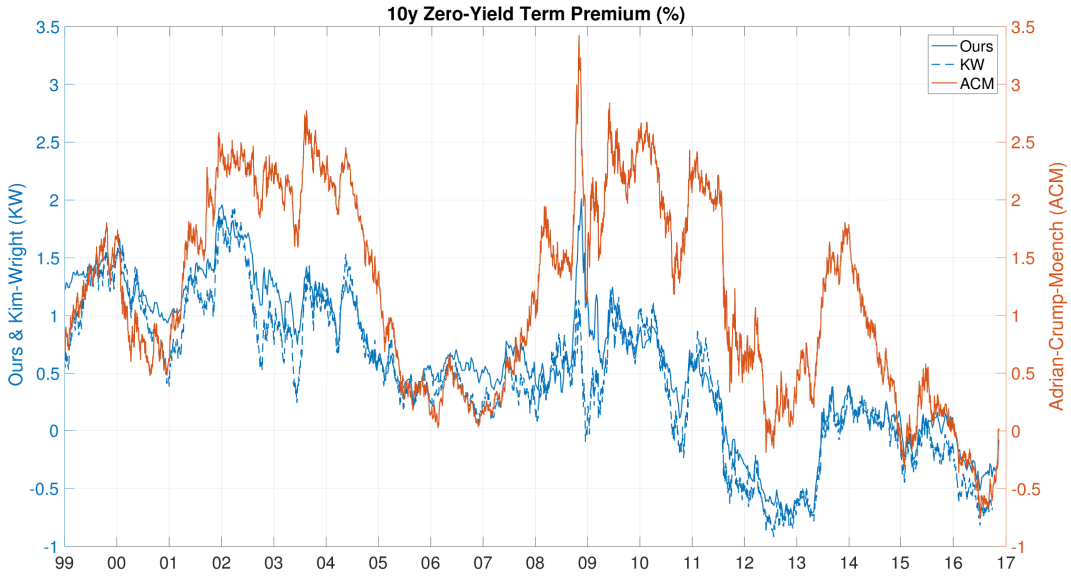

Figure 4.2: Japanese Flow was the Major Driver of Term Premium in 2016

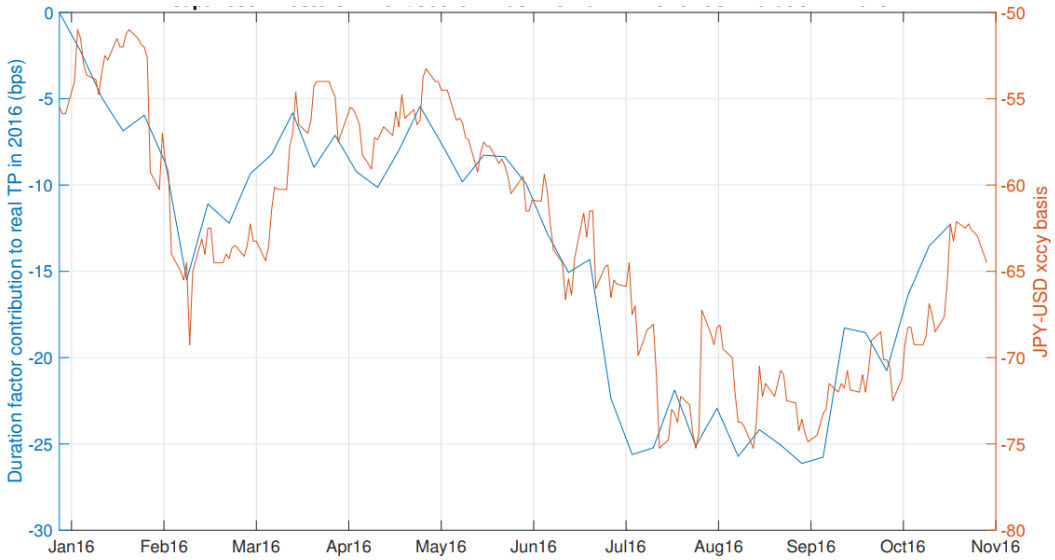

Figure 4.3: Factor Economic Meanings

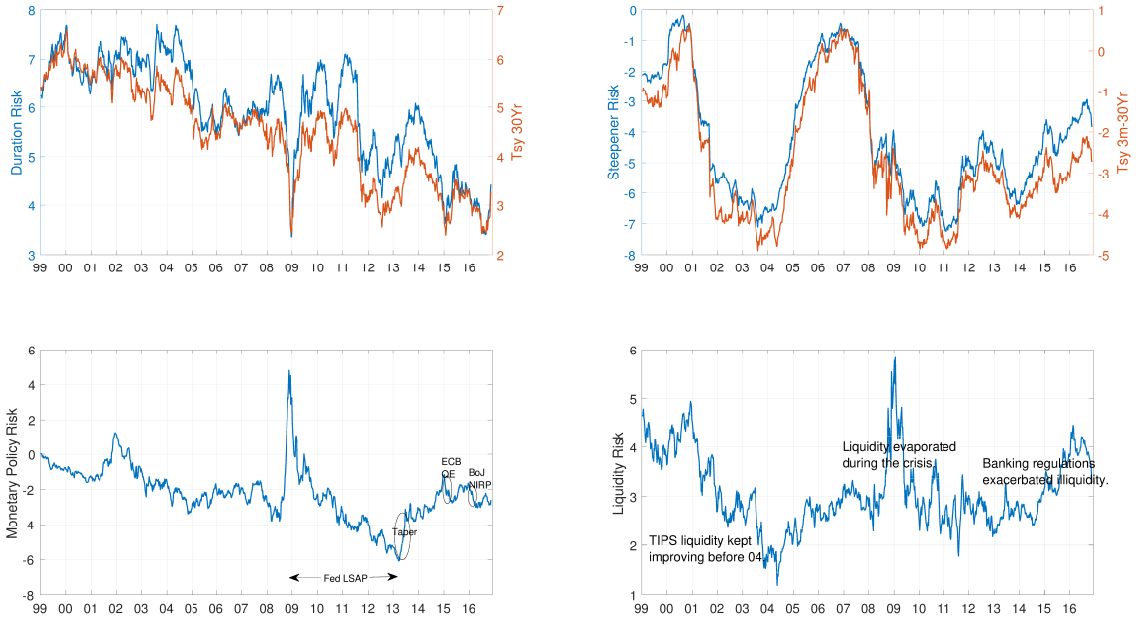

Figure 4.4: 10-Year Term Premium Decomposition

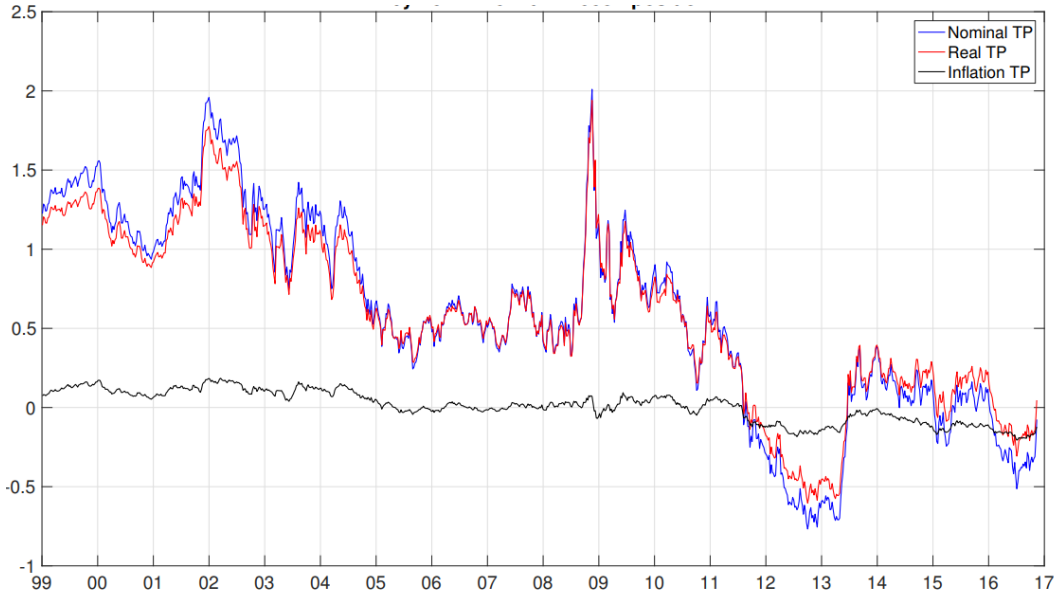

Figure 4.5: Real Term Premium Decomposition

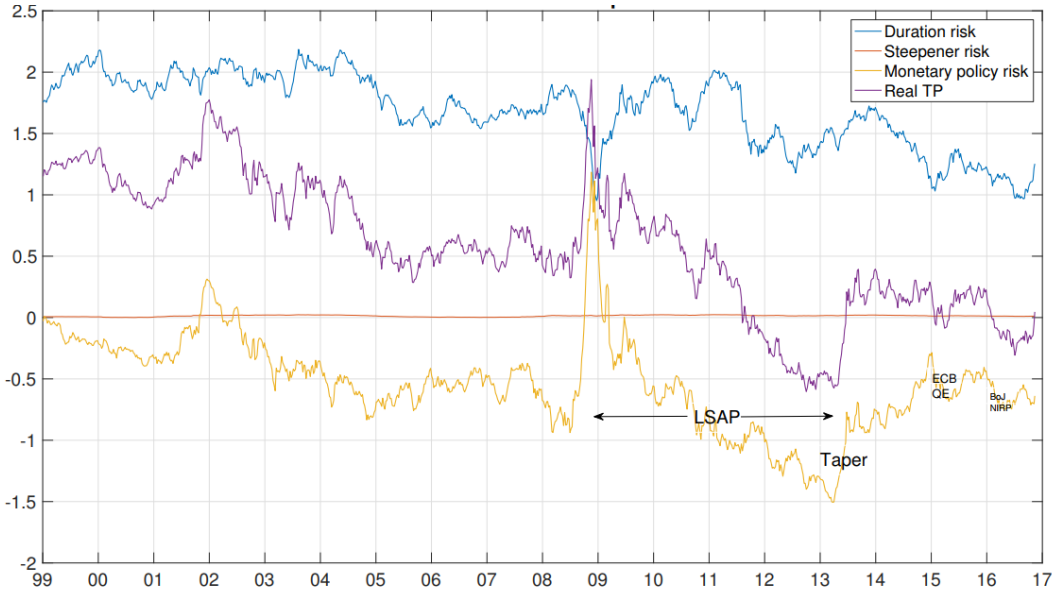

Figure 4.6: Japanese Treasury Holding Co-Moves with 10-Year UST Yields

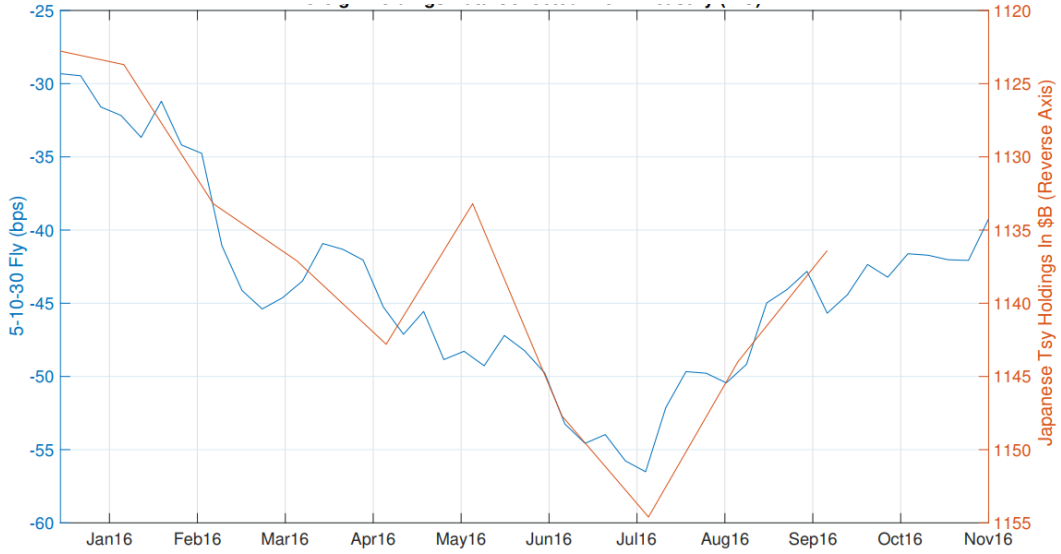

Figure 4.7: Fitted Nominal Yields: 3 Month to 14 Years

This figure shows the actual (in blue) and fitted (in red) nominal yields with maturities from 3 month to 14 years. The RMSE of the fitted yields are shown in the upper right corner of each plot. The first number is the RMSE (in bps) for the sample period excluding last half a year, while the second number is the RMSE (in bps) for last 26 weeks.

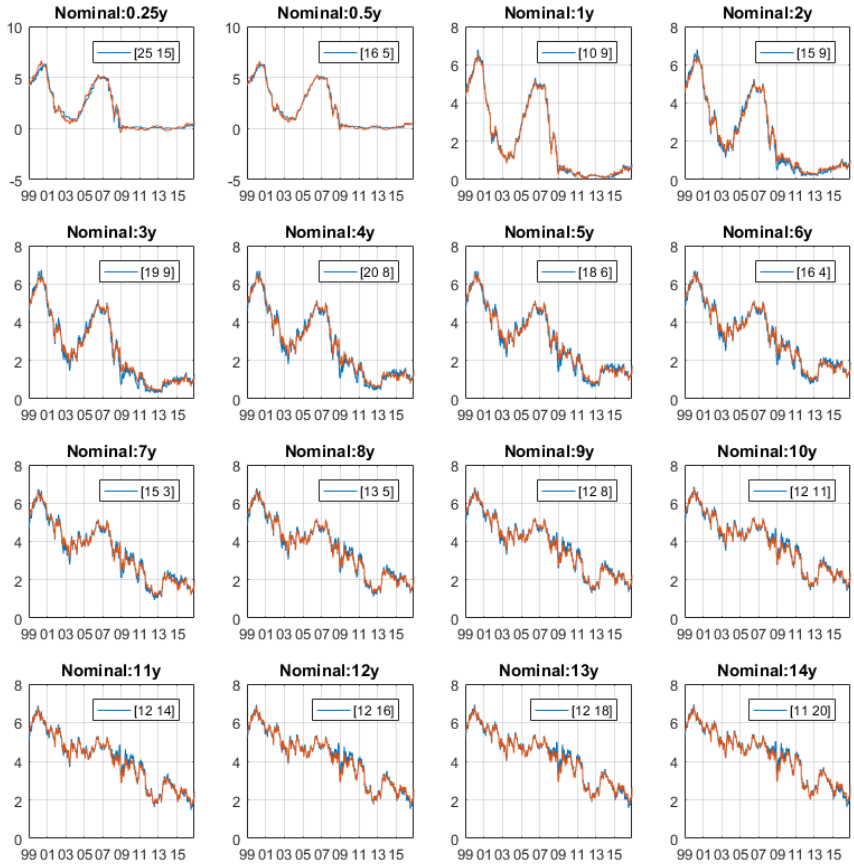

Figure 4.8: Fitted Nominal Yields: 15 to 30 Years

This figure shows the actual (in blue) and fitted (in red) nominal yields with maturities from 15 to 30 years. The RMSE of the fitted yields are shown in the upper right corner of each plot. The first number is the RMSE (in bps) for the sample period excluding last half a year, while the second number is the RMSE (in bps) for last 26 weeks.

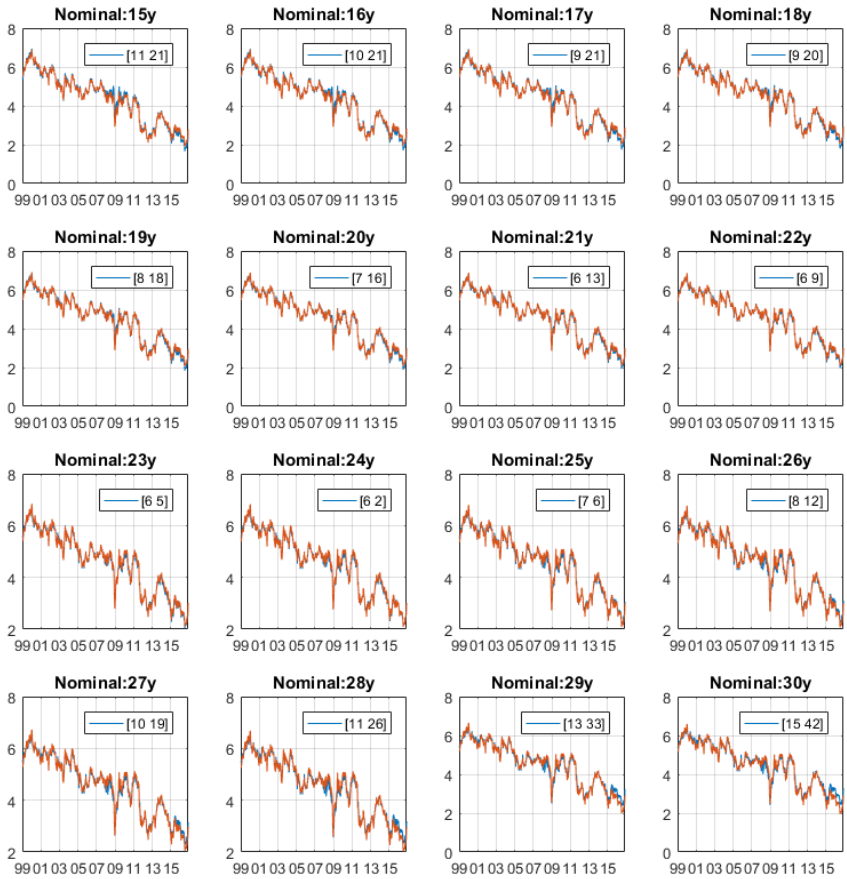

Figure 4.9: Fitted Survey Forecasts: Inflation and 3-Month Tbill Rate

This figure shows the actual (in blue) and fitted (in red) survey forecasts of average future inflation and 3-month Tbill Rate. The RMSE of the fitted yields are shown in the upper right corner of each plot. The first number is the RMSE (in bps) for the sample period excluding last half a year, while the second number is the RMSE (in bps) for last 26 weeks.

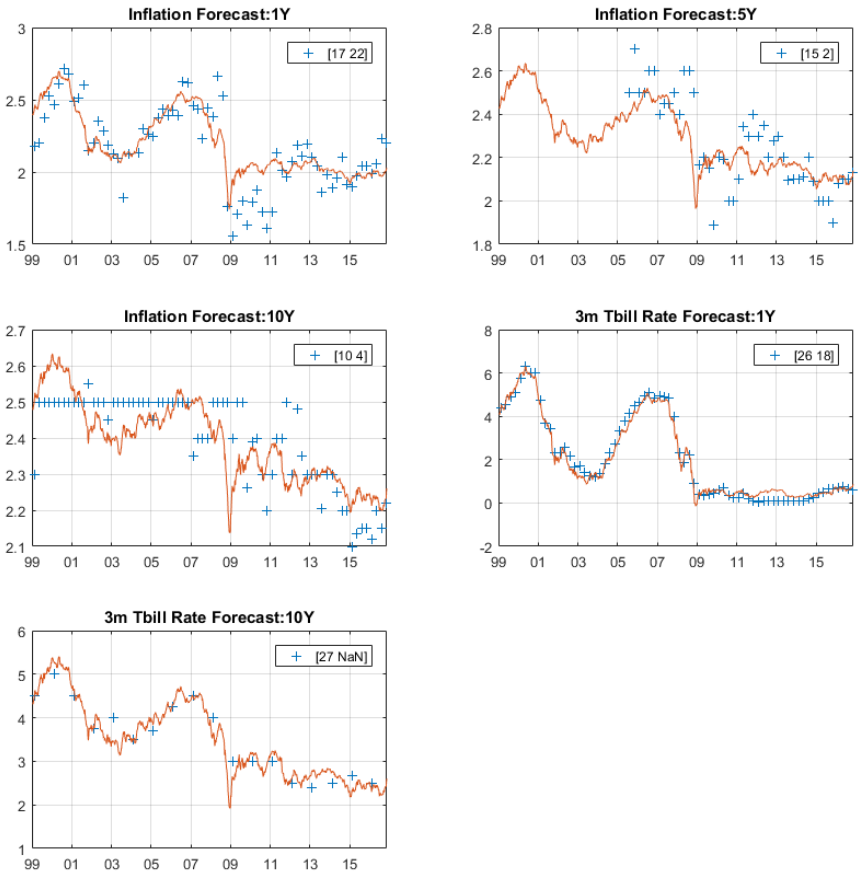

Figure 4.10: 2015-2017 Out-of-Sample Fitting RMSE across the Curve (bps)

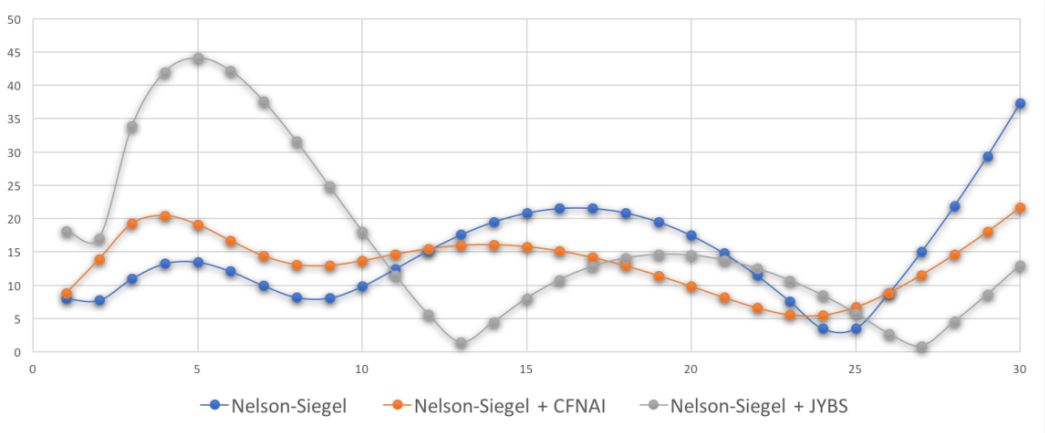

Figure 4.11: Spread between ¥-Hedged-UST and JGB (JYBS Maturity-Matched)

Figure 4.12: Real Term Premium Attribution Comparison

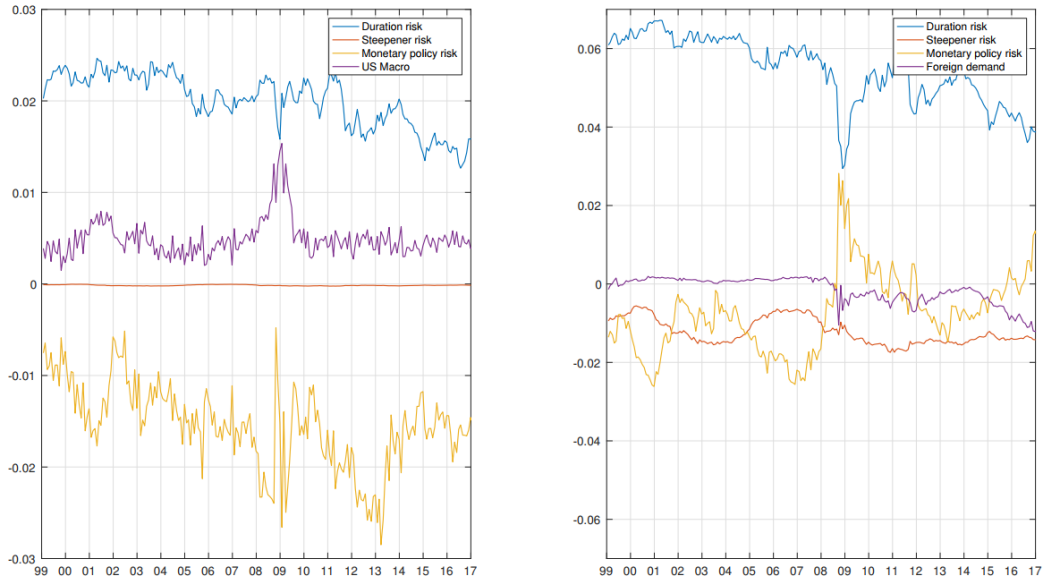

Bibliography

Abrahams, M. G., Adrian, T., Crump, R. K., and Moench, E. (2013). Pricing TIPS and treasuries with linear regressions. *Federal Reserve Bank of New York Staff Report*, (570).

Adrian, T., Crump, R. K., and Moench, E. (2013). Pricing the term structure with linear regressions. *Journal of Financial Economics*, 110(1):110–138.

Ait-Sahalia, Y., Wang, Y., and Yared, F. (2001). Do option markets correctly price the probabilities of movement of the underlying asset? *Journal of Econometrics*, 102(1):67–110.

Akaike, H. (1974). A new look at the statistical model identification. *IEEE Transactions on Automatic Control*, 19(6):716–723.

Al-Anaswah, N. and Wilfling, B. (2011). Identification of speculative bubbles using state-space models with Markov-switching. *Journal of Banking and Finance*, 35(5):1073–1086.

Amihud, Y. (2002). Illiquidity and stock returns: Cross-section and time-series effects. *Journal of Financial Markets*, 5(1):31–56.

Ang, A., Bekaert, G., and Wei, M. (2007). Do macro variables, asset markets, or surveys forecast inflation better? *Journal of Monetary Economics*, 54(4):1163–1212.

Ang, A., Bekaert, G., and Wei, M. (2008). The term structure of real rates and expected inflation. *Journal of Finance*, 63(2):797–849.

Ang, A. and Piazzesi, M. (2003). A no-arbitrage vector autoregression of term structure dynamics with macroeconomic and latent variables. *Journal of Monetary Economics*, 50(4):745–787.

Aruoba, B. S. (2019). Term structures of inflation expectations and real interest rates. *Journal of Business and Economic Statistics*, pages 1–21.

Aruoba, B. S. and Schorfheide, F. (2015). Inflation during and after the zero lower bound. *Unpublished manuscript, University of Pennsylvania*.

Badel, A. and McGillicuddy, J. (2015). Oil prices and inflation expectations: Is there a link? *Regional Economist*.

Bakshi, G., Kapadia, N., and Madan, D. (2003). Stock return characteristics, skew laws, and the differential pricing of individual equity options. *Review of Financial Studies*, 16(1):101–143.

Bali, T. G., Cakici, N., and Whitelaw, R. F. (2011). Maxing out: Stocks as lotteries and the cross-section of expected returns. *Journal of Financial Economics*, 99(2):427–446.

Bali, T. G., Hu, J., and Murray, S. (2019). Option implied volatility, skewness, and kurtosis and the cross-section of expected stock returns. *Georgetown McDonough School of Business Research Paper*.

Bali, T. G. and Murray, S. (2013). Does risk-neutral skewness predict the cross-section of equity option portfolio returns? *Journal of Financial and Quantitative Analysis*, 48(04):1145–1171.

Barberis, N. and Huang, M. (2008). Stocks as lotteries: The implications of probability weighting for security prices. *American Economic Review*, 98(5):2066–2100.

Bardgett, C., Gourier, E., and Leippold, M. (2018). Inferring volatility dynamics and risk premia from the S&P 500 and VIX markets. *Journal of Financial Economics*, 131:593–618.

Barndorff-Nielsen, O. E. (1997). Normal inverse gaussian distributions and stochastic volatility modelling. *Scandinavian Journal of statistics*, 24(1):1–13.

Barndorff-Nielsen, O. E. and Shephard, N. (2001). Modelling by Lévy processess for financial econometrics. In *Lévy Processes*, pages 283–318. Springer.

Bates, D. S. (1996). Jumps and stochastic volatility: Exchange rate processes implicit in deutsche mark options. *Review of Financial Studies*, 9(1):69–107.

Bauer, M. D. and Rudebusch, G. D. (2016). Monetary policy expectations at the zero lower bound. *Journal of Money, Credit and Banking*, 48(7):1439–1465.

Beltran, D. O., Kretchmer, M., Marquez, J., and Thomas, C. P. (2013). Foreign holdings of US treasuries and US treasury yields. *Journal of International Money and Finance*, 32:1120–1143.

Bernanke, B., Reinhart, V., and Sack, B. (2004). Monetary policy alternatives at the zero bound: An empirical assessment. *Brookings Papers on Economic Activity*, 2004(2):1–100.

Bizer, D. S. and Judd, K. L. (1989). Taxation and uncertainty. *American Economic Review*, 79(2):331–336.

Black, F. (1995). Interest rates as options. *Journal of Finance*, 50(5):1371–1376.

Blanchard, O. J. (1979). Speculative bubbles, crashes and rational expectations. *Economics Letters*, 3:387–389.

Blanchard, O. J. and Watson, M. W. (1982). Bubbles, rational expectations and financial markets. In *Crises in the Economic and Financial Structure*, volume 20 of *2*, pages 225–84. Lexington Books.

Bodenstein, M., Guerrieri, L., and Gust, C. J. (2013). Oil shocks and the zero bound on nominal interest rates. *Journal of International Money and Finance*, 32:941–967.

Bollen, N. P. and Whaley, R. E. (2004). Does net buying pressure affect the shape of implied volatility functions? *Journal of Finance*, 59(2):711–753.

Boyer, B., Mitton, T., and Vorkink, K. (2010). Expected idiosyncratic skewness. *Review of Financial Studies*, 23(1):169–202.

Brunnermeier, M. K. (2009). Deciphering the liquidity and credit crunch 2007–2008. *Journal of Economic Perspectives*, 23(1):77–100.

Brunnermeier, M. K. (2016). Bubbles. In *Banking Crises*, pages 28–36. Springer.

Brunnermeier, M. K., Gollier, C., and Parker, J. A. (2007). Optimal beliefs, asset prices, and the preference for skewed returns. *American Economic Review*, 97:159–165.

Campbell, J. Y. and Shiller, R. J. (1988). The dividend-price ratio and expectations of future dividends and discount factors. *Review of Financial Studies*, 1(3):195–228.

Carhart, M. M. (1997). On persistence in mutual fund performance. *Journal of Finance*, 52(1):57–82.

Carr, P., Geman, H., Madan, D. B., and Yor, M. (2003). Stochastic volatility for Lévy processes. *Mathematical Finance*, 13(3):345–382.

Carr, P. and Wu, L. (2003). The finite moment log stable process and option pricing. *Journal of Finance*, 58(2):753–778.

Chauvet, M. (1998). An econometric characterization of business cycle dynamics with factor structure and regime switching. *International Economic Review*, 39:969–996.

Chen, R. and Liu, J. S. (2000). Mixture Kalman filters. *Journal of the Royal Statistical Society: Series B (Statistical Methodology)*, 62(3):493–508.

Chiang, I.-H. E. and Hughen, W. K. (2017). Do oil futures prices predict stock returns? *Journal of Banking & Finance*, 79:129–141.

Chiang, I.-H. E., Hughen, W. K., and Sagi, J. S. (2015). Estimating oil risk factors using information from equity and derivatives markets. *Journal of Finance*, 70(2):769–804.

Christensen, J. H., Diebold, F. X., and Rudebusch, G. D. (2011). The affine arbitrage-free class of nelson–siegel term structure models. *Journal of Econometrics*, 164(1):4–20.

Christensen, J. H., Lopez, J. A., and Rudebusch, G. D. (2010). Inflation expectations and risk premiums in an arbitrage-free model of nominal and real bond yields. *Journal of Money, Credit and Banking*, 42:143–178.

Christensen, J. H. and Rudebusch, G. D. (2016). Modeling yields at the zero lower bound: Are shadow rates the solution? In *Dynamic Factor Models*, pages 75–125. Emerald Group Publishing Limited.

Coleman, W. J. (1991). Equilibrium in a production economy with an income tax. *Econometrica: Journal of the Econometric Society*, pages 1091–1104.

Conrad, J., Dittmar, R. F., and Ghysels, E. (2013). Ex ante skewness and expected stock returns. *Journal of Finance*, 68(1):85–124.

Cont, R. and Tankov, P. (2003). *Financial modelling with jump processes*. Chapman and Hall/CRC.

Dai, Q. and Singleton, K. J. (2000). Specification analysis of affine term structure models. *Journal of Finance*, 55(5):1943–1978.

D'Amico, S., Kim, D. H., and Wei, M. (2018). Tips from TIPS: the informational content of treasury inflation-protected security prices. *Journal of Financial and Quantitative Analysis*, 53(1):395–436.

Darvas, Z. and Hüttl, P. (2016). Oil prices and inflation expectations. *Bruegel Blog*, 21.

Datta, D., Johannsen, B. K., Kwon, H., and Vigfusson, R. J. (2018). Oil, equities, and the zero lower bound. *Federal Reserve Board Working Paper*.

Diba, B. T. and Grossman, H. I. (1988). Explosive rational bubbles in stock prices? *American Economic Review*, 78(3):520–530.

Duffee, G. R. (2002). Term premia and interest rate forecasts in affine models. *Journal of Finance*, 57(1):405–443.

Duffie, D. and Kan, R. (1996). A yield-factor model of interest rates. *Mathematical Finance*, 6(4):379–406.

Eggertsson, G. B. and Woodford, M. (2003). Optimal monetary policy in a liquidity trap. *National Bureau of Economic Research Working Papers*.

Elliott, D., Jackson, C., Raczko, M., and Robert-Skar, M. (2015). Does oil drive financial market measures of inflation expectations? *Bank of England, Bank Underground*, 20.

Evans, G. W. (1991). Pitfalls in testing for explosive bubbles in asset prices. *American Economic Review*, 81(4):922–930.

Fama, E. F. and French, K. R. (1992). The cross-section of expected stock returns. *Journal of Finance*, 47(2):427–465.

Fama, E. F. and French, K. R. (1993). Common risk factors in the returns on stocks and bonds. *Journal of Financial Economics*, 33(1):3–56.

Fama, E. F. and French, K. R. (2015). A five-factor asset pricing model. *Journal of Financial Economics*, 116(1):1–22.

Fama, E. F. and MacBeth, J. D. (1973). Risk, return, and equilibrium: Empirical tests. *Journal of Political Economy*, 81(3):607–636.

Fernández-Villaverde, J., Gordon, G., Guerrón-Quintana, P., and Rubio-Ramirez, J. F. (2015). Nonlinear adventures at the zero lower bound. *Journal of Economic Dynamics and Control*, 57:182–204.

Fisher, J. D. (2015). On the structural interpretation of the Smets–Wouters "risk premium" shock. *Journal of Money, Credit and Banking*, 47(2-3):511–516.

Foresi, S. and Wu, L. (2005). Crash–O–Phobia: A domestic fear or a worldwide concern? *Journal of Derivatives*, 13(2):8–21.

Froot, K. A. and Obstfeld, M. (1991). Intrinsic bubbles: The case of stock prices. *American Economic Review*, 81:1189–214.

Gamerman, D. and Lopes, H. F. (2006). *Markov Chain Monte Carlo: Stochastic simulation for Bayesian inference*. Chapman and Hall/CRC.

Garleanu, N., Pedersen, L. H., and Poteshman, A. M. (2009). Demand-based option pricing. *Review of Financial Studies*, 22(10):4259–4299.

Gavin, W. T., Keen, B. D., Richter, A. W., and Throckmorton, N. A. (2015). The zero lower bound, the dual mandate, and unconventional dynamics. *Journal of Economic Dynamics and Control*, 55:14–38.

Greenwood, R. and Vayanos, D. (2014). Bond supply and excess bond returns. *Review of Financial Studies*, 27(3):663–713.

Grishchenko, O. V. and Huang, J. (2013). The inflation risk premium: Evidence from the TIPS market. *Journal of Fixed Income*, 22(4):5–30.

Guerrieri, L. and Iacoviello, M. (2015). Occbin: A toolkit for solving dynamic models with occasionally binding constraints easily. *Journal of Monetary Economics*, 70:22–38.

Gürkaynak, R. S., Sack, B., and Wright, J. H. (2007). The US treasury yield curve: 1961 to the present. *Journal of Monetary Economics*, 54(8):2291–2304.

Gürkaynak, R. S., Sack, B., and Wright, J. H. (2010). The TIPS yield curve and inflation compensation. *American Economic Journal: Macroeconomics*, 2(1):70–92.

Gust, C., Herbst, E., López-Salido, D., and Smith, M. E. (2017). The empirical implications of the interest-rate lower bound. *American Economic Review*, 107(7):1971–2006.

Hamilton, J. D. and Whiteman, C. H. (1985). The observable implications of self-fulfilling expectations. *Journal of Monetary Economics*, 16(3):353–373.

Hansen, N. (2006). The cma evolution strategy: a comparing review. In *Towards a New Evolutionary Computation*, pages 75–102. Springer.

Harrison, J. and West, M. (1999). *Bayesian forecasting and dynamic models*. Springer.

Harvey, A. C. (1989). *Forecasting, structural time series models and the Kalman filter*. Cambridge University Press, Cambridge, UK.

Haubrich, J., Pennacchi, G., and Ritchken, P. (2012). Inflation expectations, real rates, and risk premia: evidence from inflation swaps. *Review of Financial Studies*, 25(5):1588–1629.

Hitzemann, S. (2016). Macroeconomic fluctuations, oil supply shocks, and equilibrium oil futures prices. *Working Paper*.

Holden, T. D. (2016). Computation of solutions to dynamic models with occasionally binding constraints. *Working Paper*.

Holden, T. D. (2017). Existence and uniqueness of solutions to dynamic models with occasionally binding constraints. *Working Paper*.

Holowczak, R., Simaan, Y. E., and Wu, L. (2006). Price discovery in the us stock and stock options markets: A portfolio approach. *Review of Derivatives Research*, 9(1):37–65.

Hong, H. and Yogo, M. (2012). What does futures market interest tell us about the macroeconomy and asset prices? *Journal of Financial Economics*, 105(3):473–490.

Hutton, A. P., Marcus, A. J., and Tehranian, H. (2009). Opaque financial reports, R square, and crash risk. *Journal of Financial Economics*, 94(1):67–86.

Ichiue, H. and Ueno, Y. (2007). Equilibrium interest rate and the yield curve in a low interest rate environment. *Bank of Japan Discussion Paper*.

Joslin, S., Le, A., and Singleton, K. J. (2013). Why gaussian macro-finance term structure models are (nearly) unconstrained factor-vars. *Journal of Financial Economics*, 109(3):604–622.

Joslin, S., Priebsch, M., and Singleton, K. J. (2014). Risk premiums in dynamic term structure models with unspanned macro risks. *Journal of Finance*, 69(3):1197–1233.

Kalman, R. E. (1960). A new approach to linear filtering and prediction problems. *Journal of Basic Engineering*, 82:35–45.

Kaminska, I., Vayanos, D., and Zinna, G. (2011). Preferred-habitat investors and the US term structure of real rates. *Bank of England Working Paper*.

Kilian, L. and Park, C. (2009). The impact of oil price shocks on the US stock market. *International Economic Review*, 50(4):1267–1287.

Kim, C. J. and Nelson, C. R. (1999). *State-space models with regime switching: Classical and Gibbs-sampling approaches with applications*. The MIT press.

Kim, D. H. and Orphanides, A. (2012). Term structure estimation with survey data on interest rate forecasts. *Journal of Financial and Quantitative Analysis*, 47(01):241–272.

Kim, D. H. and Priebsch, M. (2013). Estimation of multi-factor shadow-rate term structure models. *Federal Reserve Board Discussion Paper Series*.

Kim, D. H. and Singleton, K. J. (2012). Term structure models and the zero bound: an empirical investigation of Japanese yields. *Journal of Econometrics*, 170(1):32–49.

Kim, D. H. and Wright, J. H. (2005). An arbitrage-free three-factor term structure model and the recent behavior of long-term yields and distant-horizon forward rates. *Federal Reserve Board Working Paper*.

Kim, J. B., Li, Y., and Zhang, L. (2011a). CFOs versus CEOs: Equity incentives and crashes. *Journal of Financial Economics*, 101(3):713–730.

Kim, J. B., Li, Y., and Zhang, L. (2011b). Corporate tax avoidance and stock price crash risk: Firm-level analysis. *Journal of Financial Economics*, 100(3):639–662.

Kohn, D. (2016). Addicted to debt: Foreign purchases of US treasuries and the term-premium. *Working Paper*.

Koijen, R. S., Koulischer, F., Nguyen, B., and Yogo, M. (2016). Quantitative easing in the Euro area: The dynamics of risk exposures and the impact on asset prices. *Working Paper*.

Koijen, R. S. and Yogo, M. (2016). Shadow insurance. *Econometrica*, 84(3):1265–1287.

Krippner, L. (2012). Modifying gaussian term structure models when interest rates are near the zero lower bound. *Reserve Bank of New Zealand Discussion Paper*, (2012/02).

Krishnamurthy, A. and Vissing-Jorgensen, A. (2011). The effects of quantitative easing on interest rates: channels and implications for policy. *National Bureau of Economic Research Working Paper*.

Li, J. and Zinna, G. (2018). The variance risk premium: Components, term structures, and stock return predictability. *Journal of Business and Economic Statistics*, 36(3):411–425.

Litterman, R. and Scheinkman, J. (1991). Common factors affecting bond returns. *Journal of fixed income*, 1(1):54–61.

Livnat, J. and Mendenhall, R. R. (2006). Comparing the post–earnings announcement drift for surprises calculated from analyst and time series forecasts. *Journal of Accounting Research*, 44(1):177–205.

Mitton, T. and Vorkink, K. (2007). Equilibrium underdiversification and the preference for skewness. *Review of Financial Studies*, 20(4):1255–1288.

Mönch, E. (2008). Forecasting the yield curve in a data-rich environment: A no-arbitrage factor-augmented var approach. *Journal of Econometrics*, 146(1):26–43.

Nakata, T. (2017). Uncertainty at the zero lower bound. *American Economic Journal: Macroeconomics*, 9(3):186–221.

Nakata, T. and Tanaka, H. (2016). Equilibrium yield curves and the interest rate lower bound. *Federal Reserve Board Working Paper*.

Nelson, C. R. and Siegel, A. F. (1987). Parsimonious modeling of yield curves. *Journal of Business*, 60(1):473–489.

Nicolato, E. and Venardos, E. (2003). Option pricing in stochastic volatility models of the Ornstein-Uhlenbeck type. *Mathematical Finance*, 13(4):445–466.

Pastor, L. and Stambaugh, R. F. (2003). Liquidity risk and expected stock returns. *Journal of Political Economy*, 111(3):642–685.

Perez-Segura, A. and Vigfusson, R. J. (2016). The relationship between oil prices and inflation compensation. *Federal Reserve Board Working Paper*.

Petkova, R. (2006). Do the Fama–French factors proxy for innovations in predictive variables? *Journal of Finance*, 61(2):581–612.

Phillips, P. C., Wu, Y., and Yu, J. (2011). Explosive behavior in the 1990s Nasdaq: When did exuberance escalate asset values? *International Economic Review*, 52(1):201–226.

Ready, R. C. (2018). Oil consumption, economic growth, and oil futures: The impact of long-run oil supply uncertainty on asset prices. *Journal of Monetary Economics*, 94:1–26.

Richter, A. W., Throckmorton, N. A., and Walker, T. B. (2014). Accuracy, speed and robustness of policy function iteration. *Computational Economics*, 44(4):445–476.

Rotemberg, J. J. (1982). Sticky prices in the united states. *Journal of Political Economy*, 90(6):1187–1211.

Rudebusch, G. D., Swanson, E. T., and Wu, T. (2006). The bond yield'conundrum'from a macro-finance perspective. *Working Paper*.

Schwarz, G. (1978). Estimating the dimension of a model. *Annals of Statistics*, 6(2):461–464.

Shiller, R. J. (1981). Do stock prices move too much to be justified by subsequent changes in dividends? *American Economic Review*, 71:421–36.

Sierra, J. (2014). International capital flows and bond risk premia. *Quarterly Journal of Finance*, 4(1):1450001.

Smets, F. and Wouters, R. (2007). Shocks and frictions in US business cycles: A Bayesian DSGE approach. *American Economic Review*, 97(3):586–606.

Stilger, P. S., Kostakis, A., and Poon, S.-H. (2017). What does risk-neutral skewness tell us about future stock returns? *Management Science*, 63(6):1814–1834.

Sussman, N. and Zohar, O. (2015). Oil prices, inflation expectations, and monetary policy. *Bank of Israel Working Paper*.

Taylor, S. J., Yadav, P. K., Zhang, Y., et al. (2009). Cross-sectional analysis of risk-neutral skewness. *Journal of Derivatives*, 16(4):38.

Tirole, J. (1982). On the possibility of speculation under rational expectations. *Econometrica*, pages 1163–1181.

Vasicek, O. (1977). An equilibrium characterization of the term structure. *Journal of Financial Economics*, 5(2):177–188.

Vayanos, D. and Vila, J.-L. (2009). A preferred-habitat model of the term structure of interest rates. *National Bureau of Economic Research Working Paper*.

Warnock, F. E. and Warnock, V. C. (2009). International capital flows and US interest rates. *Journal of International Money and Finance*, 28(6):903–919.

Welch, I. and Goyal, A. (2008). A comprehensive look at the empirical performance of equity premium prediction. *Review of Financial Studies*, 21(4):1455–1508.

West, K. D. (1987). A specification test for speculative bubbles. *Quarterly Journal of Economics*, 102(3):553–580.

Wong, B. (2015). Do inflation expectations propagate the inflationary impact of real oil price shocks? evidence from the michigan survey. *Journal of Money, Credit and Banking*, 47(8):1673–1689.

Wu, J. C. and Xia, F. D. (2016). Measuring the macroeconomic impact of monetary policy at the zero lower bound. *Journal of Money, Credit and Banking*, 48(2-3):253–291.

Wu, Y. (1997). Rational bubbles in the stock market: Accounting for the US stock-price volatility. *Economic Inquiry*, 35(2):309–319.

Wurgler, J. and Zhuravskaya, E. (2002). Does arbitrage flatten demand curves for stocks? *Journal of Business*, 75(4):583–608.

Xiang, J. and Zhu, X. (2013). A regime-switching Nelson–Siegel term structure model and interest rate forecasts. *Journal of Financial Econometrics*, 11(3):522–555.

Xing, Y., Zhang, X., and Zhao, R. (2010). What does the individual option volatility smirk tell us about future equity returns? *Journal of Financial Quantitative Analysis*, 45(1):641–662.

Yan, W. (2016). The role of Asian countries reserve holdings on the US yield curve.

Zmijewski, M. E. (1984). Methodological issues related to the estimation of financial distress prediction models. *Journal of Accounting Research*, 22:59–82.